UNIVERSITÉ DU QUÉBEC

THÈSE PRÉSENTÉE À
L'UNIVERSITÉ DU QUÉBEC À TROIS-RIVIÈRES

COMME EXIGENCE PARTIELLE DU
DOCTORAT EN GÉNIE PAPETIER

PAR
CHANGBIN MAO

MÉCANISME DE RUPTURE DU BOIS SOUS COMPRESSION ET CISAILLEMENT

(MECHANISM OF WOOD RUPTURE UNDER COMPRESSION AND SHEAR)

MARS 2005

ACKNOWLEDGEMENTS

I would like to sincerely thank to Dr. Ken N. Law and Dr. Bohuslav V. Kokta for their constant supervision and supports throughout my work and studies at the UQTR.

I want to thank the Centre Intégré en Pâtes et Papiers and its professors, technicians and secretary for their kind collaborations and assistance during my study.

I also want to thank the Natural Science and Engineering Research Council of Canada, Kruger Inc. and the Fondation de UQTR for their financial supports.

Finally, I would like to thank my wife Yanfen Shen, my little daughter Jenny Mao, my parents, brothers and sister for their profound love and unwavering supports during my studies.

SUMMARY

Mechanical pulping has been well developed during the last three decades, and owing to its high yield, high bulk and high opacity, the use of mechanical pulp in printing grades is increasingly widening. However, high-energy consumption in chip refining remains a major drawback, restricting a wider expansion of this technology. Thus reducing the energy consumption in refining is one of the main technical development efforts in the mechanical pulping industry.

The main objective of this work is to conduct some basic research on the mechanism of wood rupture under compression and shear forces, especially on how and to what extent wood fiber is modified by compression. More precisely, this work intends to examine the characteristics of structural failures of wood under various conditions such as mechanical stress, compression strain, moisture content, temperature and chemical treatments. With this understanding, we might be able to find an energy-efficient way to achieve a fiber separation and an internal delamination, and finally achieve an energy saving and pulp quality improvement.

In the first series of experiments, the effect of temperature on the rupture behaviors of wood in the radial, tangential and longitudinal compressions is examined. The results indicate that wood responses similarly in both the radial and tangential compressions at various temperatures, and that fiber collapse in a transverse direction is mainly determined by the tubular structure of fiber. Further, the modulus of elasticity (MOE), first and second plateau stresses (SP1, SP2), and the specific compression energy (SCE) can be used to characterize the behaviors of wood under compression. Among these strength parameters, the second plateau stress is for the first time used to describe fiber separation at the densification stage. The relationships between these four parameters and the temperature follow the Arrhenius' Law for compressions in all three directions of specimens (radial, tangential and longitudinal directions relative to fiber axis). This means that the effect of thermal softening can be explained by the motion of polymer chain of the main components of wood (cellulose, hemicelluloses and lignin). General stress models are also developed to express the stress in the elastoplastic region in radial

and tangential compressions. These models are for first time used to predict the transverse resistance of earlywood (EW) fibers at various temperatures. According to these models, the compressive stress required to flatten EW fibers in refining is about 0.62-1.53 MPa. This force is much higher than the average stress between two refiner bars (0.45 MPa), indicating the reason of high-energy consumption in refining. However, the high strain pre-compression (70% strain) under which the wood fibers are flattened and separated, can reduce the fiber's transverse resistance by 70-85%, decreasing the compressive force required to collapse a pre-compressed fiber to 0.25-0.32 MPa. Therefore, in subsequent refining of the pre-compressed chips, an average compressive force of 0.45 MPa would be sufficient to readily flatten most of these fibers. The pre-compression of wood before refining might offer a potential change in shifting the refining process from fatigue process to a more efficient breakdown process.

The effect of sulfonation on the behavior of wood in radial compression is examined in a second series of experiment. In sulfonation, the temperature is by far the most influential factor on the level of sulfonation. The early- and latewood are sulfonated to a similar sulfonate level under the same conditions. The sulfonation decreases the physical properties of wood such as the modulus, specific compression energy, and stresses of both the first and second plastic zones. There exists a linear relationship between these physical properties and the sulfonate content. However, there is no fundamental change in the form of the compression curve at various sulfonate contents.

A systematic comparison of radial compressions with and without restraint indicates that wood responses similarly in the two compression conditions when the compression strain is low (less than 50%). However, when the compression strain exceeds 50%, there is significant lateral expansion of the wood matrix, and the wood samples behave differently. For the unrestrained compression, a second short plateau is provoked at around 60% strain, where fiber separations take place due to excessive lateral expansion. For the restrained compression, there is, however, no second plateau, and the stress increases rapidly in the densification region. The modulus at this zone is independent of the sulfonate content, indicating that the restraint controls the modulus at this zone.

The effect of compression on the strength properties of wood has also been quantitatively evaluated by shearing the pre-compressed wood blocks, in the third series experiment. The results indicate that radial compression has little effect on shear properties when the compression strain is less than 50%. Beyond this compression strain the shear properties fall sharply, indicating significant structural damages in both early- and latewood. The pre-compression conditions also have significant influence on the shear characteristics. The changes in shear properties of the specimens are closely associated with the specific compression energy in the pre-compression process.

Scanning electron microscopy (SEM) observation indicates that fibers response similarly under compression in both radial and tangential directions; longitudinal cleavages are only resulted from the transverse compressions. For the high-strain radial compression, the wood block is modified at four levels: it loosens the wood matrix, weakens the interfaces of different layers (P/S_1, S_1/S_2), weakens the linkages between micro-fibrils within S_2 layer, and flattens and flexibilizes fibers. However, the pre-compression conditions also play an important role in the process. Compression at low temperature seems to benefit fiber failure between S_1/ S_2 and within the S_2 layer. Compression with high compression strain (higher than 50%) at high temperature (120 °C) favors the modification of latewood (LW) fibers.

This study suggests that static compression with large strain (>50%) modifies the wood matrix in two aspects: first, it flattens the fibers, and greatly reduces their transverse resistance. Second, it modifies the fiber's microstructure at different levels, pre-setting a more favorite fiber separation mode and fiber development process, and rendering the wood more suitable for further processing into a mechanical pulp with improved quality. All these may potentially change the refining process from a fatigue process to a more efficient breakdown process, and finally result in an improved pulp quality and a reduced refining energy consumption.

Keywords: *Picea glauca* (Moench) Voss (white spruce), compression, shear, energy saving, chemical and thermal pretreatments, wood rupture mechanism, fiber collapse, fiber separation, scanning electronic microscopy, microstructure, Young's modulus, stress, strain, chip refining, mechanical pulps.

RÉSUMÉ

La mise en pâte mécanique a été bien développée pendant les trois dernières décennies. Dû à ses propriétés d'impression supérieures (rendement élevé, bouffant élevé et opacité élevée) l'utilisation de la pâte mécanique pour la fabrication du papier d'impression s'élargit de plus en plus. Cependant, la consommation d'énergie élevée du raffinage des copeaux demeure un inconvénient majeur, limitant un plus grand développement de cette technologie. Ainsi, la réduction de la consommation d'énergie du raffinage est toujours l'un des efforts techniques principaux dans l'industrie des pâtes mécaniques.

L'objectif principal de ce travail est de réaliser de la recherche fondamentale sur le mécanisme de rupture du bois sous les actions de compression et de cisaillement. Il est particulièrement important de savoir comment et à quel niveau le bois est modifié par une charge de compression. Plus précisément, on examine les caractéristiques des ruptures structurales du bois dans diverses conditions telles que la charge de compression «stress», la déformation de compression, le contenu d'humidité, la température, et la sulfonation. Avec une telle connaissance, nous pourrions optimiser les conditions de traitement mécanique pour réaliser une bonne séparation des fibres et une fibrillation interne de la paroi cellulaire. Ceci nous mènerait finalement à une économie d'énergie de raffinage et à une amélioration des propriétés de la pâte.

Dans la première série d'expériences, on étudie l'effet de la température sur les comportements de rupture du bois dans les compressions radiales, tangentielles et longitudinales. Les résultats indiquent que les réponses du bois sont semblables aux compressions radiales et tangentielles à diverses températures, et que l'effondrement des fibres dans la direction transversale est principalement déterminé par la structure tubulaire des fibres. Le module de l'élasticité «MOE», les «stress» du premier et deuxième plateau (SP1, SP2), et l'énergie spécifique de compression (SCE) sont employés pour caractériser les comportements du bois sous compression. Parmi eux, le «stress» du deuxième plateau (SP2) est utilisé pour la première fois afin de décrire la séparation des fibres pendant l'étape de densification. Les rapports entre ces quatre paramètres et la température suivent la loi d'Arrhenius pour les compressions dans les

trois directions de compression, soit les directions radiales, tangentielles et longitudinales relativement à l'axe des fibres. Ceci signifie que l'effet du ramollissement thermique peut être expliqué par le mouvement des chaînes de polymères des composants principaux du bois (la cellulose, les hémicelluloses et la lignine). On développe également des modèles généraux de contrainte pour exprimer la contrainte dans la région élastoplastique au cours des compressions radiale et tangentielle. Ces modèles ont été employés pour la première fois en vue de prédire la résistance transversale des fibres de bois de printemps aux diverses températures. Selon ces modèles, la contrainte de compression exigée pour aplatir des fibres de bois de printemps au raffinage est d'environ 0.62-1.53 MPa. Cette résistance est beaucoup plus grande que la contrainte moyenne entre deux barres du raffineur (0.45 MPa), ce qui explique la raison pour laquelle la consommation d'énergie est élevée dans le raffinage. Cependant, la précompression du bois avec un grand taux de déformation (70%), qui aplatit les fibres du bois et crée leur séparation, pourrait réduire la résistance transversale des fibres de 70-85%. Ceci veut dire que la précompression du bois diminue la force de compression exigée pour aplatir les fibres à 0.25-0.32 MPa. Par conséquent, lors d'un raffinage avec des copeaux précomprimés, une force de compression moyenne de 0.45 MPa aplatirait aisément la plupart de ces fibres. Cette approche de prétraitement mécanique peut potentiellement changer le processus de raffinage d'un processus de fatigue à un processus de séparation plus efficace.

Dans la deuxième série d'expériences, on étudie l'effet de la sulfonation sur le comportement du bois dans la compression radiale. On note que la température est le facteur le plus influent au niveau de la sulfonation. Autrement, les fibres de bois de printemps et les fibres de bois d'été se comportent de façon semblable dans la sulfonation sous les mêmes conditions de traitement. La sulfonation diminue les propriétés physiques telles que le MOE, le SP1, le SP2, et la SCE. Il existe une relation linéaire entre ces propriétés physiques et le contenu en groupements sulfoniques. Néanmoins, le contenu en groupements sulfoniques n'a aucun effet sur la forme des courbes de compression. Une comparaison systématique des compressions radiales (avec et sans contrainte latérale) indique que les réponses du bois sont pareilles dans les deux types de compression lorsque la compression est réalisée avec un taux de

déformation inférieur à 50%. Toutefois, quand la déformation de compression excède 50%, l'expansion latérale du spécimen se produit de manière significative, de sorte que les spécimens se comportent différemment. Dans le cas de la compression sans contrainte, un bref deuxième plateau de contrainte se produit lorsque la déformation atteint environ 60%, où une séparation des fibres a lieu en raison de l'expansion latérale excessive. Cependant, un tel deuxième plateau ne se manifeste pas quand l'échantillon est comprimé avec contrainte. Dans ce cas, la contrainte augmente rapidement dans la région de densification. D'autre part, le module de ce stade (MOE2) est indépendant du contenu en groupements sulfoniques, ce qui signifie que le module de cette région est contrôlé par la contrainte de compression.

Dans la troisième série d'expériences, on quantifie l'effet de la compression sur l'affaiblissement de la matrice du bois en utilisant un test de cisaillement des blocs de bois déjà précomprimés. Les résultats indiquent que la compression radiale a peu d'effet sur les propriétés de cisaillement quand la déformation de compression est inférieure à 50%. Au-delà, les propriétés de cisaillement tombent rapidement, indiquant des dommages significatifs dans la matrice du bois. Les conditions de précompression ont également une influence significative sur les caractéristiques du cisaillement. En fait, les changements des propriétés de cisaillement du bois sont fortement associés avec l'énergie spécifique de compression dans le processus de précompression.

L'observation à l'aide d'un microscope électronique à balayage «SEM» indique que les réponses des fibres sont pareilles suite aux les compressions radiales et tangentielles, et que le clivage longitudinal des fibres est une conséquence des compressions transversales. Pour la compression radiale à déformation élevée, le spécimen est modifié à quatre niveaux: le relâchement de la matrice du bois; l'affaiblissement des interfaces entre les différentes couches de la paroi cellulaire (P/S_1, S_1/S_2); le bris des liens entre les micro-fibrilles dans la couche S_2; et la flexibilisation des fibres. De plus, les conditions de précompression jouent également un rôle important dans le processus, par exemple, la compression à basse température favorise des ruptures entre S_1/S_2 et dans la couche S_2, tandis que la compression à haute température (120°C) en combinaison avec une haute déformation (> 50%) favorise la modification structurale des fibres de bois d'été.

En somme, cette étude suggère que la compression mécanique avec une grande déformation (> 50%) modifie le bloc du bois sous deux aspects. Premièrement, elle aplatit les fibres du bois et réduit considérablement la résistance transversale des fibres. Deuxièmement, elle modifie la microstructure de la fibre aux différents niveaux, qui peuvent prérégler le mode de séparation préférée des fibres. Ceci facilite le développement des propriétés des fibres, et rend le bois plus approprié pour la fabrication d'une pâte mécanique de qualité améliorée. Ces deux effets peuvent potentiellement changer le processus de raffinage, c'est-à-dire d'un processus de fatigue à un processus plus efficace de séparation, et peuvent donc finalement aboutir à une amélioration de la qualité de pâte et une économie d'énergie de raffinage.

Mots-clés : *Picea glauca* (Moench) Voss (épinette blanche), compression, cisaillement, économie d'énergie, prétraitement thermique, sulfonation, rupture du bois, mécanisme de rupture, effondrement de fibre, séparation des fibres, microscopie électronique à balayage, microstructure, module de Young, contrainte, déformation, raffinage des copeaux, pâtes mécaniques.

RÉSUMÉ SUBSTANTIEL

La mise en pâte mécanique a été bien développée pendant les trois dernières décennies, et dû à ses propriétés d'impression supérieures (rendement élevé, bouffant élevé et opacité élevée), l'utilisation de la pâte mécanique dans la fabrication du papier impression s'élargit de plus en plus. Cependant, la consommation d'énergie élevée au cours du raffinage des copeaux demeure un inconvénient majeur limitant une expansion plus large de cette technologie.

De nombreuses recherches ont été réalisées visant à l'amélioration des qualités des pâtes mécaniques et à l'économie d'énergie de raffinage. En général, les stratégies principales sont:

1. Nouveaux procédés (par exemple, la mise en pâte par extrusion de Bi-Vis, la bio-mise en pâte, etc.)

2. Optimisation du procédé de raffinage (par exemple, HTHC-RTS, Thermopulp ™, etc.)

3. Traitement des copeaux (par exemple, traitements chimique, mécanique, thermique et biologique)

Ces stratégies sont réussies à un certain niveau. Toutefois, il n'y a aucune percée au niveau de l'économie d'énergie et de l'amélioration des propriétés de la pâte. Ainsi, la réduction de la consommation d'énergie du raffinage est toujours l'un des efforts techniques principaux dans l'industrie de mise en pâte mécanique.

Dans la mise en pâte mécanique, des copeaux sont transformés en fibres individuelles ou fragments des fibres. Bien que le mécanisme du raffinage ne soit pas complètement compris, on accepte généralement qu'il puisse être arbitrairement divisé en deux étapes: la séparation de fibres et le développement de fibres. Dans l'étape de séparation de fibres, des copeaux sont réduits en petites particules ou en faisceaux de fibres. A mesure que la séparation de fibres continue, l'épluchage des couches externes et la fibrillation

externe dominent le processus, développant les caractéristiques des fibres par les cycles de compression-décompression répétés entre les barres du raffineur.

En général, les caractéristiques finales de la pâte sont principalement déterminées par les conditions initiales de defibrage. La façon dont la matrice du bois se désagrège en fibres individuelles est en grande partie déterminée par l'état de la lignine avant, et au moment de la rupture. Par conséquent, le changement de la microstructure du bois par une compression mécanique et la modification des composantes du bois par des produits chimiques avant le raffinage le faciliteraient. Avec un ramollissement thermique ou un traitement chimique tel que la sulfonation de la lignine, les fibres sont séparées dans la lamelle moyenne (ML). Mais ces fibres ont un potentiel relativement bas dans la fabrication du papier, car leur surface est riche en lignine, ce qui gêne l'efficacité des liaisons hydrogène. Physiquement, la structure de la fibre doit être modifiée pour augmenter la flexibilité, la conformabilité et la surface fonctionnelle pour la liaison interfibres.

Pour développer une qualité souhaitable des fibres, il est nécessaire d'enlever la lamelle moyenne, une couche hydrophobe constituée principalement de lignine, et les couches externes des parois des cellules telles que la paroi primaire (P) et probablement la couche S_1 de la paroi secondaire. En raison de l'orientation irrégulière des fibrilles dans la paroi P et de l'orientation presque perpendiculaire des fibrilles dans la paroi S_1, ces couches externes restreignent le gonflement de la couche S_2, réduisant ainsi la flexibilité et la facilité d'effondrement des fibres et, par conséquent, la liaison entre les fibres.

On sait que les régions entre la P et la S_1, et entre la S_1 et la S_2 sont les interfaces faibles dans les parois des fibres. Quand une force de compression est appliquée perpendiculairement à l'axe de la fibre, les forces de tension latérales sont créées dans la surface perpendiculaire de la force appliquée. Ces forces de tension produisent un déplacement latéral des fibres, causant la rupture entre elles. Entre-temps, les concentrations de contrainte s'accumuleraient également dans les parois des fibres, créant un mouvement relatif des diverses couches. En raison des différences dans les caractéristiques structurales entre les couches de la paroi cellulaire, des délaminations se produisent entre elles. Par conséquent, un prétraitement des copeaux qui ramolli la

lignine, et une délamination partielle des parois des fibres causée par la compression mécanique avant le raffinage, représentent une technologie de raffinage importante.

Des travaux récents conduits à l'Université du Québec à Trois-Rivières ont prouvé que la compression radiale des copeaux avant le raffinage peut réduire de manière significative l'énergie de raffinage et améliorer les propriétés de la pâte. En raison de ce résultat encourageant, il est de grand intérêt de faire de la recherche fondamentale sur le mécanisme de rupture du bois sous une force de compression et de cisaillement. Tout particulièrement, il est important de savoir comment et à quel niveau le bois est modifié par une charge de compression. Ceci peut nous éclairer pour réaliser une bonne séparation des fibres du bois et une délamination interne dans la paroi de la fibre.

L'objectif principal de ce travail est d'étudier le mécanisme de rupture du bois sous compression et cisaillement. Avec cette compréhension élargie, nous pourrions trouver une manière efficace pour réduire l'énergie de raffinage et améliorer la qualité de la pâte produite. Plus précisément, ce travail examine les caractéristiques de rupture de la structure du bois sous diverses conditions tels que la contrainte, la teneur en humidité, la température et la sulfonation. Les renseignements obtenus seront d'une grande valeur pour établir des stratégies afin de réduire l'énergie de raffinage, d'améliorer la qualité de pâte mécanique, et de mieux comprendre le mécanisme du raffinage.

La recherche effectuée inclut trois séries d'essais. La première série examine l'effet de la température sur la compression selon trois directions (radiale-R, tangentiele-T et longitudinale-L). La deuxième série étudie l'effet de la sulfonation sur la compression radiale (avec ou sans contrainte latérale) tandis que la troisième série évalue l'effet de la précompression des échantillons sur les propriétés de cisaillement du bois.

Une épinette blanche [*glauca de Picea* (Moench) Voss] de 65 ans provenant de la région du St.-Maurice dans la province de Québec a été employée dans cette étude. Des spécimens ont été préparés à partir de l'aubier contenant des cernes de croissance dans la bande externe de 50 millimètres. Pour l'expérimentation de la première et une grande partie de la deuxième série, des spécimens mesurant 10×10×10 mm (L×R×T), contenant 5 à 7 anneaux de croissance, ont été préparés de telle manière que les anneaux de

croissance soient parallèles au plan tangentiel. Pour la troisième série expérimentale, les spécimens étaient plus larges et mesuraient 11×15×28 mm (L×R×T). Tous les échantillons ont été sciés à une dimension appropriée, et ensuite polis à la dimension désirée à l'aide d'une machine de ponçage.

Des échantillons utilisés pour l'essai de sulfonation ont par la suite été cuits en phase liquide dans une lessiveuse de laboratoire de type M/K. Les essais de compressions étaient réalisés dans un système automatique d'essais de matériaux (Instron 4201). Les processus de déformation du bois sous compression étaient réalisés avec un dispositif spécial de compression et observés au moyen d'un microscope. Les surfaces de rupture des spécimens ont été caractérisées en utilisant un microscope électronique à balayage.

Dans la première série d'expériences, des blocs ont été comprimés dans trois directions (R, T, L) avec des variations de température de 22 à 140°C. L'effet de la température sur le comportement de rupture du bois dans la compression radiale, tangentielle et longitudinale a été examiné. Les résultats indiquent que le bois se comporte semblablement au cours des compressions radiales et tangentielles à diverses températures. Il passe successivement d'une étape d'élasticité à une étape d'élastoplasticité, et finalement à une étape de densification (rupture).

L'examen microscopique a indiqué qu'au début de la compression, seules les fibres de bois de printemps ont répondu au contrainte de compression dans les étapes élastique et élastoplastique. À l'étape élastique, on n'a observé aucun changement visible des échantillons. Cependant, les fibres de bois de printemps se sont effondrées successivement dans le premier plateau plastique. À la fin du premier plateau plastique, la plupart des fibres de bois de printemps étaient complètement effondrées avec leurs parois cellulaires intensivement ridées. Quelques fibres dans la zone de transition entre le bois de printemps et le bois d'été se sont également effondrées. Les fibres de bois d'été sont légèrement déformées à ce stade. Par conséquent, le module élastique et la contrainte du premier plateau (SP1) sont les propriétés des fibres de bois de printemps. Le SP1 reflète directement la résistance transversale à l'effondrement des fibres de bois de printemps.

Après le premier plateau plastique, la contrainte a augmenté rapidement. Lorsque la contrainte continue d'augmenter, un deuxième plateau de contrainte se produit à environ 60% de déformation. À ce stade-là, les parois cellulaires des fibres de bois d'été ont bouclé et les lumens des fibres ont diminué notablement. Nous avons cru que ce court plateau était provoqué par une rupture soudaine (ex. séparation des fibres) dans le spécimen. La contrainte de ce plateau (SP2) peut représenter la contrainte produisant une rupture initiale dans le spécimen ou une séparation des fibres dans le bois d'été.

Quand la déformation de compression a monté jusqu'à 70%, la force de cisaillement étendue a été créée entre les différentes couches de la paroi des fibres de bois d'été, produisant beaucoup de petites fissures ou de glissements de surface dans les spécimens. À ce moment-là, les fibres de bois d'été se sont effondrées intensivement et extensivement. La force requise pour l'effondrement des fibres de bois d'été était d'environ 10-15 fois plus grande que celle des fibres de bois de printemps.

Une compression transversale de grande déformation (70%) exige de l'énergie selon la température de compression, par exemple, 3,5-4,9 kWh/t et 0,6-0,7 kWh/t à 22°C et à 120°C, respectivement. Ces énergies représentent seulement 0,2% et 0,03% de la consommation d'énergie spécifique dans une pâte thermomécanique (PTM) typique. Cependant, le bois se comporte tout à fait différemment dans la compression longitudinale, il consomme beaucoup plus d'énergie de compression. La température de ramollissement de la lignine déterminée par les compressions selon différentes directions est autour de 90-100°C.

Le module d'élasticité (MOE), les contraintes de premier et deuxième plateau (SP1, SP2), de même que l'énergie spécifique (SCE) de compression pourraient être employés pour caractériser les comportements du bois sous compression. Parmi ces paramètres, la contrainte de deuxième plateau (SP2) est employée pour la première fois pour décrire la séparation des fibres à l'étape de densification. Les rapports entre ces quatre paramètres et la température suivent la loi d'Arrhenius pour les compressions dans les trois directions. En se basant sur nos essais, nous avons développé des groupes de modèles mathématiques pour décrire les propriétés physiques des blocs de bois soumis aux compressions selon différentes directions:

Pour la compression radiale (R^2 : 0.96-0.99):

$$RMOE = 0.378 \times e^{1833/T}$$
$$RSP1 = 0.0173 \times e^{1544.2/T}$$
$$RSP2 = 1.6977 \times e^{685.2/T}$$
$$RSCE = 0.1542 \times e^{1103.6/T}$$

Pour la compression tangentielle (R^2: 0.93-0.98):

$$TMOE = 0.2374 \times e^{1855.2/T}$$
$$TSP1 = 0.0141 \times e^{1652.8/T}$$
$$TSP2 = 1.7045 \times e^{636.9/T}$$
$$TSCE = 0.1705 \times e^{1017/T}$$

Pour la compression longitudinale (R^2: 0.92-0.98):

$$LMOE = 37.2742 \times e^{786.7/T}$$
$$LSYd = 0.3199 \times e^{1304.2/T}$$
$$LEYd = 0.0026 \times e^{1811.3/T}$$
$$LSCE = 0.0487 \times e^{1504.6/T}$$

Les résultats montrent que les valeurs prédites par les modèles s'accordent bien avec les valeurs expérimentales dans la plupart des cas. Ceci signifie que l'effet du ramollissement thermique peut être expliqué par le mouvement des chaînes de polymères des composants principaux du bois, soit la cellulose, les hémicelluloses et la lignine.

De plus, pour des compressions radiales et tangentielles, les courbes normales de compression à diverses températures s'adaptent dans une courbe unique dans les régions élastique et élastoplastique. Ceci indique l'influence prédominante de la structure tubulaire des fibres sur les comportements du bois dans ces deux régions. Toutefois, dans la région de densification, le bois se comporte tout à fait différemment à différentes températures. L'observation à l'aide du SEM confirme également cette même réponse des fibres dans les directions radiale et tangentielle. La séparation entre les interfaces de

la P/S_1, et de la S_1/S_2 était fréquente dû à la différence distincte dans l'orientation des fibrilles entre ces couches de la paroi cellulaire. Le clivage longitudinal des fibres s'est produit seulement à cause de la compression transversale.

Les modèles mathématiques généraux suivants ont été obtenus pour exprimer la contrainte dans la région élastoplastique des compressions radiale et tangentielle :

$$\sigma_r = 0.0173 \times e^{1544.2/T} \times \left[1 + 0.5112 \times \left(\frac{0.5}{0.58 - \varepsilon} - 1 \right)^{1.0297} \right]$$

$$\sigma_t = 0.0141 \times e^{1652.8/T} \times \left[1 + 0.2322 \times \left(\frac{0.5}{0.58 - \varepsilon} - 1 \right)^{1.3598} \right]$$

Le modèle se compose de deux facteurs indépendants: le facteur de température (T) et le facteur de déformation (ε). Ces modèles ont été employés pour la première fois en vue de prédire la résistance des fibres de bois de printemps à diverses températures. D'après ces modèles, la contrainte de compression exigée pour aplatir des fibres de bois de printemps au raffinage est d'environ 0,62-1,53 MPa. Cette résistance est beaucoup plus grande que la contrainte moyenne entre deux barres de raffineur (0,45 MPa), conduisant à une consommation d'énergie élevée lors du raffinage. Néanmoins, la précompression au taux de déformation élevée (70%), qui aplatit et sépare les fibres du bois, pourrait réduire la résistance transversale de la fibre de 70-85%, ce qui veut dire que la force de compression exigée pour effondrer une fibre précomprimée pourrait être substantiellement réduite à 0,25-0,32 MPa. Par conséquent, dans un raffinage des copeaux précomprimés, une force de compression moyenne de 0,45 MPa serait suffisante pour aplatir aisément la plupart de ces fibres. Cette approche de précompression peut potentiellement changer le procédé de raffinage d'un processus de fatigue en un processus plus efficace de séparation.

Dans la deuxième série d'expériences, on a utilisé un design expérimental CCD (Central Composite Design) pour réaliser des essais sur la sulfonation des échantillons à 15 niveaux (8,4-236,9 mmol/kg) de contenu en groupements sulfoniques. Les effets de la sulfonation sur le comportement du bois sous des compressions radiales (avec et sans

contrainte) ont été examinés. Des essais additionnels ont également été effectués afin d'étudier la différence entre le bois de printemps et le bois d'été lors de la sulfonation et de la compression.

L'analyse de RSM (Response Surface Method) a indiqué que la température est le facteur le plus influent au niveau de la sulfonation. Malgré leurs différences morphologiques, le bois de printemps et le bois d'été peuvent être sulfonés au même degré de contenu en groupements sulfoniques sous les mêmes conditions de cuisson.

La sulfonation diminue les propriétés mécaniques du bois telles que le module d'élasticité (MOE), l'énergie spécifique de compression (SCE), les contraintes du premier et du deuxième plateau de compression (SP1, SP2). Pourtant, il n'y a aucun changement fondamental de la forme de la courbe de compression des échantillons de bois entier (spécimen se composant de bois de printemps et de bois d'été) sous divers niveaux de contenu en groupements sulfoniques.

Les courbes normalisées de compression des échantillons sulfonés et celles des échantillons comprimés à diverses températures peuvent être adaptées dans une courbe unique représentant les régions élastique et élastoplastique. Ceci confirme une autre fois que les comportements élastiques et élastoplastique du bois sont principalement dépendants de la structure cellulaire des fibres du bois. L'augmentation de la température de compression ainsi que du contenu en groupements sulfoniques diminue toutes les propriétés physiques étudiées (MOE, SP1, SP2, SCE). Cependant, les mécanismes de ramollissement sont différents: le ramollissement thermique, qui est réversible, est le résultat des ajustements des mouvements des chaînes de polymères de tous les composants du bois. Le rapport entre les propriétés physiques et la température suit la loi d'Arrhenius. Au contraire, la sulfonation est une modification chimique irréversible des composants du bois, en particulier de la lignine. Dans ce dernier cas, les propriétés physiques du bois diminuent linéairement avec l'augmentation du contenu en groupements sulfoniques.

Une comparaison systématique des compressions radiales (avec et sans contrainte) a été faite sur des échantillons sulfonés. Les résultats indiquent qu'avec une basse

déformation (inférieure à 50%) les échantillons ont répondu pareillement dans les deux types de compression (avec ou sans contrainte): les modules d'élasticité (MOE) et la contrainte du premier plateau (SP1) sont semblables dans les deux cas. À l'inverse, quand le taux de déformation excède 50%, où l'expansion latérale de l'échantillon se produit de façon significative, les échantillons se comportent différemment entre les deux sortes de compression. Quand les échantillons sont comprimés sans contrainte, un bref deuxième plateau de contrainte se produit à environ 60% de déformation. À ce moment-là, la séparation des fibres a lieu en raison de l'expansion latérale excessive. Au-delà de ce point, la contrainte augmente de nouveau avec l'augmentation du taux de déformation. Ce deuxième module (MOE2) diminue linéairement avec l'augmentation du contenu en groupements sulfoniques. Par contre, un tel deuxième plateau n'existe pas quand l'échantillon est comprimé avec contrainte. La contrainte augmente alors rapidement dans la région de densification. Évidemment, l'apparition du deuxième plateau de contrainte et le changement de module (MOE2) à ce stade sont contrôlés par la contrainte qui limite l'expansion latérale des échantillons sous compression.

La compression individuelle des échantillons de bois de printemps et de bois d'été indiquen que ces deux types de bois (fibre) se comportent différemment. Les courbes de compression pour le bois de printemps montrent un plateau plastique prolongé à cause de l'effondrement et du déplacement latéral des fibres de bois de printemps. Par contre, ce plateau plastique prolongé n'est pas évident dans le cas du bois d'été, ce qui suggère que l'effondrement des fibres de bois d'été a eu lieu plutôt de façon progressive.

La compression radiale d'un bloc de bois indique que les propriétés mécaniques du bois sont contrôlées par les caractéristiques morphologiques cellulaires. La rupture mécanique suit alors la théorie du faible-lien dans la structure du bois. Dans le bois entier, le bois de printemps constitue une zone faible où les fibres sont grandes et à parois minces en comparaison avec celles dans la zone de bois d'été; les fibres d'été ont en effet une paroi cellulaire très épaisse et un diamètre relativement plus petit.

Par conséquent, nous prévoyons que le bois de printemps absorbe la majorité de l'énergie de compression et s'effondre ensuite dans la zone plastique prolongée bien avant la rupture du bois d'été. Ceci pourrait fort bien arriver au cours du raffinage où les

fibres de printemps subissent plus de fragmentation par rapport aux fibres de bois d'été. Par ailleurs, on pourrait s'attendre qu'au cours d'un raffinage de copeaux de différentes densités, ceux de basse densité devraient être rupturés de façon différente de ceux de haute densité comme c'est le cas pour le bois de printemps et le bois d'été au cours d'une compression statique.

Dans la mise en pâte chémicomécanique ou chémicothermomécanique, les copeaux ont subi un changement crucial de leurs propriétés mécaniques, mais leur comportement au raffinage serait tout à fait différent dépendant du traitement chimique. La sulfonation du bois de printemps et du bois d'été favoriserait une meilleure séparation des fibres dans le raffinage (comme dans les procédés CMP et CTMP), minimisant ainsi le dommage des fibres, en particulier les fibres celui des bois de printemps. Par conséquent, le ramollissement thermique ou chimique de la matrice du bois rend les fibres (bois de printemps et bois d'été) plus flexibles, fournissant une meilleure distribution d'énergie de raffinage.

Dans la troisième série d'expériences, les effets de la compression sur l'affaiblissement de la matrice du bois ont été quantitativement évalués par des essais de cisaillement des blocs de bois précomprimés. Les résultats indiquent que le degré de déformation permanente des blocs provoqué par la compression transversale est affecté par la température de compression et par le contenu en groupements sulfoniques. Ainsi la compression à 80°C est celle qui produit la plus grande déformation permanente. D'un autre côté, les spécimens sulfonés ont la plus basse déformation permanente.

Généralement, la compression radiale a peu d'effet sur les propriétés de cisaillement si le taux de déformation est inférieur à 50%. Au-delà de ce taux de déformation les propriétés de cisaillement chutent brusquement, indiquant des dommages structuraux significatifs dans le bois de printemps et le bois d'été. Les conditions de précompression ont aussi une influence significative sur les caractéristiques du cisaillement du bois; la sulfonation étant la plus importante d'entre elles. Cependant, dans toutes les circonstances, les propriétés de cisaillement du bois tels que le module de cisaillement, la contrainte de fléchissement de cisaillement, la contrainte maximum, et l'énergie de

fléchissement sont fortement associées avec l'énergie spécifique de compression consommée par les spécimens dans les processus de précompression.

L'observation au moyen de la microscopie électronique à balayage (SEM) indique que les réponses des fibres sont pareilles lors des compressions en directions radiale et tangentielle, tandis que les clivages longitudinaux des fibres ont été créés seulement par la compression transversale. La SEM indique également que la compression à grand taux de déformation modifie le bloc du bois à quatre niveaux possibles: relâchement de la matrice du bois; affaiblissement d'endroits entre les différentes couches de la paroi cellulaire (P/S_1, S_1/S_2); bris des liens entre les micro-fibrilles dans la couche S_2; et finalement assouplissement des fibres. Il est à noter que les conditions de précompression jouent également un rôle important. Par exemple, la compression à basse température favorise des ruptures entre S_1 et S_2 de même que dans la couche S_2, tandis que la compression à haute température (120°C) et au taux de déformation élevée (> 50%) favorise quant à elle la modification des fibres de bois d'été. Tous ces effets de précompression peuvent mener finalement à une économie de l'énergie de raffinage et une amélioration des propriétés de la pâte.

La technique des tests de cisaillement développée dans cette recherche peut être utilisée de façon satisfaisante pour évaluer l'affaiblissement structurel d'une matrice de bois produite par une compression radiale statique. Elle peut aussi être une bonne méthode pour l'évaluation de l'affaiblissement du bois sous des compressions semblables tels que les processus de la fatigue et de compression cyclique du bois.

En somme, cette étude suggère que la compression statique avec un grand taux de déformation (> 50%) modifie le bois sous deux aspects. Premièrement, elle aplatit les fibres, ce qui réduit considérablement leur résistance transversale. Deuxièmement, elle modifie la microstructure de la fibre à différents niveaux qui peuvent ensuite prédéterminer le mode de séparation des fibres au cours du raffinage. Ces modifications faciliteraient le développement des propriétés des fibres, en rendant le bois plus approprié pour la fabrication d'une pâte mécanique de qualité améliorée. Par conséquent, la précompression du bois avant de le raffiner peut potentiellement changer le procédé de raffinage d'un processus de fatigue en un processus plus efficace de

TABLE OF CONTENTS

LIST OF FIGURES

LIST OF TABLES

LIST OF SYMBOLS & ABBREVIATIONS

APMP	Alkaline Peroxide Mechanical Pulping
Car.	Carboxylate
CCD	Central Composite Design
C_s	Sulfonate Content, mmol/kg
CSF	Canadian Standard Freeness, mL
CML	Compound Middle Lamella
CMP	Chemimechanical Pulping
CTMP	Chemithermomechanical Pulping
CV	Coefficient of Variance, %
E	Active Energy, KJ/mol
E_t	Shear Total Energy, J
EW	Earlywood
E_y	Shear Yield Energy, J
FSP	Fiber Saturation Point
G	Shear Modulus, MPa
GW	Stone Ground Wood
HC	Hemicelluloses
HTHC	High-temperature/High-compression Pretreatment
IC	Inter-cell
IW	Intra-wall
KCL	Finnish Pulp and Paper Research Institute
L	Longitudinal direction
LCC	Lignin-Carbohydrate Complex
LEY_d	Yield Energy at Longitudinal compression, J
LSY_d	Yield Stress at Longitudinal compression, MPa
LW	Latewood
LWC	Light Weight Coated grade
MOE	Modulus of Elasticity (Young's Modulus, MPa)
P	Primary Wall
R	Radial Direction

RL	Radial-Longitudinal Plane
RS	Restraint (Compression)
PGW	Pressurized Stone Groundwood
RMP	Refiner Mechanical Pulping
RSM	Response Surface Method
RTS	Residence Time–Temperature–Speed
S_1	Outer Layer of Secondary Wall
S_2	Middle Layer of Secondary Wall
S_3	Inner Layer of Secondary Wall
SCE	Specific Compression energy (Energy/Sample Volume, KJ/m^3)
SCA	Super Calendar Grade A
SEC	Specific Energy Consumption
SEM	Scanning Electron Microscopy
SP1	First Plateau Stress, MPa
SP2	Second Plateau Stress, MPa
STFI	Swedish Pulp and Paper Research Institute
T	Tangential Direction or Absolute Temperature
T_c	Temperature in Celsius
TL	Tangential-Longitudinal plane
TMP	Thermomechanical Pulping
TW	Trans-wall
W/G	Water Glycerol Mixture
c	Strength Coefficient
m	Strain Hardening Coefficient
σ	Compression Stress, MPa
σ_n	Normalized Compression Stress, MPa
ε	Compression Strain, %
τ_y	Shear Yield Stress, MPa
τ_{max}	Shear Maximum Stress, MPa

Chapter 1 - Introduction

1.1 Background

Mechanical pulping has been well developed during the last three decades or so, and is now a mature technology. It appears that the development of mechanical pulping went through a rapid increase in design production from 1974 to 1987, and a relatively slow development since 1988 (Figure 1.1) [1]. In 2000, the global design capacity of thermomechanical pulp (TMP) and associated high-yield pulp was about 41 million tons

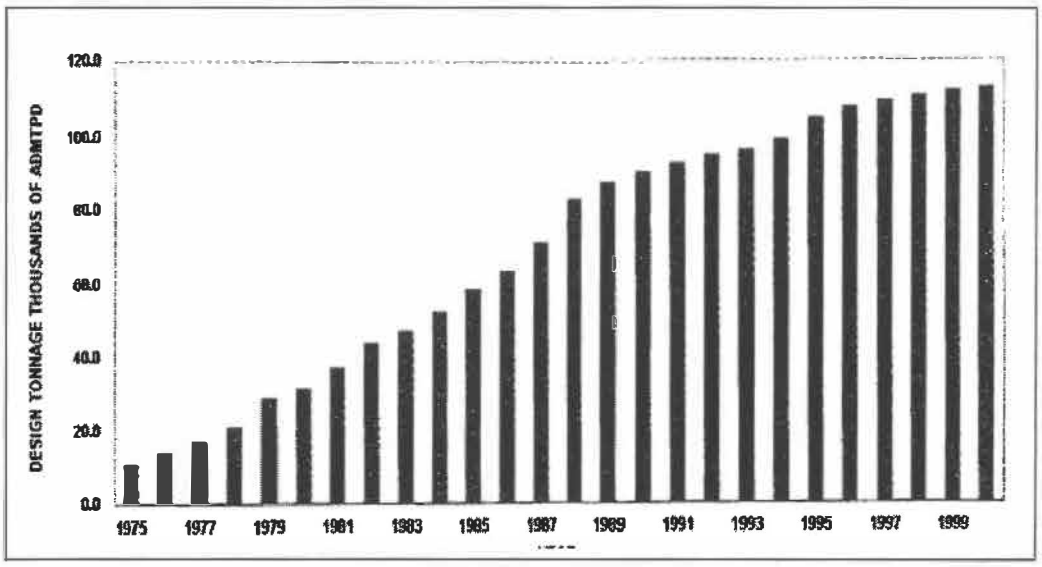

Figure 1.1 Cumulative daily production from 1975 [1]

per year. The world mechanical pulp production reached its peak of 42.4 million tons in 1999, and experienced a little decline in recent years (Table 1.1). In Canada, mechanical pulp production varied from 10.2 to 12.3 million tons in last decade, representing about 45% of total pulp [2].

There are two main factors that are responsible for the relatively slow growth of mechanical pulp in recent years. First, yellowing or color reversion of lignin-rich mechanical pulps limits its usage in high-value printing and writing grades. However, the successful use of a ultra-violet absorber and a radical scavenger [3], could lead to a breakthrough in overcoming such a problem. Second, the high energy consumption in

chip refining remains another major drawback restricting a wider expansion of this technology, particularly in regions where the cost of electrical power is exorbitant. The specific energy consumption for TMP is about 2-3 MWh/ton, which is considerably higher than that of groundwood (GW) and pressurized groundwood (PGW), about 1.5-2.5 MWh/ton, as Figure 1.2 shows [4]. The energy requirement can be as high as 3.5 MWh/ton for the pulp of TMP used in top quality magazine paper [5]. Therefore, reducing the energy consumption in refining remains one of the main technical development efforts in the mechanical pulping industry [6].

Table 1.1 Pulp production from 1991 to 2001 (million tones) [2]

Year	1991	1992	1993	1994	1995	1996	1997	1998	1999	2000	2001
Canada:											
Mech. pulp	10.65	10.21	10.59	11.00	11.55	10.97	11.40	10.48	11.22	12.29	11.41
Total pulp	23.33	22.84	22.90	24.65	25.40	24.35	24.97	23.60	25.40	26.41	24.92
World:											
Mech. pulp	34.71	33.31	33.47	34.92	36.60	34.68	35.48	41.92	42.39	37.12	34.72
Total pulp	162.4	164.1	162.5	166.7	174.3	174.0	178.2	176.1	179.1	188.7	179.4

In mechanical pulping, wood is treated under extreme conditions to produce a papermaking pulp [7]. The mechanism of refining, although not completely understood, is widely accepted that it may be arbitrary divided into a fiber separation stage and a fiber development stage [8, 9, 10, 11]. In the fiber separation stage, chips are reduced to small particles or fiber bundles. As the fiber separation continues, peeling of the outer layers and external fibrillation dominate the process [10], developing the papermaking characteristics of fibers through repeated compression-decompression cycles between refiner bars. These two stages are not distinct; they overlap in practice. Atack et al. [7, 8] regarded the refining process as a "highly specialized attrition process in which the objectives are to produce 'debris' with certain physical characteristics". They believed that some kind of fatigue failure mechanism is involved in the process of fiber separation. Refining is also considered as a cooperative process in which a large part of the energy is consumed in mixing, that is, creating new configurations [12].

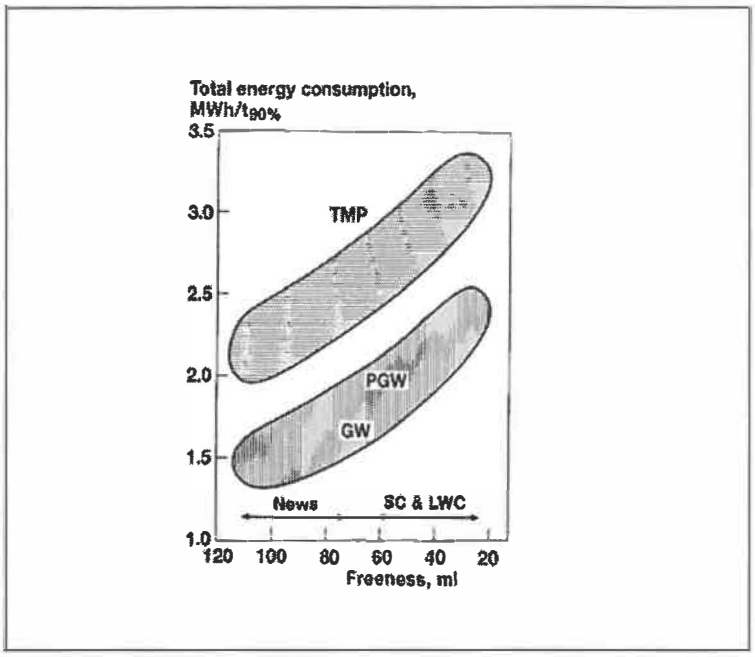

Figure 1.2 Total electric energy consumption for GW, PGW, and TMP as a function of freeness and end use, Norway spruce [4]

There are two principal elements that involved in a refining process: wood and refiner. They both influence the energy consumption and pulp properties (Figure 1.3). Thus, to improve the energy efficiency one must understand the behavior of raw material in refining and optimize the process. The fundamentals of refining and the characteristics of wood will be discussed in chapters 2 and 3, respectively.

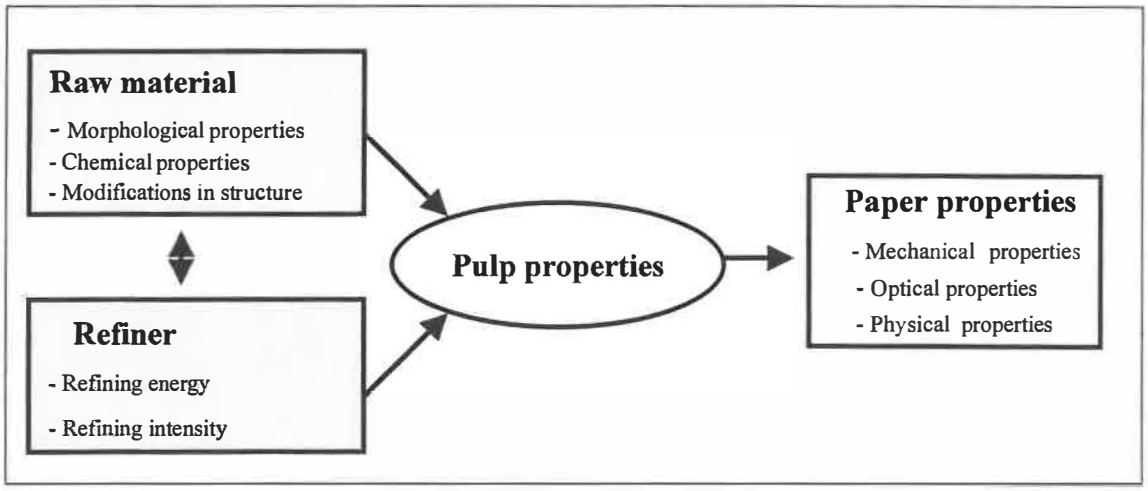

Figure 1.3 Factors affecting pulp and paper properties

1.2 Means for Reducing Refining Energy

Extensive research aiming at reducing the refining energy has been conducted during the last two decades. Pearson [9] stated that "It will be impossible to greatly reduce the energy of mechanical pulping once efficient use has been established". However, Sundholm [4] estimated that energy reduction by 40-60% is possible, and suggested that "In the long term, some sort of compressive pretreatment or enzyme treatment could be part of a new energy–efficient technology." Efforts are made in this area at the Finnish Pulp and Paper Research Institute (KCL) which launched a series of programs aiming at improving energy efficiency in mechanical pulping [13, 14]. Recently, the KCL and Swedish Pulp and Paper Research Institute (STFI) joined forces in a 3-year mechanical pulp research program [1]. They focus on two major areas: development of mechanical pulping processes with minimum energy consumption and utilization of mechanical pulp for optimum cost performance. So far, no real breakthrough has been made. Hence, the high energy consumption remains one of the major technical barriers in mechanical pulping. Generally, the main strategies in reducing energy consumption may include:

1. New processes (e.g. Bi-Vis extrusion pulping, biopulping, etc.)

2. Optimization of refining process (e.g. HTHC-RTS, Thermopulp^{TM}, etc)

3. Pretreatment of chips (e.g. chemical, mechanical, thermal and biological)

1.2.1 New processes

Some promising advances have been made during the past decades. For instance, many new processes had emerged, including the Bi-Vis screw extruder [15], the reciprocating apparatus [16], fungal or enzymatic treatment [17, 18], and explosion pulping [19, 20]. The Bi-Vis extruder utilizes compression and shear forces to fiberize the chips. However, the fiberized mass requires a subsequent refining to produce an acceptable pulp. It was claimed that 30% saving in specific energy could be achieved by this technique [15]. Despite these efforts, there has been no real breakthrough.

1.2.2 Optimization of refining process

Energy saving and better pulp quality can be obtained by optimizing the refining process. In the Multistage process developed at KCL [21], refining is conducted in three stages; each stage uses a different refining speed (e.g., 2000, 1800, and 1500 rpm, respectively) and a different temperature (e.g., 165, 140, and 100°C, respectively). The process configuration results in energy saving of 10%-15% and lower shive content and improved tensile strength.

The Thermopulp™ process of Metso Corporation (former Sunds Defibrator) [22] operates with a conventional low-temperature/low-energy primary stage (600 kWh/t) and a high-temperature (160-170°C) second stage. The high temperature in the second stage improves fiber flexibility and enables the fiber to develop its papermaking quality more rapidly. It was claimed that this process resulted in an energy saving up to 10-20%.

The RTS (Residence time–Temperature–Speed) process of Andritz-Sprout Bauer Inc [23] uses a short residence time, and a high temperature and a high rotational speed in the primary stage. As reported, this process reduces the specific energy by 6-12%. It was also reported that using new plate segment geometries, such as unidirectional plates [24] and LE-segments (Valmet, now Metso paper) [25], could result in an energy saving by 13% and 10%-20%, respectively.

These modified processes were successful to a certain degree in reducing the energy requirement. However, they have some drawbacks. For example, the high temperature leads to decreased brightness, and high rotation speed causes fiber cutting and other problems. There still remain many technical obstacles in the way for achieving the anticipated potential of 50% energy reduction while still meeting the rising end-product demands. These obstacles could be overcome through further fundamental researches on raw material and processing equipment.

1.2.3 Pretreatment of chip

Any pretreatment of chips that weakens the cell wall or modify the wood components may allow refining to take place more readily and produce stronger pulps by providing more favorable conditions for energy absorption [26]. These pretreatments include chemical, thermal, mechanical, and biological actions. It was believed that some kinds of compressive or enzyme pretreatments that modify wood chips before the refining could be part of a new energy-efficient technology.

1.2.3.1 Chemical Pretreatments

Mild chemical treatments are used to improve the physical properties of pulps. The common treatment chemicals employed include sodium hydroxide, sodium sulfite, and alkaline/hydrogen peroxide. Depending on the degrees of treatment and the chemicals used, the mechanical pulps can be categorized as chemimechanical (CMP) or chemithermo-mechanical (CTMP) or alkaline peroxide mechanical pulp (APMP).

1. Alkali (NaOH) pretreatment

In alkali pretreatment low concentrations of sodium hydroxide (0.25-2.5%) [27] are used at temperature generally between 20 and 30°C. The impregnation times vary from 15 to 120 min. The treatment is followed by a refining stage to produce a usable pulp.

The alkali treatment may involve in hydrolysis of pre-existing esters or lactones of hemicelluloses [28]. Acidic group content of the pulp could be substantially increased by such a treatment. The counter-ions of the acidic groups draw additional water into the cell wall, increasing the swelling capacity of fibers. In a mild alkali treatment, the main reaction is deacetylation of hemicelluloses. The reaction may cause a weight loss of the treated chips by 3-10%, and bond breakage between the lignin and hemicelluloses [29, 30]. These chemical modifications of the hemicelluloses weaken the wood matrix, facilitating the mechanical separation of fibers in refining. The main disadvantages of alkaline pulps are poor brightness and low opacity. These drawbacks can be overcome by an addition of a bleaching agent such as hydrogen peroxide in the system [30, 31]. The effectiveness of this

approach is evidenced by the success of a relatively recent process called alkali-peroxide mechanical pulping (APMP) [32, 33, 34, 35].

2. Sulfite pretreatment (Na_2SO_3)

Sodium sulfite is one of the most common agents used in mechanical pulping such as in CTMP and CMP. The sulfite treatment or sulfonation softens the lignin in wood. Thus, it reduces the shear modulus of the treated wood, and flexibilizes fibers [36]. In sulfonation, hydrophilic sulfonic acid groups are introduced to the hydrophobic lignin, rendering it hydrophilic and flexible. As a result, sulfonation facilitates fiber separation, particularly in the middle lamella, minimizing the adverse effect of fiber shortening during refining. According to [37], there are 3 reactive lignin groups defined as X, Z, and B groups, as shown in Figure 1.4. The B group can only be sulfonated in strong acidic conditions (pH: 1 to 2). The most common groups are of X and Z types which can be sulfonated at pH 4 to 9. Figure 1.5 depicts the major sulfonate reactions of lignin [38]. Kinetic studies indicated that the X group reacts relatively fast, whereas the Z group reacts relatively slower. Thus, it may be assumed that X group can be sulfonated in relatively gentle conditions such as those used in the CTMP, and both groups of X and Z types can be sulfonated in more severe conditions such as those used in the CMP. Whereas, the B type will not be sulfonated in both CTMP and CMP processes. Table 1.2 shows the typical pulping conditions for CMP and CTMP.

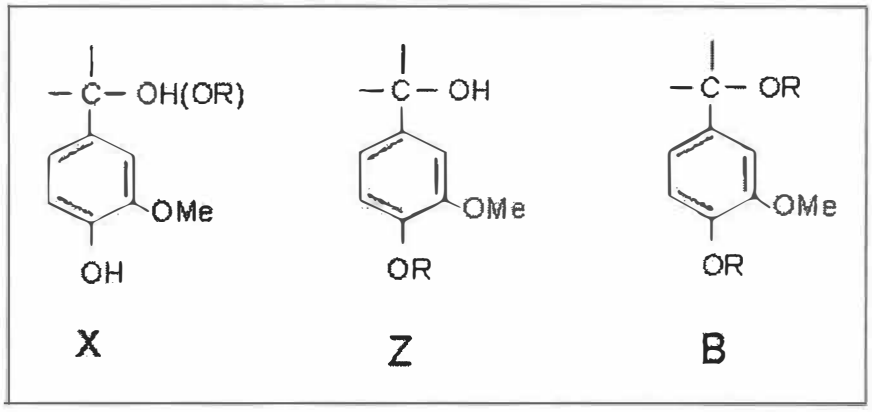

Figure 1.4 Different basic groups in lignin that can be sulfonated under suitable conditions

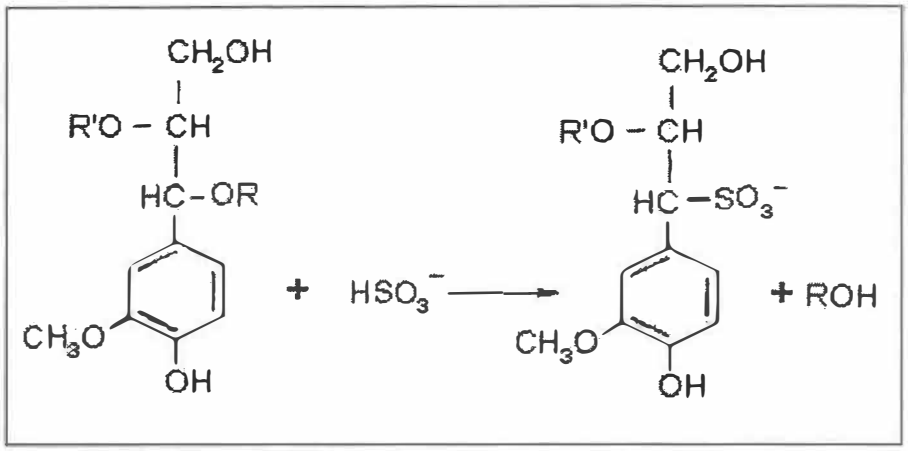

Figure 1.5 The reaction introducing sulfonate groups into lignin

Table 1.2 Typical pulping conditions for CTMP and CMP [39]

Process/ Species	Atmospheric steaming, min	Chemicals, %	Preheating time, min	Temp., °C	Unbleached pulp yield, %
CTMP					
Softwood	10	1-5% Na_2SO_3	2-5	120-135	91-96
Hardwood	10	1-3% Na_2SO_3 + 1-7 % NaOH	0-5	60-120	88-95
CMP					
Softwood	10	12-20% Na_2SO_3	10-60	140-175	87-91
Hardwood	10	10-15% Na2SO3	10-60	130-160	80-88

The degree of sulfite treatment can be determined by measuring the sulfonate content of the pulp. In general, the sulfonate content of pulp is about 0.24-0.75 % for CTMP and about 1-2% for CMP. The level of sulfonation is affected by the treatment temperature and its relationship with the latter is shown in Figure 1.6 [40]. Softening of lignin and partial dissolution of lignin and carbohydrates weaken the middle lamella and make the fiber walls flexible and less brittle. This chemical modification could affect the mode of fiber rupture in refining (Figure 2.3) and influence the development of fiber properties.

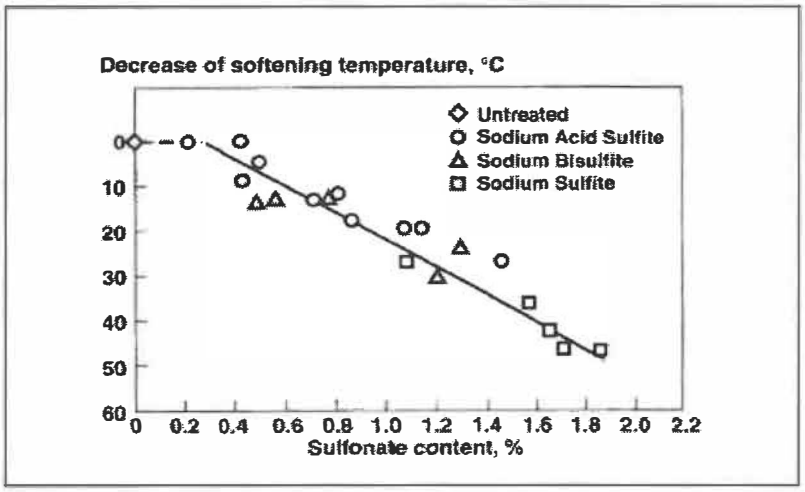

Figure 1.6 Softening temperature reduction of residual lignin in black spruce as a function of the degree of sulfonation [40]

1.2.3.2 Thermal Pretreatment

It was reported that [41] steaming of chips at elevated temperature increases the crystallinity of cellulose, and causes cleavage of hydrogen bond and lignin-hemicelluloses linkages. As shown in [42], steaming also increases the solubility of hemicelluloses, the accessibility of cellulose, and the modification of lignin. Further, it increases the permeability by weakening the pit membrane [43]. Evidently, steaming can improve the refining efficiency and the pulp quality. Although high temperature steaming in refiner housing provides improved strength properties of TMP [44] but it negatively affects the pulp brightness [45]. Therefore, the time for high temperature steaming should be kept as short as practical.

1.2.3.3 Biological Pretreatment

Biological treatment of chips prior to refining (bio-mechanical pulping) has advanced significantly in the past decade or so [26]. The principle of biotreatment is to use a natural fungus (e.g. ligninase) to degrade the lignin in wood. Once the lignin, which is the cementing agent in wood, is degraded or weakened or disintegrated, the cellulosic fibers can be readily separated in refining. The fungal treatment involves in enzymatic

softening and swelling of the cell wall, thinning and fragmentation of the cell walls in localized areas, as reported in [46]. White-rot fungus is the most effective lignin-degrading medium. The most commonly studied species include *Phaneorchaete chrysosporium* [46, 47], *Ceriporiopsis subvermispora* and *Phlebia subserialis* [26].

As anticipated, the bio-treatment substantially lowers the electric energy consumption in refining, improves certain strength properties, and reduces the environmental impact. A 33% saving in refining energy could be obtained for chips after 2-week incubation [26]. In chemical pulping (e.g. Kraft process), the fungal pretreatment of chips reduces pitch content and the active alkali requirement by up to 18%. Additionally, the sulphidity requirement is also decreased by up to 30%, and the cooking time by up to 33%. The pulp quality is also significantly improved in terms of bleachability, brightness gain and strength properties [48].

The main drawback of fungal pretreatment is time-consuming (2-4 weeks). For economical reason, it is imperative to enhance the treatment technique to reduce the required incubation period. It was suggested that a precompression stage before fungal treatment might accelerate the bioreation [11, 47].

1.2.3.4 Mechanical Pretreatment

Interests in wood compression in relation to mechanical pulping grew increasingly during the last two decades or so. The researches are focus in two aspects: wood compression in related to refining and basic theoretical researches.

1.2.3.4.1 Wood compression and refining

It was believed that the breakdown of wood matrix during mechanical pulping is a fatigue process, and that high temperature, high stress amplitude and high frequencies favor the structural breakdown of wood, but not necessary benefit the final pulp properties.

Plug-screw pressing is currently used to pretreat chips prior to refining. However, as reported by Murton [49], screw pressing of chips did not yield significant differences in

energy saving or pulp quality when compared to the conventional TMP if the compression ratio is relative low (e.g. 3:1). With this compression ratio, an average strain for chips is only about 16.5% (see Table 4.2). Other works [50, 51] showed that higher compression ratios significantly improve chemical impregnation, leading to higher fiber flexibility and pulp strength. But high compression ratio (e.g. 5:1) causes noticeable fiber breakage, resulting in reduced fiber length.

To minimize fiber damage, a combined high-temperature/high-compression (HTHC) pretreatment of chips has been incorporated in the RTS process of Andritz Inc. [52, 53, 54]. It was found that the HTHC-RTS process (compression ratio: 5:1) reduced the specific energy consumption (SEC) by 440-550 kWh/t for northeastern spruce and Norway spruce when compared with a baseline TMP, meaning an energy saving of about 20%. The HTHC-RTS process also produces pulps of increased sheet density, tear index, tensile index, opacity, brightness and light scattering, and reduces shives. Recently, Andritz introduced RT – Fiberizer^{TM} (RTF) to replace HTHC press [55]. The method involves a gentle separation of fibers in wood chips using a combination of pressafining and refining actions in a pressurized environment. This pretreatment resulted in 10-14% reduction in energy consumption compared to control high-intensity pulp. Since the method separates fibers prior to refining, the effect of compression on fiber is quite low. Hence, its potential use in improving fiber properties remains questionable.

Axial compression of wood blocks [74] prior to refining could also result in substantial energy savings, for example 9% for TMP and nearly 40% for CTMP. But this compression is not practical in reality, and may also cause excessive fiber damage in high compression ratio.

Obviously, all these compression methods are limited by the compression ratio. High compression ratio benefits the energy saving, but leads to more fiber damage, and produces short fiber and more fines in final pulp, which is detrimental to pulp properties.

Meanwhile, static mechanical compression of softwood chips [56, 57, 58] causes fiber separation between the primary wall (P) and the S_1 layer of the secondary wall or

between the S_1 and the S_2 layers. The precompressed chips produced TMP (100-200 ml CSF) with 18-25% less specific energy consumption (SEC) when compared with the untreated chips, while the SEC saving for the screw-pressed chips was 10-20%. Considerable improvement in paper properties was also observed for platen-pressed chips such including:

- ~13% increase in long fiber (R28 + R48).
- ~15% and 19% increase in tensile index and TEA.
- ~8% and 11% reduction in fiber coarseness for R28 and R48 respectively.

These works show that static compression is more advantageous than the screw pressing. However, the compression ratio, and the energy consumption in platen compression were not presented in these works. In light of these interesting findings, further basic researches in this area are worth pursuing.

1.2.3.4.2 Basic research on wood compression

Wood is very complicated physically and chemically (as discussed in chapter 3). Wood fibers response differently under compression in different conditions. Therefore, the compression conditions are critical in determining the wood behaviors. These conditions include compression directions, compression speed, temperature, compression strain, sample moisture content, density and wood species.

1. **Effect of loading directions on wood compression**

Many works have been conducted on radial [59, 60, 61, 62, 63, 64, 65, 66, 67] and tangential directions [68, 69, 70, 71]. Longitudinal compression of small specimens received relatively less attention [72, 73, 74, 75].

Table 1.3 summarizes main results of these works. The results indicated the physical properties vary greatly between species. For the same species, modulus in radial direction is higher than that of tangential in most cases, but the relationship is reversed for jack pine and *Pinus radiata*. This is the same for yield stress. The stresses for these

two directions remain at the same level in most cases, but a huge difference was observed for jack pine. For longitudinal direction, the modulus and plateau stress is much higher than that of radial and tangential directions. The difference is due to the difference in fiber orientation in axial and transversal directions. As discussed later, many factors affect the modulus and compressive stress. Therefore, simple comparison of these properties obtained by different authors may lead to erroneous conclusion.

Table 1.3 Modulus and yield stress of some wood species

Researchers (Speed)	Species	Sample,		Modulus, MPa (CV%)			Stress at 5%, MPa (CV%)		
		R×T×L mm	W/D	R	T	L	R	T	L
Renaud M. [68] Low	Birch	(Cylinder, R7×20)	W	470 (20.8)	270 (30.7)	2620 (24.0)	2.7	2.3	20.3
High				1800	1700	4900	19.5	19.7	85
			D	1260 (22.9)	780 (21.0)	5670 (19.9)	5.7	7.3	65.1
	Trembling aspen	(Cylinder, R7×20)	D	840 (26.5)	440 (33.4)	4900 (32.0)	3.6	3.1	51.4
Tabarsa T. [69] Low	White Spruce	8×8×8	W	139 (18)	104		2.9 (9)	4.96	
	Jack pine	8×8×8	W	83 (24)	153		1.7 (28)	10.9	
	Aspen	8×8×8	W	95 (17)			2.6 (14)		
Watanabe U. [70] (11Hz)	Pinus Radiata	22×2×1.5	W	400	900				
Ethington.R.L [71] (N.A)	Larch	20 ×50 ×150	15%				9.36 (17)	6.11 (17)	
Berg J.-E. [75] (6mm/min)	Norway spruce	20×20×20	W				2	2	12

* Tests were conducted at room temperature. Some data were got form plot graphs. W/D: water saturated or dry sample.

2. Effect of compression rate on wood compression

Compression speed is another parameter that has gained much attention [63, 68, 76, 77, 78, 79]. Since wood is a viscoplastic material, the strain rate has an important effect on the energy dissipation during loading. Wood morphology may also be an important

factor in relation to the effect of strain rate. The heterogeneous nature of wood structure can influence stress propagation in the material. However, the effect would only become important for the very high strain rates.

Researches indicated (Table 1.3) that high compression rate resulted in high modulus and plateau stress at all compression directions. The difference could be significant if liquid is present in fiber lumen. This is attributed to the inability of the liquid to flow out readily. High strain rate also generates localized damages and long cracks in specimen, particularly on the specimen surface. This suggests an inability to distribute applied stresses evenly in the sample at high strain rate. On the contrary, low strain rate develops small fissures evenly in the samples, and the EW fibers are collapsed uniformly. Thus, the compression rate should be set as low as practical to generate a reproducible and smooth stress-strain curve.

3. Effect of temperature on wood compression

Effect of temperature on wood compression has been discussed by many researchers [59, 60, 61, 62, 64, 74, 75, 80, 81]. Most of these works are conducted in radial direction. In many cases, glycerol was used as a heating medium when a temperature above 100 °C was used. Table 1.4 presents some results of these researches. As shown in the table, the plateau stress decreased steadily with increasing temperature. A total reduction of 76% was obtained when the temperature increased form 25 °C to 150 °C.

Table 1.4 Effect of temperature on plateau stress (10%) at radial compression [61]

Sample (W/G)	Temperature, °C	25	50	80	95	115	150
Water	Stress, MP	2.31	1.79	1.06	0.85		
	CV, %	3	4	7	2		
Ethylene Glycol	Stress, MPa	2.46	1.76	1.08	0.93	0.78	0.59
	CV,%	5	4	4	3	4	9

* Norway spruce, Sample size: 10×10×10 mm; test speed: 0.05 mm/min.

Berg et al conducted longitudinal compression on Norway spruce [75]. They obtained a mean compressive strength of 17 MPa when glycerol-impregnated samples were tested

at room temperature. This value decreased to 6.2 MPa when the temperature was raised to 120°C. It was further reduced to 4.0 MPa when the tests were carried out at 180 °C. The relative modulus was decreased by 75% when the temperature increased from room temperature to 180 °C. These results also show that the compressive strength and modulus remained fairly constant in three directions when moisture content is higher than 40%. It was believed that there is no effect on the strength and elastic modulus when the moisture content is higher than fiber saturation point (FSP), which is around 23-32% [75]. It was also recommended that the compression be carried out at temperature well below 120°C to achieve substantial changes in wood structure. Frazier et al. [74] also confirmed that pre-compression at low temperature (20°C) is desirable to improve pulp properties.

The decrease in the mechanical properties with increasing temperature is related to the increase in the mobility of the polymeric chains, particularly of the lignin which softens at about 90°C (1Hz), as explained by Dumail et al. [61]. However, there is no systematic research on the effect of temperature on the compression in three directions, especially in tangential and longitudinal directions. There is also no relation established between the temperature and the plateau stress or modulus.

4. Other considerations

Standard test method ASTM D143 was developed to test large wood specimens. However, for small specimens, other considerations should be considered to obtain reproducible results, especially in sample preparation. They include sample size, aspect ratio (height to width ratio of specimen), EW/LW ratio, density, relative annual ring direction, moisture content, surface quality, non-parallel surface and defects.

Wolcott et al. [82] demonstrated that the modulus in transversal compression increased with specimen height. Rough and non-parallel surface could lead to a decrease in modulus. On the other hand, the yield stress was not affected by these parameters.

In summary, owning to the lack of standard testing methods for small specimens most of the published results from different researchers are not comparable. For this reason, the understanding of the mechanism of wood rupture under compression remains unclear.

1.3 Objectives of the research

A literature survey indicates that any pretreatment that weakens the cell wall or modify the wood components may allow refining to take place more readily and produce stronger pulps by providing more favorable conditions for energy absorption. Our previous study also demonstrates that pretreatment of wood chips by static compression could be an effective way in improving refining efficiency and pulp quality [56, 57, 58].

The main objective of this work is to study the mechanism of wood failures under mechanical compression and shear. With this understanding, we might be able to find an energy-efficient way to achieve fiber separation and internal delamination, leading to energy saving and pulp quality improvement. More precisely, this work is intended to examine the characteristics of structural failures of wood under various conditions such as mechanical stress, moisture content, temperature and chemical treatments. Such information will be of a great value for reducing the current refining energy requirement and improving mechanical pulp quality. In this work the following three principal aspects will be examined:

1. The rupture behaviors of wood under compression in radial, tangential and longitudinal directions;

2. The effect of sulfonation on the wood behavior in radial compression;

3. The effect of pre-compression in radial direction on the shear properties of wood.

Justification: Wood is an anisotropic viscoelastic material, which is complicated physically and chemically. Wood fibers respond differently under compression in different directions. However, most published works were conducted in radial direction, using a relatively small compression strain (less than 50%). Our experiences indicate

that when the wood is compressed with a small strain, the total deformation is practically attributed to the collapse of the thin-walled earlywood fibers while the thick-walled latewood fibers are not affected [67]. In fact, the collapse and flexibilization of the latewood fibers are also essential in producing a good quality mechanical pulp.

Secondly, the behavior of wood under compression load is still unclear because little information has been reported other than the change in modulus. This property only reflects the elastic property of the specimens, and gives a little information on modifications in wood structure. Other parameters should be defined and employed to describe the wood's behaviors in different compression stages. The relationships between these parameters and compression conditions should also be established.

Further, despite its effectiveness in modifying wood properties, the influence of chemical pretreatment on wood compression receives little attention [83]. Sodium sulfite is one of the most common agents used in mechanical pulping such as in CTMP and CMP. Sulfonation introduces hydrophilic sulfonates to the hydrophobic lignin, rendering it hydrophilic and flexible. As a result, sulfonation facilitates fiber separation, and improves the collapsibility of wood fibers. Thus, a systematic study on the effect of thermal and chemical modification of wood on the compression would provide us with new information on the breakdown of the wood matrix.

Additionally, shear failure of wood is directly related to defiberation in refining [84, 85, 86, 87], but it has received little research attention. It is known that compression and shear are the two principal forces involved in chip refining. It would be of great interest to examine the effect of compression on the shear properties of wood. The nature of physical failure of the pre-compressed specimens should also be investigated.

The repeated compressive action of refining collapses the fibers and the shearing action of refiner bars fibrillates the fiber surface. The repeated compression and relaxation of the fibers disrupt the bonds between the compound middle lamella (CML) and the secondary wall, reducing the transverse stiffness of fibers. It is widely accepted that the final pulp characteristics are mainly determined by the initial defiberation conditions, and that the manner in which the wood matrix disintegrates into pulp fibers is largely

determined by the condition of the lignin prior to, and at the instant of fracture. Hence, mechanical compression and chemical modification of the wood components and micro-structure before refining would facilitate the refining process. Such treatments would improve energy absorption by fibres, yielding stronger pulps. Therefore, detailed studies on wood compression would provide us with a better understanding regarding the influences of compression directions, temperature, and chemical treatment on the failure characteristics of wood. Such information may shed some light on the mechanism of refining, and hopefully it might lead to a more energy-efficiency refining configuration.

Structurally, this thesis consists of seven other chapters. Chapter 2 and chapter 3 review briefly the nature of mechanical pulping and the characteristics of wood, respectively. Chapter 4 describes the experimental plan and the experimental procedures employed, while chapter 5 to 7 present the results and the discussions. Finally, chapter 8 gives a general conclusion.

Chapter 2 - Mechanical pulping

The purpose of all pulping processes is to liberate fibers from the wood matrix and process them into a usable furnish for papermaking. There are two major types of mechanical processes that are currently used in the pulping industry: wood grinding and chip refining. The scope of discussion within the framework of this study is, however, restricted to the latter.

2.1 Fundamentals of Refining

2.1.1 Characteristics of a refiner

A typical industrial refiner (for example, a single disk refiner) composes of a rotor and a stator within the refiner housing. The refining surface of a refiner plate consists of, in general, three sections: a breaker bar section located near the inlet of refiner (center of a refiner disk), a fine bar section on the disk periphery, and an intermediate section in between [88]. The basic design parameters of the refiner segments are the width of the bars and grooves, the height of the bars, the number, placement, and design of the dams, the selective grooves, the taper, and the angle of the bars. The design and functions of elements are given in [5, 89].

2.1.2 Refining mechanism

Hypothetically, the refining process may be divided into a fiber separation and a fiber development stages (Figure 2.1) [4]. Fiber separation occurs as the chips enter into contact with the breaker bars that break down the chips. The disintegration continues in the intermediate section, producing smaller particles. It is widely accepted that most of the characteristics of the final pulp are determined by the conditions in the initial fiber separation. The mode of fiber separation is largely determined by the condition of the lignin prior to, and at the instant of fracture [90].

As shown in Figure 2.2 [91], there are three possible modes of fiber fracture. They are trans-wall failure (TW, across the cell wall), intra-wall failure (IW, within the cell wall)

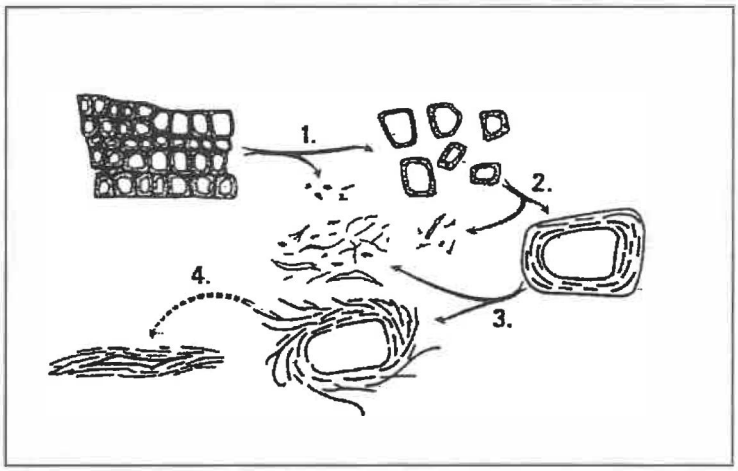

Figure 2.1 A hypothetical chip refining stages [4]

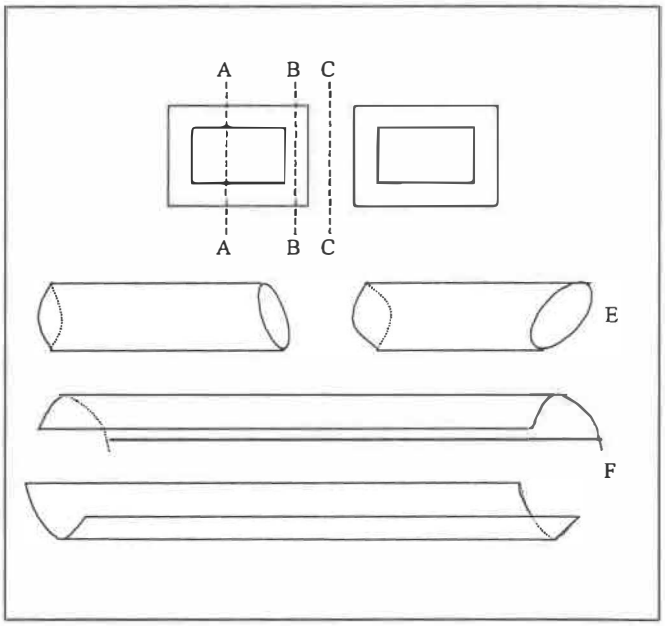

Figure 2.2 Schematic illustrating different type of failure. A-A, B-B, C-C are Transwall, Intrawall ad Intercell respectively, E, F are radial and tangential transwall failure [91]

and inter-cellular failure (IC, in middle lamella). With a softening effect, the temperature will regulate the location of failure in the wood matrix (Figure 2.3) [92]. For example, in TMP, where the refining temperature is above the lignin softening point, one would expect an inter-cellular failure. However, Johnsen et al [93] reported that, in TMP, intra-wall rupture could occur mainly through the S_1, the S_1/S_2 interface or

through the S_2 layer. At a lower temperature such as that in atmospheric refining (e.g. refiner mechanical pulping, RMP) both intra-wall and trans-wall could occur.

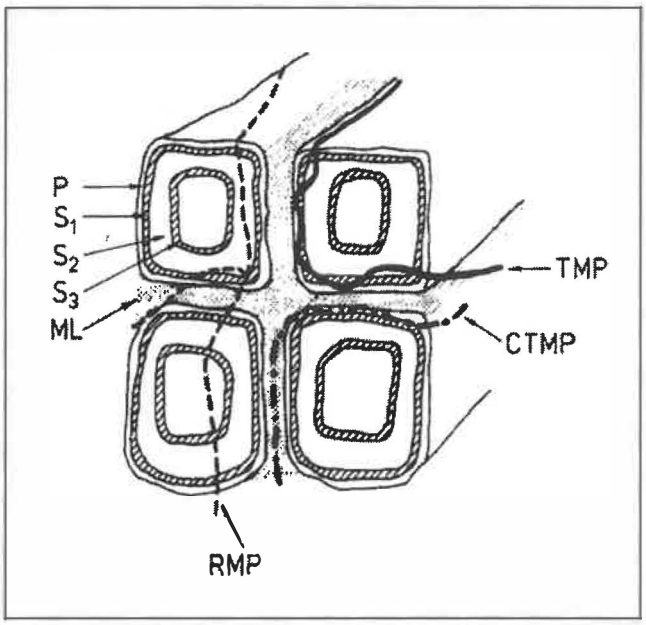

Figure 2.3 The fracture zones in softwood in different mechanical processes [92]

The second phase of refining, a fiber development stage, takes place through repeated attrition by compression and shearing, as the separated fibers and fiber bundles enter the fine refining section. This action allows us to achieve the desired papermaking properties such as external and internal fibrillation (delamination) of fibers. In addition, the refining action also shortens fibers. Hence, refining promotes changes in fiber length, specific surface, wetness and fiber flexibility. Considerable studies [8, 94, 95, 96, 97, 98] have been made on the mechanisms of refining and significant progress has been achieved towards a unified theory.

2.1.3 Refining theories

Numerous theories have been put forward to explain the mechanism of pulp refining. Generally, the theories require two major variables to satisfy the correlation between the changes in pulp properties and refining. The changes in physical properties of pulp are related to both the quantity (N) and the intensity (I) of the refining treatment:

$$\Delta(\text{Pulp property}) = F(N, I) \qquad \text{Eq. 2.1}$$

Three prevalent theories are briefly presented in the followings:

1. Specific edge load (SEL) theory by Brecht in 1967 [99]

$$\Delta(\text{Pulp property}) = f(\hat{E}_{net}, S_e) \qquad \text{Eq. 2.2}$$

Where, $\hat{E}_{net}$ = Net specific energy = N,

S_e = Specific edge load = I

2. Number of impact theory by Leider and Nissan in 1977 [100]

$$\Delta(\text{Pulp property}) = f(E, N_f)\ [101] \qquad \text{Eq. 2.3}$$

Where, E = Energy per impact = N,

N_f = Number of impacts per fiber = I

3. C-Factor theory by Kerekes in 1990 [102]

The C-factor was defined as the capacity of a refiner to impose impacts on pulp fibers passing through the refiner.

$$\Delta(\text{Pulp property}) = f(N, I) \qquad \text{Eq. 2.4}$$

$N = C/F_d$ = Number of impacts per unit mass dry fiber

$I = P_{Net}/C$ = Energy per impact

Where, P_{Net} = Net power, F_d = Flow rate of fiber through the refiner

2.2 Influence of Refining Conditions

Refining conditions have a significant impact on paper quality. These variables [103, 104, 105, 106, 107, 108, 109] include the throughput, stock consistency, rotation speed, refining temperature, residence time, and plate gap. The combination of all these

variables results in different specific energy and refining intensity. In refining, these parameters determine the fiber properties. Figure 2.4 [104] indicates how the specific energy consumption and the refining intensity affect the freeness and long fiber content in a TMP. Generally, for a given specific energy, an increase in the throughput and rotation speed and a decrease in residence time and plate gap would result in an increase in refining intensity. The refining consistency also plays an important role in determining the pulp quality and the specific energy consumption.

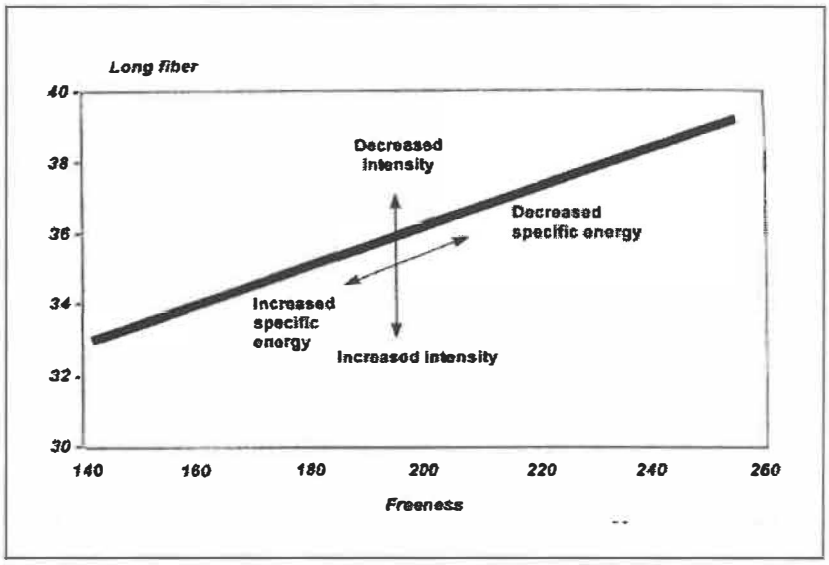

Figure 2.4 Schematic illustrating the relationship between specific energy, intensity of refining and pulp characteristics [104]

Alami et al [105] showed that, ideally, a refining system should operate within a consistency range of 22-36%. This condition will provide the maximum energy saving while producing high quality pulp with minimum dependence on consistency variations. It is reported [105, 109] that using high intensity refining in the first stage could efficiently break down the material and separate the fibers. When a refiner is operated at higher production rates the energy required to reach a given freeness could be reduced by as much as 25%, but the shives content would increase and the pulp quality decreases [106].

2.3 Difference between Grinding and Refining

In grinding [88], wood logs are pressed against a revolving grinding stone and, therefore, the fibers are immobilized and continuously compressed and sheared until they are set free from the logs (Figure 2.5). The process is harsh and energy efficient. On the other hand, chips are used in refining. As such, fiber separation in refining is stochastic [4, 94] due to the relatively mobile state of the chips in a fixed gap between the refiner bars. It occurs as a result of the compressive and shear actions, which disintegrate the wood matrix into fibers and fiber bundles (Figure 2.6). Hence, chip refining is comparatively gentler than the grinding of wood logs. Meanwhile, the energy efficiency is much lower for refining than for grinding. On the other hand, refiner pulps have better strength property than the groundwood pulp does.

2.4 Desirable Characteristics of Mechanical Pulp

Owing to its high yield (low wood cost), high bulk and high opacity, the use of mechanical pulp in printing grades is increasingly widening. The trend in papermaking is to produce whiter and lighter sheets with good printing quality. This means that there is a need for a strong mechanical pulp with a good optical properties and printability. An increase in a strength property of the mechanical pulp component could thus reduce the chemical pulp component in the furnish and lower the manufacturing cost. Mechanical pulp can also contribute to the bulk of paper, particularly for the low weight coated grade (LWC). Its high light scattering coefficient constitutes another positive attribute in printing and writing grades. On the other hand, there is a certain undesirable quality of mechanical pulp due to its relatively poor contribution to the paper smoothness. This negative impact can, however, be minimized by various strategies such as a pretreatment of chips prior to refining, optimization of refining conditions and proper selection of raw material.

It has been shown that pretreatment of chips produces sheet with decreased roughness and improved smoothness [110, 111, 112, 113]. Previous studies [113] taught us that the refining conditions, particularly those used in the primary stage, such as temperature, consistency and intensity, etc, have an important influence on the final pulp quality. The

influence of raw material on sheet quality is also well recognized; uniform thin-walled fibers tend to yield better inter-fiber bonding (better tensile strength) and improved surface smoothness.

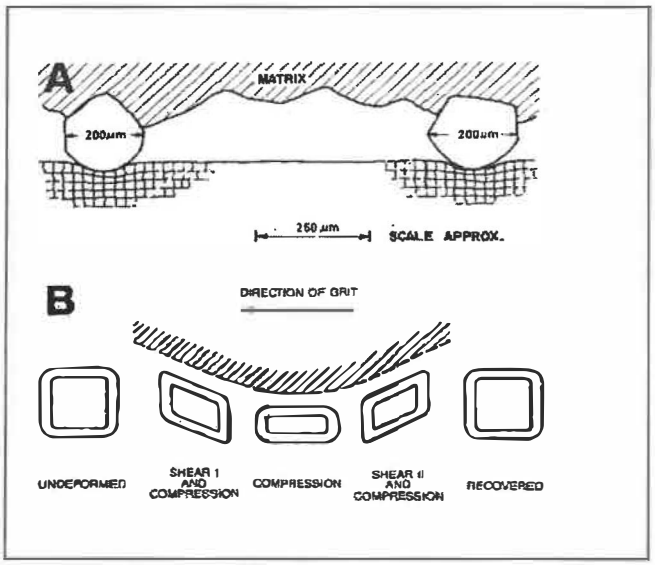

Figure 2.5 Presentation of idealized grinding zone conditions [88]

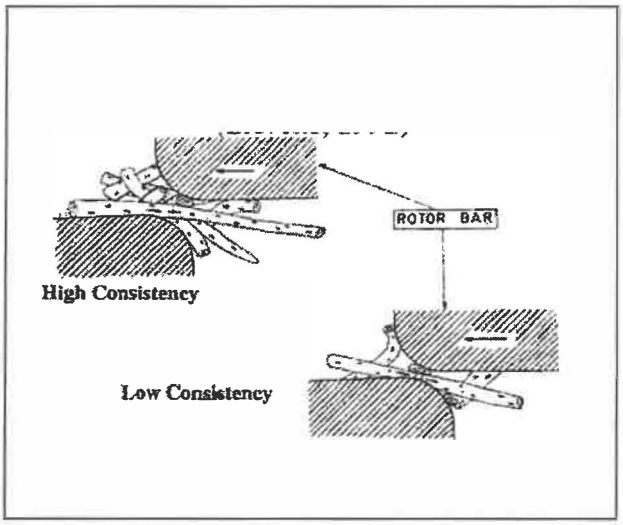

Figure 2.6 Fiber treatment at leading edges [94]

2.5 Summary

Refining is a stochastic process that requires extensive specific energy to produce a good quality mechanical pulp when compared with stone grinding. However, the former gives a better pulp quality than the latter does. The mode of fiber failure in refining is affected by the condition of lignin in the cell wall before and at the instant of fracture. Therefore, pretreatment of chips to weaken the lignin, and to create partial delamination in the fiber wall by mechanical compression prior to refining represents an important process step in a modern refining technology. Characteristics of raw material also play an important role in determining the final pulp quality; uniform, long and thin-walled fibers are desirable in the mechanical pulping.

Chapter 3 - Characteristics of wood

The characteristics of wood have a dominating influence on the pulp quality of both the chemical and mechanical pulps [114, 115, 116, 117, 118, 119, 120, 121]. In addition to their effects on refining energy requirement the basic wood properties also exert no negligible impact upon the final pulp quality. The important characteristics include basic density, fiber length, fiber diameter, cell wall thickness, fiber coarseness, flexibility, etc.

3.1 Wood and Cell Wall Structure

3.1.1 Macroscopic structure of softwood

Wood is composed of concentric growth increments or growth rings. The most striking variation in softwood properties within a single tree is the presence of early- and latewood, the former being larger in radial width and thinner in cell wall when compared with the latter. In general, softwood (coniferous tree) is made up with 90-95% (by volume) of fiber (tracheid) and 5-10% parenchyma cell. Softwood fibers (tracheids) are elongated cellular elements with a length of 3-5 mm and a width of 30-45 μm while the parenchyma cells (mostly ray cells) are brick-like in shape and are usually less than 0.5 mm long and about 10 μm wide [122, 123].

A wood log may be pictured as a truncated cone through which three sections may be cut perpendicularly to each other. These planes are defined as cross-section (X) perpendicular to the grain, radial section (R) perpendicular to the growth increments, and tangential section (T) in respect to the concentric growth increments. The definitions of these planes are useful for describing the mechanical properties of a wood specimen because wood is anisotropic in nature.

3.1.2 Microstructure of fiber (tracheid)

Essentially, a typical softwood fiber (tracheid) has a spirally layered wall structure. The structure has an outer layer called primary wall (P) and an inner layer called secondary wall that in turn consists of three distinct layers, S_1, S_2 and S_3. The S_2 layer constitutes

the main bulk of the structure as depicted in Figure 3.1 [123,124]. Fibril orientation in the P is indicated as random, in the S_1 and S_3 as about perpendicular to the fiber axis, and in the S_2, as approximately parallel to the fiber axis. The nature of fibril orientation has a tremendous influence on the behavior of the wall structure under mechanical stresses such as in refining [125, 126]. The physical characteristics of cell wall layers and their chemical components are presented in Table 3.1 [127, 128], which shows that the middle lamella (ML) is particularly rich in lignin. The outer layers including the P and S_1 layer have relatively large fibril angle, and hence, they could play a role in restricting the swelling of the S_2. On the other hand, the S_2 layer constitutes the main bulk of cell wall and has low fibril angle, meaning that it plays the most important role in determining the characteristics of pulp fibers. In summary, the proportion and concentration of the three major wood components are not uniformly distributed across the cell wall.

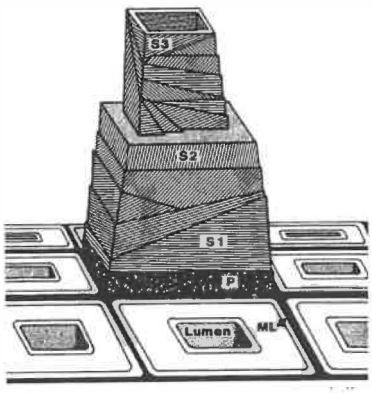

Fig. 3.1 Diagrammatic representation of softwood fiber wall. ML -middle lamella, P - primary wall, S1, S2, S3 -layers of secondary wall. [94]

Figure 3.1 Diagrammatic representation of softwood fiber wall. ML–middle lamella, P – primary wall, S_1, S_2, S_3, - layers of secondary wall.

Different models of cell wall organization had been discussed in details [129, 130]. In general, the cell wall is made up with various lamellae, which in turn is composed of macrofibrils. Each bundle of macrofibrils consists of numerous of microfibrils that are 100-300 Å in diameter. The latter can be further broken down into elemental fibrils

(40Å) that consists about 40 basic units of cellulose chain (Figure 3.2). A conventional model indicates that microfibrils of cellulose are embedded in a hemicelluloses-lignin matrix, arranged in an interrupted lamellar structure, as shown in Figure 3.3 [131].

Table 3.1 Chemical composition and physical properties of fiber wall layers [127, 128, 132]

	Fibril angle, Degree	Thickness, Microns	Cellulose, %	Hemicelluloses, %	Lignin, %
Middle lamella	Non ordered	0.50	8	36	56
Primary wall	Non ordered	0.10	15	32	53
S_1 layer	±70	0.15	28	31	41
S_2 layer	+15	4.00	50	31	19
S_3 layer	-70	0.04	48	36	16
Density, kg/m^2			1550	1500	1300
DP, 10^3			5-10	0.1-0.2	--
MW, 10^5			0.8-1.6	--	0.02
Young's modulus, (axial) , GPa			134	8(0.02)	4
Young's modulus, (trans.) , GPa			27.2	4(0.01)	4
Shear modulus, GPa			4.4	2(0.005)	1.5

+, -: Right-handed and left-handed, respectively; DP: degree of polymerization; MW: molecular weight. Modulus is the value below the T_g, and that of hemicelluloses in brackets is the modulus above T_g

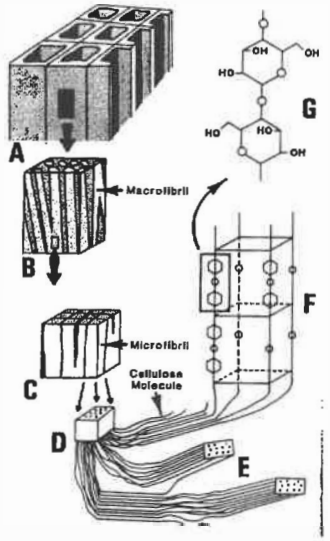

A. Transverse/longitudinal view of several wood fiber.

B. Portion of a fiber S2 layer, shown here to consist of macrofibrils.

C. Portion of a macrofibril, shown here to consist of aggregates of microfibrils, which are in turn composed of aggregates of cellulose molecules.

D. Cross-section of a single microfibril.

E. Region of a microfibril where the cellose chains exhibit a high degree of order

F. Organization fo cellulose molecules into a series of 'unit cells', showing the basic repeating unit of cellulose.

G. A cellobiose unit

Figure 3.2 Diagrammatic representation of cellulose in the wood fiber wall [123]

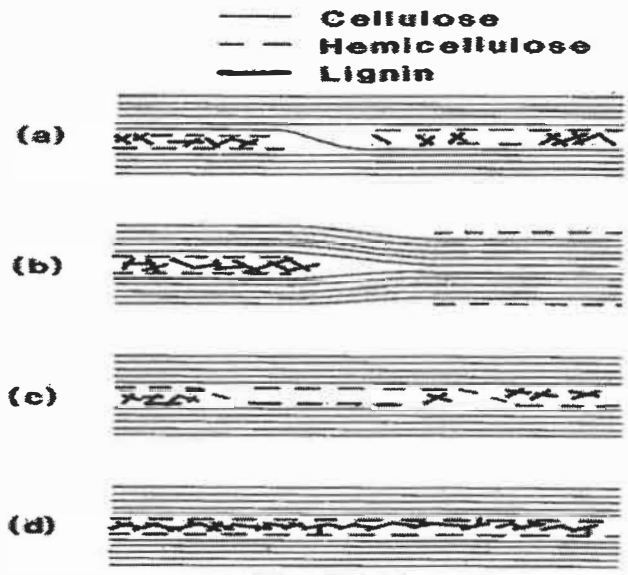

(a) Bridging by cellulose molecules
(b) Cellulose fibril cocrystallization
(c) Bridging by cocrystallized hemicelllose molecule
(d) Cocrystallized hemicellulose molecules cross linked by lignin

Figure 3.3 Four possible ways that holds fibrils together in the cell wall [131]

3.2 Chemical Composition of Wood

Lignin, cellulose, and hemicelluloses are the three main chemical constituents in wood. Softwoods have different chemical composition as compared to hardwoods, as indicated in Table 3.2 [122, 131]. The most significant difference is the higher lignin content in the conifers than in the deciduous species. This difference dictates the choice of pulping methods for the two types of species. The distribution of chemical constituents across the cell wall is not uniform, as illustrated in Table 3.1 and Table 3.3 [127], and Figure 3.4 [133]. Evidently, the nonuniform distribution of chemical constituents, particularly the lignin, across the cell wall can be attributed to the difficulty in obtaining uniform cooking in chemical pulping, and the characteristics of fiber separation and fibrillation in mechanical pulping.

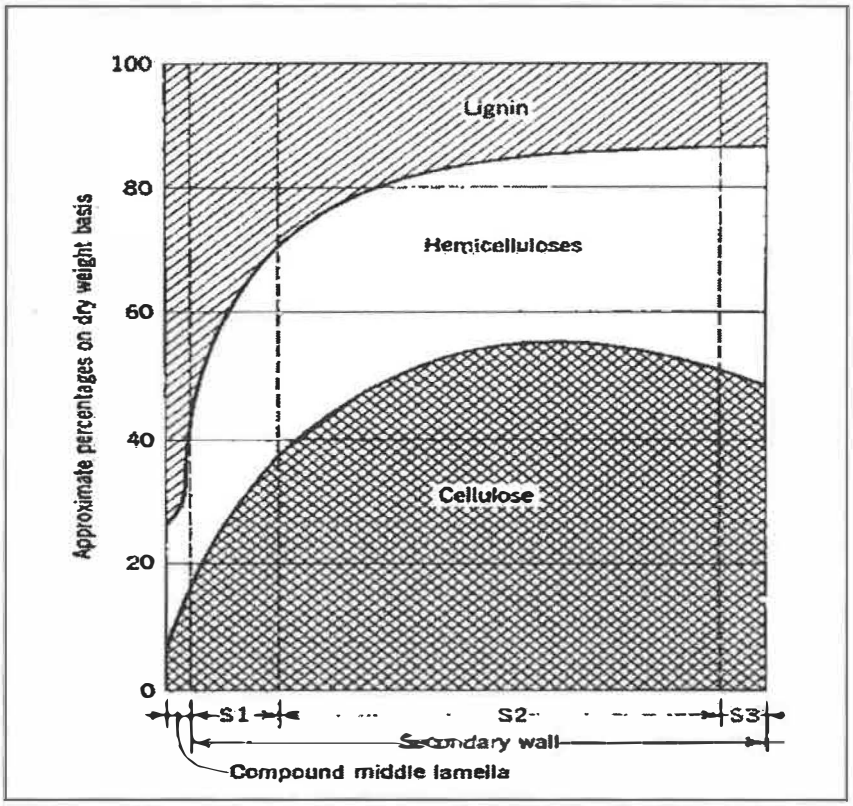

Figure 3.4 An approximate perceptual distribution of the chemical components in different softwood tracheid [8]

Table 3.2 Approximate chemical composition of softwoods and hardwoods [122, 134]

	Constituents, %			
	Lignin	Cellulose	Hemicelluloses	Extractives
Hardwoods	20 ± 4	45 ± 2	30 ± 5	5 ± 3
Softwoods	28 ± 3	42 ± 2	27 ± 2	3 ± 2
White spruce	31	41	29	1

Table 3.3 Distribution of lignin in black spruce tracheid [122, 134]

	Region	Volume, %	Lignin, %	Lignin Concentration, %
Earlywood	Secondary wall	87	72	23
	Middle lamella	9	16	50
	Cell corner	4	12	85
Latewood	Secondary wall	94	82	23
	Middle lamella	4	10	60
	Cell corner	2	9	100

3.3 Chemical Properties of Major Wood Components

The chemical properties of the three major wood components (lignin, cellulose and hemicelluloses) will be briefly discussed in the following in respect to pulping and papermaking [127].

Lignin is a complex, crosslinked, three-dimensional thermoplastic polymer formed by phenolic units. The number of building units varies from a few to several hundreds. The basic unit of softwood lignin is guaiacyl. The polydispersity of softwood lignin is 2.5, which is much higher than that of cellulose. The aromatic nature of the phenolic units renders lignin hydrophobic, and the three dimensional network provides rigidity and optimum resistance to external stresses. The softening temperature for isolated (water-saturated) lignin is 80°-90°C. Additional water does not significantly lower its softening

point. Under conditions typical for mechanical pulping, the softening temperature for *in situ* lignin ranges from 100° to 130°C. The softening property of lignin plays an important role in fiber separation and internal delamination. In general, fiber separation below the lignin softening temperature improves energy efficiency of the refining process, but sacrifices the fiber length. High temperature refining is beneficial to the development of fiber properties and maintaining the fiber length.

Cellulose is a homopolysaccharide composed of β-D-glucopyranose units. The molecules are completely linear and have a strong tendency to form intra- and intermolecular hydrogen bonds. The cellulose microfibrils contain both crystalline and amorphous regions. The crystallinity for wood pulp cellulose is 60-70%. The native cellulose in the secondary cell wall of plants is monodisperse, that is, it contains only molecules of one size. The cellulose in the primary cell wall is polydisperse, and has a lower average molecular weight. The softening temperature of dry cellulose, and amorphous cellulose in water-saturated condition are 220°C and 20°C, respectively [126]. In refining, the fibers are kept in water-saturated condition, improving fiber flexibility that is beneficial for minimizing the adverse effect of fiber cutting.

Hemicelluloses (HC) are heteropolysaccharides. Galactoglucomannans and arabino-glucuronoxylan are two principal hemicelluloses in softwoods, which represent about 20% and 5-10% of wood, respectively. Their backbones are linear or possibly slightly branched. Acids easily depolymerize the galactoglucomannans, and the acetyl groups are easily cleaved by alkali. The softening temperature of HC under dry condition and water-saturated conditions are 180°-220°C and 20C°, respectively [124]. It is recognized that there is probably no chemical bond exits between cellulose and hemicelluloses, but sufficient mutual adhesion is provided by hydrogen bonds and van der Walls force. Chemical linkages probably exist between the hemicelluloses and the lignin. These two components make up a so-called lignin-carbohydrate complex (LCC) [127, 135]. In high-purity pulps, most of the HC and lignin are removed. However, in paper-grade pulps, HC are retained as much as possible to maintain pulp yield and to promote desirable fiber properties. Owing to their hydrophilic properties [136], the HC promote

internal lubrication of the fiber during the beating and refining, leading to improved flexibility, ease of mechanical refining, and increased sheet density.

3.4 Summary

Wood is a heterogeneous material, physically and chemically. Also, it is anisotropic in nature. Due to this particularity, pulping and papermaking are relatively complex processes. Optimization of the processes at various stages requires serious considerations to produce paper products of the best possible quality that meets the consumers' demand. In papermaking, wood fiber alone cannot always meet the desired requirement, and, therefore, some chemical or mechanical modification of wood prior to pulping is necessary, and extraneous materials such as pigments and fillers are incorporated into the paper structure to enhance its quality.

Chapter 4 - Experimental

4.1 Background

In mechanical pulping, wood chips are transformed into individual fibers or fragments of fibers. The characteristics of fiber separation are related to the pretreatments to which the chips are subjected. With a thermal softening or a chemical treatment such as sulfonation of lignin, fibers are separated in the middle lamella, but they have relatively low papermaking potential because their surface is enriched with lignin, hindering effective hydrogen bonding. Physically, the fiber structure has to be modified to promote fiber flexibility, conformability, and functional surface for inter-fiber bonding.

To develop desirable fiber quality it is necessary to remove the lignin-rich middle lamella (ML), an hydrophobic layer, and the outer layers of cell wall such as the primary wall (P) and probably the S_1 layer of the secondary wall. Due to the random fibril orientation in the P and nearly perpendicular fibril orientation in the S_1, these outer layers could compromise the swellability of the bulk layer of S_2, reducing the flexibility and collapsibility of fibers and consequently the inter-fiber bonding.

It is known that the regions between P and S_1, and between S_1 and S_2 are the structural weak links within the fiber wall. When a compressive force is applied normal to the fiber axis lateral tensile forces are created in the plane perpendicular to the applied force. These tensile forces produce a lateral displacement of fibers, causing rupture between them. Meanwhile, stress concentrations would also build up within the fiber wall, creating a relative movement of various layers. Due to the differences in structural characteristics between the layers, delaminations between them are expected to occur. Some recent research works conducted at the Université du Québec à Trois-Rivières have shown that radial compression of wood chips prior to refining can significantly reduce the refining energy requirement while improving the mechanical properties of the resulting pulps [56, 57, 58]. In view of this encouraging finding, it is of great interest to do some basic research on the mechanism of wood rupture under compression force, especially on how and to what extent the wood fibers were modified by compression.

This may shed some lights on energy-efficient ways to achieve fiber separation in wood and internal delamination in fiber wall.

Since wood is an anisotropic material it is important to find out the most efficient way to apply a mechanical force to the wood matrix. There are many kinds of mechanical forces that can be used such as compression, shear, tensile, bending and torsion, etc. However, it is well recognized that in chip refining only two major forces are involved, that is the compression and shear. In this respect, these two forces will be examined in the study.

4.2 Experimental design

The research includes three series of tests. The first series examines the effect of temperature on compression in three directions (radial, tangential and longitudinal). The second series studies the effect of sulfonation on the radial compression (restrained and unrestrained compression) while the third series investigates the effect of pre-compression of samples on the shear properties of wood. The main experimental procedures are presented in Figure 4.1 and Figure 4.2. While the experimental parameters are given in Table 4.1. A minimum of 5 specimens was tested in sulfonation study (Series 2). Ten replicates were used for each condition in other compression tests.

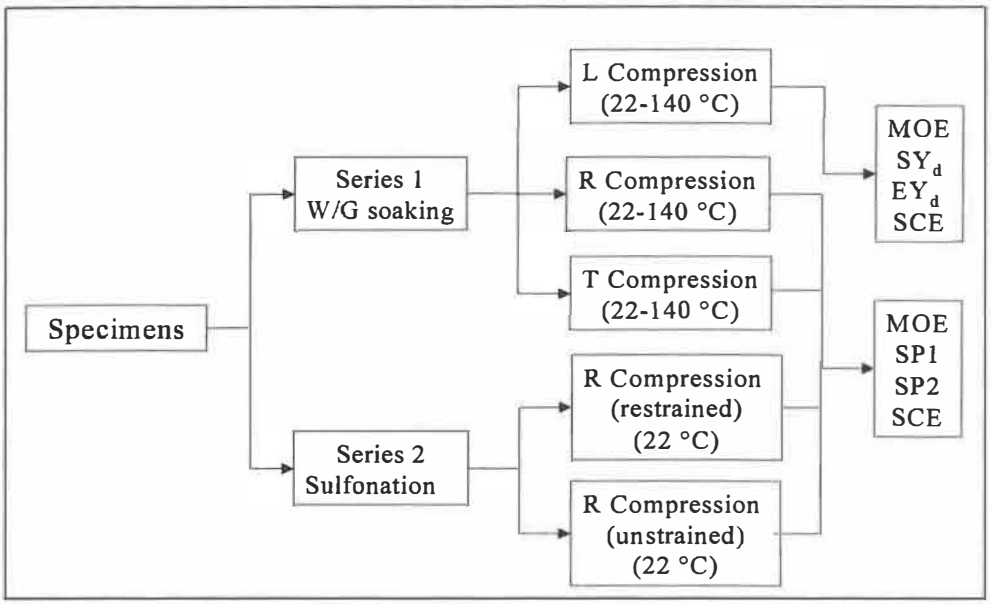

Figure 4.1 **Flow diagram showing the main experimental procedures of the first two series of experiments (L: longitudinal, T: tangential; R: radial direction)**

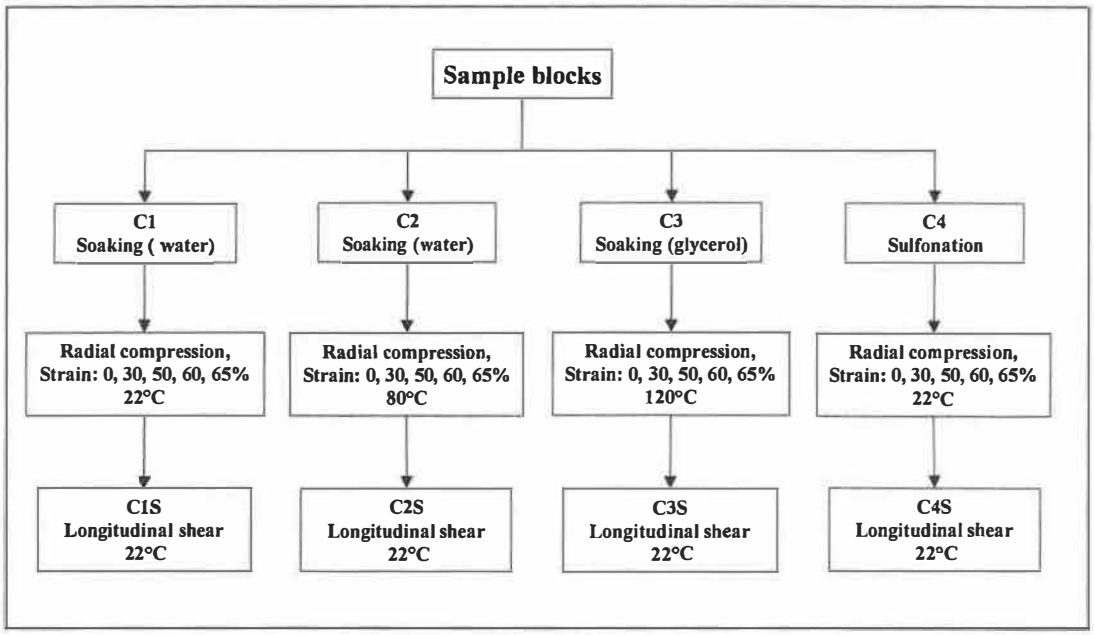

Figure 4.2 **Flow diagram showing the main experimental procedures of the third series of tests on the effect of pre-compression on shear properties**

4.3 Experimental conditions

4.3.1 Material

A 65-year-old white spruce [*Picea glauca* (Moench) Voss] obtained from the St.-Maurice region in the Province of Quebec was used in this study. The wood logs were air-dried and were sawed to discs of about 10 cm in thickness. The discs were stored in room temperature before sample preparation.

4.3.2 Preparation of samples

It is known that juvenile wood (the central portion of a tree trunk) has different physical and chemical properties than the mature wood, and that heartwood has dissimilar chemical composition as compared with the sapwood. For these reasons the experimental specimens were prepared from the sapwood portion containing growth increments in the outer 50 mm band. The specimens were free of knots, compression wood, cracks, decay and other visible defects.

For the first and most of the second experimental series, specimen measured 10 x 10 x 10 mm (L x R x T), contained 5 to 7 growth rings, were prepared in such a way that the growth rings are (more or less) parallel to the tangential plane (Figure 4.3 A). The overall average volumetric proportion of earlywood was determined to be 78 %; the latewood represented 22%. Specimens containing only EW or LW measuring 10 x 3 x 10 mm (L x R x T) and 10 x 1.9 x 10 mm (L x R x T), respectively, were also prepared for certain tests in the second series. For the third experimental series, the specimen measured 11x 15 x 28 mm (L x R x T). The other properties are the same as those of the first two series. All samples were first sawn to an appropriate dimension, and then trimmed to the desired dimension using a sanding machine. The exact dimension of specimens in water or water/glycerol (W/G) saturated condition was measured using a digital sliding caliper to the nearest 0.01 mm at 22°C. This dimension was used in all calculations in the following tests.

Table 4.1 Experimental parameters

Tests	Specimen treatment	Testing direction	Number of specimens	Test temp. °C
Series 1 Effect of temperature on compression	W/G saturated	Radial (R)	70	22-140
		Tangential (T)	70	
		Longitudinal (L)	70	
Series 2 Effect of sulfonation on compression	Sulfonated (15 sulfonates levels)	R (Restrained)	95	22
		R (unrestrained)	95	
Series 3 Effect of pre-compression on shear properties	Water saturated	R-compression + RL shear	50	22
	Water saturated		50	80
	W/G saturated		50	120
	Sulfonated		50	22

* W/G: Water/Glycerol mixture (8:1)

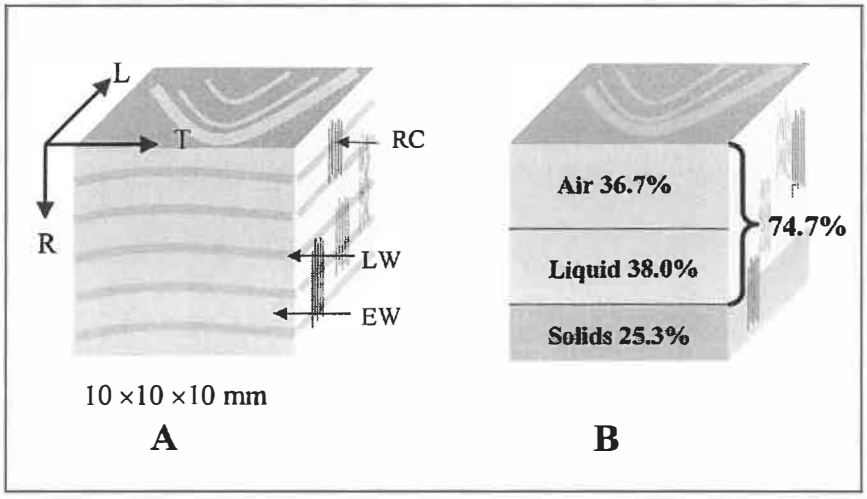

Figure 4.3 Schematic diagram illustrating the characteristics of a specimen.

* L: longitudinal, R: radial, T: tangential, RC: ray cells, LW: latewood, EW: earlywood

The white spruce samples had the following characteristics: basic density = 380 kg/m^3, density of solids = 1500 kg/m^3, density of liquid = 1000 kg/m^3, and moisture content 50%. Thus the volume of solid is 25.3%, as shown in Figure 4.3 B, and a maximum compression strain is 74.7%. Based on the assumption that the bulk density of a loosely

packed chip is 150 kg/m^3, and the solid contents of two typies of compressions at equivalent compression deformations are same, the compression ratio in a plug-screw and the corresponding compression strain in platen compression can be estimated as shown in Table 4.2.

Table 4.2 Comparison between plug-screw compression ratio and static compression strain

Solid content, %	20	30	40	50	60	70	80	90	100
Screw Compression Ratios	2/1	3/1	4/1	5/1	6/1	7/1	8/1	9/1	10/1
Static Compression Strain, %	0	15.7	36.7	49.4	57.8	63.8	68.4	71.9	74.7

4.3.3 Pre-treatment of specimens

Samples used in the experiments were pretreated as follows:

1. Air-drying

All the specimens will be first air-dried in a conditioning room (23 ± 1°C, 50 ± 2% relative humidity) for a week, allowing them to reach a uniform moisture content of 9.13%. The moisture content was determined by drying 4 samples in an oven at 105°C until a constant weight is reached. The conditioned samples were kept in sealed plastic bags for further testing.

2. Water or water/glycerol (W/G) soaking

Water or W/G soaking was conducted at room temperature. A predetermined number of air-dried samples were soaked in tap water or W/G mixture (1:8 ratio) under vacuum for 48 hours. The treated samples were stored in corresponding liquid before testing. Four samples were used for the determination of moisture content of the saturated wood.

3. Na_2SO_3 treatment (sulfonation)

(1). For the second series of tests, a Central Composite Design (CCD) and Response Surface Method (RSM) were employed to generate different levels of sulfonate content

in the wood samples. The variables used are presented in Table 4.3. A total of 19 runs were conducted, which generated a series of samples with 15 different sulfonate levels. These sulfonated samples were then compressed with or without restrain.

Table 4.3 Central Composite Design (CCD) of sulfonation conditions (19 runs)

Code value(Cv)		- 1.682	- 1	0	1	1.682	Cv/Av
Actual value (Av)	Temp., °C	20	48	90	132	160	Cv= 90 + 41.62Cv
	Time, min	5	21	45	69	85	Cv= 45 + 23.78Cv
	Con., %	0	6.1	15	23.9	30	Cv= 15 + 8.92Cv

Before the sulfonation, the samples were soaked, overnight, under vacuum in predetermined concentration of Na_2SO_3 solution. Sulfonation at temperatures below 90°C was conducted in beakers containing the required preheated liquor while sulfonation above 90°C was carried out in a liquid phase cooking using a M/K laboratory digester. In the process, 20 specimen blocks (approximately 10g, o.d.) were placed in a stainless steel basket and cooked with 1.2 liter of chemical solution. The initial pH of the solution was 9.7, which dropped slightly after cooking. The chemical solution was preheated in digester to 90°C before the wood blocks were added. It took about 15 minutes to reach the desired temperature. This initial heating time was not included in the sulfonation time. The treated samples was thoroughly washed with running tap water and kept in water in a conditioning chamber at 4°C until further testing.

Additional sulfonation trials were conducted to study the difference between EW and LW in sulfonation and compression. The sulfonation conditions were: 132 °C; 15% Na_2SO_3 and 15, 45, and 75 min, following the same procedures and other conditions used for the 19 runs described earlier.

(2). Samples used in the third series of test (C4) were sulfonated using a 10% Na_2SO_3 solution at 132 °C for 75 minutes.

Additionally, ten samples were used to determine the ionic group content of the sulfonated specimens.

4.3.4 Ionic group content

The sulfonated blocks were first compressed using an hydraulic press and then disintegrated in a blender before being refined in a PFI mill (5,000 - 20,000 revolutions). The resulting pulps were treated with 0.1N HCL, twice, each for 45 minutes and then thoroughly washed with distilled water. The ionic groups were measured by conductivity titration [137].

In the process, the treated pulp was dispersed in 450 ml of 0.001N sodium chloride prepared in deionized water. A quantity of 5 mL of 0.1N HCL was added to the suspension prior to titration. The titration was carried out with 0.1N sodium hydroxide dispensed by the titration unit while the suspension was stirred under a nitrogen atmosphere. The alkali was added at a rate of 0.5 mL every 45 seconds so as to allow sufficient time for equilibrium to be reached between readings. After titration, the pulp was filtrated and oven dried at 105 °C to determine the exact dosages of pulp.

The titration was carried out by means of an automatic titration system composing of a titration unit (Ω Metrohm, Brinkmann, 765 Dosimat), a conductivity meter (Thermo Orion Model 150) and a computer with data processing software.

Figure 4.4 shows the titration curves of sample S19, which was sulfonated in a 15% Na_2SO_3 solution at 160°C for 45 minutes. Intersection of the three linear branches gives the V1=12.62 mL, V2 = 17.31 mL. In the titration, 5 mL (V0) of 0.1N HCL was added and 3.22 g (o.d.) pulp was used in the titration. The acid groups were obtained as follows:

Sulfonates = $[(V1 - V0)\times N]/m\times 0.001$

$= [(12.62 - 5)\times 0.1]/3.22\times 0.001$

$= 236.6$ mmol/kg

Carboxylates = $[(V2 - V1)\times N]/m\times 0.001$

$= [(17.31-12.62)\times 0.1]/3.22\times 0.001$

$= 145.6$ mmol/kg

The contents of sulfonic and carboxylic groups were calculated by the computer when the input of the exact dosage of pulp used was entered. The coefficients of variation were approximately 1% and 3% for sulfonates and carboxylates, respectively, in two parallel tests. Therefore, only one test was conducted in most cases. However, two parallel tests were conducted for the specimens of sulfonated EW and LW, as described in the second series of tests.

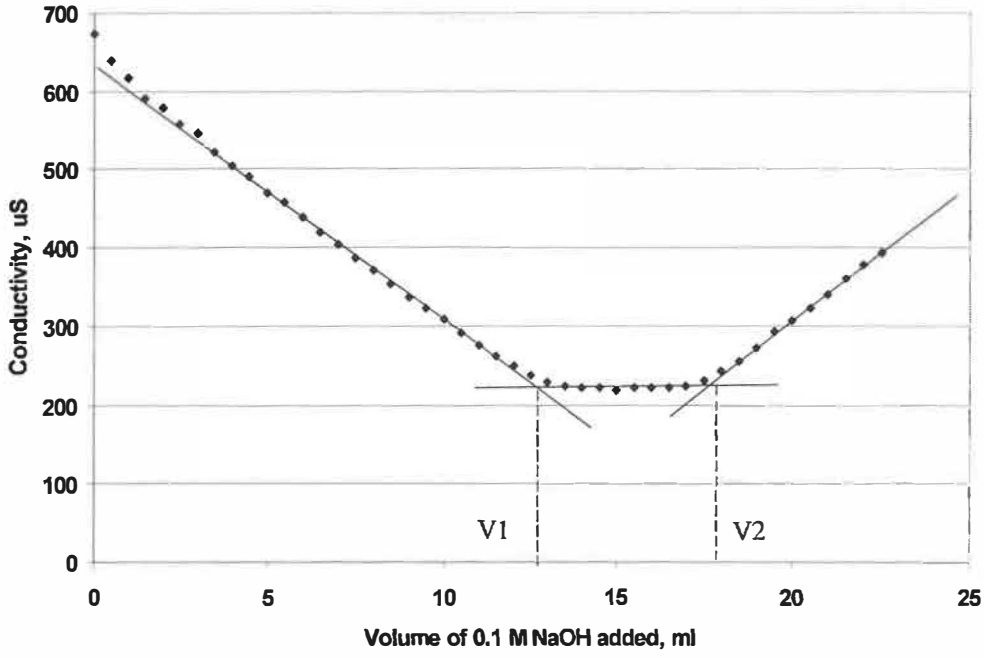

Figure 4.4 Conductivity titration curve of sample S19

4.4 Mechanical testing

4.4.1 Instruments for testing

1. Instron machine

The compression tests were conducted using an Instron machine (model 4201). The Instron machine consists of three main units: mechanic compression unit (1, load cell of 5 kN), machine control unit (2) and a computer control unit (3) as show in Figure 4.5.

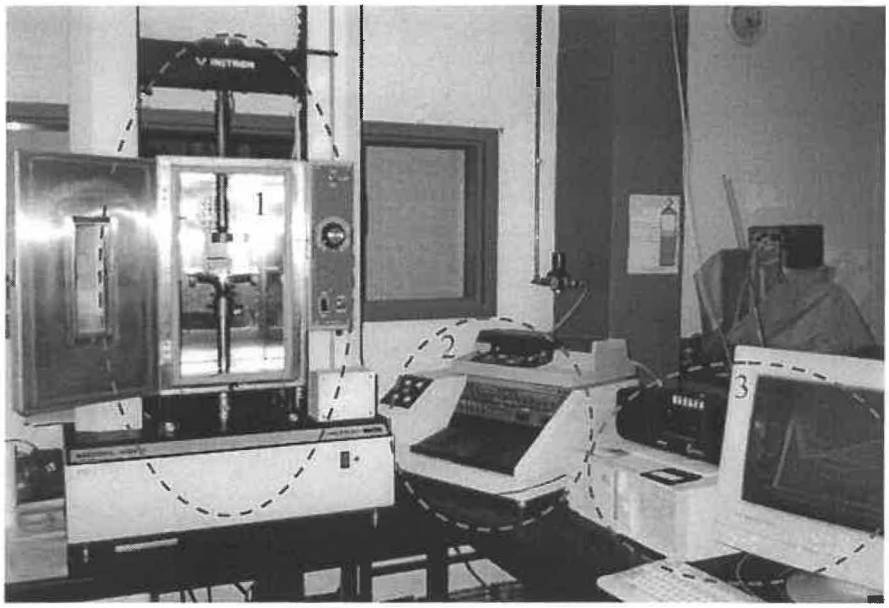

Figure 4.5 Instron machine (Model 4201)

The controllable parameters include temperature, compression speed, and data collecting rate. The computer control unit provides various calculations based on the recorded displacement and load, including stress, strain, modulus, compression energy etc. Most of these data can be obtained directly in the test report by carefully presetting the control programs. However, the compression curves presented in this thesis could not be obtained directly from the output. They were constructed by transforming the raw data file (MRD file) into MAD file and then processed using Microsoft Excel. The information on the Instron testing system and the calculation methods are given in the

reference guide of "Instron Series IX Automated Materials Testing System, Version 5, M22-12410-3 (1990)".

2. Self-design devices

Three stainless steel devices and several accessories are designed and made for different specific purposes.

Device 1: Temperature control container

To conduct the compression tests at elevated temperatures, an Instron heating chamber with an electronic hot air heater was used. Since the sample blocks were heated in a medium of water/glycerol mixture, a special container was made and fixed onto the compression platform. One side of the container was made of transparent plastic, allowing direct observation during the compression process. The test sample was fixed onto the bottom of the container by means of a spring clip. Several other temperature control accessories were also made to be used with the Instron machine.

Device 2. Device for restrained compression

We conducted a series of radial compression tests where the sample was restrained from lateral expansion. To perform these tests, a special specimen holder was made, as shown in (Figure 4.6). In radial compression, only tangential direction was expanded significantly. The longitudinal direction (fiber axial direction) only experiences a very small expansion. Thus, to simplify the device, only tangential direction will be restrained by tightening the screw handle. Relative restrain in longitudinal direction is obtained by matching the sample size with the slot of compression device. As such, the device minimizes the lateral expansion of sample under compression, allowing us to identify the real wood failure caused by a compressive force. In contrast, the structural failures of wood induced by compression without restraint are generated not only by the compressive action but also by the tensile and shear forces created by lateral expansion of specimen under a compressive load. This device can also be used to observe, microscopically, a sample under restraint compression.

To examine the physical changes of specimen under compression without restraint using a light microscope, a small compression device was fabricated as shown in Figure 4.7. This small device can be fixed onto the stage of a light transmission microscope. The compression was operated manually.

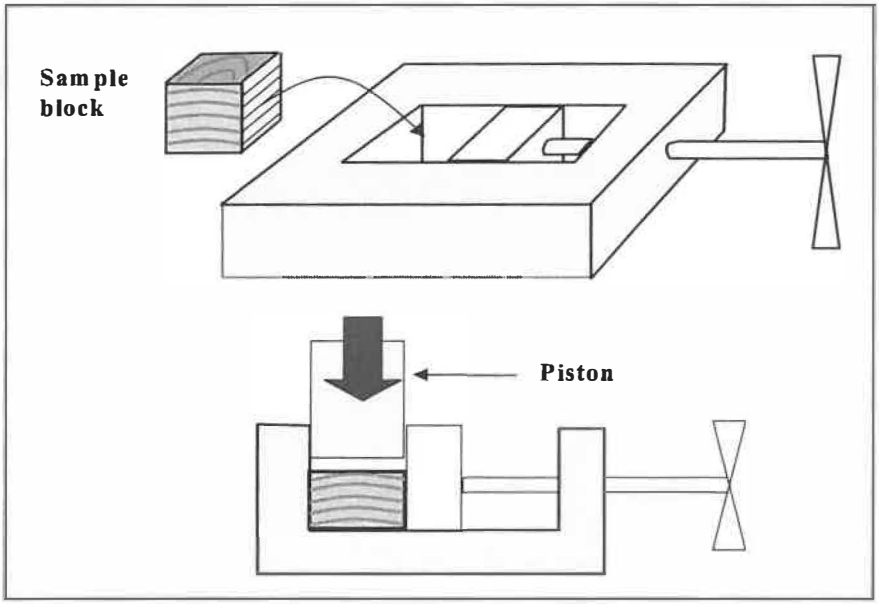

Figure 4.6 Restrained compression device

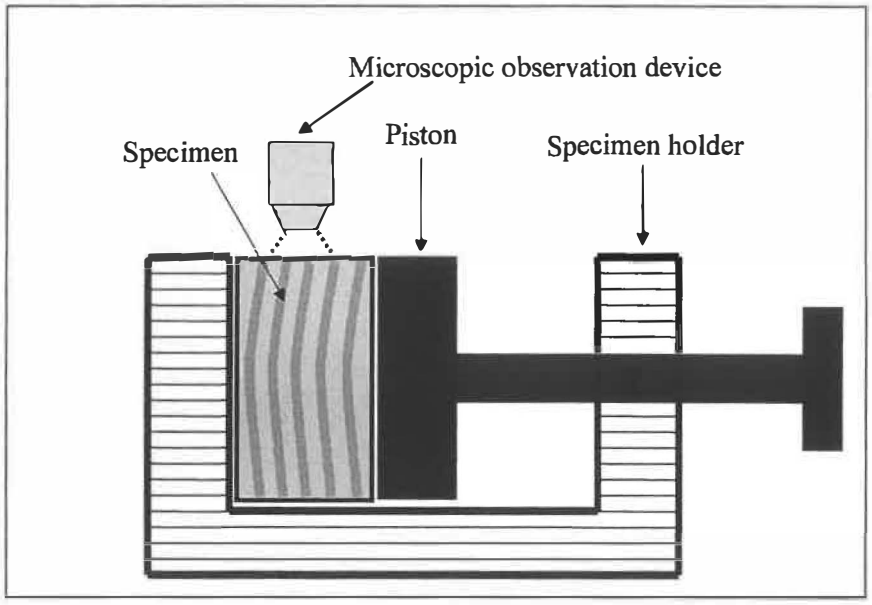

Figure 4.7 Manual compression device for microscopic observation

Device 3. Shear device

The influence of structural damages in wood caused by compression on mechanical strength cannot be revealed by mere optical evaluation. For this reason we conducted a series of shear tests using precompressed sample blocks. The shear results would reveal the degrees of structural weakness of samples induced by compression. Several shear methods have been used by different researchers [138, 139]. However, shear is more complicated than compression. Since wood begins to deform when stress is applied, the deformation produces stress concentration that occurs differently in different samples. In most cases the wood tends to cleave rather than shear. Having performed several initial trials, we designed and fabricated a shearing device (Figure 4.8) that can be adapted to the Instron machine. As shown in the figure, the wood specimen can be retained in a slot, minimizing its lateral movement during the shear test. The distance between two platforms is 11 mm, and the sample width is 10 mm. In this test, two pairs (4 failure planes) of shear surface were generated.

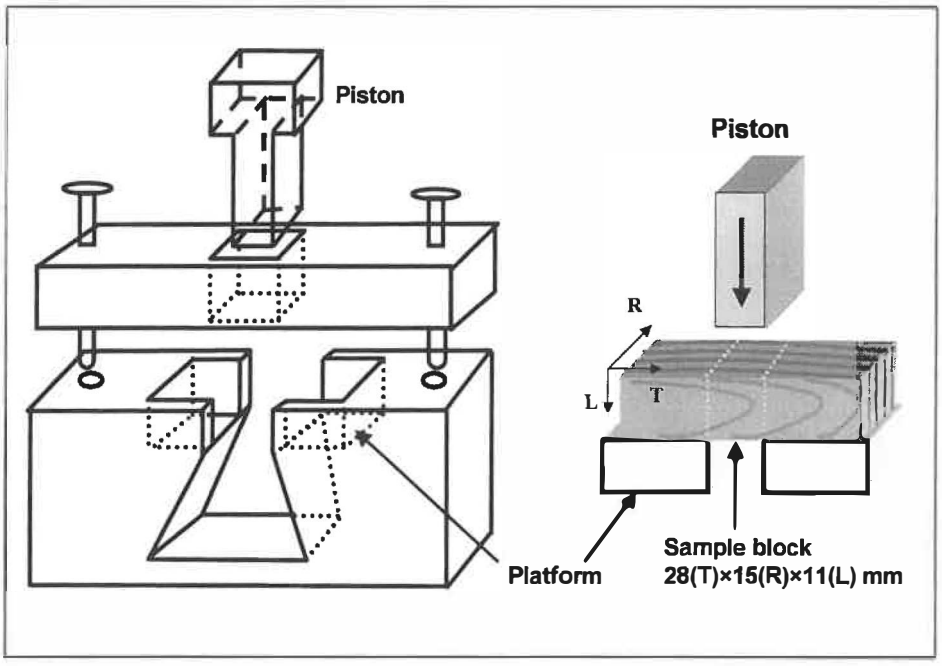

Figure 4.8 Specimen holder for shear test

4.4.2 Compression tests

The conditions of compression tests are presented in Table 4.4. Due to the maximum load limit of the load cell used (5 kN), in some cases the preset end strain of 65% cannot be reached, particularly when the compression tests were carried out with restraint (e.g. tests of series 2 and 3). This situation should not influence most of the evaluated properties. However, it does cause some levels of variation in the calculation of specific compression energy (SCE) because a change of the base of the comparison.

Characterization of compression and shear properties was based mainly on stress-strain curves obtained in various trials conducted, as presented in Table 4.4.

Table 4.4 Test conditions on Instron machine

Tests	Samples	Compression direction	Test temp. °C	End strain %	Strain rate mm/Min.	Data collection rate Data/Sec.
Series 1 Compression	W/G Saturated	Radial	22-140	70	3	5 for first 30 seconds, then reduce to 1 after that
		Tangential	22-140	70		
		Longitudinal	22-140	50		
Series 2 Compression	Sulfonated	Radial (Restrained)	22	70		
		Radial (unrestrained)	22	(70)		
Series 3 Pre-Compression (for shear test)	W/G Saturated	Radial	22	0		
			80	30		
			120	50		
	Sulfonated	Radial	22	60		
				65		

* Note: W/G: water/glycerol (1/8)

For radial and tangential compression ('R' and 'T' will be added in front of parameter to indicate the compression direction, such as RMOE, TSP1).

(1). Young's modulus (MOE, MPa)

(2). First plateau stress (SP1, MPa)

(3). Second plateau (SP2, MPa)

(4). Specific compression energy (SCE, MJ/m^3)

For longitudinal compression:

(1). Young's modulus (LMOE, MPa)

(2). Yield stress (LSY_d, MPa)

(3). Yield energy (LEY_d, J)

(4). Specific compression energy (LSCE, MJ/m^3)

4.4.3 Shear tests

Albeit the main mechanical action in chip refining is a compression-shear phenomenon, these two actions occur concurrently. It is, therefore, difficult to simulate the same refining action at laboratory level. In fact, the compression and shear actions are inter-related; the shear action in a refiner depends on the compression of chips between refiner plates. For a given input of chips, the compressive and shear forces are small when the refiner clearance is large. As the clearance decreases, both the compression and shear actions increase. When there is no compression, the shear action may not exist. We adopted a simplified approach to investigate the influence of compression on the shearing of wood blocks by employing pre-compressed samples for the shear tests. It is hoped that this step-wise approach would yield useful information regarding the mechanism of wood failure under external stresses.

In this part of experimentation, four groups of sample (series 3) were first pre-compressed to different strains (0%, 30%, 50%, 60%, 65%) under various conditions as indicated in Table 4.4. These samples were then sheared in the radial-longitudinal plane. The RL-shear will indicate the effect of compression on the strength weakening in wood matrix. The conditions used in the shear tests were as follows:

(1). Specimen dimension: 11x 15 x 28 mm (L x R x T)

(2). Shear type: RL-shear (longitudinal direction shear to generate shear surfaces in RL-plane)

(3). Loading speed: 10 mm/min.

(4). Data collecting rate: 10 data/Sec.

(5). End strain 27%

The following parameters are evaluated using the shear stress-strain curves. Discussions on these parameters are given in Chapter 7.

(1). Shear modulus (G, MPa)

(2). Shear yield stress (τ_y, MPa)

(3). Shear maximum stress (τ_{Max}, MPa)

(4). Shear yield energy (E_y, J)

(5). Shear total energy (E_t, J)

4.5 Microscopic Analyses

The characteristics of wood failure under compression and shear loading were examined by means of light microscopy and scanning electron microscopy. The features of interest included the location of an initial fracture, the mode of rupture, and structural changes in fiber wall, etc.

4.5.1 Analyses by light microscopy

A transmission light microscope (Zeiss Photomicroscope III, West Germany) and a stereo-microscope (Wild TYP 352837, Heerbrugg Switzerland) were used in this study. Photomicrographs were taken with the former. To observe surface characteristics of sample blocks using the transmission light microscope, two external light sources (Intrlux® 6000-1) were used to provide incident light to the sample under observation.

The surface of sample to be observed was prepared in water saturated condition using a sliding microtom prior to the compression. The compression was performed manually using a specially designed device (Figure 4.6 and Figure 4.7).

4.5.2 Analyses by scanning electron microscope (SEM)

Surface failure characteristics of samples compressed by the Instron machine were studied by means of a scanning electron microscope (JSM-5500, from JEOL). Twenty samples were examined as listed in Table 4.5.

Table 4.5 Samples subjected to SEM analysis

Samples	Samples code	Compression temp, °C	End strain, %	SEM code	Observed planes
Series 1 Compressed W/G - saturated samples	R120	120	70	RRL RTL	Manually cleaved radial-longitudinal and tangential-longitudinal planes
	T120	120	70	TRL TTL	
	L120	120	50	LRL LTL	
Series 3 Compressed water - saturated samples	MC2	22	0	A0RL A0TL	Sheared radial-longitudinal planes, & Manually cleaved tangential-longitudinal planes
	MC65	22	65	A65RL A65TL	
Series 3 Shearing of precompressed W/G - saturated samples	MCS0	120	0	B0RL B0TL	
	MCS50	120	50	B50RL B50TL	
	MCS65	120	65	B65RL B65TL	
Series 3 Compressed sulfonated samples	MCSS0	22	0	C0RL C0TL	
	MCSS65	22	65	C65RL C65TL	

Chapter 5 - Results and discussions: Effect of temperature on wood compression

This chapter consists of two parts. Part one describes the general technical considerations of wood compression and the behaviors of wood compressed in different directions. Part two discusses the wood behaviors under compression at three different directions and effect of temperature on the compression.

5.1 Temperature control

Temperature is an important parameter affecting the compression behavior of wood. It can be easily controlled during the compression tests. The best approach would be conducting the tests in an autoclave [62], but this technique requires a special load cell, and the compression system could be rather complicated. A simple alternative is to use a heating medium such as glycerol because glycerol has a high boiling point of 290°C and has physical and chemical properties similar to those of water [59, 61]. This method eliminates the use of a pressurized system when only water is used.

The use of glycerol as a heating medium requires tedious preparation of glycerol-saturated samples such as that described by Sadoh [140]. Basically, the samples were first immersed in 50% glycerol for 48 hours at 60°C, under vacuum. They were then oven-dried before again being immersed in glycerol for 24 hours at 60°C, under vacuum. However, this procedure may affect the wood properties due to long exposure at that high temperature.

The heating chamber (electrically heated air) of the Instron machine was used to maintain the desired temperature throughout the testing process. As indicted in Figure 5.1, it took about 7 min to reach 120°C in the testing chamber, and 35 min was required to obtain this temperature in the center of samples. However, the moisture content of sample was only 0.08% at this stage, meaning that it cannot be heated above 100°C until it was completely dried. To overcome this difficulty and to obtain the desired temperature and moisture content we used glycerol as a heating medium.

The heating medium actually used in this study was a mixture of water and glycerol (W/G = 1:8 by volume) instead of 100% glycerol. This formulation minimized the tedious procedures in sample preparation and the possible thermal alteration of sample properties as mentioned earlier [140]. The mixture had a boiling point of 150°C, which was sufficiently high for our maximum required temperature (140°C).

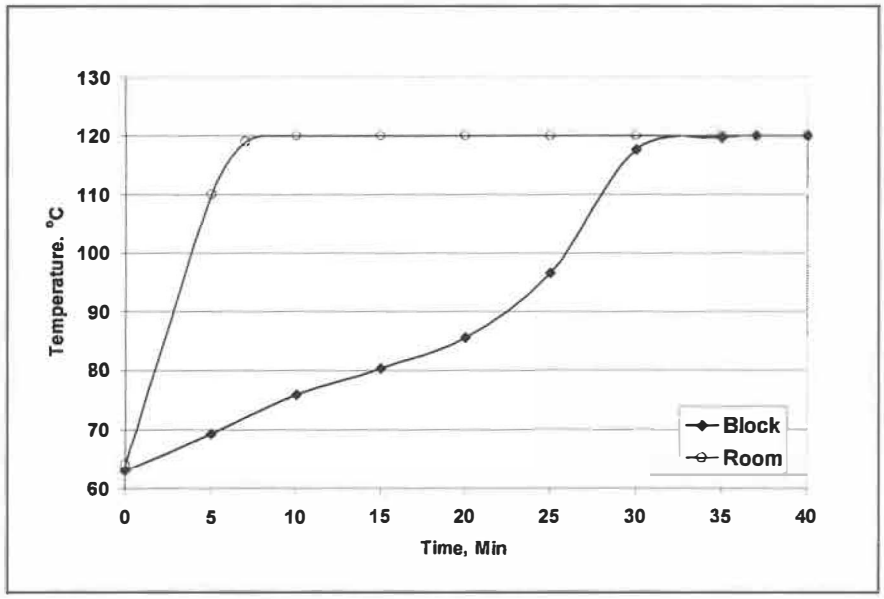

Figure 5.1 Temperature in the center of sample by hot air heating

Figure 5.2 shows the radial compression curves for dry samples and those treated and tested with water, glycerol and W/G mixture. The quantitative information for these four samples is presented in Table 5.1 and Figure 5.3. Note that there are noticeable differences in modulus (MOE), first plateau stress (SP1) and specific compression energy (SCE) between the sample groups, the water treated samples being the lowest while the dry samples the highest, as shown in Figure 5.3. The values for the glycerol or W/G treated samples lied between. It is also noted that the water treated samples tended to have slightly higher second plateau stress (SP2) when compared to those treated with glycerol or W/G mixture. We found that the compression curves for the dry samples did not show a second plateau (SP2), and it exhibited some degrees of fluctuation in the early stage of the first plateau region. This characteristic was noted in all compression curves of dry samples, which was probably due to the unstable response of the EW fibers in dry condition.

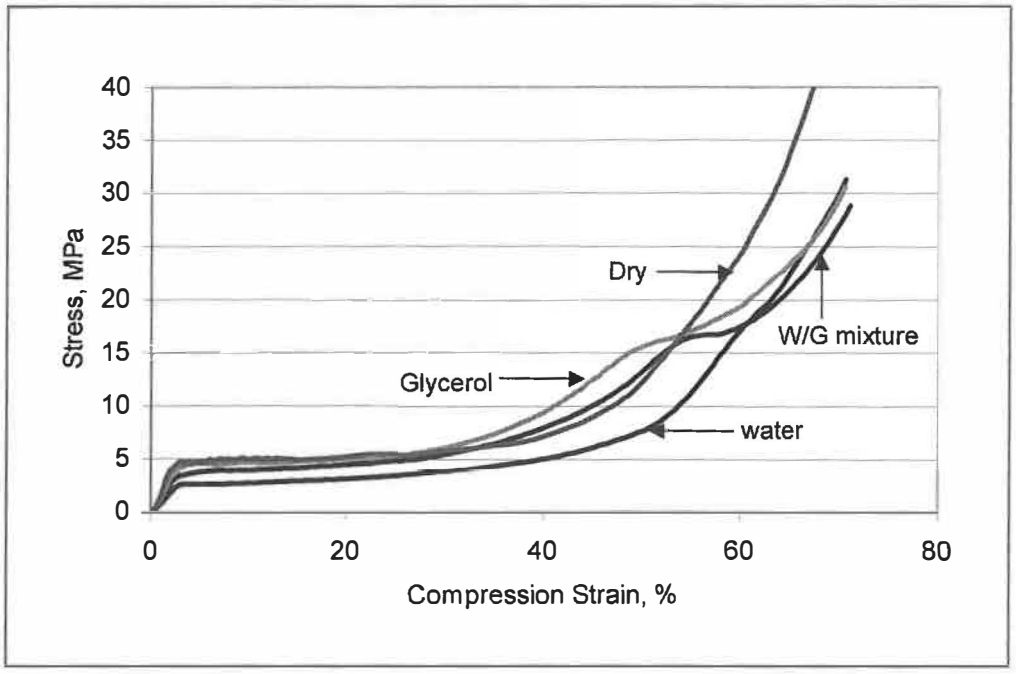

Figure 5.2 Radial compression curves of samples of four different treatment conditions (22°C)

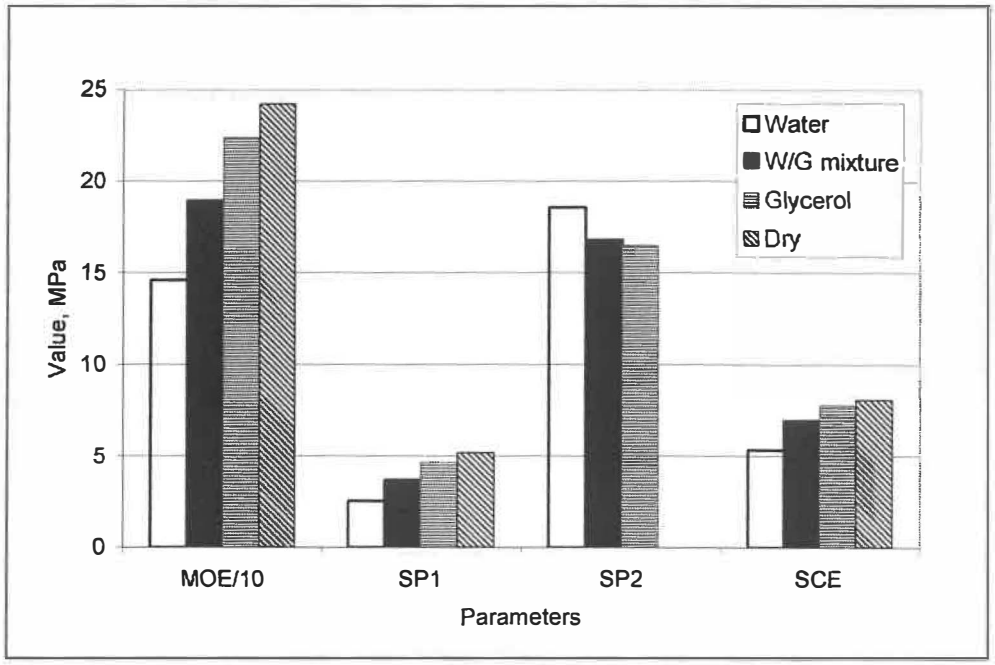

Figure 5.3 Compression properties of four different treatment conditions

Table 5.1 Physical properties of different liquid-saturated samples

Medium	MOE, MPa	SP1, MPa	SP2, MPa	SCE, MJ/m^3
Water	146 (26.6)[a]	2.56 (8.1)	18.55 (10.9)	5.33 (14.0)
W/G mixture	189.2 (31.4)	3.69 (8.3)	16.78 (5.4)	6.96 (17.7)
Glycerol	223.5 (27.9)	4.52 (8.5)	16.47 (14.7)	7.77 (11.6)
Air-dry	241.7 (18.2)	5.20 (8.3)	--	8.08 (9.0)

[a] Data in brackets are the coefficient of variation in percentage (CV,%).

The compression curves for water treated samples differed from those sample treated either with 100% glycerol or W/G mixture not only in magnitude (Table 5.1) but also in its form. This was particularly evident when the compression strain was greater than 50%. The extent of the second plateau of the glycerol-related samples was relatively longer when compared with that for the water treated samples, which might be due to the possible effect of plasticization of water or the larger molecular size of glycerol, lowering its displacement rate from lumens during compression. In contrast, their SP2 was about 10% lower in comparison with the water saturated samples, indicating the possibility that glycerol could facilitate fiber separation under compression force. Despite these differences, it was generally believed that water and glycerol had similar softening ability as reported in [61, 75]. Our results are in line with their findings, and indicated that W/G mixture could be a good substitute of water or glycerol as a heating medium. However, the physical properties of samples saturated with different liquids may not be compared directly.

There were differences in heat transfer ability between the three heating mediums, as shown in Figure 5.4. It shows that water heated faster than glycerol and that any addition of water to glycerol reduced the heating time for a given temperature. Figure 5.5 shows the increases in temperature at the center of samples treated with glycerol and W/G mixture. The time required to reach 140°C in the center of samples was similar for both heating mediums, about 7 min. In our tests, we preheated all samples in W/G

mixture for 15 minutes before conducting compression tests, ensuring a uniform heating for all samples.

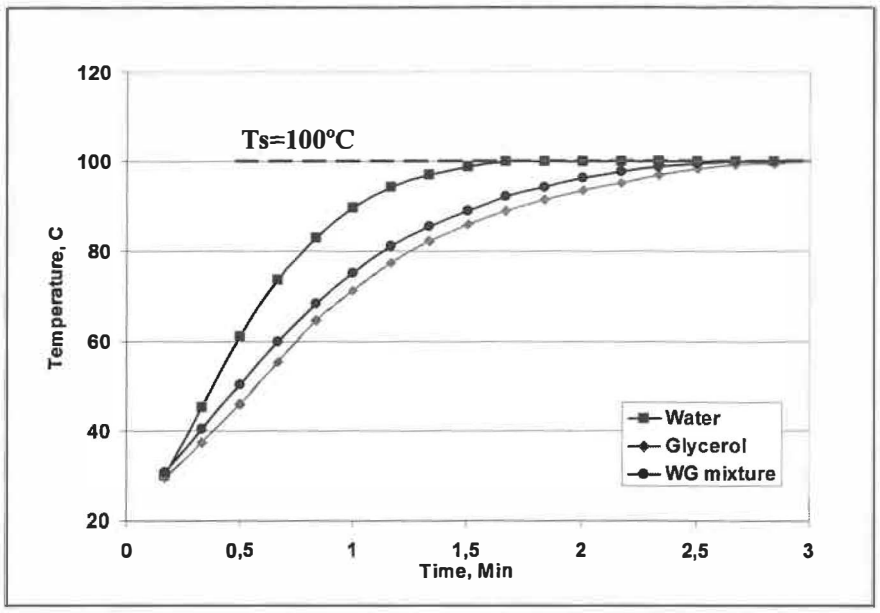

Figure 5.4 Temperature increase in samples in three different heating mediums (testing room temperature 100°C)

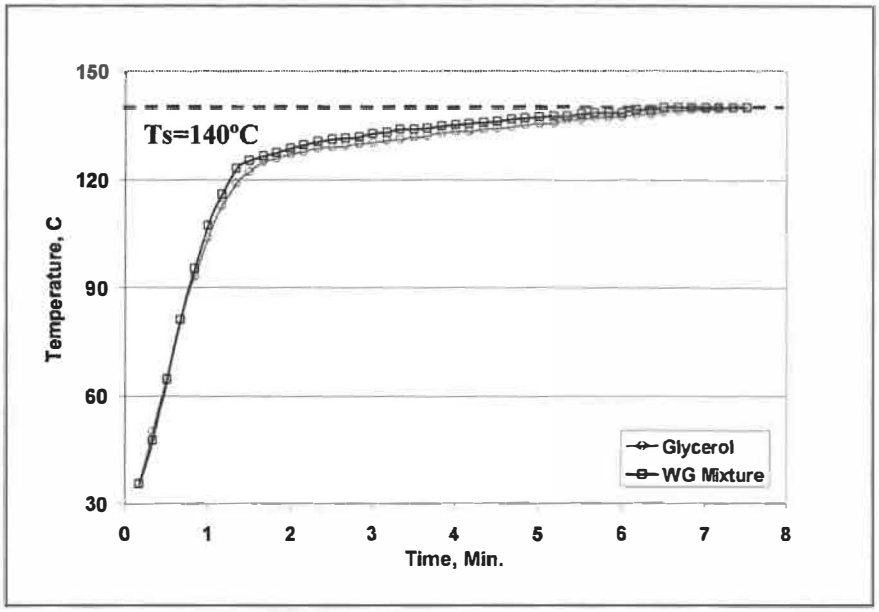

Figure 5.5 Temperature increase in samples in glycerol and W/G mixture (testing room temperature 140°C)

5.2 Effect of temperature on wood compression

This part discusses the influence of the direction of compression in relation to fiber axis and the effect of temperature of wood under compression. The samples used in this study were all saturated and heated with a mixture of water and glycerol (W/G = 1:8). Other experimental variables were kept constant and similar to those used in other trials, as described in chapter 4.

The term "stress" was defined as the applied force divided by the initial cross-sectional area of sample under load, while the term "strain" was defined as the ratio of the displacement of the crosshead of the testing machine and the initial height of specimen. The reported property values were the average of 8-10 replicates in most cases. To identify the properties at different directions, letters 'R, T, and L' were added in front of those properties, indicating the compression directions of radial, tangential and longitudinal direction, respectively. For examples, RMOE, TMOE represent the modulus at radial and tangential direction, respectively.

5.2.1 Radial compression

5.2.1.1 Characteristics of radial compression

Figure 5.6 presents 10 compression curves for the W/G saturated samples compressed in radial direction at 140°C. The characteristics of these curves are similar to those reported by other researchers [61, 62, 65]. A typical curve shows an elastic region (I) followed by an extended plastic plateau (II) and then a densification region (III) with sharp increase in stress.

Microscopic examination indicated that in the early state of compression only the EW responded to the compress stress. In the elastic stage, no evident changes could be observed in samples. However, the EW fibers were collapsed successively in the first plateau stage (Figure 5.7 A to C). At the end of the first plastic plateau, most of the EW fibers were completely collapsed and their cell wall buckled extensively. Some fibers in the transition zone between EW and LW were also collapsed. The LW fibers deformed only slightly at this stage. Hence, the elastic modulus and the first plateau stress are the

properties of EW fibers. The stress at this plateau reflects directly the transverse resistance to collapse of EW fiber.

In this study, the first plateau stress (SP1) is defined as the stress at 10% compression strain, as show in Figure 5.8. The stress also termed as offset yield stress or zero slope yield stress. The stress value may also be set at 5% strain in some investigations. The stress at 5% strain may represent the stress of the EW fibers developed in the very early stage of the growth season (near the LW of last season). These fibers have the biggest lumen and very thin cell wall. The stress at 40% strain may represent the stress of EW fibers in the later portion of EW zone. These fibers tend to have thicker cell wall and smaller lumen when compared to the initial EW fibers. For these morphological variations, a compromise was made to set the first plateau stress at 10% compression strain. The extent of the first plastic plateau is associated with the EW/LW ratio; high proportion of LW means shorter plastic region.

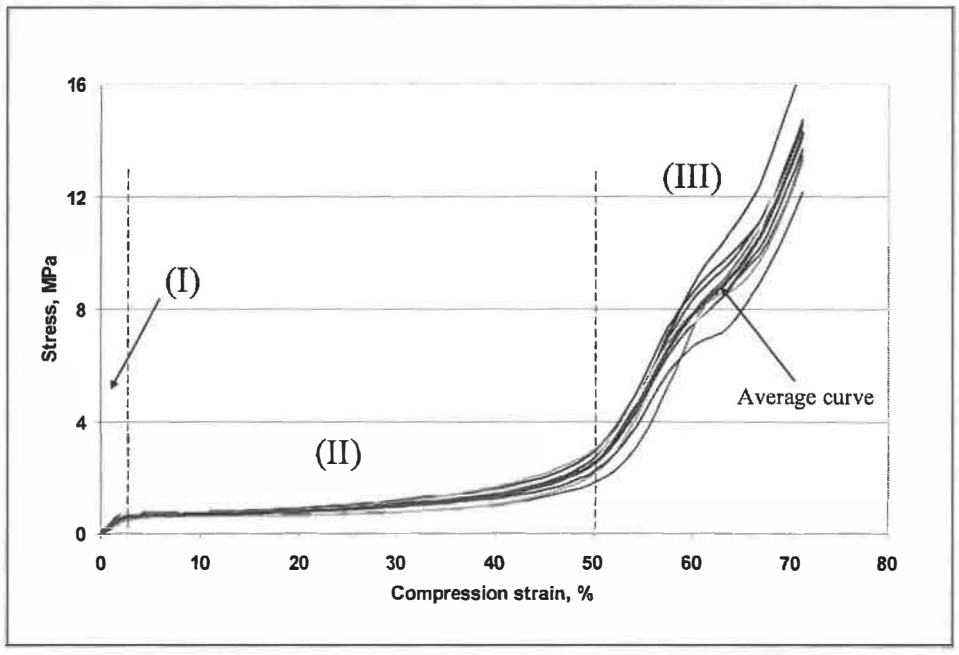

Figure 5.6 Typical radial compression curves (140 °C). (I) Elastic region, (II) Plastic plateau, (III) Densification region

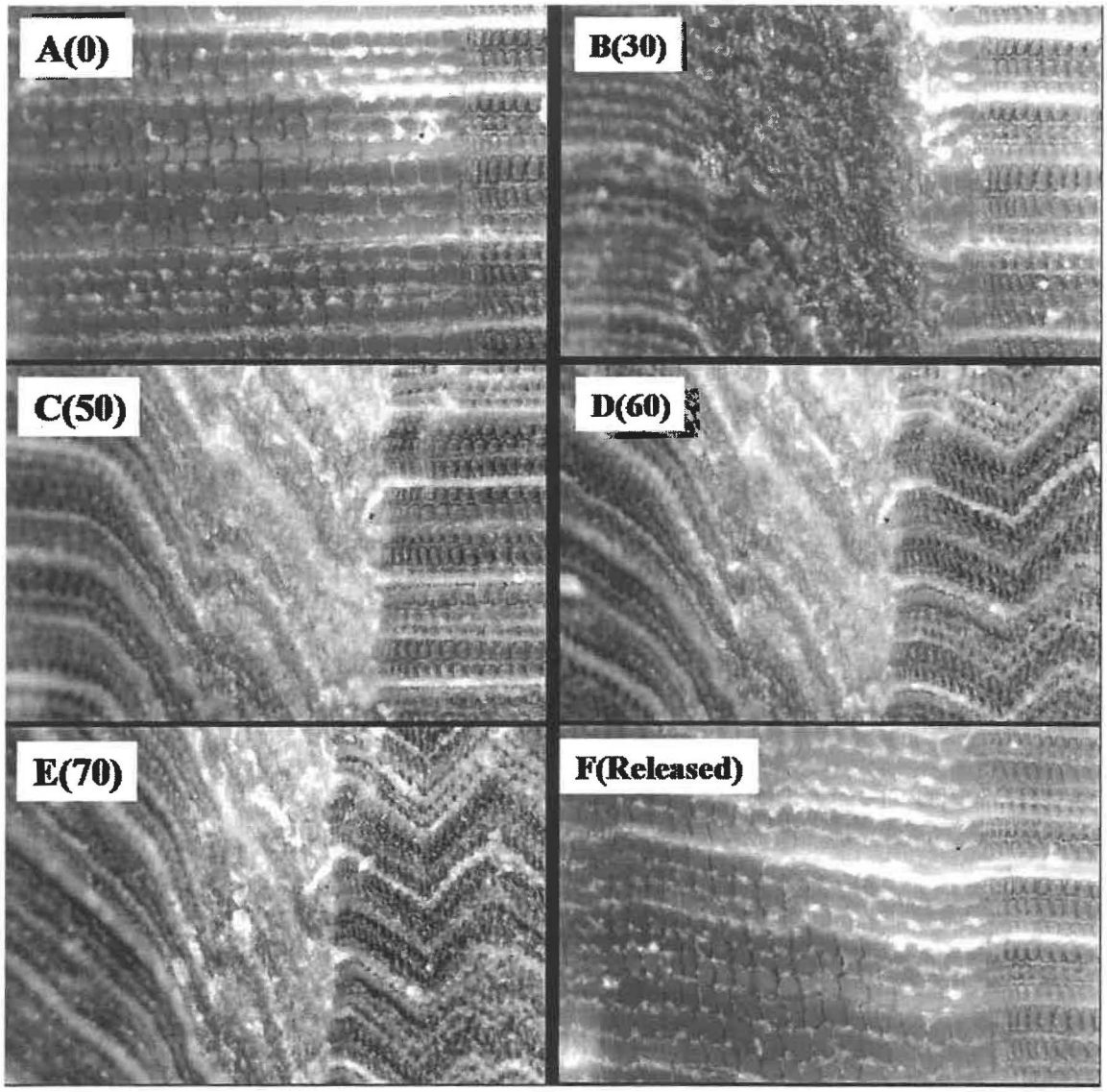

Figure 5.7 Progressive deformation of fiber under various radial compression strains of water saturated sample (22°C, number in bracket represents compression strain in percentage)

Generally, the stress at 10-20% compression strain is quite stable. This is also one of the reasons why the first plateau stress (SP1) was defined at strain of 10% in this investigation. This property can be used to characterize the collapsibility of EW fibers in different compression conditions. In fact, it is a quantitative parameter that could be used to characterize the behavior of wood in the plastic plateau (region II).

Following the first plastic plateau was a stage with sharp increase in stress. As the stress increased a second stress plateau occurred at about 60% strain, which was relatively short when compared to the first stress plateau. This brief stress plateau is usually ignored in many investigations because in most studies a maximum compression strain of 50% or less has been used. Uhmeier et al [59] noted this short second stress plateau in a study on heated spruce wood, and accounted it as a result of fracturing of the test samples. However, our microscopic observation (Figure 5.7 E, F) indicated that the wood specimens remained integral even when they were compressed to 70% strain. We believed that this short plateau was caused by sudden failure (fiber separation) developed in specimen, particularly in the LW region.

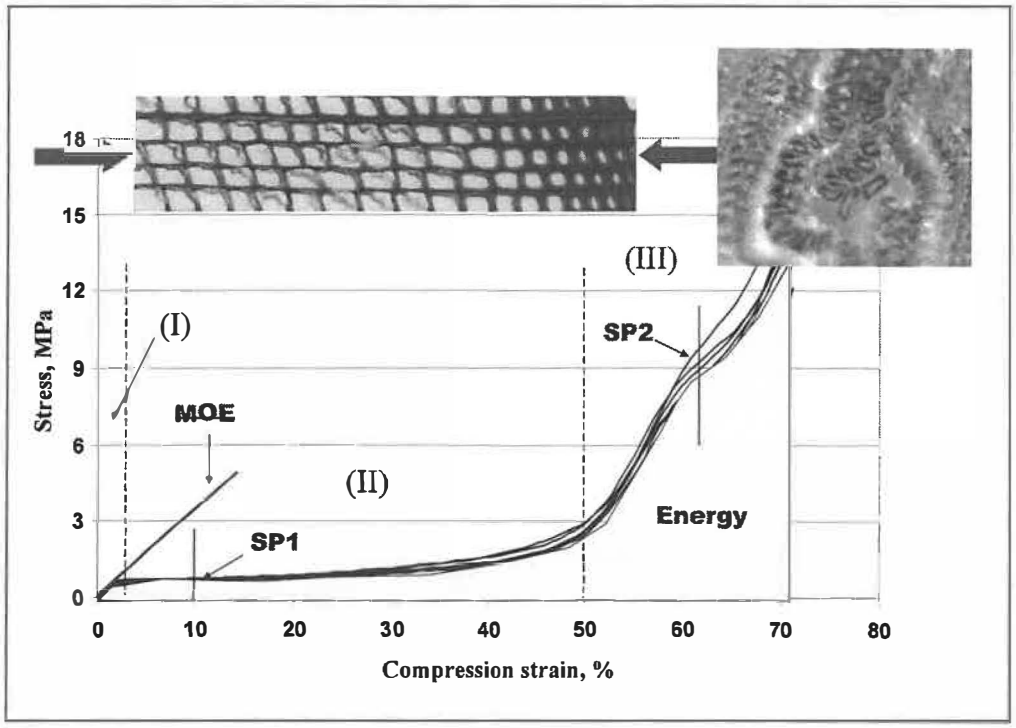

Figure 5.8 Definition of four parameters used to characterize wood compression

MOE: Young's modulus, MPa (Region I)

SP1: 1st plateau stress, MPa (Region II, collapse of EW fibers)

SP2: 2nd plateau stress, MPa (Region III, separation of LW fiber)

SCE: Specific energy consumption (Energy/Volume), MJ/m^3

We termed the stress at this plateau as the second plateau stress (SP2). It is determined by the slope curve of the stress-strain curve and is located at the point corresponding to the bottom of the slope curve' valley, in the neighborhood of 60% strain (Figure 5.9). To simplify the data processing, the value of SP2 will be obtained directly by an embed-sensor from stress-strain curve during the test on Instron machine.

At this second plateau stage, the cell wall of LW fibers buckled and the fiber lumen decreased noticeably (Figure 5.7 D). As such, the SP2 may represent the stress generating the initial failure in LW (fiber separation). This fiber separation was evident between the fibers (tracheids) and ray cells in radial plane. Note that the SP2 occurred only when the compression strain exceeded about 50%. The position of second plateau on the stress-strain curve depended on the EW/LW ratio. It might occur at a strain less than 60% when the wood sample contained large proportion of LW. Sample dimension also has an important influence on the second plateau. When the dimension is relatively large (in tangential direction), the friction between the sample surfaces and the two-compression plates increases, restraining the sample from lateral expansion. The second plateau might not appear because there is no sudden failure. This situation can be seen later in the third series of trial. However, despite the absence of the second plateau, the fiber separations were still occurred at correspondent stage as was proofed in later shear test. The SP2 was used for the first time as a quantitative parameter to characterize the response of wood at high compression strain (densification region, or region III) in this work.

When the compression strain increased to 70%, extensive shear force was created between different layers of LW, generating many small cracks or slip planes in the specimens. The LW fibers collapsed extensively (Figure 5.10). They remained partially collapsed (Figure 5.11) even when the compression force was released. The force required to collapse the LW fibers was about 10-15 times higher than that for the EW fibers. In compression without restraint the LW fibers did not collapse uniformly throughout the cross-section of specimen. Because of the lateral expansion in tangential direction the LW fibers on the radial edges of sample were less affectted and they

remained unflattened. This result is different form the observation of Tabarsa et al. [65] who claimed that latewood cells did not collapse under compression.

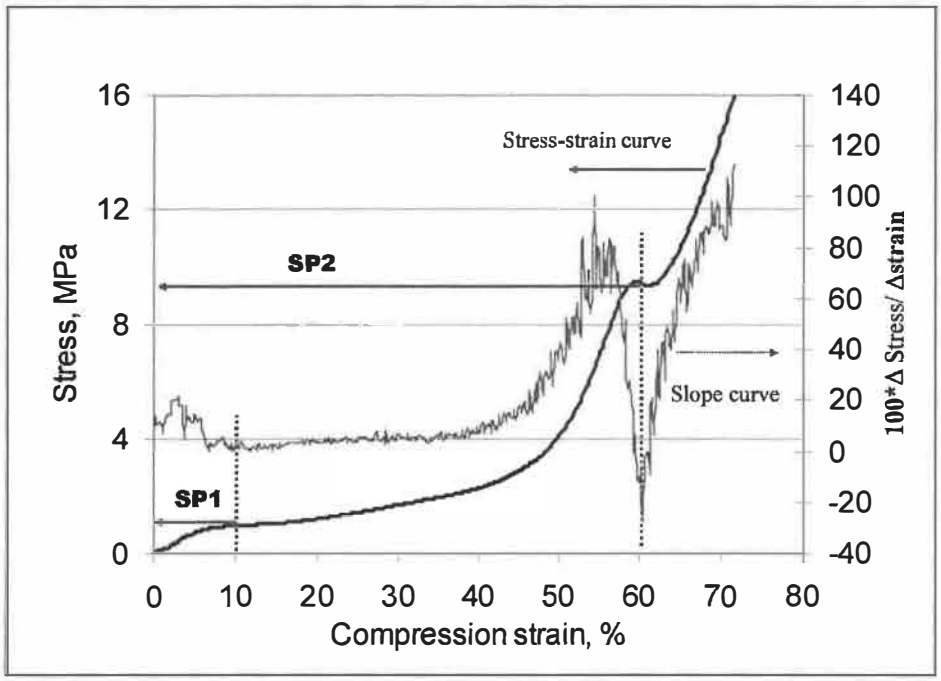

Figure 5.9 Mathematic definition of second plateau stress (SP2)

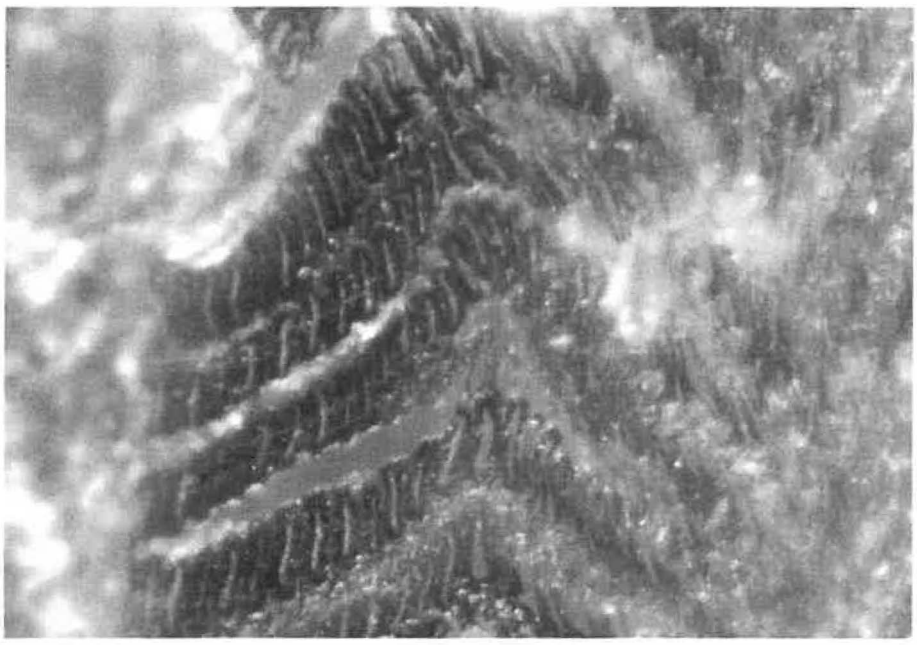

Figure 5.10 Extensive collapse of latewood fibers at compression strain of 70% (22˚C)

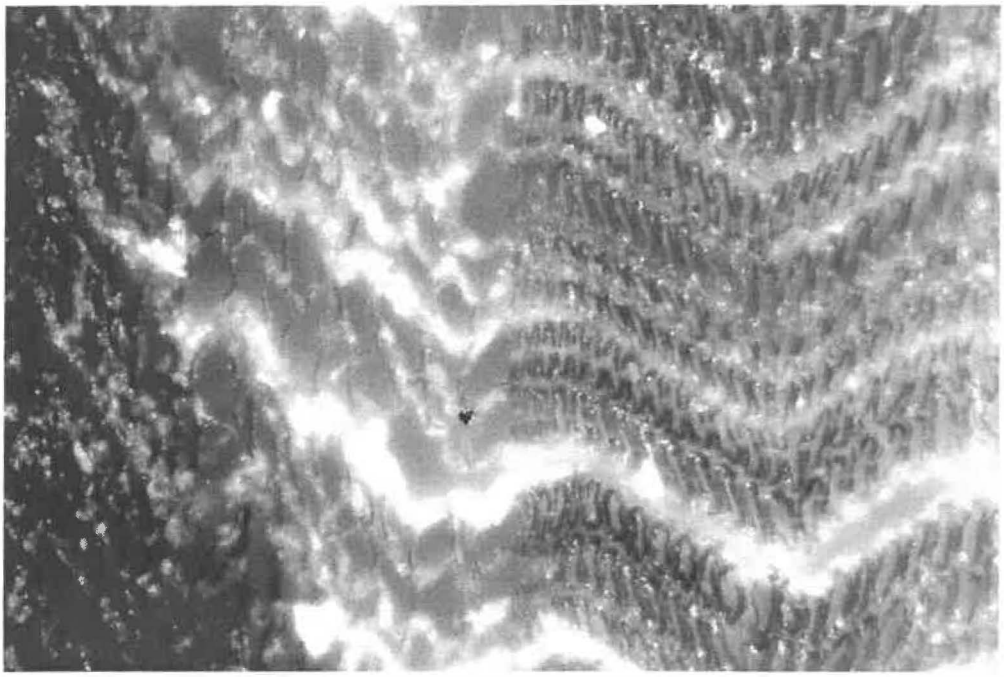

Figure 5.11 Deformation of fiber pressed to 70% and released in air for 2 minutes (22°C)

Occasionally, the collapse of LW fibers was noted by Uhmeier et al [59]. As it was noted in this study the collapse of the LW fibers depends on the compression strain. Strain at 50% or less may not be enough to flatten LW fibers. Additionally, if the loading speed or strain rate is too high, the sample may fracture and disintegrate into pieces before the LW fibers are collapsed.

It was observed that both the EW and LW fibers recovered almost completely their original form when the specimen was released from compression load, especially in the presence of water (Figure 5.7 F). The permanent deformation was less than 5% in most cases. The fissures produced by compression would be the locations of initial failure in subsequent treatments. The influence of precompression on shear properties will be discussed later in chapter 7.

Specific compression energy (SCE, MJ/m^3 or MPa) is the energy per unit volume of specimen consumed during compression. It is also termed as toughness in some cases. The SEC can also be expressed in kWh/t. For white spruce, energy of one 'MJ/m^3' correspondent to 0.731 'kWh/o.d.t'.

Modulus of elasticity (MOE), or Young's Modulus, is defined as the slope of initial linear portion of a stress-strain curve. The MOE is widely used to characterize the modification of wood structure by compression. In this study, four parameters, SP1, SP2, SEC and MOE (Figure 5.8) are employed to characterize the responses of wood under compression.

5.2.1.2 Effect of temperature on radial compression

The effect of temperature on the wood compression is mainly determined by the softening temperatures of its main components (cellulose, hemicelluloses, and lignin). Figure 5.12 shows the stress-strain curves of radial compression at various temperatures (22-140˚C), and Table 5.2 summarizes the physical properties at these temperatures. The stress-strain curves indicate that the compression stress decreased steadily with increasing temperature. However, the form of the compression curves remained similar within the range of strain tested, suggesting that there is no fundamental difference in wood behaviors within the limit of temperatures employed. Under compression, they all exhibit an elastic, a plastic and a densification regions.

Table 5.2 Results of radial compression at different temperatures

Temp.	RMOE		RSP1		RSP2		RSCE	
˚C	MPa	CV, %	MPa	CV, %	MPa	CV, %	MJ/m^3	CV, %
22	205	31.4	3.17	8.34	17.2	5.42	6.67	17.7
40	125	31.8	2.36	8.83	14.5	10.6	4.96	12.1
60	86.0	41.3	1.79	10.2	13.3	10.3	4.20	14.6
80	69.4	30.0	1.48	8.23	12.4	11.1	3.57	19.2
100	51.9	29.7	1.10	9.72	11.5	11.8	3.11	18.4
120	38.7	22.2	0.84	8.60	9.62	11.9	2.55	13.6
140	33.6	21.9	0.71	7.48	8.36	11.3	2.16	8.43
Dec. %	83.6		77.6		51.4		67.6	
Av.(CV,%)		29.8		8.8		10.3		14.9

* Note: CV – coefficient of variation, Dec.- total decrease from 22 to 140 ˚C .

As the temperature increased from 22°C to 140°C, the modulus decreased by 83.6%, the first plateau stress by 77.6%, the second plateau stress by 51.4%, and the specific energy by 67.6%.

Despite numerous works on radial compression, there is little quantitative information available. Tabarsa [69] reported a modulus (MOE) of 139 MPa for water saturated white spruce compressed at room temperature. With similar condition we obtained a value of 146 MPa for water saturated and 205 MPa for W/G -impregnated white spruce samples. The value of MOE for our water-saturated samples is comparable to that of Tabarsa. The W/G-impregnated sample showed an increase of 40% in comparison with the water-saturated samples. A similar increase in MOE of glycerol treated specimens was also observed by other researchers [61, 75].

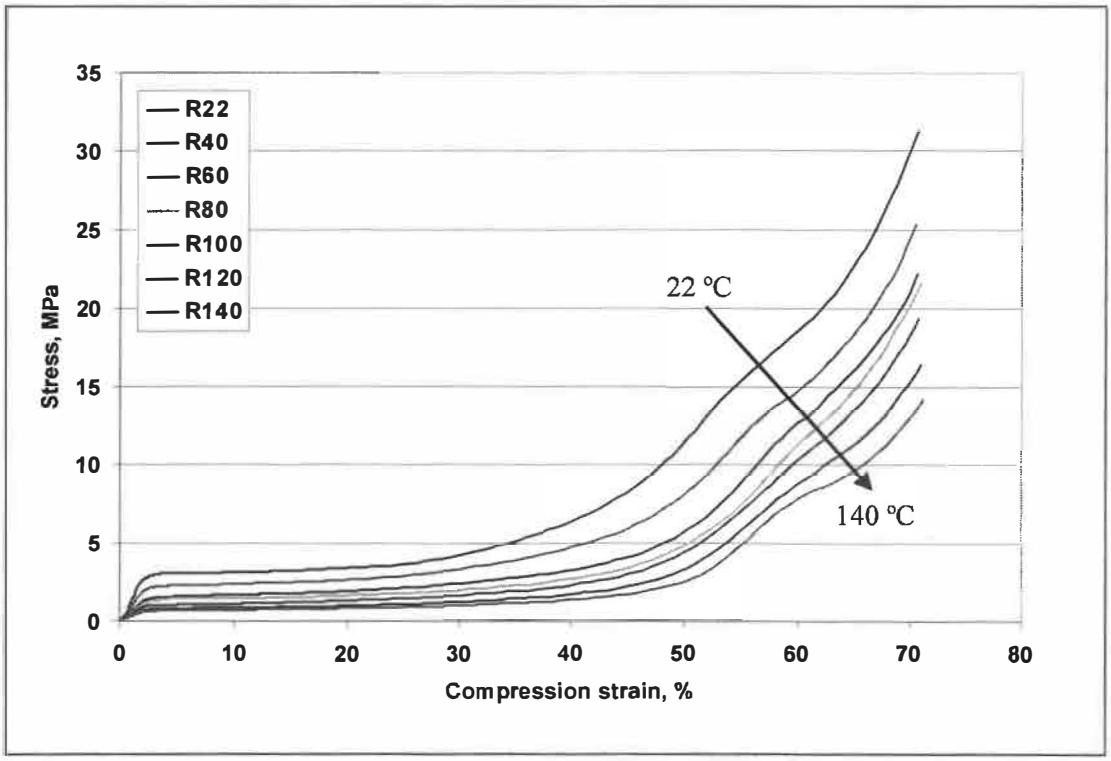

Figure 5.12 Radial compression at various temperatures. Each curve is the average of 8-10 replicates. Number in sample name indicates compression temperature

Figure 5.13 compares the first plateau stress (SP1) obtained in this study with those reported by other researchers. The figure indicates that our SP1 values are about 15 to

20 % higher than those reported by others [61, 75]. The difference might be due to the difference of species used. However, the figure reveals that Norway spruce and white spruce behaved similarly as a function of temperature increase. Note that sample II shown in the figure had been steamed at 120 °C for 30 minutes before tests [61] while sample III had been treated in glycerol at 60 °C for 72 hours and oven dried once [62]. Such thermal treatments might affect properties of wood. A reduction by 13% in SP1 was observed by Uhmeier et al [62] when the wood is boiled in water for 30 minutes and tested at 20 °C. Considering this result the increase by 15-20% in SP1 for our untreated white spruce specimens is reasonable.

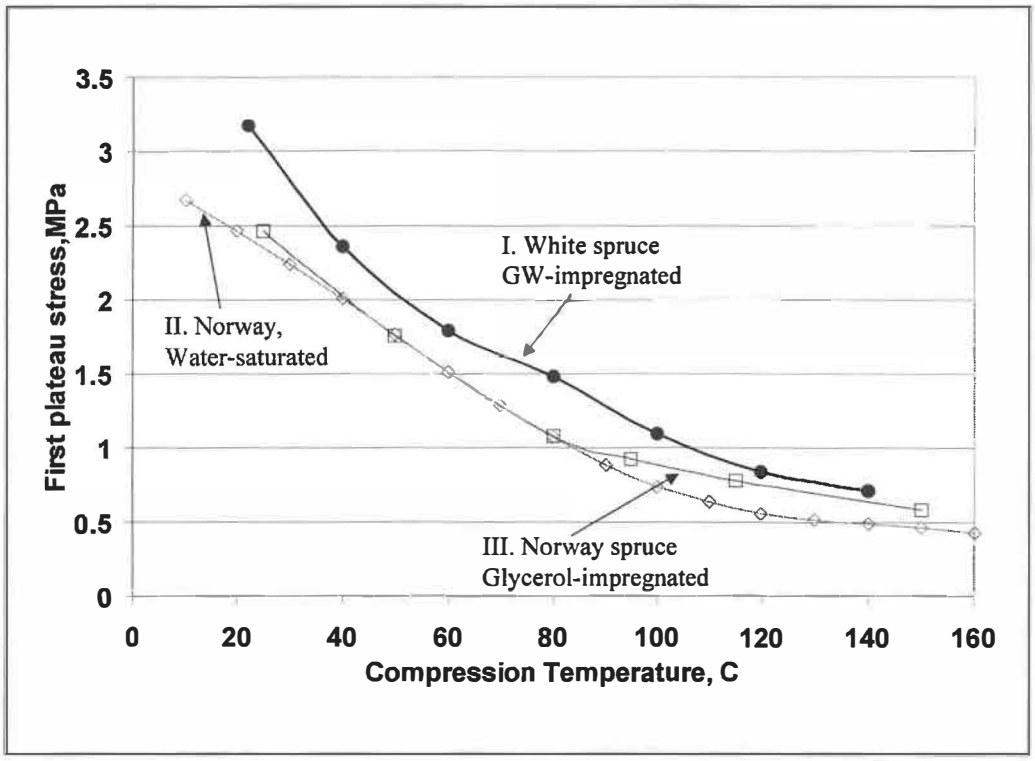

Figure 5.13 Comparison of first plateau stress at various temperatures with results of others

I. W/G- impregnated white spruce (RTL, 10×10×10), test speed: 3 mm/min
II. Water-saturated Norway spruce (RTL, 10×10×10), test speed: 2.4 mm/min [61]
III. Glycerol-impregnated Norway spruce (RTL, 10×10×20, test speed: 0.05 mm/min [62]

5.2.2 Tangential compression

5.2.2.1 Characteristics of tangential compression

Figure 5.14 shows the typical tangential compression curves. Obviously, the tangential compression curves are quite similar with those of radial compression. They also show an elastic region, a plastic plateau and a densification region. However, the LW behaved differently in tangential compression. After the elastic region, it began to bend and buckled, and deviated from its original straight line. Meanwhile, the weak EW fibers began to collapse at the regions where the compression force was concentrated. This dislocation of LW and the collapse of EW happened throughout the whole plastic region. The EW fibers collapsed completely at about 50% strain. Similar to the radial compression, tangential compression also showed a short second stress plateau at about 60% strain, where fiber separation occurred and the sample was locally fractured. The samples were deformed into a 'C' form, having a typical fracture in the mid height of the sample due to excessive bending. The collapse of LW fibers was also observed at 70% strain. But the collapse was not as uniform as that observed in radial compression.

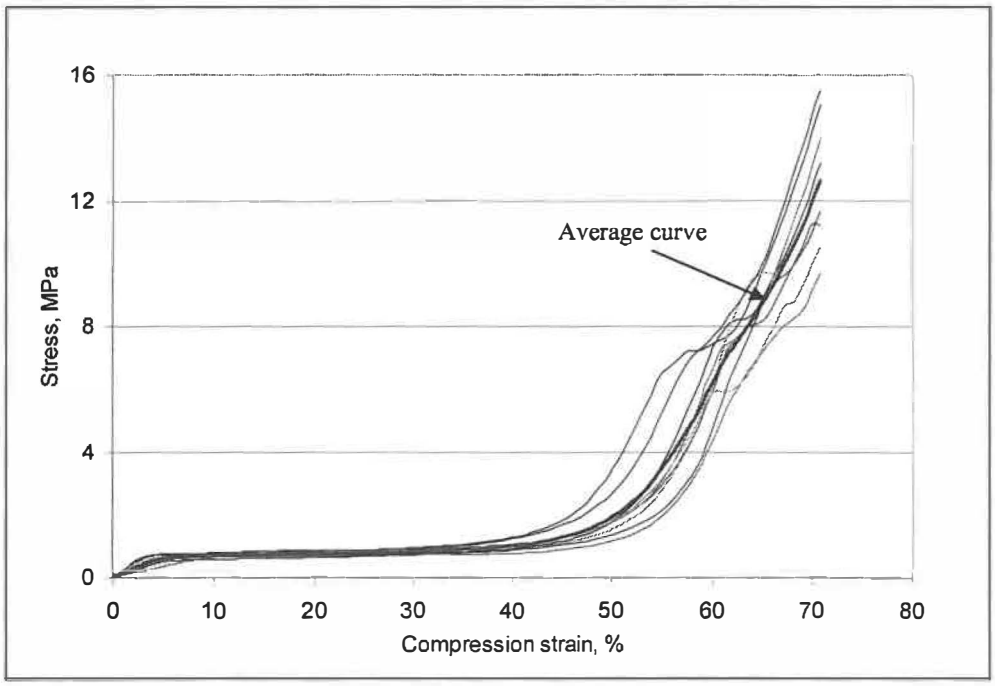

Figure 5.14 Typical tangential compression curves (140°C)

In general, the wood fibers behaved similarly in both radial and tangential compression. The four parameters (MOE, SP1, SP2 and SCE) used for characterizing the response of wood in radial compression were also employed to characterize tangential compression.

5.2.2.2 Effect of temperature on tangential compression

The effect of temperature on tangential compression is shown in Figure 5.15. The extend of the first plastic plateau was similar to that of radial compression except that the increase in stress was more gradual in the latter part of the plateau when compared to the radial compression.

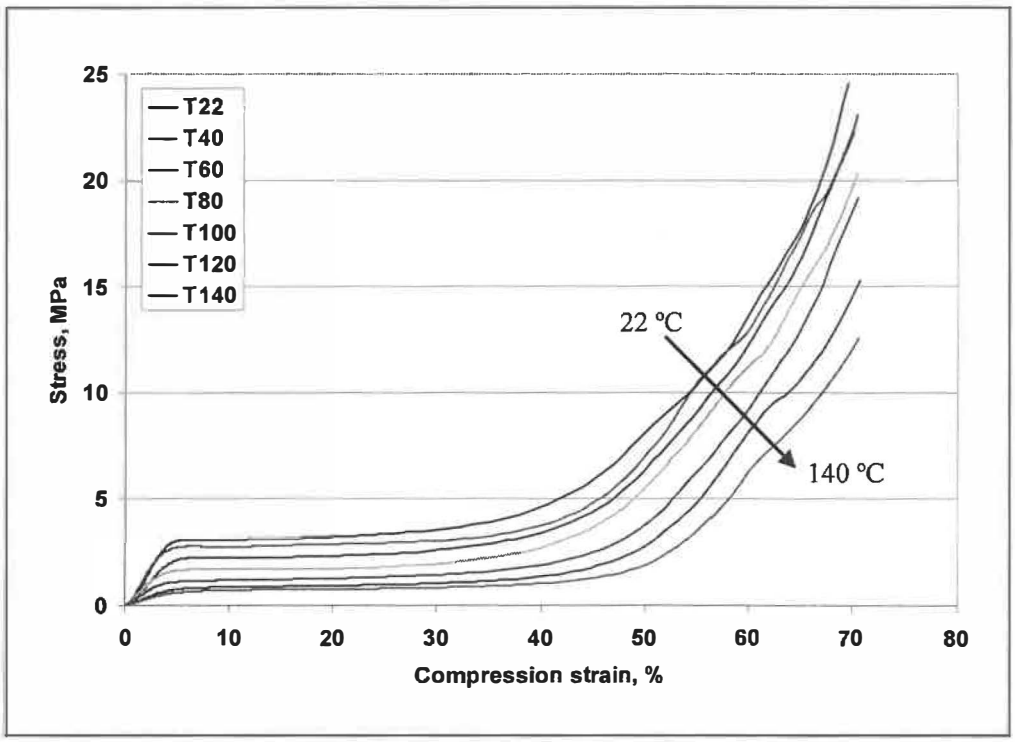

Figure 5.15 Tangential compression at various temperatures

As indicated in Table 5.3, the MOE was decreased by 82% in tangential compression. The levels of decrease in other properties (SP1, SP2 and SCE) were also similar to those observed for radial compression, revealing the similarity in radial and tangential compression. In fact, there are no absolute radial and tangential compressions since the compressions (radial and tangential) were carried out without restrain. In both cases, the

specimen deformation is quite complicated with fiber collapse, fiber dislocation and rotation, and lateral displacement, etc.

Table 5.3 Results of tangential compression at different temperatures

Temperature	TMOE		TSP1		TSP2		TSCE	
°C	MPa	CV, %	MPa	CV, %	MPa	CV, %	MJ/m^3	CV, %
22	101	21.3	3.42	9.42	14.6	17.2	4.79	14.3
40	96.5	21.2	2.77	10.9	12.7	17.6	4.51	10.5
60	67.0	32.0	2.23	16.1	12.3	13.9	4.06	14.9
80	56.2	24.1	1.69	10.2	10.4	15.3	3.01	13.7
100	40.6	20.3	1.19	7.56	9.14	19.4	2.80	13.7
120	23.0	24.7	0.89	12.0	8.60	15.6	2.32	14.2
140	17.9	34.6	0.73	8.36	7.96	14.9	1.78	17.0
Dec., %	82.3		78.7		45.5		62.8	
Av.(CV,%)		25.5		10.6		16.3		14.0

5.2.3 Longitudinal compression

5.2.3.1 Characteristics of longitudinal compression

Wood responds differently in longitudinal compression when compared to transversal compression, Figure 5.16 indicates. As shown in Figure 5.17, the stress increased linearly in the elastic region. When it reached a turning point A, where the fibers buckled and 'slip planes" or "kinks' took place, indicating the occurrence of the first slight permanent structural change [72]. The stress at this turning point was about 70% of the ultimate stress. The latter was noted at about 4% strain (point B). Beyond the point B, there was a region where the stress remained relatively stable (from point B to point C). When the specimen was strained beyond the point C, the stress dropped rapidly and leveled off (D).

Microscopic observation showed that most failures were initiated in the region A-B. The plateau from B to C represented the propagation of micro-cracks, which might not significantly decrease wood's longitudinal compressive strength because the sample remained intact at this stage. The length of this B-C region may represent the ability of wood sample to remain intact. Beyond the point C, the stress began to decrease rapidly, probably due to the development of macro-cracks (point C to point D). The cracks took place at the EW/LW boundary and between the ray cells and fibers. Complete fracture of specimens was also observed in a few cases. When the specimen was strained beyond the point D, the stress began to increase steadily, which is partly due to the combined effect of longitudinal and transverse compressions of wood fibers.

Longitudinal compression is rather complicated. Discussions on the failure process [73] and fracture morphology produced by longitudinal compression have been reported in [72]. Our discussions in this study are mainly focused on the effect of temperature on the longitudinal compression. Four parameters, MOE, SCE, yield stress (SY_d) and yield energy (EY_d) were used to characterize the longitudinal compression. The definitions of these parameters are illustrated in Figure 5.17. Briefly, the MOE and SCE are same as defined previously for the radial and tangential compression. The yield stress (SY_d) is

defined as 1% offset yield stress (MPa) while the yield energy (J) is the energy accumulated to the yield point.

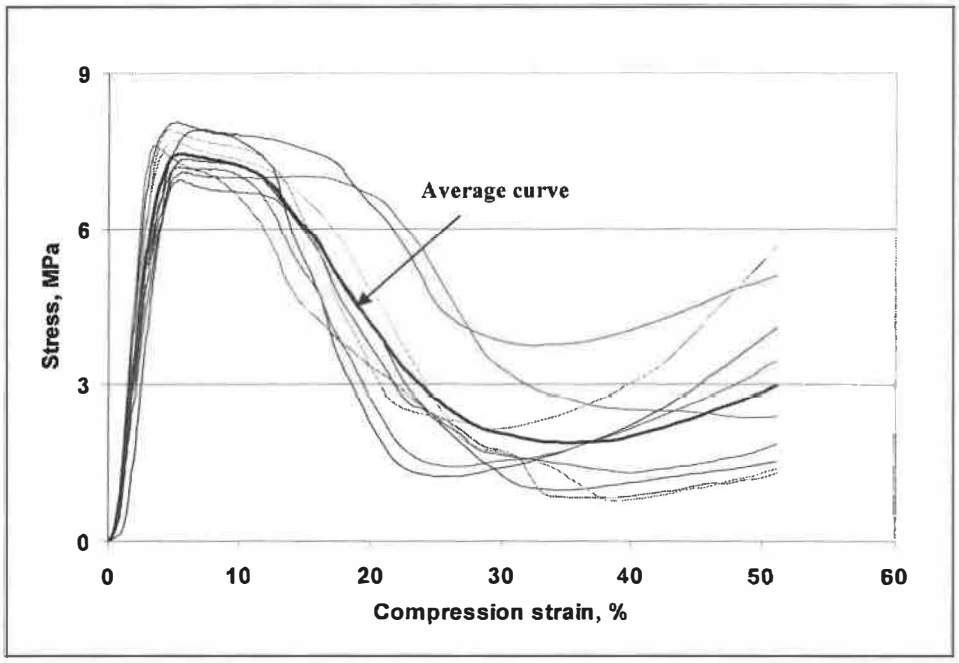

Figure 5.16 Typical longitudinal compression curves (140°C)

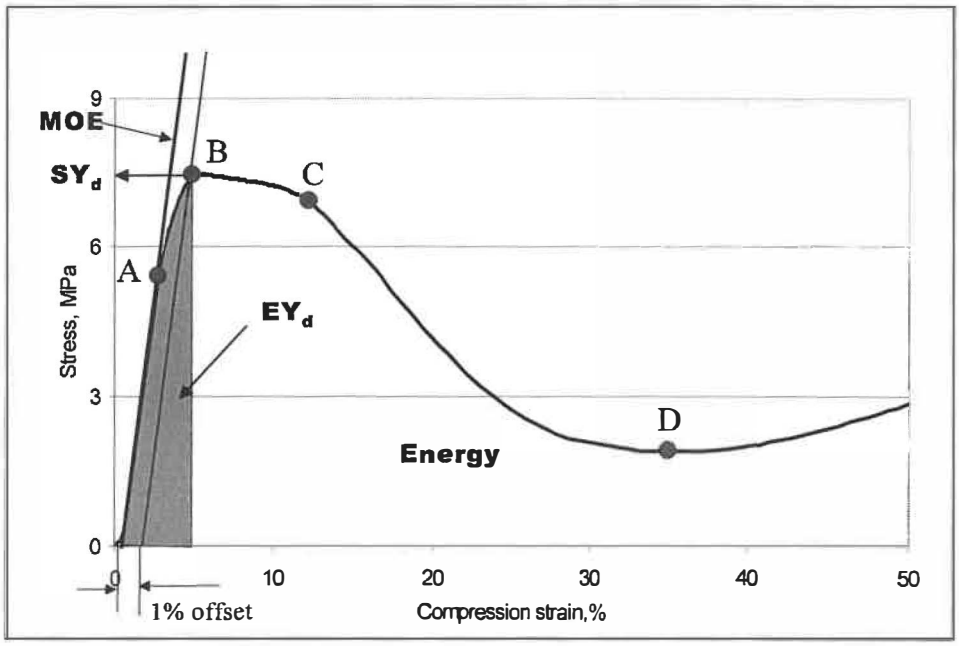

Figure 5.17 Longitudinal compression processes and some definitions

5.2.3.2 Effect of temperature on longitudinal compression

Figure 5.18 illustrates that the effect of temperature on the longitudinal compression is more complicated than that on transverse compression. The form of the compression curves changed when the temperature increased. First, at low temperatures, the drop in maximum stress was abrupt and the peak was narrow. The width of the peak increased gradually with increasing temperature; it was almost flattened out at 140°C. Second, the second part of the compression curves, after the fall in maximum stress, tended to increase with increasing compression strain when the temperature was low. This tendency leveled off at high temperatures.

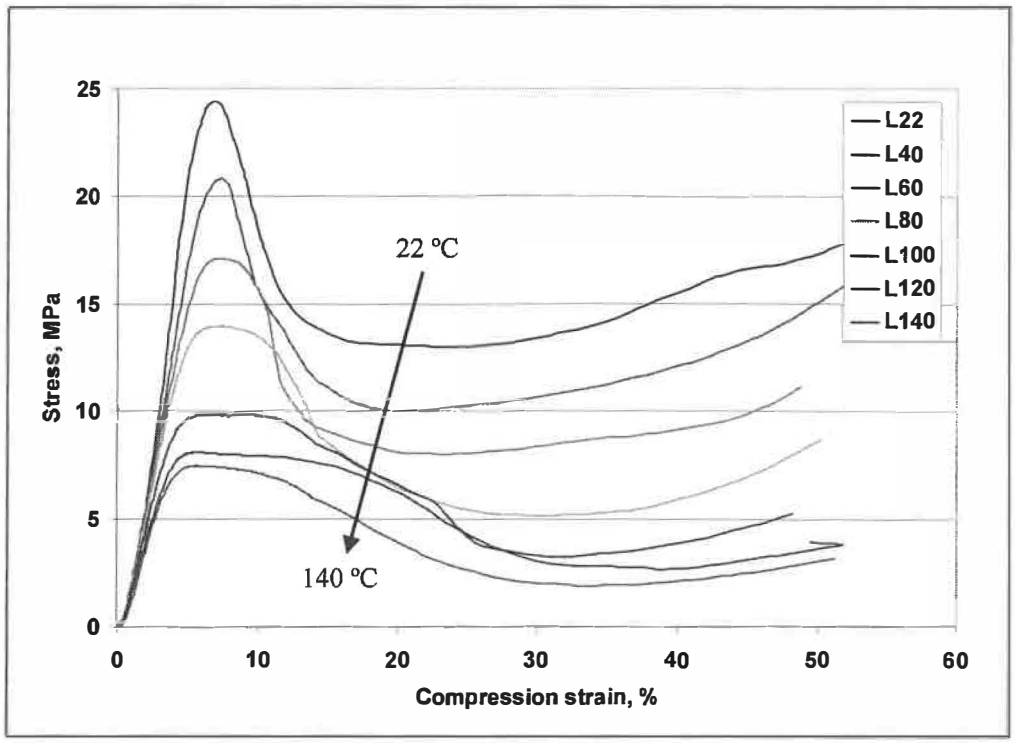

Figure 5.18 Longitudinal compression at various temperatures. Each curve is the average of 8-10 replicates.

The characteristics observed in longitudinal compression are associated with the softening effect of high temperature on the behavior of wood components. At low temperature, the wood matrix was stiff and cracks or fiber separation was more localized under the compression load. As the temperature rose the wood components were somewhat softened and became more pliable and ductile, minimizing the creation of

cracks and generating long cracks. This failure phenomenon may be illustrated in (Figure 5.19). There were two possible types of deformations in longitudinal compression: Type A, extensive local small cracks occurred at low temperature, and type B, several large cracks took place throughout the whole specimen at high temperature. The dominant deformation changed slowly from type A to type B failure when the temperature rose from 22°C to 140°C (Table 5.4). This implies that compression at low temperature facilitated fiber separation and generated small cracks, while high temperature created slip planes that could become long and large cracks.

The temperature played an important role in determining the compression energy; the total energy consumption decreased from 5.36 kWh/t at 22°C to 1.25 kWh/t at 140°C. Our result is in accordance with that of Franzier and Williams [74], who concluded that optimal conditions for energy saving in pulping were to precompress the wood to 65% at 20°C with an energy of 5 – 10 kWh/t. Berg and Gradin [75] used acoustic emission to monitor failures in wood during the longitudinal compression, and claimed also that the compression should be carried out at temperature well below 120°C in order to introduce many failures in the wood. However, no one else had pointed out that there are two types of failure modes in longitudinal compression.

Table 5.4 Results of longitudinal compression at different temperature

Temp. °C	LMOE		LSY_d		LEY_d		LSCE		Number of failures	
	MPa	CV,%	MPa	CV,%	J	CV,%	MJ/m^3	CV,%	A	B
22	608	17.5	24.49	6.4	0.965	13.1	7.338	16.6	9	1
40	416	16.0	21.07	5.9	0.935	8.2	5.818	18.2	9	1
60	365	6.6	17.26	8.1	0.716	7.8	4.952	17.6	6	4
80	336	16.5	14.08	7.9	0.536	16.3	3.768	11.7	6	4
100	324	8.4	10.11	9.1	0.286	12.6	2.738	21.1	5	5
120	273	14.9	8.16	9.2	0.231	14.8	2.243	24.6	4	6
140	260	19.0	7.60	4.4	0.210	11.8	1.704	29.1	3	7
Dec. %	57.2		69.0		78.2		76.8			
Av.(CV%)		14.1		7.29		12.1		19.8		

The compression temperature also influenced other properties such as modulus, yield stress and yield energy. These properties were reduced by 57.2%, 69% and 78.2%, respectively, when the temperature raised form 22°C to 140°C. Berg et al [75] also obtained similar decrease in modulus and yield strength by 59% and 63.5% when the compression temperature was raised from 23°C to 120°C. Comparable decreases were also noted in the present study: 55% reduction in modulus and 66.6% drop in yield stress within the same range of temperature.

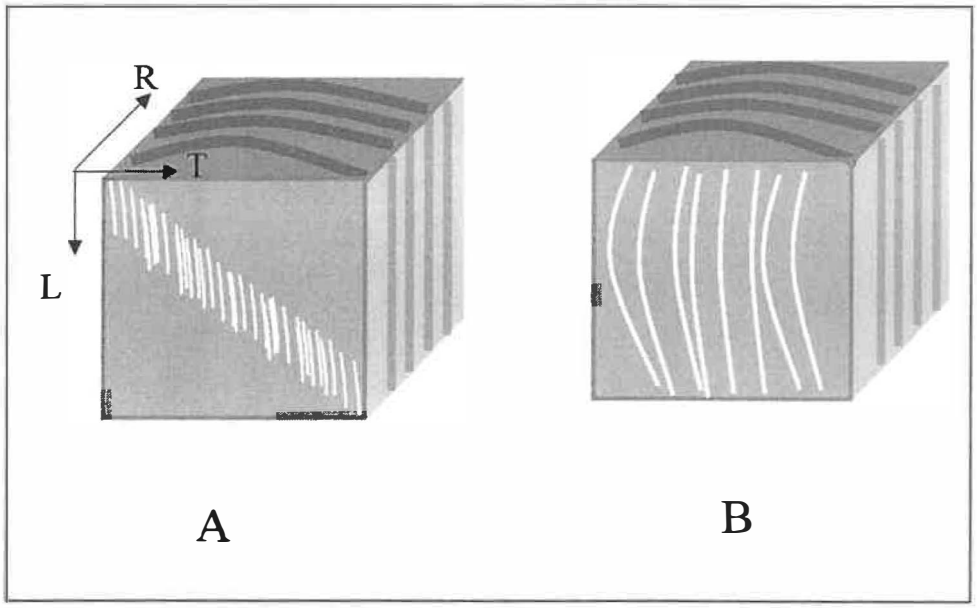

Figure 5.19 Possible failure types in longitudinal compression

5.2.4 Comparison of compression in different directions

5.2.4.1 The effect of compressions on modification of wood matrix

Wood responses differently when compressed in different directions. As a consequence, the wood matrix and the fiber wall were modified in a different manner depending on the direction of compression. The changes in fiber wall can be revealed by scanning electronic microscopy (SEM). For the SEM study, samples were first compressed at 120°C with predetermined strain and then split with a knife to yield surfaces in radial and tangential planes. In the tangential plane only EW fibres were exposed on the surfaces.

Figure 5.20 to Figure 5.23 show the radial and tangential surfaces of sample compressed to 70% strain in radial direction. Since the compression force was applied perpendicular to the grain and parallel to the radial plane, the radial walls supported most of the stress until the fiber was completely collapsed. Thus, large concentrations of stress would occur, forcing the radial walls to buckle (either inward or outward) and causing the fibers to separate in radial plane. Figure 5.20 shows that the fracture plane went through several fiber layers, indicating the pre-separation resulted from compression. Note that the separations were induced by compression particularly at the interface of tracheid and ray cell. These separations can also be seen in the cross-section view, as shown in Figure 5.10 and Figure 5.11. Slippage between cell wall lamellae caused by cell wall buckling was also evident. Separations between P/ S_1, S_1/ S_2 were frequent owing to the distinct difference in fibril orientation between these layers. Figure 5.22 shows a separated and collapsed fiber with S_2 exposed. Furthermore, owing to extensive buckling at high compression strain, the fibers dislocated and expanded laterally. This movement introduced high tensile and shear stress in the plane perpendicular to the compression direction, resulting in longitudinal cleavage of fibers, as indicated in Figure 5.20 and Figure 5.23. The characteristics of fiber separation caused by radial compression under different conditions will be further discussed in chapter 7.

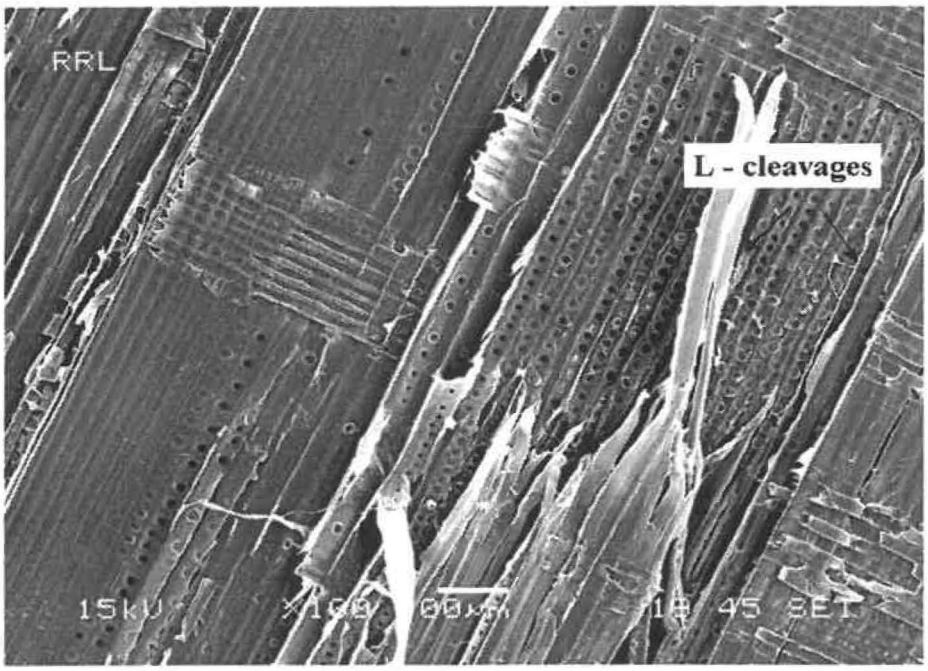

Figure 5.20 SEM micrograph showing failures occurred at several fiber layers in radial plane of sample compressed to 70% strain in radial direction (120 °C)

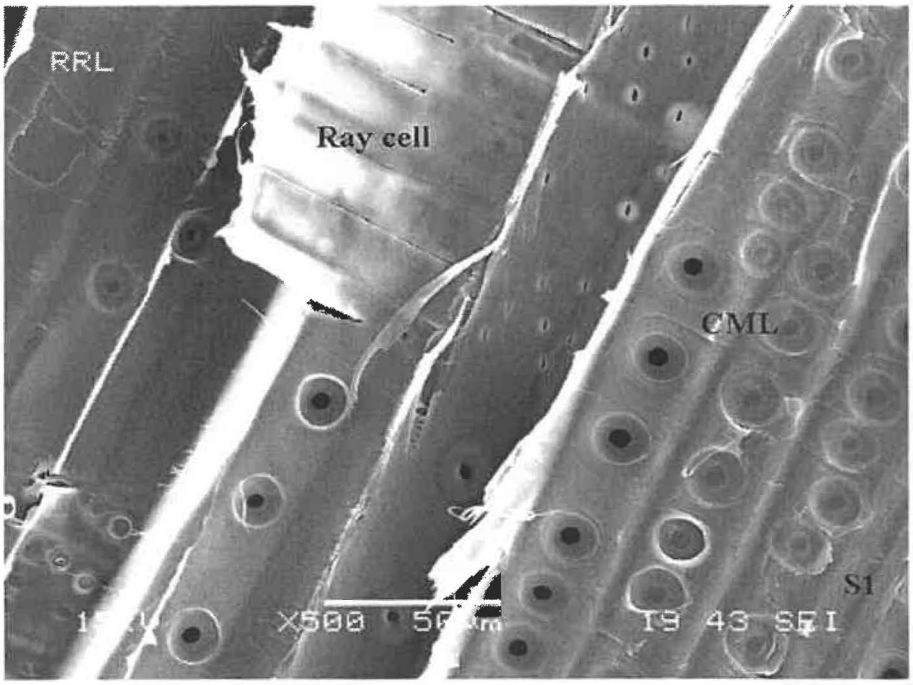

Figure 5.21 SEM micrograph showing longitudinally broken fiber on radial plane of sample compressed to 70% strain in radial direction (120 °C)

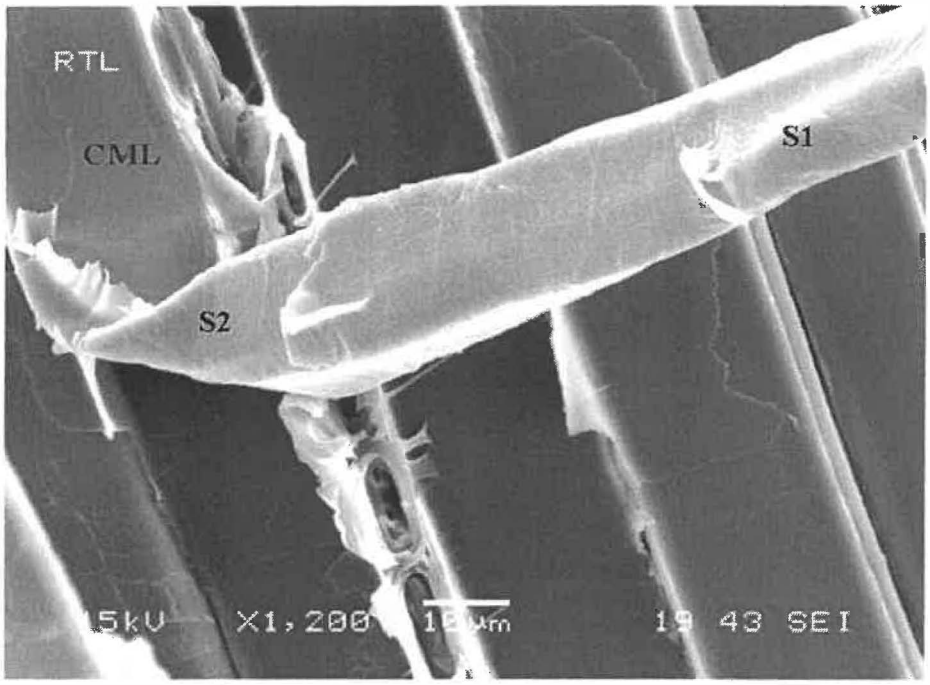

Figure 5.22 SEM micrograph showing separated fiber with S_2 exposed on tangential plane of sample compressed to 70% strain in radial direction (120 °C)

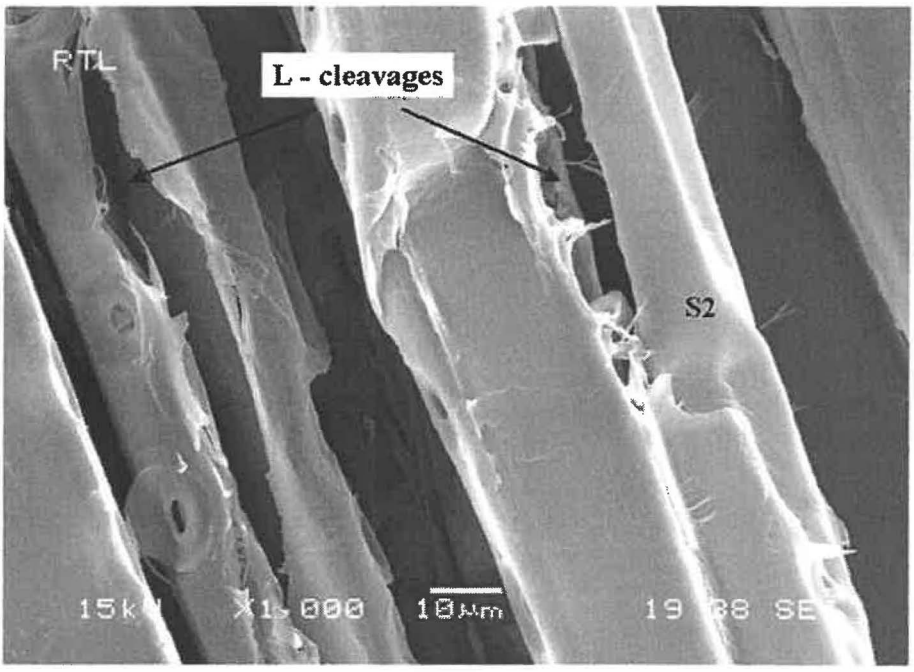

Figure 5.23 SEM micrograph showing longitudinal cracks on fibers in tangential plane of sample compressed to 70% strain in radial direction (120 °C)

Figure 5.24 to Figure 5.27 show the radial and tangential surfaces of sample compressed to 70% strain in tangential direction. Generally, the characteristics of the surface were similar to those seen in radial compression. The samples were also separated at several layers of fibers in radial plane (Figure 5.24). The fibers were separated mainly between P/S_1; exposition of S_2 can be seen in some parts of the exposed surface (Figure 5.26 and Figure 5.27). Longitudinal cleavage was also observed (Figure 5.25).

Figure 5.28 to Figure 5.31 show the radial and tangential surface of samples compressed to 50% strain in longitudinal direction. The surface characteristics generated in tangential plane were quite different from those in radial plane. In tangential plane the fiber deformation was localized as shown in Figure 5.19 and Figure 5.31. However, the fibers in the compressed area were well separated with either S_1 or S_2 exposure as observed in radial plane (Figure 5.28 to Figure 5.30). No longitudinal cleavage was observed in longitudinal compression.

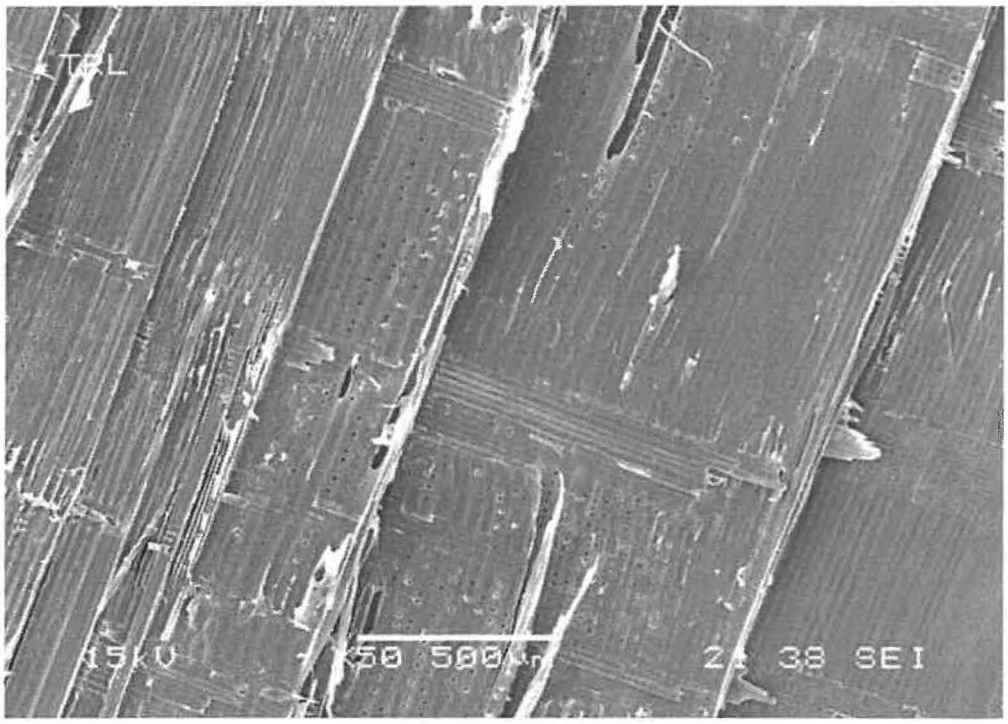

Figure 5.24 SEM micrograph showing failures occurred at several fiber layers in radial plane of sample compressed to 70% strain in tangential direction (120 °C)

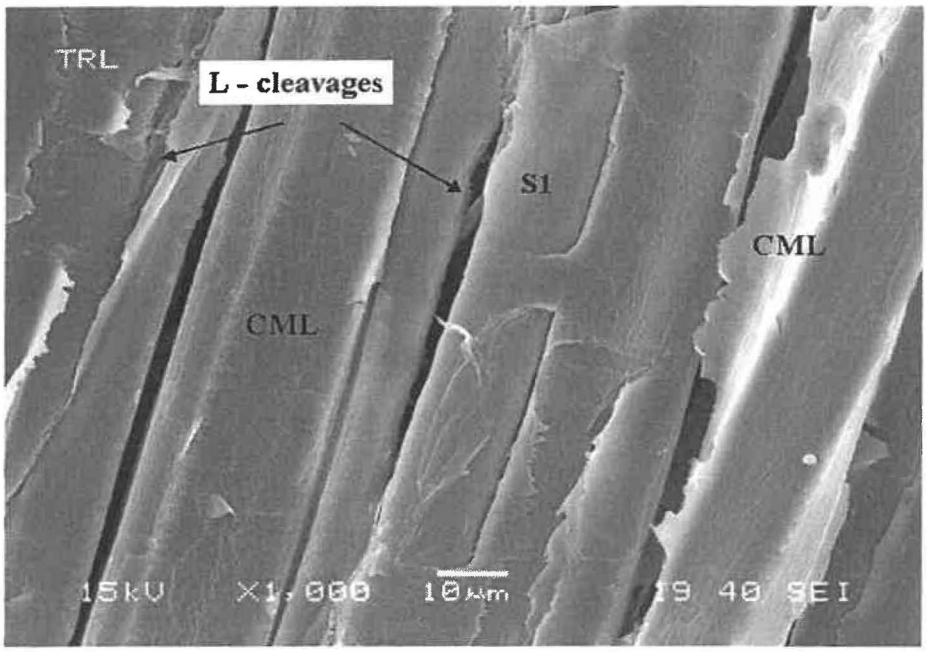

Figure 5.25 SEM micrograph showing fiber separations on radial plane of sample compressed to 70% strain in tangential direction (120 °C)

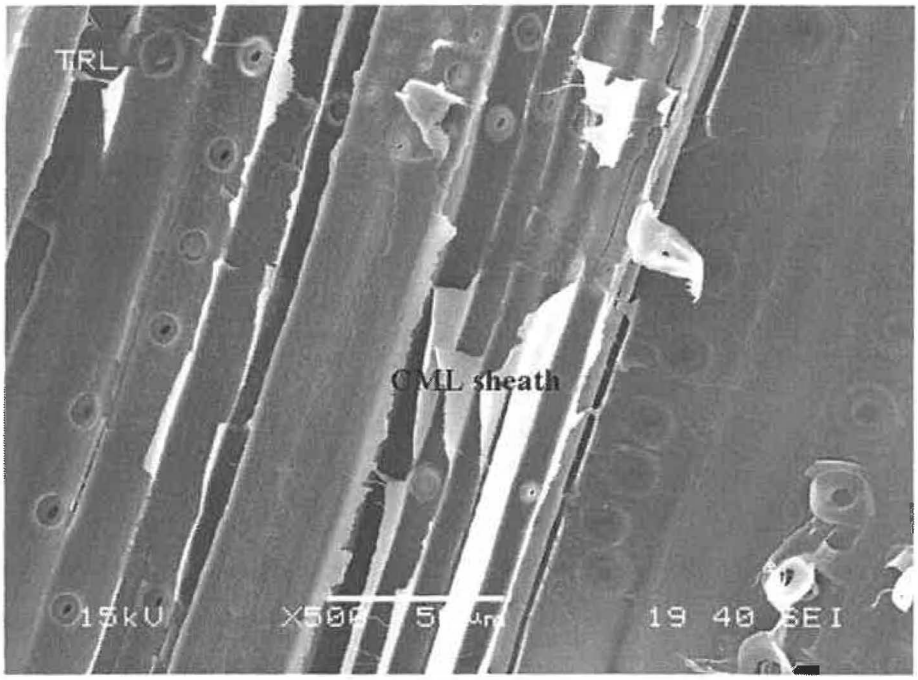

Figure 5.26 SEM micrograph showing the locations where the fibers were stripped away with CML sheath left on radial plane of sample compressed to 70% strain in tangential direction (120 °C)

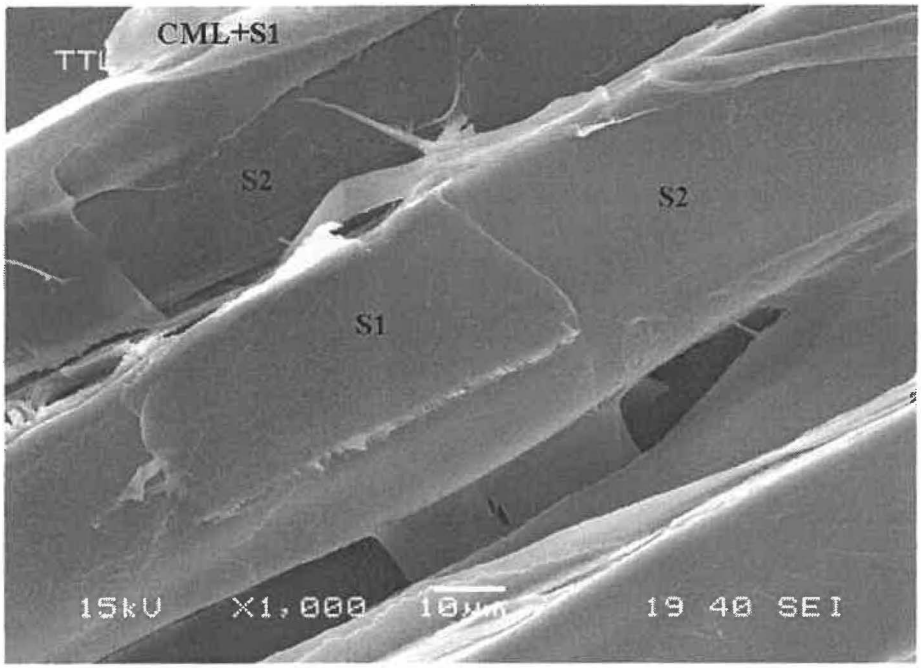

Figure 5.27 SEM micrograph showing separated fiber covered with broken CML and with S_2 exposed on tangential plane of sample compressed to 70% strain in tangential direction (120 °C)

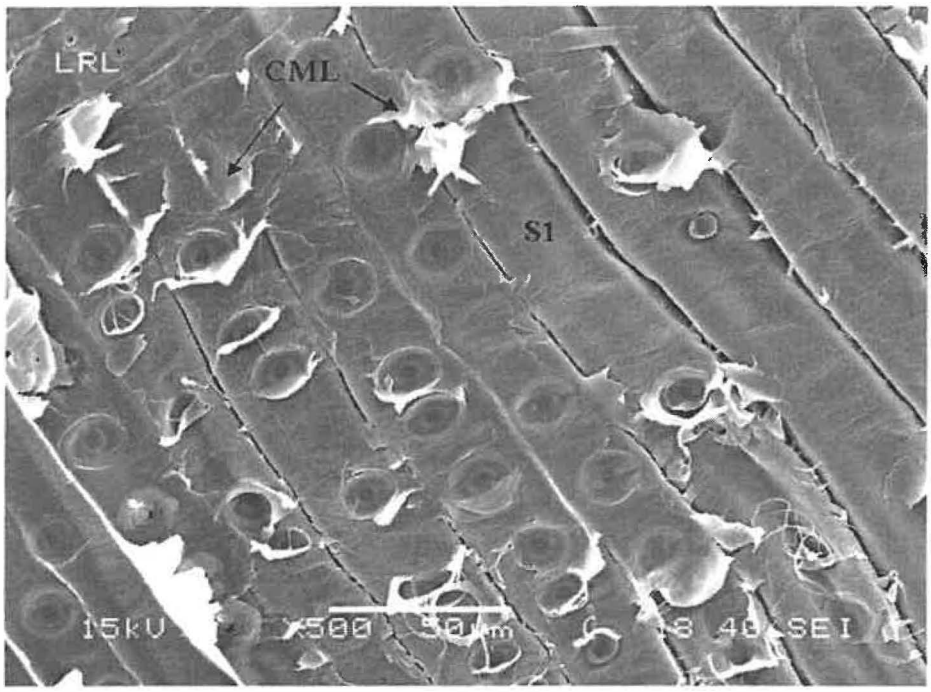

Figure 5.28 SEM micrograph showing fiber separation on radial plane of sample compressed to 50% strain in longitudinal direction (120 °C)

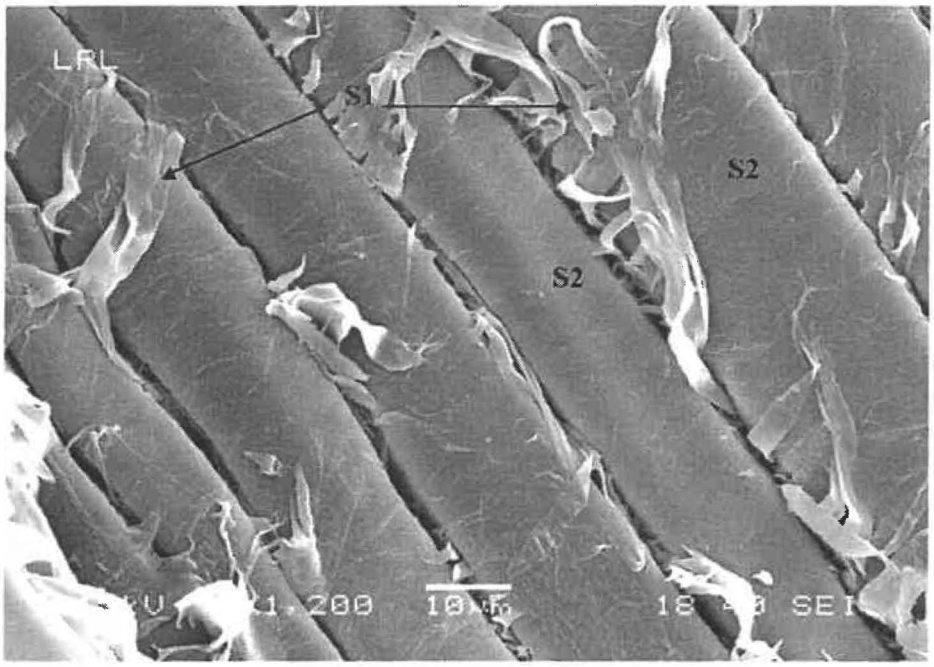

Figure 5.29 SEM micrograph showing separated fibers with S_1 strips loosely attached on radial plane of sample compressed to 50% strain in longitudinal direction (120 °C)

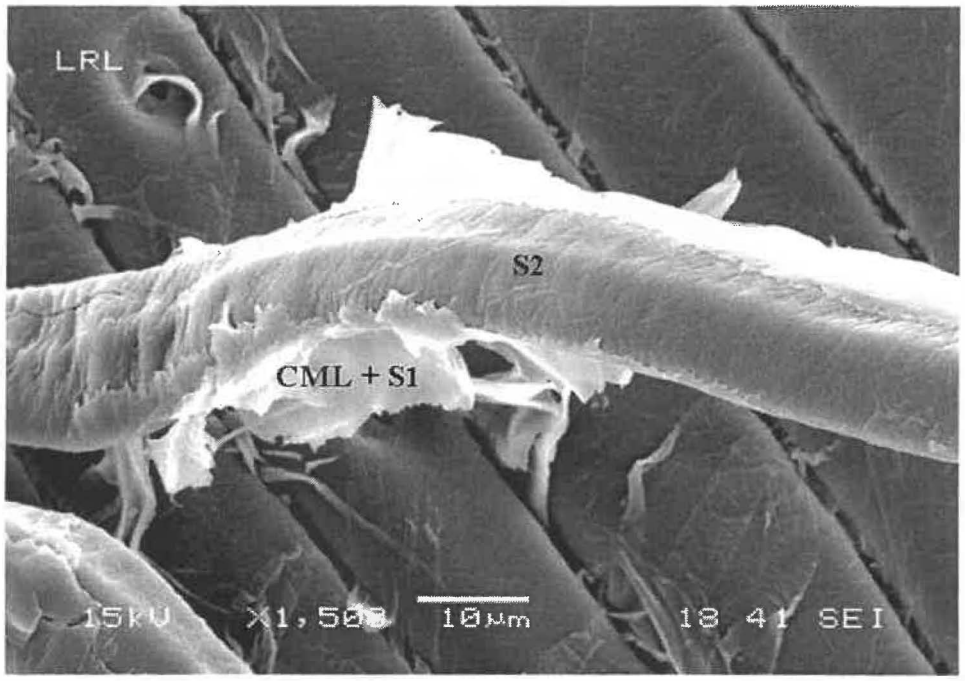

Figure 5.30 SEM micrograph showing separated fibers with S_2 exposed on radial plane of sample compressed to 50% strain in longitudinal direction (120 °C)

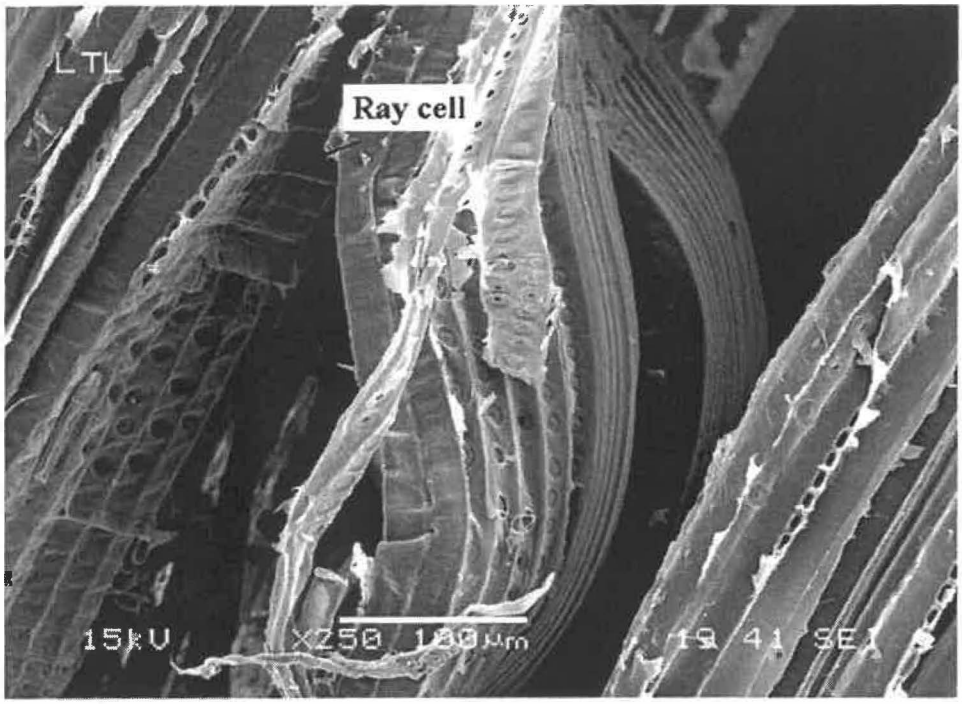

Figure 5.31 SEM micrograph showing fibers separated at fiber/ray cell interface on tangential plane of sample compressed to 50% strain in longitudinal direction (120 °C)

5.2.4.2 Physical properties in different directions

1. First plateau stress

Figure 5.32 compares the first plateau stress (SP1) between the radial and tangential compression at various temperatures. At low temperatures (< 80°C) the tangential compression yielded a slightly higher SP1 (about 15%) when compared to the radial compression. The difference was gradually diminished as the temperature rose. As discussed earlier, the EW fibers played the sole role in determining the SP1 in radial compression. In tangential compression the situation was quite different; both the EW and LW fibers jointly determined the SP1. As such, the SP1 was higher for tangential compression than for the radial compression. However, as the temperature increased, softening both the EW and LW, the difference gradually disappeared. The magnitude of dissimilarity in SP1 between radial and tangential compression may also be affected by

the EW/LW ratio in the growth increments. If the ratio is low (such as in Jack pine), the SP1 in tangential compression could be much higher than that of the radial compression (10.9 MPa and 1.7 MPa, respectively) [69]. The magnitude of difference would be small for white spruce because it has small proportion of LW (about 20%).

2. Second plateau stress

Figure 5.33 compares the second plateau stress (SP2) between the radial and tangential compression. The figure clearly indicates that the radial compression gave 15 - 20% higher SP2 in comparison with the tangential compression. This difference was diminished at high temperature (higher than 120°C). The difference between the radial and tangential comparison in SP2 could be explained by the dissimilarity in fracture mechanism. In radial compression the EW fibers are first to collapse, densifying the wood specimen. As the compression strain increases, the radial files of LW fibers are forced to distort and buckle, causing fiber separation while maintaining the specimen intact. On the other hand, in tangential compression, the LW bands tend to bend under stress, creating separation between EW and LW zones and reducing the compression stress (e.g. SP2). The bending and fracturing of the LW bands is unavoidable because these bands are usually not completely parallel to the direction of force. Additionally, there is no densification effect on the specimen; the specimen is usually broken, in contrast to the specimen compressed at radial direction.

3. Modulus of elasticity

Wood has the highest compression strength in longitudinal direction (the axial direction of fibers). As seen in Figure 5.34, the longitudinal compression gave a modulus approximately 5 times higher than that for the transverse compression. The radial and tangential compressions were relatively comparable in modulus under various temperatures.

Further, the compression temperature had significant influence upon the modulus of wood, regardless of the direction of compression. There was a decrease by 57% in MOE for the longitudinal compression when the temperature increased from 22°C –140°C.

The percentage reduction in MOE was significantly higher for the transverse compression, approximately 82%. This indicates that the modulus of longitudinal compression is largely determined by the fiber resistance in its axial direction. In this direction, fiber wall strength is much higher than that of middle lamella. Thus, the effect of thermal_softening of lignin on modulus at longitudinal direction may be minimized. While for the transverse compression, the modulus is largely depended on fiber transverse resistance that mainly was determined by both the fiber wall and the middle lamella of EW fibers. Thus, the thermal softening on the middle lamella can decrease transverse modulus more significantly. The strong correlation between the SP1 and the MOE for both radial and tangential compression (Figure 5.35) seems to support this view.

4 Specific compression energy (SCE)

The difference in SCE between the three compression directions was dependent on the temperature used, as revealed in Figure 5.36. At temperatures inferior to 80°C, the longitudinal compression had the highest SCE while the tangential compression the lowest; the radial compression lied in between. As the temperature rose above 80°C the difference was relatively negligible. In view of this, it is suggested that any mechanical pretreatment of wood chips before refining be performed at elevated temperature, preferably above 100°C, minimizing the required energy and fiber breakage in compression. However, the direct comparison is not available, because the longitudinal compression was conducted only up to 50% strain (transverse compression is up to 70%). But, it is still evident that longitudinal compression consumes much more energy than the transverse compressions if samples are compressed to same compression strain, especially at low temperature (Figure 5.37). However, even at low temperature (22 °C), the energy consumption for these compressions is quite small. It is about 6.7-7.3 MJ/m^3 (5-5.3 kWh/t), which is only 0.2% of the specific energy consumption (SEC) of a typical TMP (2500 kWh/t). At high temperature (120°C), the compression energy is 2.24-2.55 MJ/m^3 (0.64-0.7 kWh/t), which is only 0.03% of the SEC for TMP.

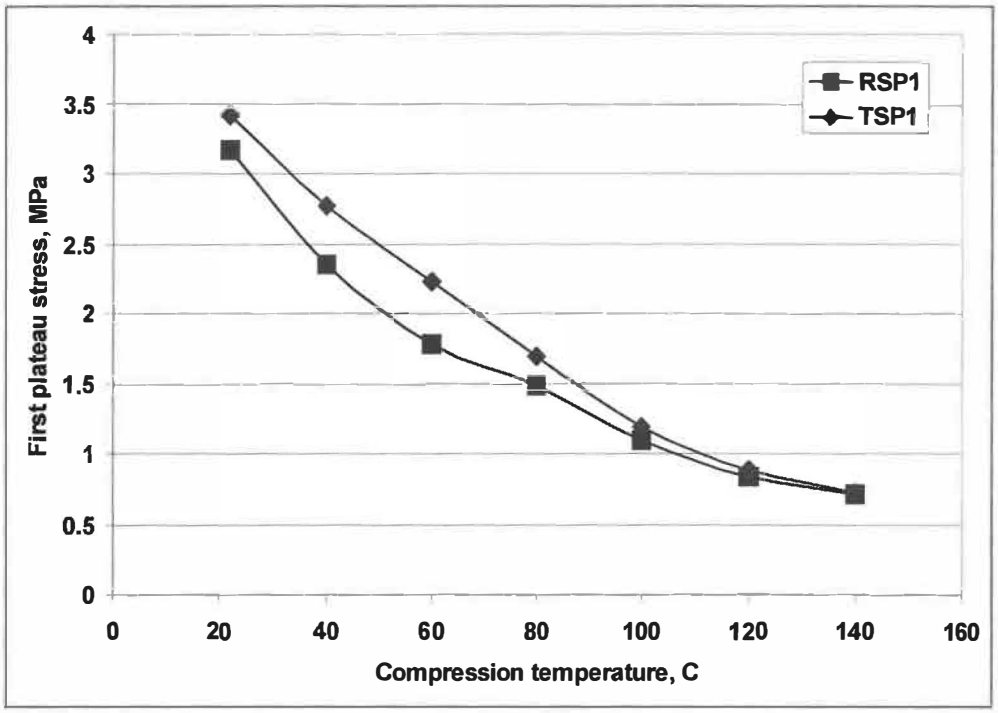

Figure 5.32 First plateau stress in radial and tangential compression at various temperatures

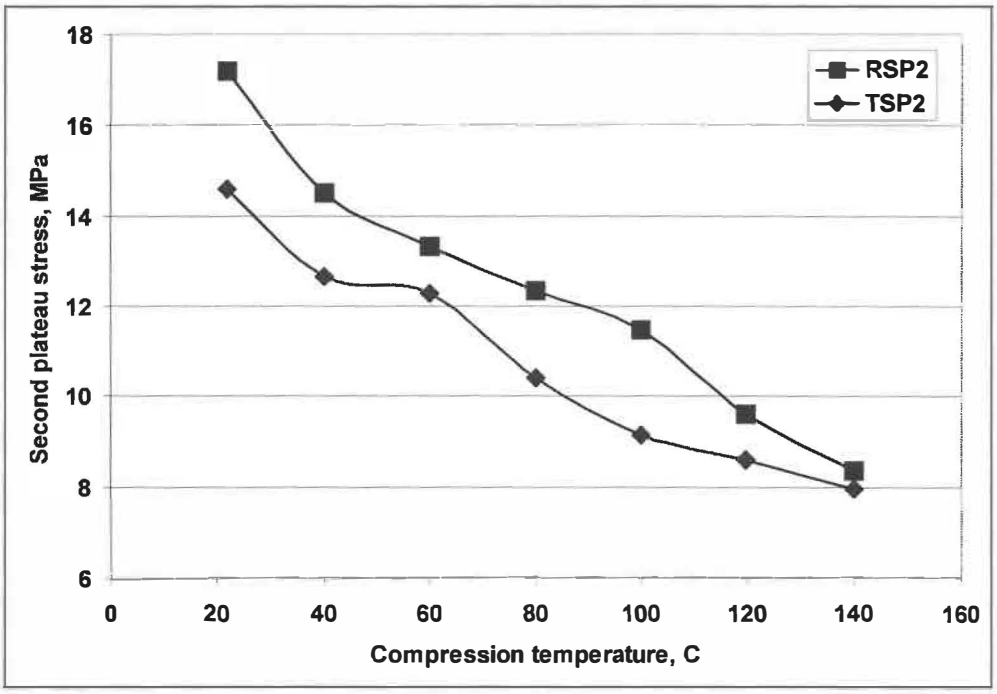

Figure 5.33 Second plateau stress in radial and tangential compressions at various temperatures

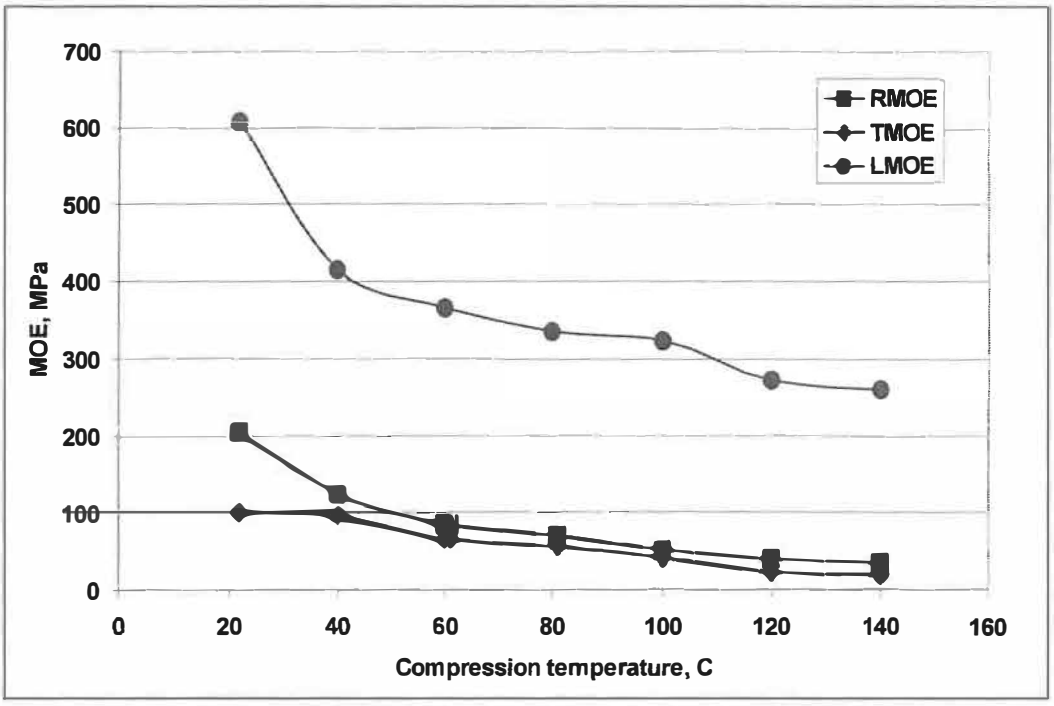

Figure 5.34 Modulus for three compressions at various temperatures

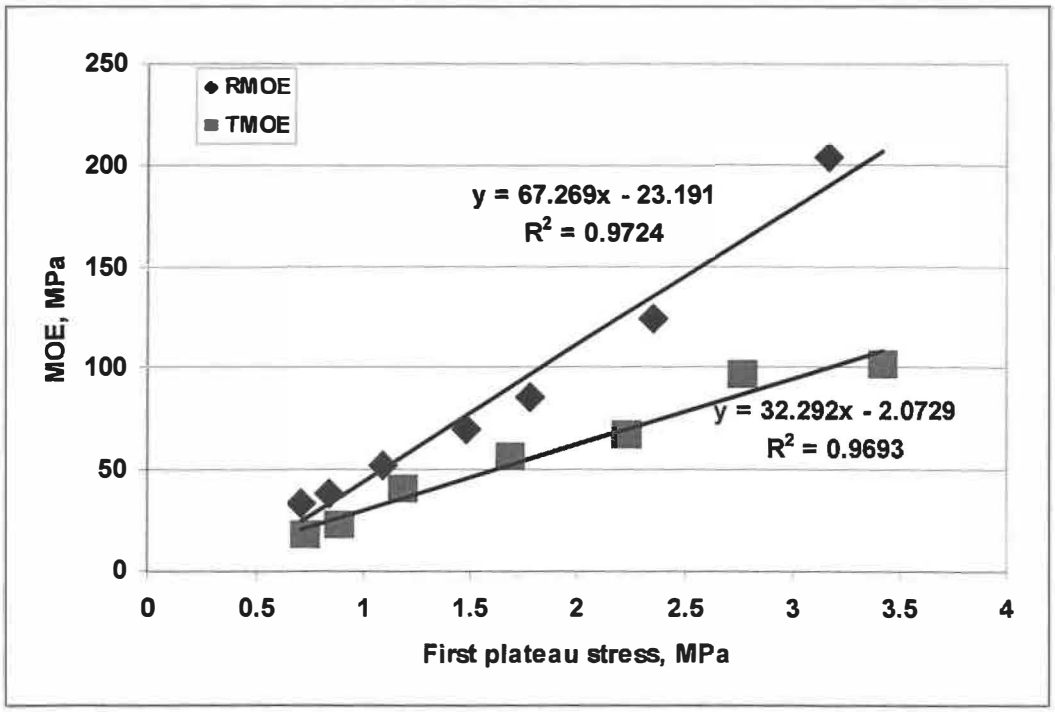

Figure 5.35 Relation between SP1 and MOE in transverse compressions

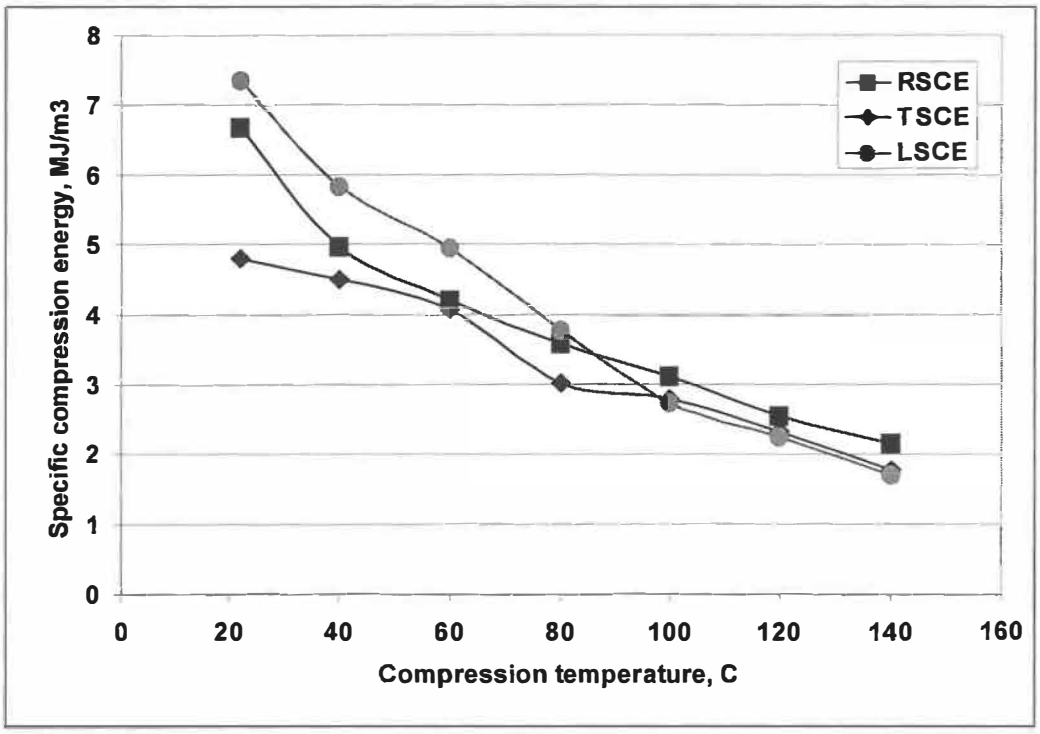

Figure 5.36 Specific compression energy for three compressions at various temperatures (compression strain for transverse and longitudinal directions are 70% and 50% respectively)

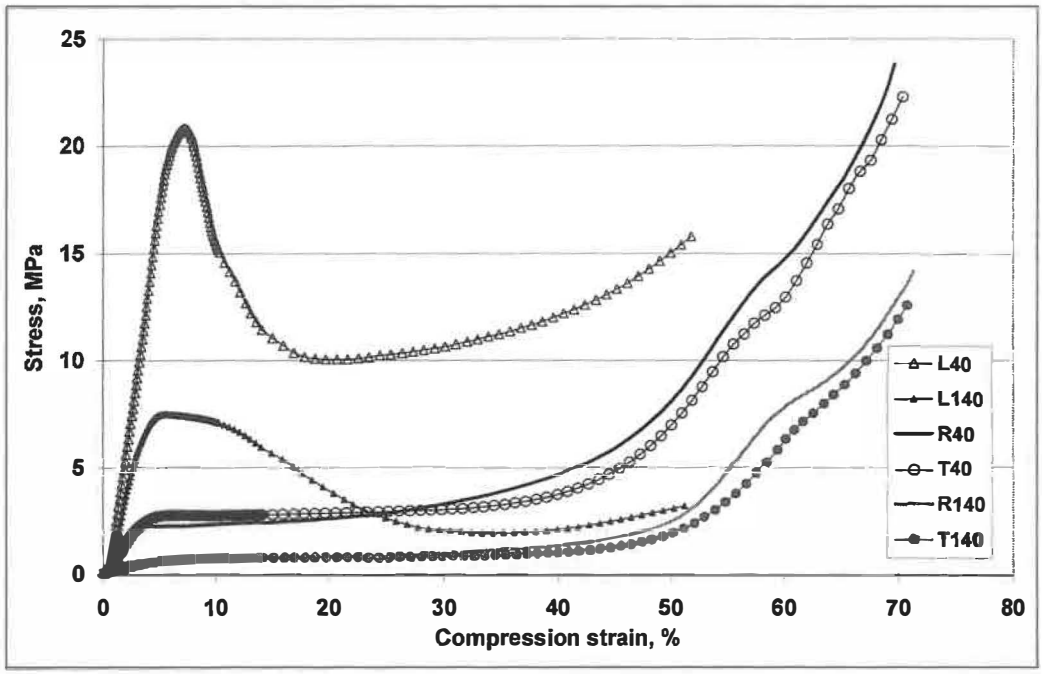

Figure 5.37 Compression curves for three directions at 40°C and 140°C

5.2.4.3 Softening temperature of wood components

As discussed in section 3.3, the softening temperature of water-saturated cellulose and hemi-cellulose is comparatively low, about 20°C in comparison with that of isolated (water-saturated) lignin, 80°-90°C [124, 126]. Under conditions typical for mechanical pulping, the softening temperature for *in situ* lignin is in the range of 100°-130°C [127]. However, a complete softening of the lignin cannot be obtained until temperature of 150-160°C is reached [141]. Since our compression temperature ranged from 22°C to 140°C, the effect of temperature on compression is mainly controlled by the thermal softening of lignin.

The measurement of the physical properties such as MOE, SP1, SP2, SY_d, etc. may not directly reflect the softening properties of lignin because of the chemical and structural complexity of the wood matrix. But after some transformation, most of these properties indicate the thermal softening of lignin at 80 °C to 100°C.

The stress in transverse direction (SP1) mainly determined by the middle lamellar and the double cell wall that is parallel to the applied force. For a given cell wall thickness, the variation in SP1 of radial and tangential compression may indicate the influence of lignin softening. But, the SP1-temperature curve of transverse compression didn't directly show a definite point of change. However, in its relative slope curve, as shown in Figure 5.38 and Figure 5.39, the point of change can be clearly identified (the slope was obtained from the most fit model of SP1-temperature curve). The relative slope defined as the slope divided by the stress at that temperature. This point of change occurred in temperature range of 80-100°C (with a peak value at 90°C). This range is believed to indicate the softening of lignin.

Fiber buckling and separation are the two main failures observed in longitudinal compression. The yield point obtained in longitudinal compression may correspond to the crack propagation between the compound middle lamellar and the secondary wall or in the middle lamella, depending on the temperature of test specimen. Thus, the yield stress (SY_d) of longitudinal compression might also reflect the property of lignin. Figure

5.40 indicates a rapid drop in yield stress in a temperature range of 80°-100°C, suggesting a softening of lignin around 90°C.

The SP1 and SP2 represent, respectively, the stress where fiber collapse and fiber separation occurred. A SP2/SP1 ratio of 13 was reported for radial compression of water saturated Norway spruce at 98°C [59]. In this study, the SP2/SP1 ratio varied from 5.5 to 12 and 4 to 11 for radial and tangential compression, respectively (Figure 5.41). The SP1 is mainly determined by rigidity of middle lamellar and the double cell wall that is in parallelism with the direction of the loading force, while the SP2 is influenced by both properties of middle lamella and the resulting lateral expansion (fiber separation). Thus, we may conclude that the SP2/SP1 ratio reflects the relative resistance of fiber separation. The SP2/SP1 ratio increased with increasing temperature, indicating either a relative increase in resistance in fiber separation or an increase in fiber collapsibility. A rapid increase in SP2/SP1 ratio was noted at about 80°C for both radial and tangential compression, an indicator of lignin softening. With softened lignin, the fibers collapse more readily and as a consequence, the lateral expansion and shear would decrease, resulting in less fibers separation. This characteristic was evident in SEM photomicrographs (in 7.3), which shows that compression at low temperature generated relatively more cracks. Thiruvengadaswamy et al. [81] also reported that low temperature favored fiber separation.

The lignin softening temperature in the neighborhood of 80°C obtained in this work is in line with that noted by other researchers. Sadoh and Ohgoshi [142] reported a transition temperature of 80°C for the viscoelastic behavior of wood. Uhmeier et al [62] obtained similar result (maximum value at 85 °C) for radial compression of Norway spruce. Further, Dumail et al [61] also reported a permanent deformation in radial compression (50% strain) increased greatly after 80°C, and attributed it to thermal softening of lignin at this temperature.

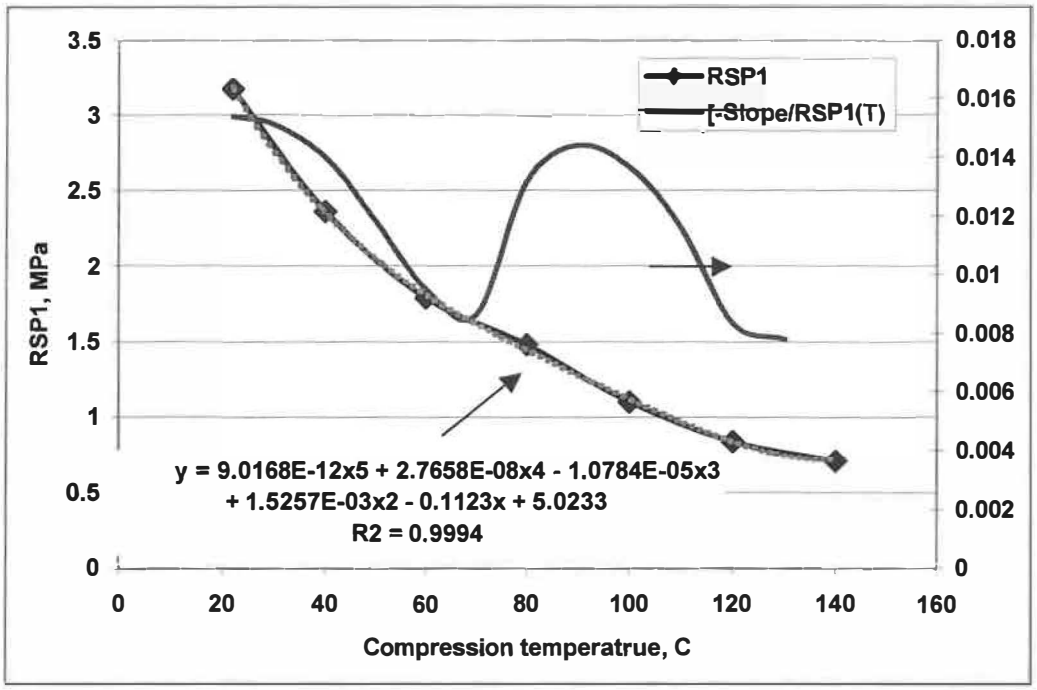

Figure 5.38 Variation of first plateau stress and its relative slope curve at various temperatures in radial compression, indicating a possible softening region at 80-100 °C

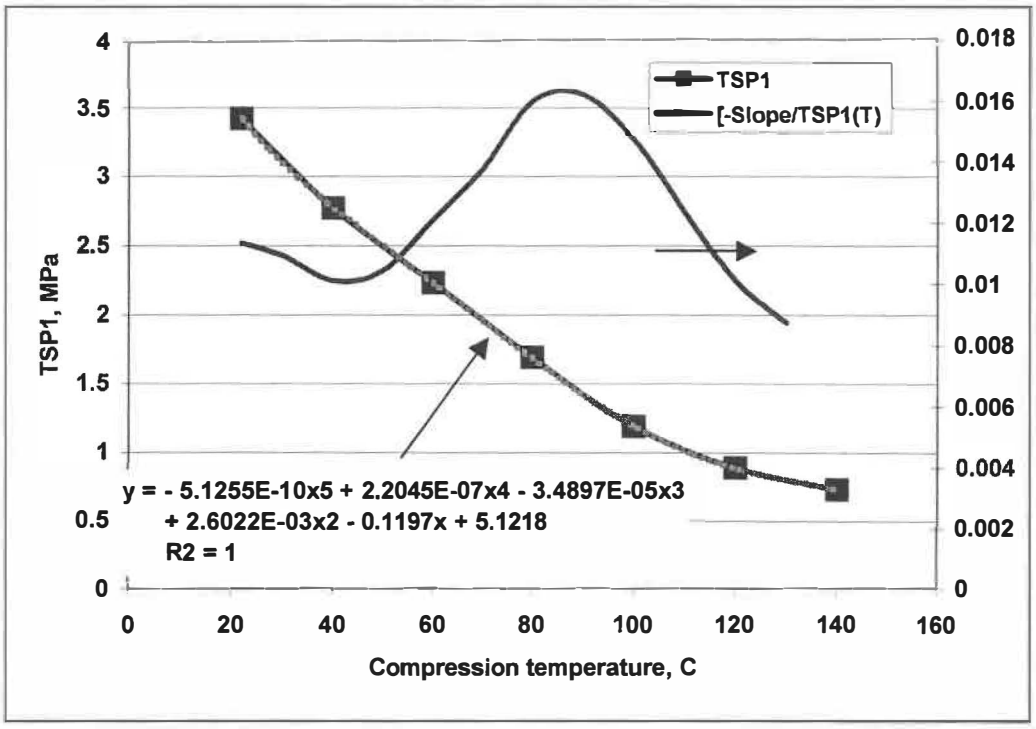

Figure 5.39 Variation of first plateau stress and its relative slope curve at various temperatures in tangential compression, indicating a possible softening region at 80-100 °C

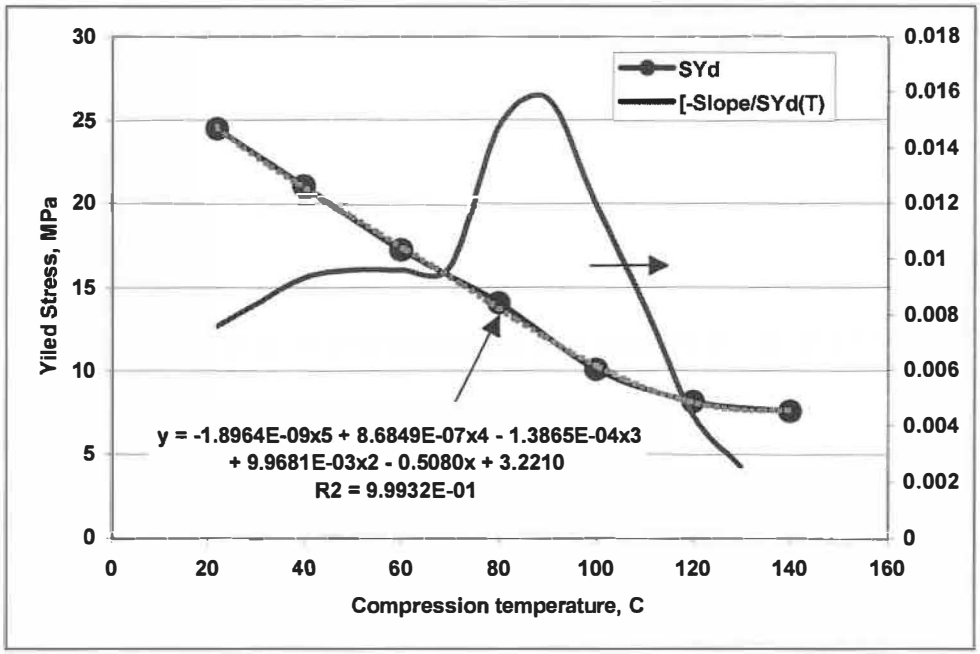

Figure 5.40 Variation of yield stress and its relative slope curve at various temperatures in longitudinal compression, indicating a possible softening region at 80-100 °C

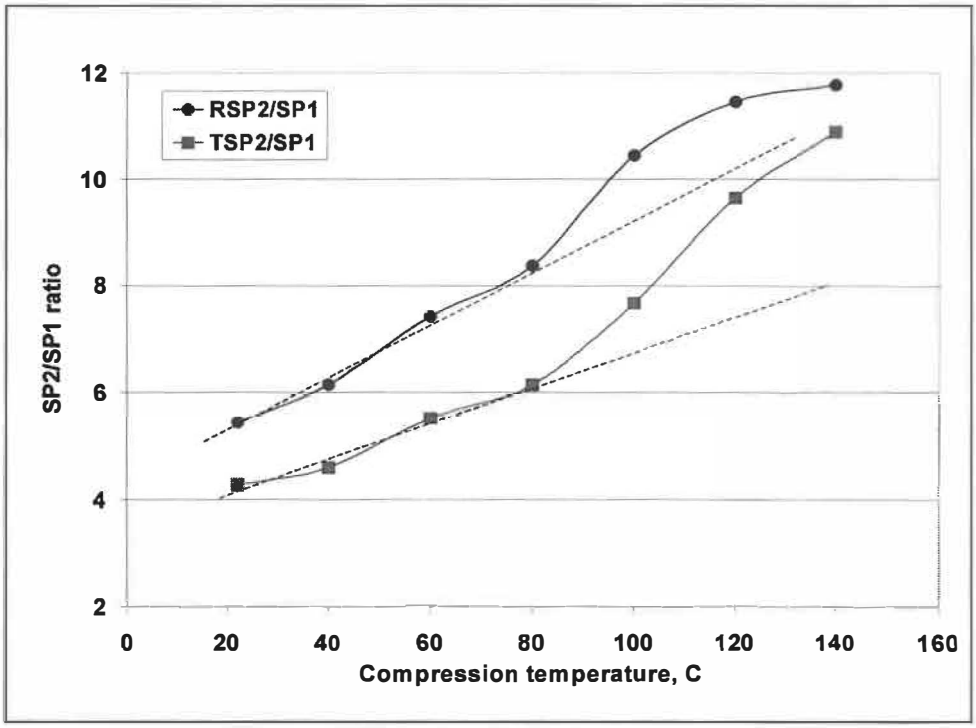

Figure 5.41 Variation of SP2/SP1 ratio at various temperatures in radial and tangential compressions

5.2.5 Mathematical models for physical properties of wood under compression

The data obtained from the study on the effect of temperature on wood compression could be used to develop mathematic models. The models would be useful for predicting the compression properties of wood under certain specific conditions. A software called *Statgraphics plus 4.1* offers a simple technique to directly relate the test temperature and the property parameters. Table 5.5 summarizes the results for all the parameters studied. Since all the P-Value in the ANOVA (Analysis of Variance) is less than 0.01, there exist statistically significant relationships between the temperature and property parameters, at 99% confidence level. Most of the correction coefficients are higher than 0.99, indicating a strong relationship between the temperature and the property parameters. The R-squared indicates that most of the models can explain more than 98% of the variability in the property parameters.

Table 5.5 Mathematic models obtained by *Statgraphics plus 4.1*

Compression Directions	Mathematic model	P-Value	Correlation coefficient	R^2
Radial	$RMOE = 7.98 + 4416.09/T_c$	0.0000	0.996	0.991
	$RSP1 = 7.31 - 1.34*Ln(T_c)$	0.0000	0.999	0.998
	$RSP2 = 22.38 - 1.15*Sqrt(T_c)$	0.0000	0.990	0.981
	$RSCE = 13.85 - 2.36*Ln(T_c)$	0.0000	0.998	0.995
Tangential	$TMOE = (11.54 - 0.053*T_c)^2$	0.0000	0.992	0.984
	$TSP1 = Exp(1.57 - 0.014*T_c)$	0.0000	0.997	0.995
	$TSP2 = 1/(0.06 + 0.00050*T_c)$	0.0000	0.992	0.984
	$TSCE = 5.37 - 0.026*T_c$	0.0000	0.986	0.973
Longitudinal	$LMOE = 220.65 + 84/T_c$	0.0000	0.993	0.987
	$LSY_d = Exp(3.46 - 0.011*T_c)$	0.0000	0.994	0.988
	$LEY_d = Exp(0.44 - 0.015*T_c)$	0.0002	0.978	0.956
	$LSCE = Exp(2.29 - 0.012*T_c)$	0.0000	0.998	0.995

* T_c: Temperature in Celsius degree. Sqrt: Square root

These mathematical models are different form each and do not explain the mechanism of wood failure under compression at various temperatures. However, it is known that, on a molecular level, the change in the properties of a material caused by temperature is mainly due to the molecular (or polymer chain) motion at different temperatures. These temperatures related mechanism of change can be expressed by Arrhenius' law:

$$Y = A \times e^{-E/RT}$$

Eq. 5.1

Where, 'A' is frequency or pre-exponential factor; 'E' activation energy of reaction; 'R' the gas constant (8.314J/Mol·K), and 'T' true temperature [T(K)= T_c(°C) + 273.15]. This expression fits well for lots of experiments over a wide range of temperature, and is a very good approximation of the true temperature dependency [143]. It has been widely used in thermally activated process such as the intrinsic conductivity of semiconductors, the catalytic reaction of emission control, the diffusion processes in metals, the creep in plastics, and the viscosity of fluids [144].

Taking 'Y' to represents the properties of MOE, SP1, SP2, SCE etc. obtained by axial and transverse compressions, if they follow the Arrhenius' law, then:

Ln (Y) = a(1/T) + b.

Thus, Ln(Y) and (1/T) will have a linear relationship; Figure 5.42 to Figure 5.44 show that there is a linear relationship between Ln(Y) and (1/T) for all the compressions at three directions. From these linear functions we can get a group of mathematical models in the form of Arrhenius' law for the property parameters for the three compression directions:

For radial compression (R^2: 0.96-0.99):

$$RMOE = 0.378 \times e^{1833/T}$$
$$RSP1 = 0.0173 \times e^{1544.2/T}$$
$$RSP2 = 1.6977 \times e^{685.2/T}$$
$$RSCE = 0.1542 \times e^{1103.6/T}$$

Eq. 5.2

For tangential compression (R^2: 0.93-0.98):

$$TMOE = 0.2374 \times e^{1855.2/T}$$
$$TSP1 = 0.0141 \times e^{1652.8/T}$$
$$TSP2 = 1.7045 \times e^{636.9/T}$$
$$TSCE = 0.1705 \times e^{1017/T}$$

Eq. 5.3

For longitudinal compression (R^2: 0.92-0.98):

$$LMOE = 37.2742 \times e^{786.7/T}$$
$$LSYd = 0.3199 \times e^{1304.2/T}$$
$$LEYd = 0.0026 \times e^{1811.3/T}$$
$$LSCE = 0.0487 \times e^{1504.6/T}$$

Eq. 5.4

Thus, universal temperature-dependent models are obtained as shown above. These models are much simpler than that obtained by relating two variables directly (Table 5.5). These models may also imply that the effect of temperature on wood properties could be explained by the effect of temperature on the molecular motion of wood components (cellulose, hemicelluloses, and lignin).

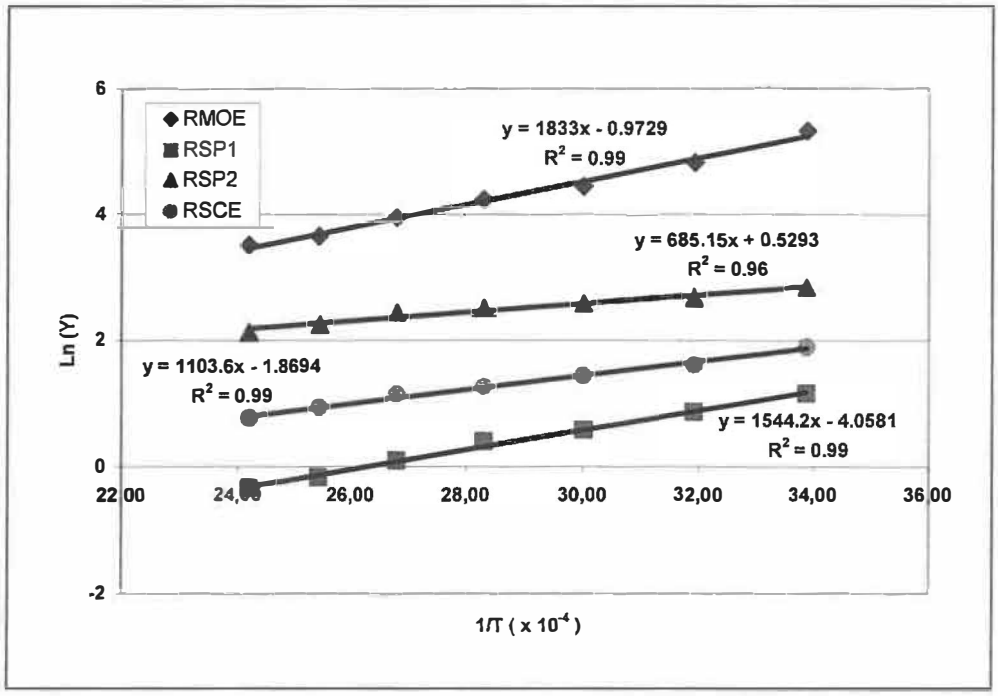

Figure 5.42 Linear relationship between Ln (Y) and 1/T for radial compression

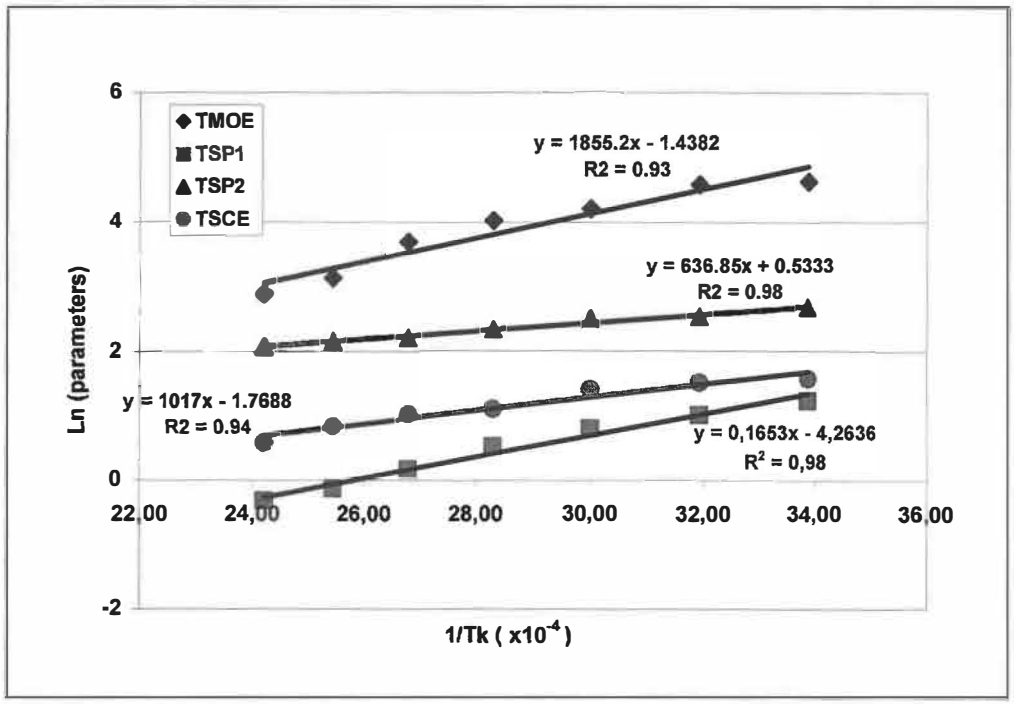

Figure 5.43 Linear relationship between Ln (Y) and 1/T for tangential compression

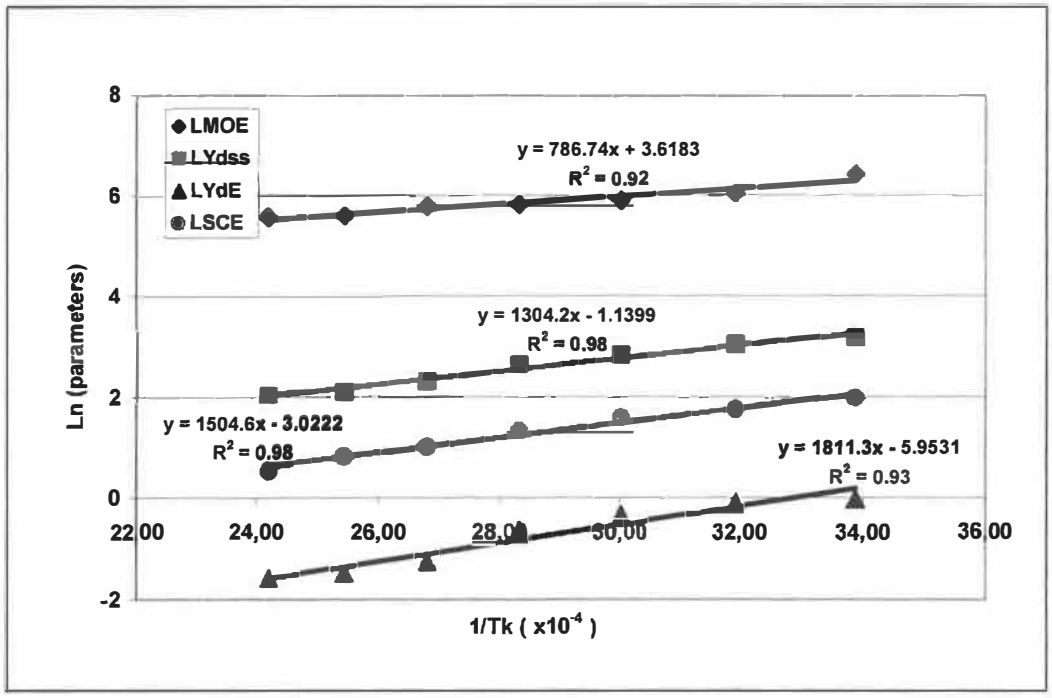

Figure 5.44 Linear relationship between Ln (Y) and 1/T for longitudinal compression

It should be pointed out that the significance of 'E' in the equation is not very clear here. In the origin of Arrhenius' law, 'E' is the activation energy of the chemical reaction. It was also reported that the viscosity of materials also follows Arrhenius' law [143], and 'E' represents the activation energy for viscous flow. Activation energy of 320 and 230 KJ/mol for spruce and birch were reported in thermal softening of dry wood samples [145]. But no one has tried to express the wood physical properties by Arrhenius' law. Considering the complexities of wood compression and wood components, 'E' may represent the combination activation energy of polymer-chain's motion of the main components of wood or the activation energy of process.

Table 5.6 shows the activation energy for wood under compression in three directions. 'E' is somewhat different in the three directions for a given property. This phenomenon is reasonable because the activation energy depends not only on temperature, but also on how the molecules are bonded in position. For example, the activation energy for carbon in diffusion is different in different host structure. They are 34, 29.3 and 43.5 KJ/mole in

fcc iron, *bcc* iron and *hcp* titanium respectively [144]. Wood is an anisotropic material; it is reasonable to have different activation energy for the same property in different directions. The activation energy for different properties in different directions ranges from 5 to 15 KJ/mole. However, for radial and tangential compression, the activation energy has only a minor difference for the same properties (CV less than 5%). Thus, for radial and tangential compression, the activation energy for same properties can be roughly regarded as the same. It is well known that there is a direct relationship between the mechanical or viscous behavior of polymeric materials and their molecular behavior [143]. Our result may suggest that, at molecular level (chemical compositions, polymer chains, and microstructures), the radial and tangential compressions are similar. This similarity in molecular level determines how the wood behaviors similarly in radial and tangential compressions as observed earlier.

Table 5.6 Activation energy for wood under compression in three directions

	Activation Energy (E), KJ/mol				CV (RT)
Directions	L	R	T	Av. (RT)	%
MOE	6.541	15.240	15.424	15.332	0.111
SCE	12.509	9.175	8.455	8.815	2.940
SP1 (LSYd)	(10.843)	12.838	13.741	13.290	3.067
SP2 (LEYd)	(15.059)	5.697	5.295	5.496	1.467

* CV: Coefficient of variance in percentage. L, R, T: longitudinal, radial and tangential directions respectively.

According to these mathematical models, the physical properties of wood in three directions can be calculated. Table 5.7 to Table 5.9 present the calculated values and our experimental data. The calculated values and the experimental values are plotted in Figure 5.45 to Figure 5.48. These figures reveal that the calculated values fit well with the experimental values. Most of the values are within the range of $Y = (1\pm10\%)\ X$ (between the dash lines) at various temperatures. Among these parameters, the modulus in tangential compression and the yield energy in longitudinal compression exhibit a relatively large variation. Generally, these universal models predict well of the compression properties of wood under various temperatures in the three directions.

Table 5.7 Experimental value Vs calculated value in radial compression

Temp.	RMOE, MPa		RSP1, MPa		RSP2, MPa		RSCE, MJ/m^3	
°C	Exp.	Calc.	Exp.	Calc.	Exp.	Calc.	Exp.	Calc.
22	205	188.8	3.17	3.25	17.2	17.32	6.67	6.50
40	125	132.1	2.36	2.40	14.5	15.16	4.96	5.24
60	86.0	92.9	1.79	1.79	13.3	13.29	4.20	4.24
80	69.4	68.0	1.48	1.37	12.4	11.83	3.57	3.51
100	51.9	51.5	1.10	1.09	11.5	10.66	3.11	2.97
120	38.7	40.1	0.84	0.88	9.62	9.71	2.55	2.56
140	33.6	32.0	0.71	0.73	8.36	8.92	2.16	2.23

Table 5.8 Experiment value vs. calculated value in tangential compression

Temperature	TMOE, MPa		TSP1, MPa		TSP2, MPa		TSCE, MJ/m^3	
°C	Exp.	Calc.	Exp.	Calc.	Exp.	Calc.	Exp.	Calc.
22	101	127.8	3.42	3.82	14.6	14.76	4.79	5.36
40	96.5	89.0	2.77	2.77	12.7	13.04	4.51	4.39
60	67.0	62.4	2.23	2.02	12.3	11.54	4.06	3.61
80	56.2	45.5	1.69	1.52	10.4	10.36	3.01	3.04
100	40.6	34.3	1.19	1.18	9.14	9.40	2.80	2.61
120	23.0	26.6	0.89	0.95	8.60	8.62	2.32	2.27
140	17.9	21.2	0.73	0.77	7.96	7.97	1.78	2.00

Table 5.9 Experimental value vs. calculated value in longitudinal compression

Temp.	LMOE, MPa		LSY_d, MPa		LEY_d, MJ/m^3		LSCE, MJ/m^3	
°C	Exp.	Calc.	Exp.	Calc.	Exp.	Calc.	Exp.	Calc.
22	608	536.6	24.49	26.60	0.965	1.21	7.338	7.99
40	416	460.3	21.07	20.63	0.935	0.85	5.818	5.96
60	365	395.8	17.26	16.06	0.716	0.60	4.952	4.46
80	336	346.2	14.08	12.87	0.536	0.44	3.768	3.46
100	324	307.2	10.11	10.56	0.286	0.33	2.738	2.75
120	273	275.9	8.16	8.83	0.231	0.26	2.243	2.24
140	260	250.4	7.60	7.52	0.210	0.21	1.704	1.86

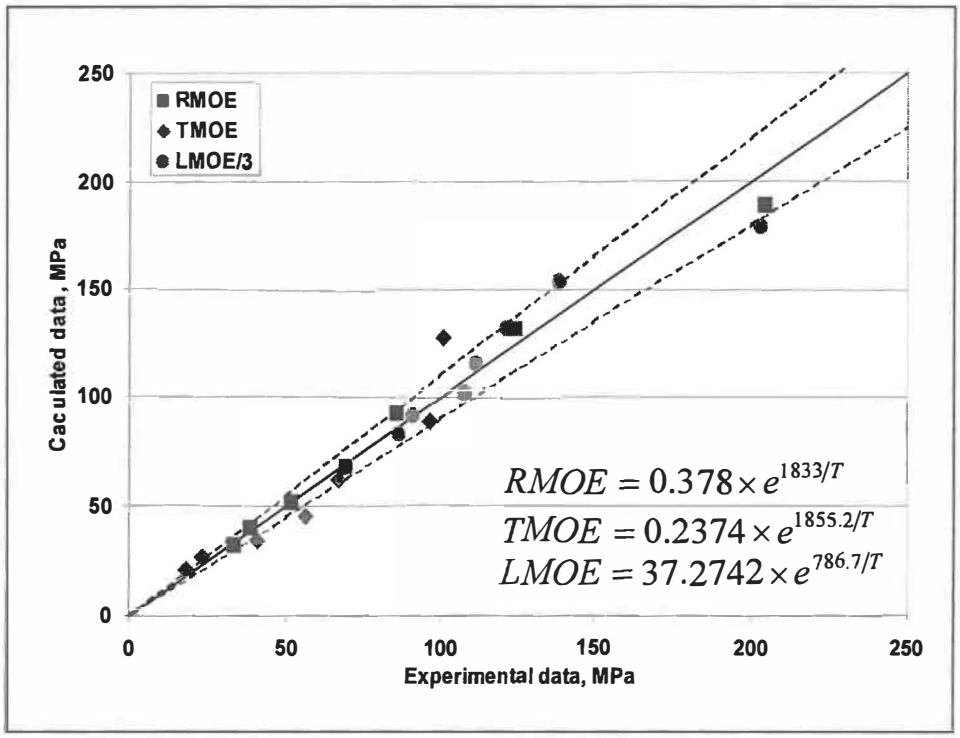

Figure 5.45 Model validation for MOE for three compression directions at various temperatures

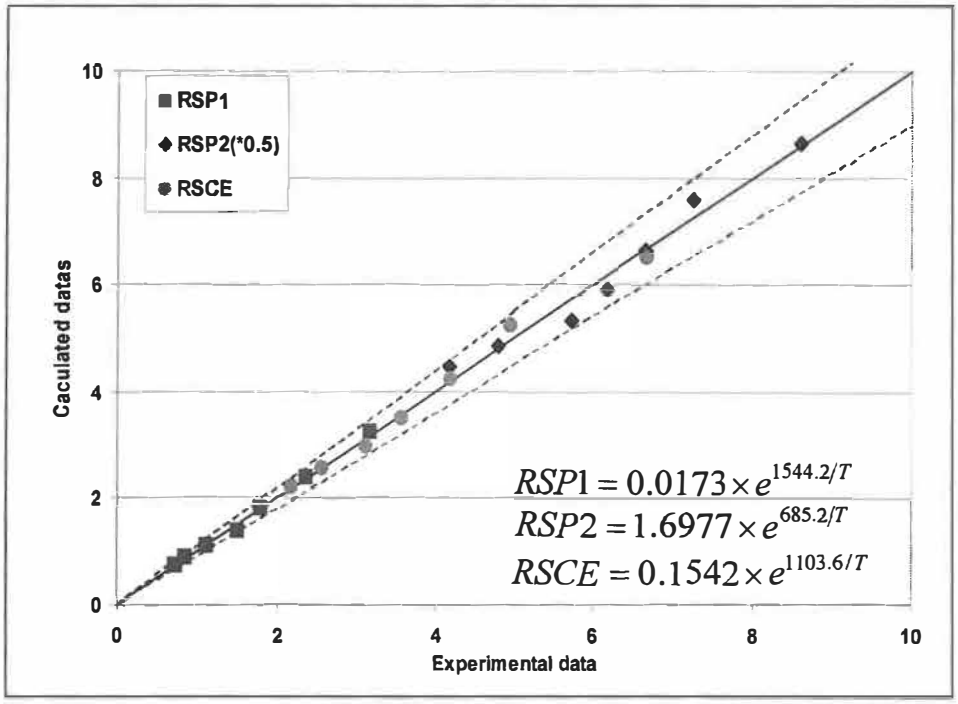

Figure 5.46 Model validation for radial compression at various temperatures (Units see Table 5.7)

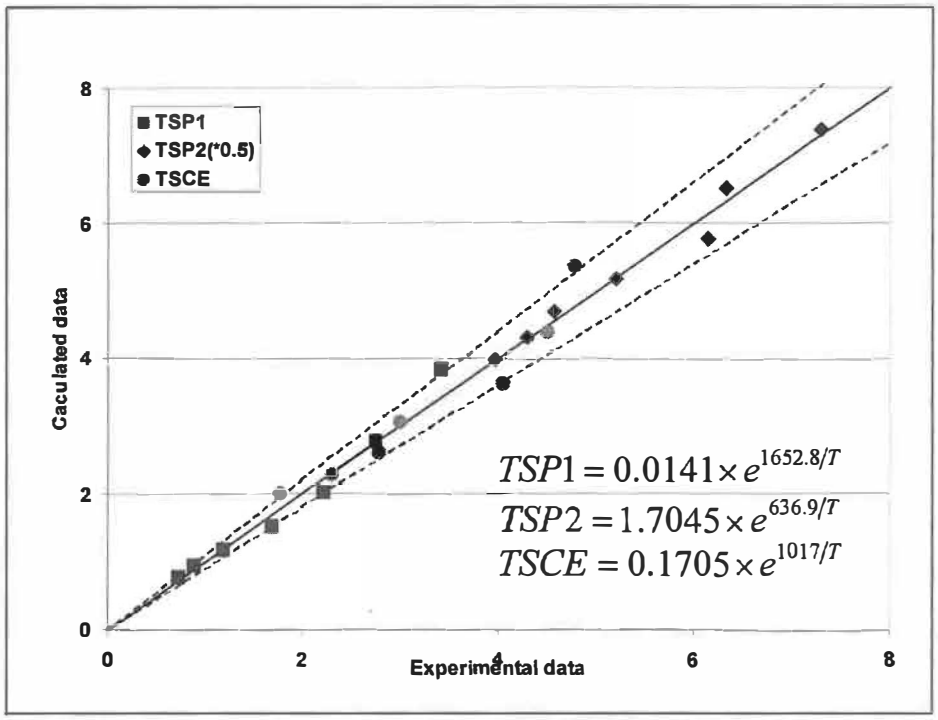

Figure 5.47 Model validation for tangential compression at various temperatures (Units see Table 5.8)

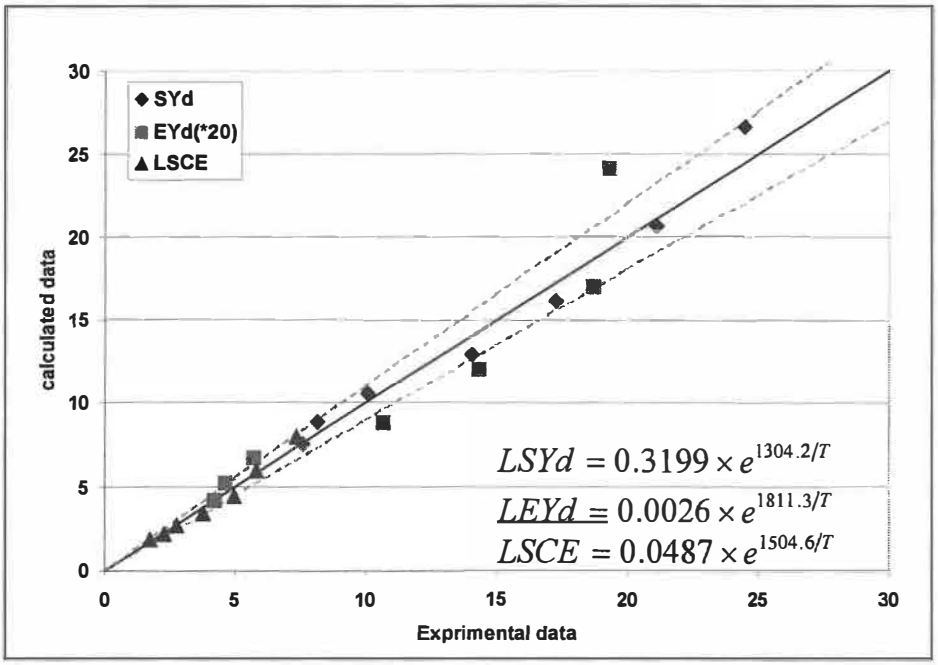

Figure 5.48 Model validation for longitudinal compression at various temperatures (Units see Table 5.9)

5.2.6 Elastic and elastoplastic behavior of wood

Theoretically, a purely elastic material is one complying with Hook's law and a purely plastic material yields indefinitely after reaching a certain stress. Material that possesses both elastic and plastic properties is called elastoplastic (elastico-plastic, viscoelastic) material. Wood is a material that has the elastoplastic property [77, 78,146].

Under a compression load wood exhibits a linear stress-strain relationship within a relatively small compression, about 5% in most cases. This elastic region represents an initial linear cell wall bending of the EW fibers in radial compression. As the compression load increases the EW fibers collapse gradually until all the EW fibers were completely collapsed. This nonlinear cellular collapse usually occurs at strain from 5% to 50%. The deformation can recover but not completely when the load is released. In this region, the wood behaves as a typical elastoplastic material. With further loading, the wood densifies and the structural failure is too complicated to describe because of the complexity in the compression process at this stage. In the followings, we treat only the elastic and visco-elastic behavior of wood under compression.

1. Elastic behavior of wood

In the elastic region (region I), the stress-strain relationship follows Hook's Law, that is $\sigma = K\varepsilon$, where ε is compression strain, and 'K' is elastic modulus which has been shown in Eq. 5.2 and Eq. 5.3 for both radial and tangential compressions. Thus the stress:

For radial compression:

$$\sigma_r = 0.378e^{1833/T} \times \varepsilon, (\varepsilon \le \varepsilon_y)$$

Eq. 5.5

For tangential compression:

$$\sigma_t = 0.2374e^{1855.2/T} \times \varepsilon, (\varepsilon \le \varepsilon_y)$$

Eq. 5.6

2. Elastoplastic behavior of wood

Both the Voigt-Kelvin and Maxwell models, which contain springs and dashpots, can be used to describe the linear viscoelastic behaviors of materials in the elastoplastic region (region II). For non-linear viscoelastic behaviors, a combination of groups of non-linear spring and dashpot will be necessary to construct a model. Analysis of such systems can become extremely complex [147]. Ludwik [148] proposed an alternative solution to describe viscoelastic behavior by the following empirical equation:

$$\sigma = \sigma_0 + c\varepsilon^m$$

Eq. 5.7

Where, σ_0 is the yield stress, c the strength coefficient, and m the strain-hardening coefficient, which could be determined from the best fits to experimental data. This equation may be used to characterize the stress-strain curve in the elastoplastic region (region II) of transverse compression.

Figure 5.49 and Figure 5.50 indicate that, after normalization ($\sigma_n=\sigma/\sigma_y$, σ_y = SP1), the normalized curves for radial and tangential compressions at different temperatures (22°C -140 °C) can be, respectively, fitted into one curve in the elastic region (region I) and elastoplastic region (region II). In these regions, the temperature does not change the form of the stress-strain curves; the wood behaves similarly at different stress levels at different temperatures. Thus, the possibility of fitting the data into one normalized curve implies that, in transverse compression, the deformation behavior of wood is independent of temperature in the elastic and elastoplastic regions, but dependent on its cellular structure. This finding is in accordance with that of Wolcott et al. [149] and other researchers [150,151]. These researchers constructed a model by modifying the Hook's Law to describe the linear and nonlinear stress-strain relationship [$\sigma=\varphi(\varepsilon)E\varepsilon$]. They claimed that, for most synthetic polymer foams and wood, the strain-stress function is independent of the properties of the material matrix or the cell wall, and is dependent only on the cellular structure. They also claimed that the effect of loading

conditions, temperature, and moisture content should not influence the strain function φ(ε), but only the Young's modulus E.

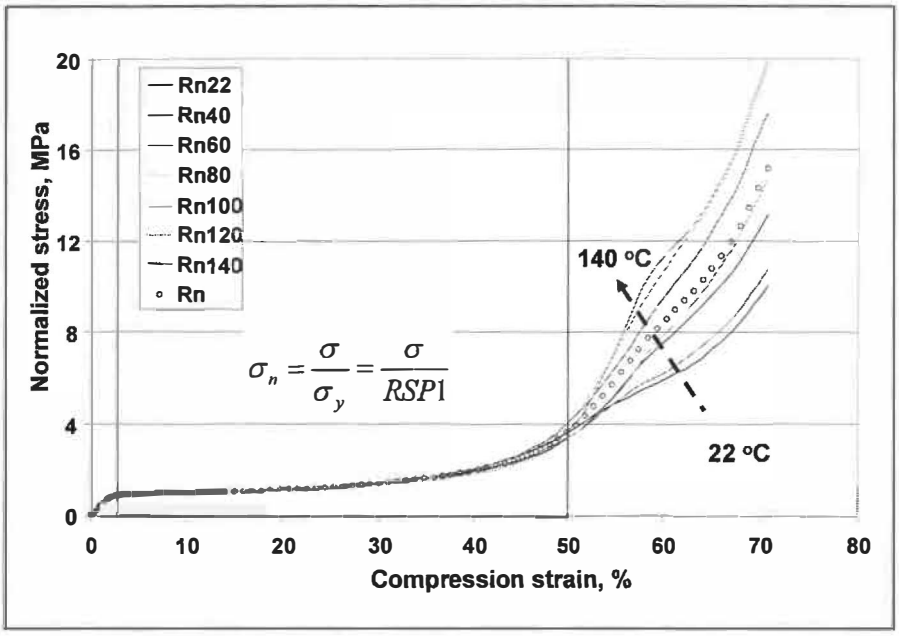

Figure 5.49 Normalized curves for radial compression at various temperatures

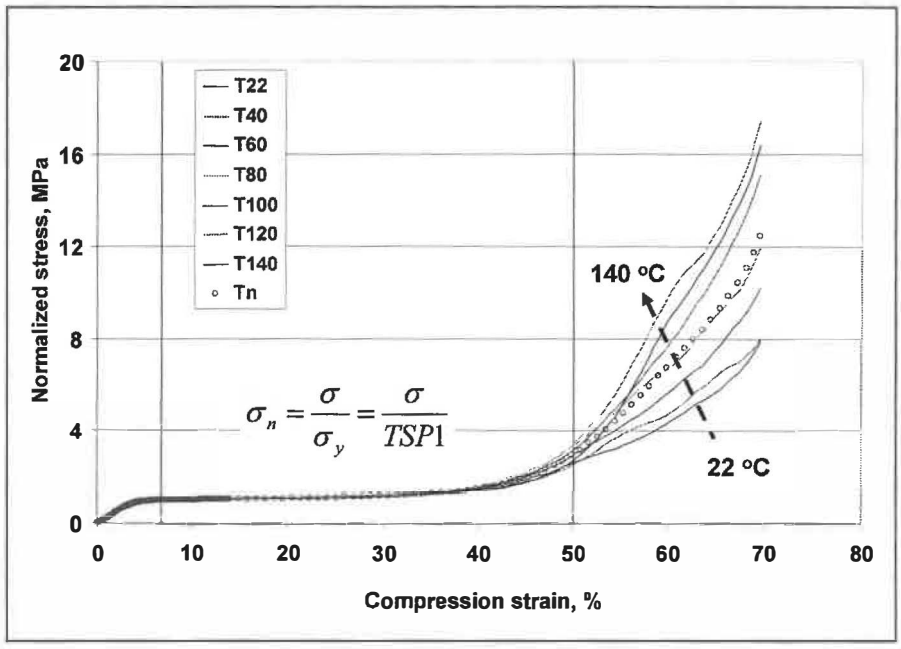

Figure 5.50 Normalized curves for tangential compression at various temperatures

However, in the densification region (region III), the compression curve varies with temperature in both radial and tangential compression. As discussed earlier, after the collapse of most of the EW fibers in region II, the wood begins to expand laterally, and fiber dislocation and separation dominate the deformation process. This phenomenon suggests that wood behaves quite differently in lateral expansion and fiber separation at different temperatures. In fact, the values of second plateau stress in the normalized curves correspond to the SP2/SP1 ratio. This ratio increases with increasing temperature, indicating a relative increase in fiber separation resistance at higher temperature. This characteristic has been discussed in section 5.2.4.3.

Since the normalized curves can be fitted into one curve, this resultant curve can be used to represent the normalized curves for describing the elastoplastic region (region II) at various temperatures. Based on an average normalized curve, a mathematical model could be constructed as proposed by Liu et al (152,153).

$$\frac{\sigma}{\sigma_y} = 1 + c \times \left[\frac{\varepsilon_d}{\varepsilon_d - (\varepsilon - \varepsilon_y)} - 1 \right]^m$$

Eq. 5.8

The parameters in this equation can be obtained as follows:

Taking $X = \log\left[\frac{\varepsilon_d}{\varepsilon_d - (\varepsilon - \varepsilon_y)} - 1 \right]$ and $Y = \log(\frac{\sigma}{\sigma_y} - 1)$

Then $Y = a + mX$

Since the wood matrix begins to yield at approximately 8% strain, and densify at about 50% strain (in radial and tangential compressions) therefore we can set the yield strain (ε_y) and densification strain (εd) as 0.08 and 0.5, respectively. A linear relationship for the radial and tangential compressions is presented in Figure 5.51 and Figure 5.52. The values of R^2 are 0.995 and 0.998, respectively, indicating a high linearity for both directions. From the regression equation $Y = a + mX$, the parameters 'c' ($=10^a$) and 'm'

can be obtained for both radial and tangential compressions. Table 5.10 shows the linear relationship of *X*/*Y* and mathematical models for the normalized curve of radial and tangential compressions. The strength coefficients *c* for both radial and tangential compression are, respectively, 0.5112 and 0.2322. These values are only about 0.1-0.05% of that of 0.05% C killed steel sheet (503.67 MPa). But for the strain-hardening coefficient *m*, the value for wood is 4-6 times higher than that of 0.05% C killed steel (0.234) [154].

Figure 5.53 shows that the normalized models (σ_n) fit well with the average normalized curves for the elastoplastic region (8-50%) in radial and tangential compressions.

Table 5.10 X/Y linearships and mathematical models for normalized curves at radial and tangential compressions

Sample	X/Y relationship	a	*c*, MPa	*m*	σ_n Models
Radial Comp.	Y= 1.0297X – 0.2914 R^2= 0.9950	-0.2914	0.5112	1.0297	$\sigma_n = 1 + 0.5112 \times [(0.5/(0.58-\varepsilon) -1]^{1.0297}$
Tangential Comp.	Y= 1.3598X –0.6341 R^2= 0.9926	-0.6341	0.2322	1.3598	$\sigma_n = 1 + 0.2322 \times [(0.5/(0.58-\varepsilon) -1]^{1.3598}$

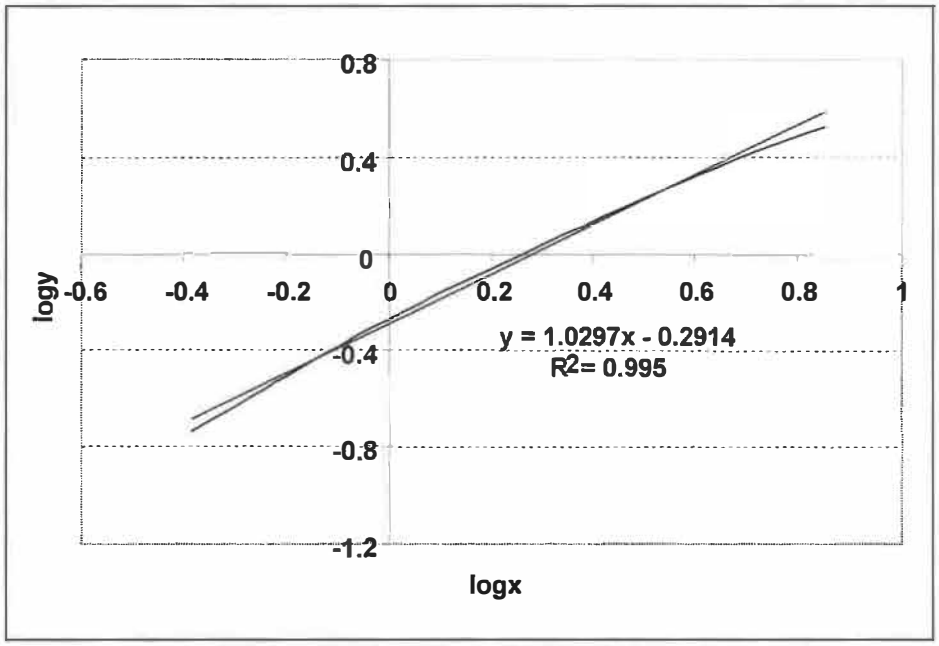

Figure 5.51 Linear relationship of normalized curve for radial compression

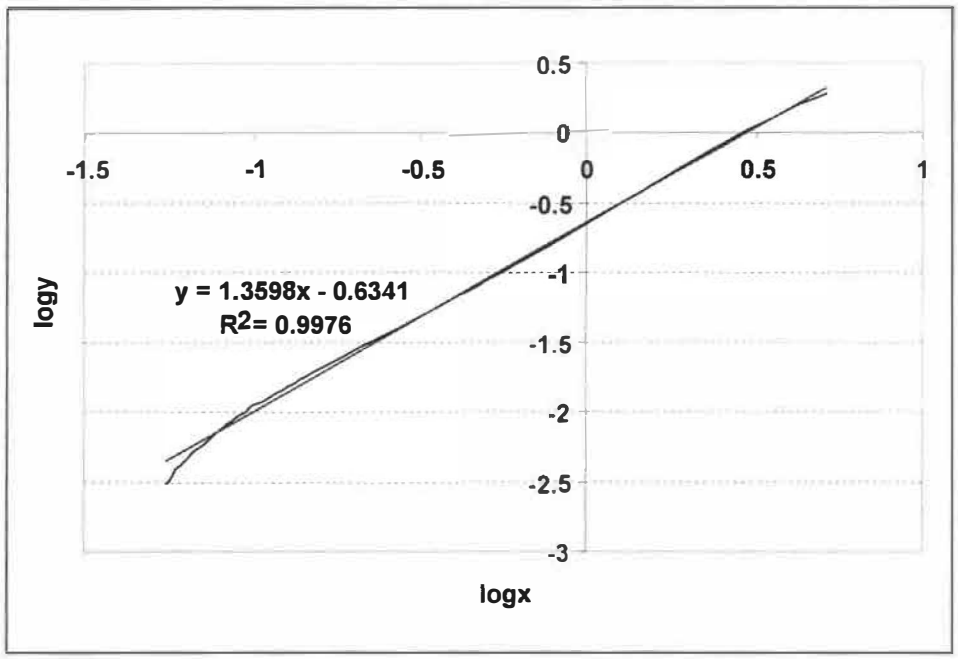

Figure 5.52 Linear relationship of normalized curve for tangential compression

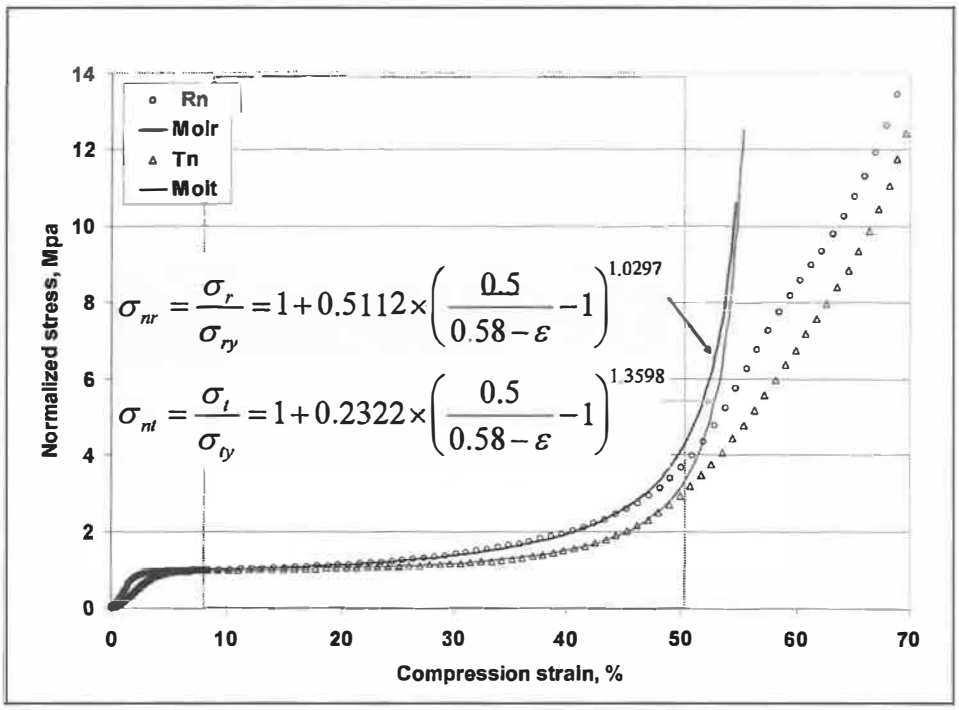

Figure 5.53 Models and normalized compression curves for radial and tangential compressions

The general models for compression stress at various temperatures and different compression strains in this region can be derived from this normalized stress (σ_n).

$$\sigma = \sigma_n \times \sigma_y$$

The general model includes two parts, strain factor [$\sigma_n = f(\varepsilon)$], which is independent of temperature, and the temperature factor [$\sigma_y = f(T)$], which is independent of compression strain. In radial and tangential compression, σ_y can be directly obtained from experiments or equal to RSP1 (radial) and TSP1 (tangential) in Eq. 5.2 and Eq. 5.3 developed earlier. Thus:

For radial compression:

$$\sigma_r = RSP1 \times \left[1 + 0.5112 \times \left(\frac{0.5}{0.58 - \varepsilon} - 1\right)^{1.0297}\right]$$

Eq. 5.9

$$\sigma_r = 0.0173 \times e^{1544.2/T} \times \left[1 + 0.5112 \times \left(\frac{0.5}{0.58 - \varepsilon} - 1\right)^{1.0297}\right]$$

Eq. 5.10

For tangential compression:

$$\sigma_t = TSP1 \times \left[1 + 0.2322 \times \left(\frac{0.5}{0.58 - \varepsilon} - 1\right)^{1.3598}\right]$$

Eq. 5.11

$$\sigma_t = 0.0141 \times e^{1652.8/T} \times \left[1 + 0.2322 \times \left(\frac{0.5}{0.58 - \varepsilon} - 1\right)^{1.3598}\right]$$

Eq. 5.12

Figure 5.54 and Figure 5.55 show that the general models fit very well at two temperatures when the experimental values of yield stress were used in both radial and tangential directions. To simplify the validation of Eq. 5.9 and Eq. 5.11 for all temperatures tested, Figure 5.56 and Figure 5.57 compare the model values and experimental values at various temperatures (22°C – 140 °C) for a series of compression strains (10%, 20%, 30%, 40%, 50%) in radial and tangential compressions. Clearly, the model values and experiment values fit very well; the variation is less than 10% in most cases. However, the model values in both compression directions are somewhat higher than the experimental values, when the compression strain is high (e.g. 50%), which is evident as shown in Figure 5.53.

Figure 5.58 and Figure 5.59 show that the general models (Eq. 5.10 and Eq. 5.12) fit well at two temperatures when the model of yield stress is used in both radial and tangential directions. Figure 5.60 and Figure 5.61 show the plot of the model values and experimental values at various temperatures, and a series of compression strains for the radial and tangential compressions. Again, the model values and the experiment values fit well. The variations are, however, a little higher than those of the models where the experimental yield stress were used, especially at low temperature and at relative high strain (above 45%) for tangential compression. This variation is introduced by the model of yield stress (TSP1) at this direction, since the general model fit quite well when experimental values of yield stress were used (Figure 5.57). However, the variation in the model is still acceptable because the model variations for the tangential yield stress (stress at 10% strain) are 8-16% in actual tests. The variation comes mainly from the variation of strength in wood fibers. For example, the variation of stress could be higher when the fibers in the transition zone between the EW and LW play a role in high strain compression. This situation can be seen in Figure 5.6 which shows that the variation of stress become more evident at 30-50% compression strain. In fact, this variation is quite large at low temperature.

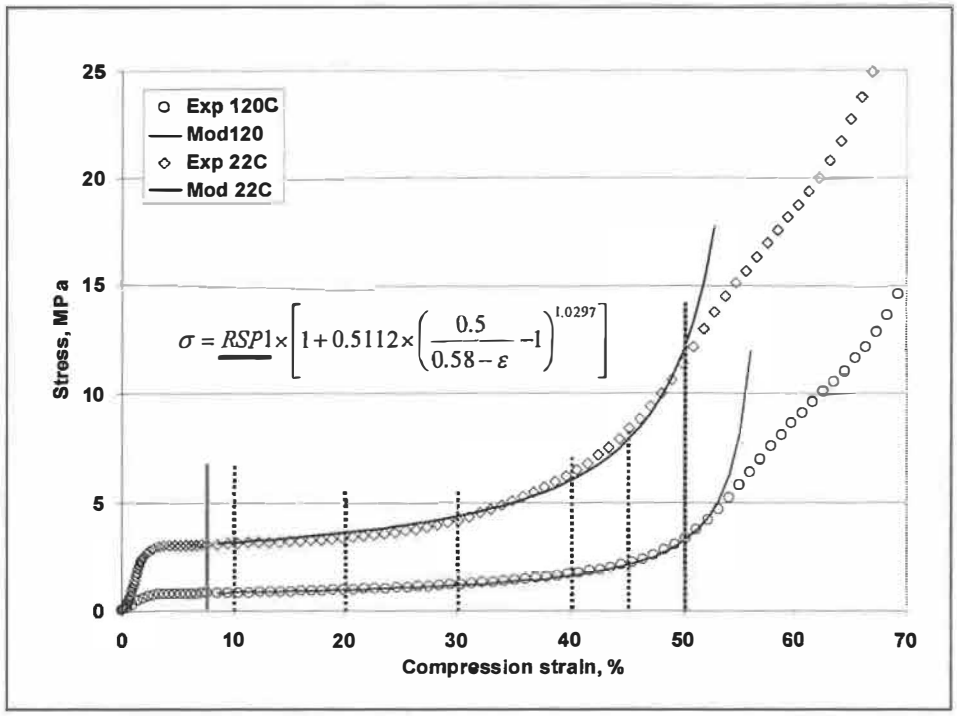

Figure 5.54 Model validation for radial compression at 22°C and 120°C (RSP1, experimental value)

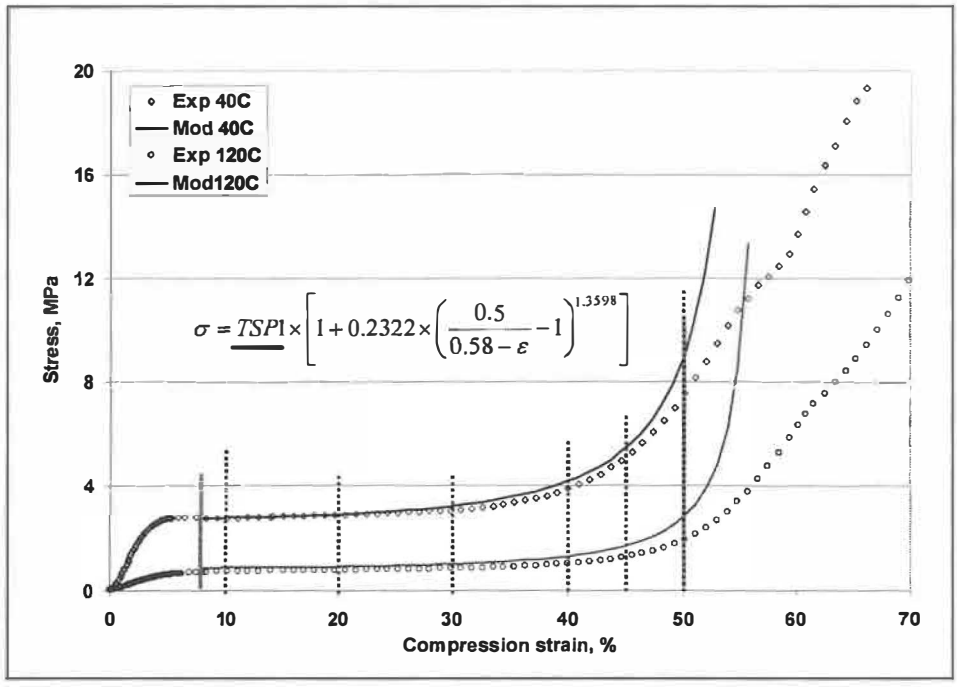

Figure 5.55 Model validation for tangential compression at 22°C and 120°C (TSP1, experimental value)

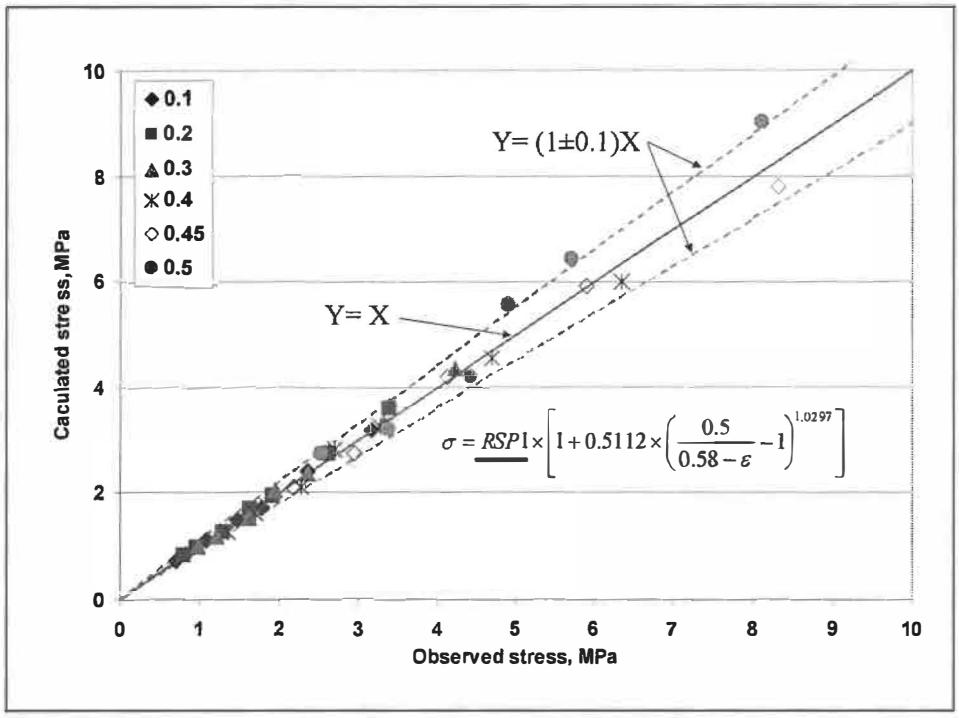

Figure 5.56 Model value and experimental value at various compression strains and temperatures for radial compression (RSP1, experimental value)

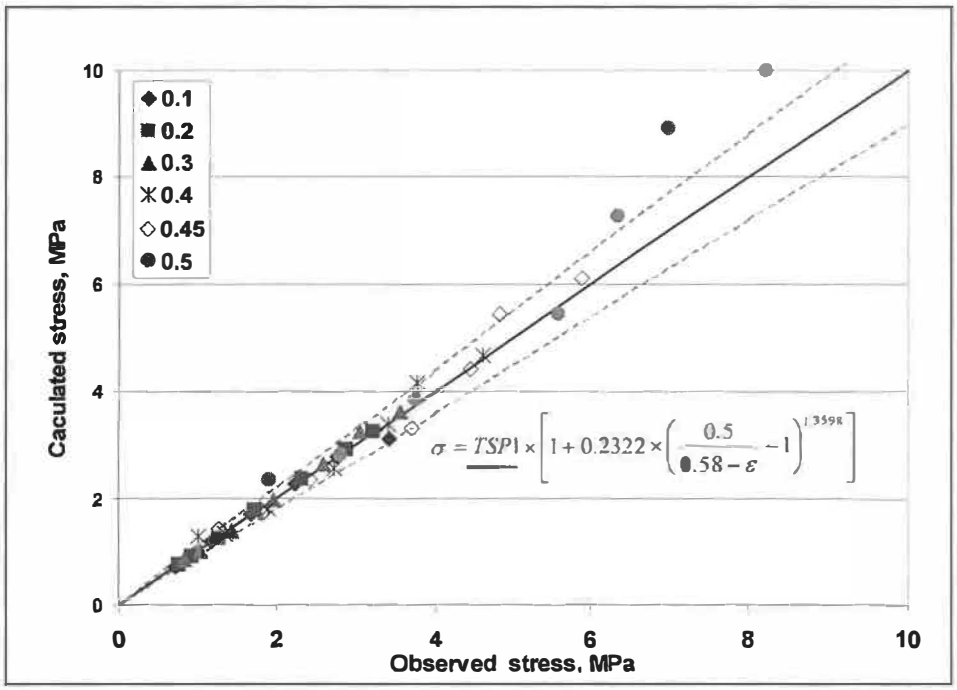

Figure 5.57 Model value and experimental value at various compression strains and temperatures for tangential compression (TSP1, experimental value)

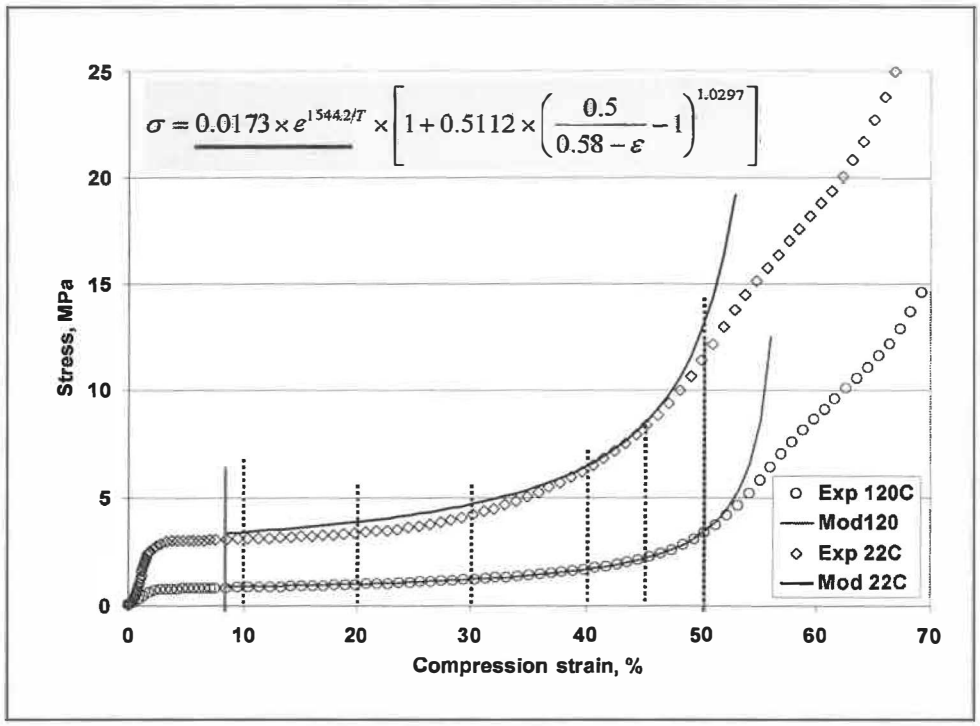

Figure 5.58 General model validation for radial compression at 22°C and 120°C

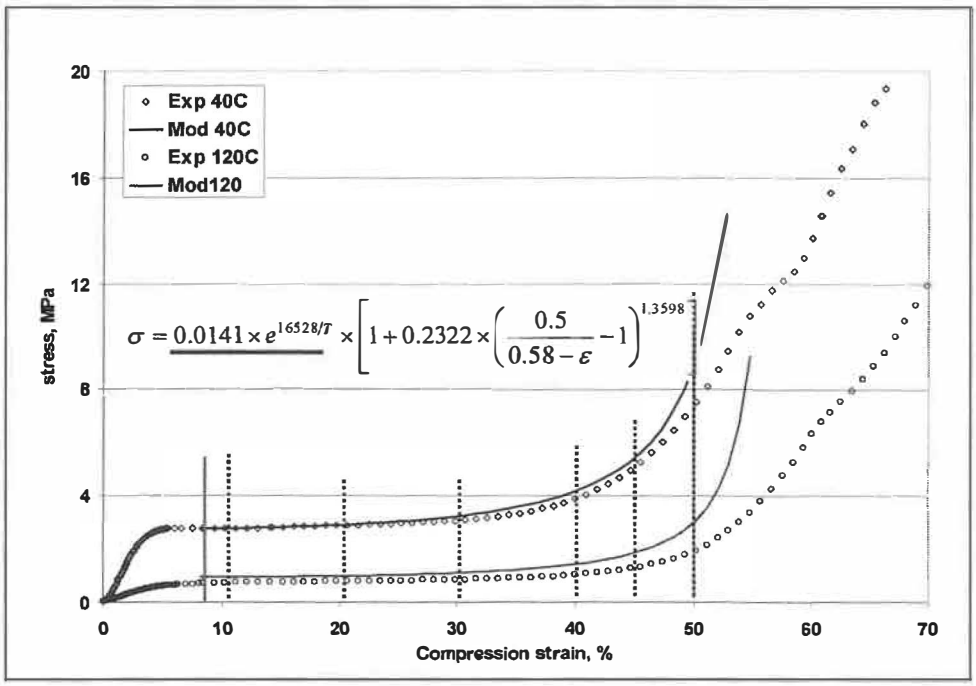

Figure 5.59 General model validation for tangential compression at 22°C and 120°C

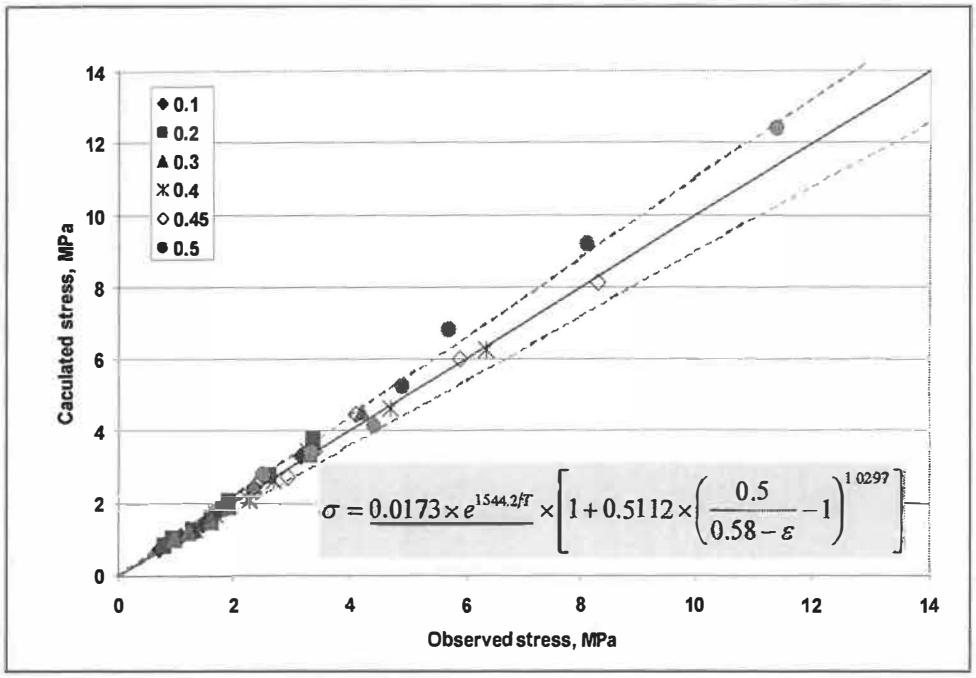

Figure 5.60 General model value and experimental value at various compression strains and temperatures for radial compression

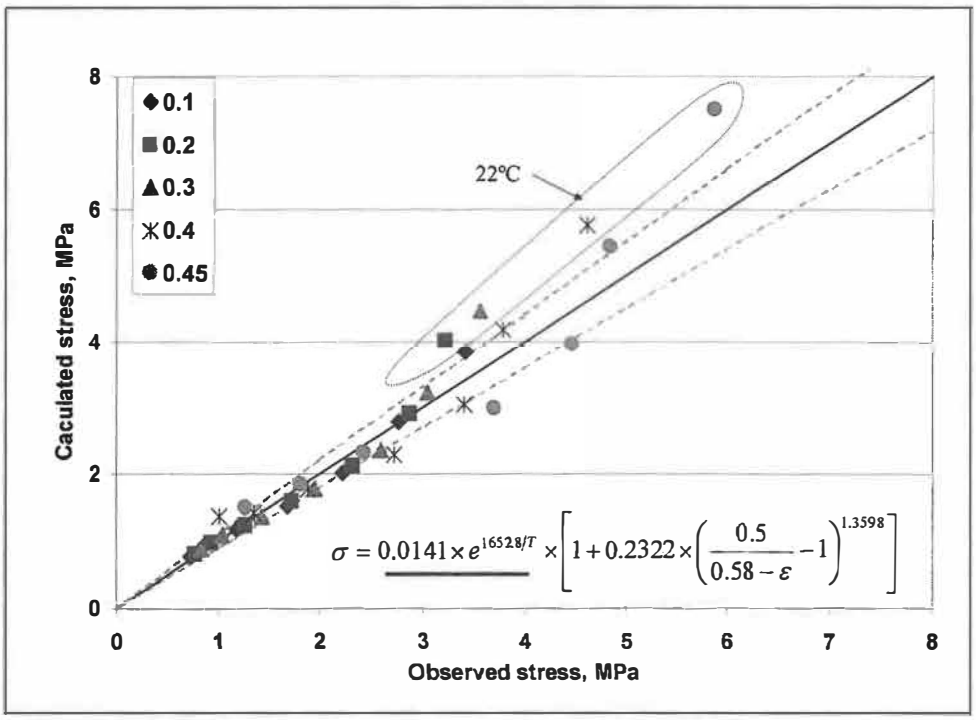

Figure 5.61 General model value and experimental value at various compression strains and temperatures for tangential compression

5.2.7 Fiber collapse stress in transverse directions and its relation with refining mechanism

According to the mechanism of wood compression, the first plateau is the result of the successive collapse of earlywood fibers (see sections 5.2.1.1 and 5.2.2.1). Thus, the stress of this plastic region (region II) represents the transverse resistance of EW fibers. This resistance stress at different temperatures can be calculated by using Eq. 5.10 and Eq. 5.12 for the radial and tangential directions. Since the EW fibers constitute a group of fibers with relatively different strength property (owning to different cell wall thickness and lumen diameter etc.), the stress values at 10% compression strain can be used to represent the low-strength EW fibers and the stress values at 45% strain represent relatively high-strength fibers.

Table 5.11 presents the transverse resistance at various temperatures obtained from experiments (Obs.) and those values calculated from the general models (Mod.). The table indicates that the model values and the experimental values fit well, especially for the radial compression, and that the transverse resistances at the same temperature are similar.

Table 5.11 Transverse resistance of EW wood fiber at various temperatures

		Transverse stress, MPa											
T, °C		22		80		120		140		160		180	
		low	high	low	high	low	high	low	high	low	high	low	high
R	Obs.	3.17	8.30	1.48	3.40	0.84	2.18	0.71	1.72				
	Mod.	3.30	8.12	1.40	3.44	0.90	2.20	0.74	1.82	0.62	1.53	0.53	1.31
T	Obs.	3.42	5.88	1.69	3.70	0.89	1.82	0.73	1.28				
	Mod.	3.84	7.50	1.83	2.99	0.95	1.86	0.77	1.51	0.64	1.26	0.54	1.06

* R – radial; T – tangential

Several authors have studied the transverse resistance of wood fibers. Bardage et al. [155] demonstrated that the collapse behavior of delignified fibers may be determined by fiber structure and external force. Jang [156] have formulated a general equation (collapse index, CI) for the collapse of wood pulp fibers in terms of transverse

dimensions, transverse elastic modulus of the fiber wall, and collapse pressure. The equation is rather complicated and only an index of collapsibility of wood-pulp fibers was predicted. However, the exact external force required to collapse a fiber has not been identified by these researchers.

Several researchers [157,158,159] have conducted the compression on single wood pulp fibers. Table 5.12 compares the fiber collapse force obtained in this study with those reported by others.

Table 5.12 Force required to collapse a wood fiber at room temperature

Reference	Species	Treatments	Collapse force, MPa
Nyren [158]	Spruce (Latewood)	Sulfite	7.85
Nyren & Hartler [159]	Norway spruce (Earlywood)	Kraft	4.28 - 5.14
	Norway spruce (Earlywood)	Sulfite	2.85 - 3.14
This study	White spruce (Earlywood)	Water-saturated	R 3.17 - 8.30 (Exp.) (3.30-8.12) (Mod.)
			T 3.42-5.88 (Exp.) (3.84-7.50) (Mod.)

* R – radial direction; T – tangential direction; Exp. – test value; Mod. - Model value

The fiber collapse force from this investigation was obtained by radial compression of solid wood blocks containing EW and LW. Considering the variation of the strength of the EW fiber, the stress values were taken at 10 % and 45% compression strains to represent the lower and higher strength of EW fibers, thus, most of EW fibers were evaluated in the test. This may explain why our data show a wider range in comparison to those reported for chemical fibers (Nyren and Hartler).

There are some advantages of testing wood blocks instead of single chemical fibers. Using untreated blocks means that the fibers suffer little or no structural and chemical modification. Further, testing thousand of fibers in a block is more realistic and accurate than using a single fiber. The technique using single fiber is rather tedious and time consuming in fiber selection and testing. Most importantly, our test can be done easily at different temperatures. A general model can be developed to calculate the collapse force at various temperatures.

In this work the collapse force models are developed using data collected at 22-140°C. As we know, hydrolysis and decrystalization of hemicelluloses and cellulose mainly occur above 200°C and 230°C, respectively [62]. Lignin is more stable than these two components. Thus, wood remains relatively stable at temperatures below 200°C. There should be no sudden change in wood properties at temperature between 140°C and 180°C. Therefore, the reliability of these models may be extended to predict properties up to 180°C. If the presumption holds, the general model can, for the first time, be used to calculate the fiber collapse force in a refiner during the refining which takes place about 130-160°C.

The mechanical actions of a refiner are commonly characterized using energy-based methods. Hence, a good knowledge of the forces acting on fibers would lead to a better understanding of the refining process [160]. Many researches have been conducted to characterize the forces and pressures acting between bars in an operating refiner. A maximum peak stress in a refiner was found to be 4.4-7.2 MPa [161, 162], which corresponds to the stress at the leading edge of a refiner bar. The peak was followed by a plateau that was about an order of magnitude lower, with an average of 0.45 MPa.

Figure 5.62 compares the compressive stress in a refiner and the stress required to flatten EW fibers. According to the model developed in this study, a compressive force of 0.62 –1.53 MPa is required to collapse a white spruce EW fiber at 160°C (that of LW fiber could be 10-15 times higher). This is somewhat higher than the compressive force between two refiner bars that is about 0.45 MPa in average. Therefore, the compressive force between two refiner bars is not enough to efficiently flatten the EW fibers. In fact, only the compressive stress at the leading edge is sufficient to collapse the EW fibers, if the compression strain is great enough. In reality, the refiner gap is fixed and is much larger than the fibers diameter (transverse dimension). Thus, even those fibers were trapped on the leading edges; they are not likely to collapse completely. Therefore, most compression on fibers will remain on the elastic region during the refining. These small compressions evidently have no effect on the breakdown of the structure unless thousands of these small compressions were applied repeatedly. The number of these small impacts in refining has been estimated to be 10,000 [163]. This process is called

fatigue process and consumes tremendous amount of energy. However, this process is not desirable and should be avoided if possible in order to improve the energy efficiency in refining.

The concern over the lack of compressive force during refining has been discussed by Law [164]. He claimed that the predominant refining action might actually come from the shear force rather than from the compression in the current refining technology. He also suggests that there must be a desirable balance between these two actions, and most of the compression must precede the shear to establish favorable conditions for the benefit of the latter. However, the current refining technology does not permit the two forces to operate independently in a single refiner, and thus the benefits of compression cannot be fully exploited. The finding of the present work shows that the compressive force is not enough to collapse most of the EW fibers, strongly support these concerns. Therefore, a compressive pretreatment of wood chips prior to refining would improve the pulp qualities and energy efficiency in a refining.

The path of conventional fiber development (I: fiber separation stage, II: fiber develop stage) and that of a new approach can be schematically illustrated in Figure 5.63. In the new approach, chips are pre-compressed, normal to fiber axis, to a large strain of 70% before refining. The high strain pre-compression (70% strain), which flatten wood fibers and create fiber separation, could reduce the fiber transverse resistance by 70-85% (Table 5.13), decreasing the compressive force required to collapse a pre-compressed fiber to 0.25-0.32 MPa. Therefore, in subsequent refining of the pre-compressed chips, an average compressive force of 0.45 MPa will flatten most of these fibers. This approach will potentially change the refining process from fatigue process to a more efficient breakdown process. As discussed earlier, the energy consumption for such transverse compression is only about 4.79-6.67 MJ/m^3 (3.5-4.9 kWh/t) at 22 °C and 2.32-2.55 MJ/m^3 (0.6-0.7 kWh/t) at 120°C, representing only 0.2% and 0.03%, respectively, of the specific energy consumption in a typical TMP (2500 kWh/t).

Table 5.13 First plateau stress (SP1) at multi-compression at the first three compression cycles

Sample	Compression conditions			SP1, MPa		
	Temp. °C	Rate, mm/Min.	Strain, %	1st Comp.	2nd Comp.	3rd Comp.
1A	22	3	50	2.021	0.632	0.511
2B	22	3	70	2.264	0.319	0.108
5A	90	3	50	0.813	0.358	0.343
6A	90	3	70	0.904	0.253	0.206

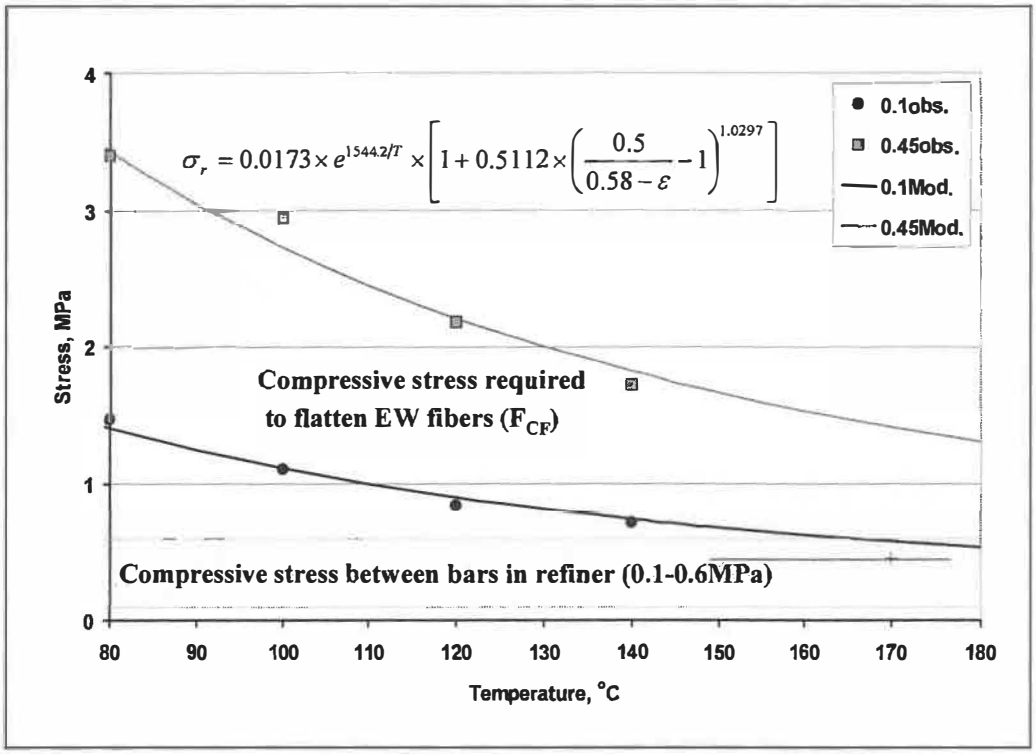

Figure 5.62 Stress required to flatten EW fibers at various temperatures and the stress in a refiner (0.1obs. and 0.45 obs. represent fiber resistance values at compression strain of 10% and 45% getting from test. 0.1Mod. and 0.45Mod. represent the model value at those compression strain)

Emphasis on re-thinking the refining technology has also been made recently [165]. Needs were suggested to characterize refining action by the forces and strains on fibers rather than the energy during bar crossing. Jocco Deckker [165] also suggested that creation of internal fibrillation with minimal fine production should be the target of

refining, which is best achieved by compression rather than shear action. A new refiner based on this principle is under development in Netherlands [165]. The fiber resistance model developed in this investigation could serve as a base for such researches.

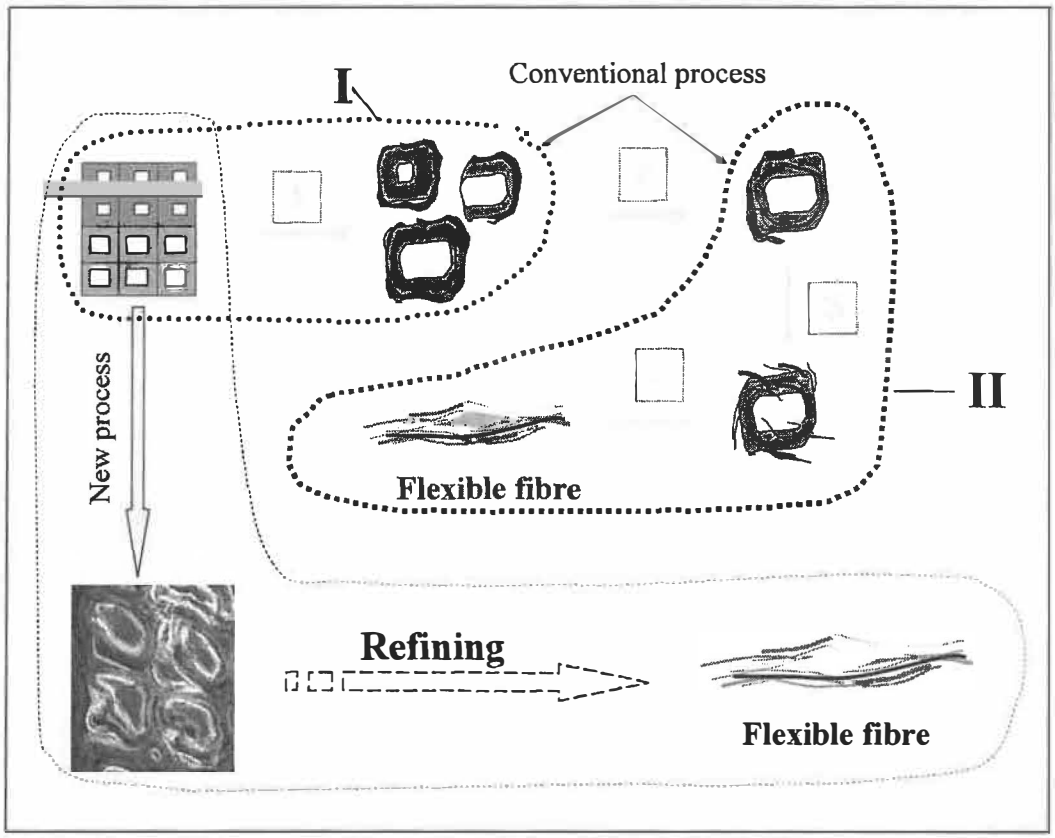

Figure 5.63 Conventional refining processes and proposed new processes

5.3 Concluding remarks for this part

Wood responds similarly in both radial and tangential compressions at various temperatures by successively going through an elastic, an elastoplastic, and a densification (fracturing) stage. It behaves, however, quite differently in longitudinal compression. A single large strain (70%) compression requires, respectively, 3.5-4.9 kWh/t and 0.6-0.7 kWh/t at 22°C and 120°C. These energies represent only 0.2% and 0.03% of the specific energy consumption in a typical TMP.

The modulus (MOE), first and second plateau stresses (SP1, SP2), and the specific compression energy (SCE) have been used to characterize the behaviors of wood under compression at different stages. Among them, the second plateau stress was defined and used for the first time to describe the fiber separation at densification stage. The relationships between these four parameters and the temperature follow the Arrhenius' Law. This means that the effect of thermal softening can be explained by the motion of polymer chain of the wood main components. The softening temperature of lignin obtained by compression at different directions is around 90-100°C.

For radial and tangential compressions, the normalized compression curves at various temperatures fit into one unique curve, respectively, in the elastic and elastoplastic regions, indicating the predominant influence of the tubular structure of fibers upon the behaviors of wood in these two regions. However, in the densification region, the wood behaves quite differently at different temperatures. The SP2/SP1 ratio varies from 5.5 to 12 and 4 to 11 for radial and tangential compression, which increases with increasing temperature, indicating that the low temperature favors fiber separation. However, the fiber separation stress (SP2) is relatively high at low temperatures.

SEM observation also confirms that fiber response similarly under compression at radial and tangential directions. Separation between P/S_1, S_1/S_2 was frequent owing to the distinct difference in fibril orientation between these layers, and the longitudinal cleavage was only resulted from the transverse compression.

General mathematic models are developed to express the stress in the elastoplastic region in radial and tangential compressions. The models consist of two independent factors- the temperature factor and strain factor. These models were used for the first time to predict the resistance of EW fibers at various temperatures. According to these models, the compressive stress required to flatten EW fibers in refining conditions is about 0.62-1.53 MPa. This force is much higher than the average stress (0.45 MPa) between two refiner bars, indicating the reason for the high-energy consumption in refining. However, the high strain pre-compression (70% strain), which flattens wood fibers and create fiber separation, could reduce the fiber transverse resistance by 70-85%, decreasing the compressive force required to collapse a pre-compressed fiber to 0.25-0.32 MPa (at 90°C and 22°C). Therefore, in subsequent refining of the pre-compressed chips, an average compressive force of 0.45 MPa will readily flatten most of these fibers. This approach may potentially change the refining process from fatigue process to a more efficient breakdown process.

The results obtained in this study suggest that pretreatment of wood by static compression with a large compression strain flattens fibers, reduces fiber transverse resistance, and creates fiber separation before refining may be an effective mean to reduce the refining energy.

Chapter 6 - Results and discussions: Compression behavior of sulfonated samples

Due to the morphological structure of wood, radial compression generates relatively more stable stress-strain curves. Therefore, we studied the effect of sulfonation on wood behavior in radial compression.

Sulfonation is an important technique for producing mechanical pulp (CTMP, CMP) with improved papermaking properties. We used a central composite design (CCD) [166], to conduct study on samples of 15 different levels of sulfonation. The sulfonated samples were compressed with and without restraint. In addition to the investigation on the difference between these two types of compression techniques, we also examined the response of early- and latewood to sulfonation, and their mechanical behavior under a compression force.

6.1 Sample sulfonation

6.1.1 Factors effecting sulfonation

Table 6.1 presents the sulfonation conditions and the content of acid groups. An analysis using Response Surface Method (RSM) [166] indicated that the reaction temperature is the most influential factor on the level of sulfonation (Figure 6.1 to Figure 6.3). When the temperature is below 90°C, prolonged reaction time does not significantly influence the sulfonate content. However, at a high temperature, an increase of reaction time improves significantly the sulfonate content (Figure 6.3). The effect of sodium sulphite concentration and treatment time are also significant, but to a lesser extent when compared to the temperature. The results are in line with those of Beatson et al [167] who reported that the total SO_2, pH, and reaction time have significant effect on the sulphur content of lignin in the treated spruce wood.

Table 6.2 shows the analysis of variance (ANOVA) and regression coefficient for the sulfonate contents. The ANOVA table partitions the variability in sulfonate content into

Table 6.1 Experiment conditions (CCD) and results of sulfonation

	Sulfonation conditions Code value			Sulfonation conditions Actual value			Acid groups	
Run	A Temp. °C	B Time min	C Na_2SO_3 Con. %	Temp. °C	Time min	Na_2SO_3 Con. %	Sulfonate (Predict, Cs) mmol/kg	Carboxylate mmol/kg
1	1	1	-1	131.6	68.8	6.1	157.3 (149.3)	117.0
(2)	0	0	0	90	45	15	78.7 (78.1)	110.9
3	-1	1	1	48.4	68.8	6.1	33.3 (21.5)	94.8
4	1	-1	-1	131.6	21.2	6.1	118.9 (105.7)	134.5
5	1	1	1	131.6	68.8	23.9	212.3 (208.1)	136.5
6	-1	-1	-1	48.4	21.2	6.1	20.1 (14.1)	95.6
(7)	0	0	0	90	45	15	78.4 (78.1)	110.9
8	0	-1.682	0	90	5	15	42.9 (49.7)	104.4
9	0	1.682	0	90	85	15	91.2 (98.8)	122.3
10	-1.682	0	0	20	45	15	29.1 (34.3)	92.9
11	0	0	-1.682	90	45	0	8.4 (26.7)	80.6
(12)	0	0	0	90	45	15	78.3 (78.1)	111.3
13	0	0	1.682	90	45	30	95.8 (91.9)	119.9
14	1	-1	1	131.6	21.2	23.9	155.3 (157.0)	123.3
(15)	0	0	0	90	45	15	77.8 (78.1)	110.1
16	-1	-1	1	48.4	21.2	23.9	35 (32.9)	105.7
17	-1	1	1	48.4	68.8	23.9	44.7 (47.7)	117.2
(18)	0	0	0	90	45	15	78.3 (78.1)	111.7
19	1.682	0	0	160	45	15	236.9 (246.1)	145.4

* Note, data in brackets indicate the value predicted from Eq. 6.1

separate parts for each of the effects. It then tests the statistical significance of each effect by comparing the mean square against an estimate of the experimental error. In this case, 6 effects have P-values less than 0.05, indicating that they are significantly different from zero at 95% confidence level. Therefore, the relationship of sulfonate content (C_s) and reaction conditions can be simplified as shown in the following equation:

$$C_s = 78.09 + 62.99\times Temp + 14.61\times Time + 19.38\times Con. + 21.95\times Temp^2 + 9.06\times Temp\times Time - 6.65\times Con.^2 \quad (R^2 = 0.97).$$

Eq. 6.1

Where, Temp. Time and Con. are code values for these reaction conditions, which can be obtained from the actual values as shown in Table 4.3. The R-Squared indicates that the model as fitted explains 98.6% of the variability in sulfonate content. The adjusted R-squared, which is more suitable for comparing models with different numbers of independent variables, is 97.2%. The standard error of the estimate shows that the standard deviation of the residuals has a value of 10.62. The predicted sulfonate content (from Eq. 6.1) is presented in Table 6.1 and illustrated in Figure 6.4. The figure indicates that the model values fit very well with the experiment values.

Table 6.2 Analysis of Variance (ANOVA) and regression coefficient for sulfonate content (C_s)

Source	Sum of Squares	Df	Mean Square	F-Ratio	P-Value	Regression Coefficient.
Constant						78.09
A:Temp.+block	54178.20	1	54178.20	480.73	0.0000	63.00
B:Time+block	2915.20	1	2915.20	25.87	0.0007	14.61
C:Con.+block	5130.03	1	5130.03	45.52	0.0001	19.38
AA	6579.63	1	6579.63	58.38	0.0000	21.95
AB	657.03	1	657.03	5.83	0.0390	9.06
AC	529.75	1	529.75	4.70	(0.0583)	(8.14)
BB	25.32	1	25.32	0.22	(0.6468)	(-1.36)
BC	28.50	1	28.50	0.25	(0.6271)	(1.89)
CC	603. 21	1	603.21	5.35	0.0460	-6.05
Total error	1014.30	9	112.70			
Total (corr.)	72548.80	18				
R^2 = 98.60 %, R^2 (adj.) = 97.20 % , Standard Error of Est. = 10.62, Mean absolute error = 5.45, Durbin-Watson statistic = 1.05						

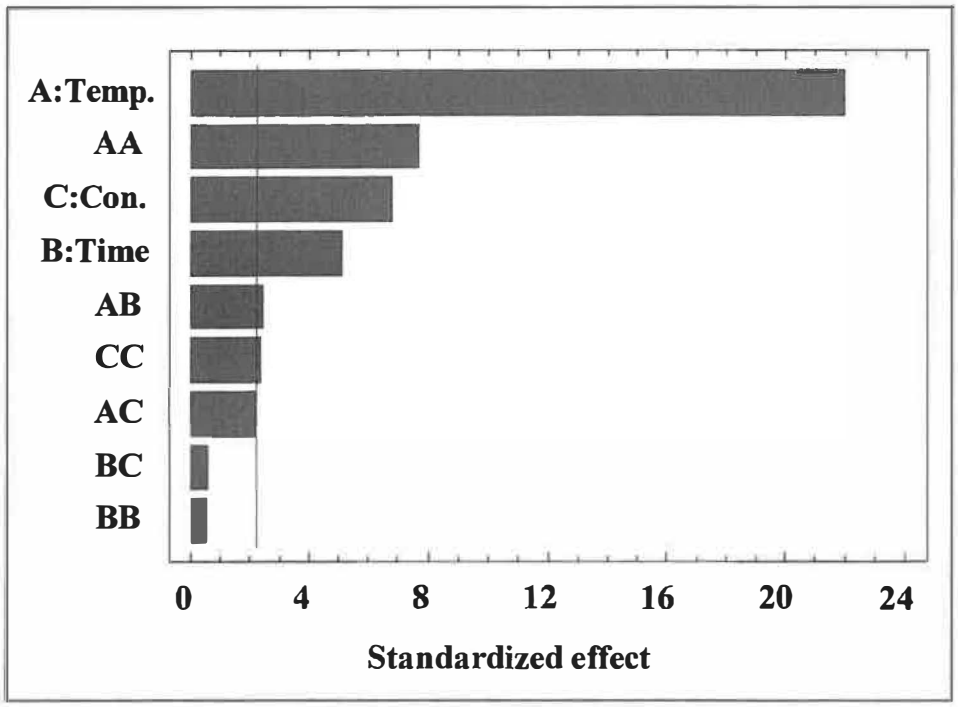

Figure 6.1 Standardized Pareto Chart for sulfonated content (Cs)

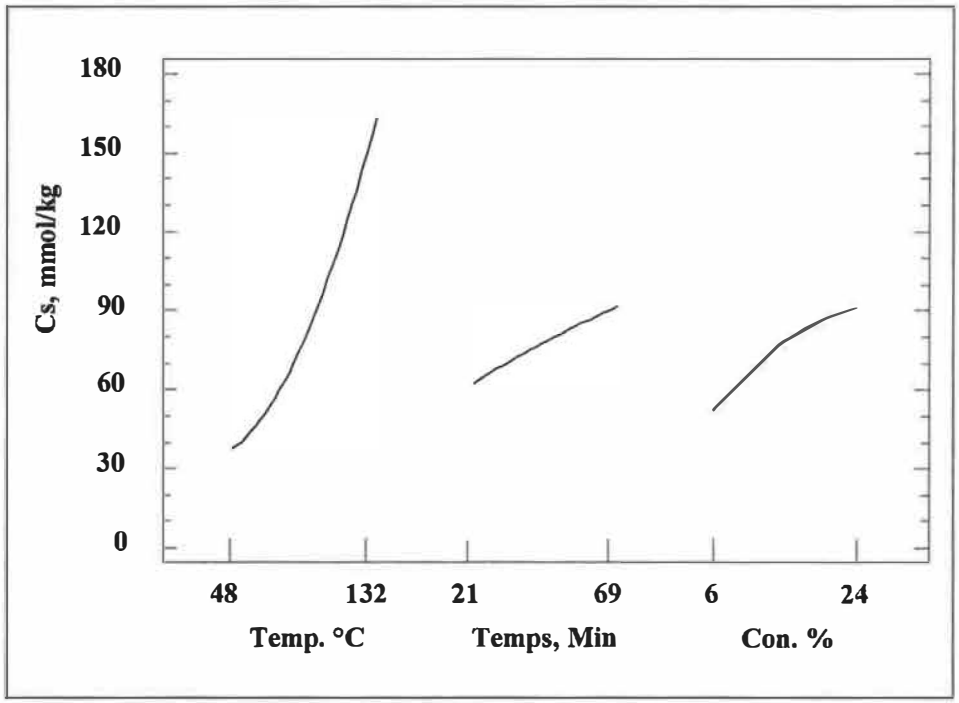

Figure 6.2 Plot of main effects on sulfonate content (Cs)

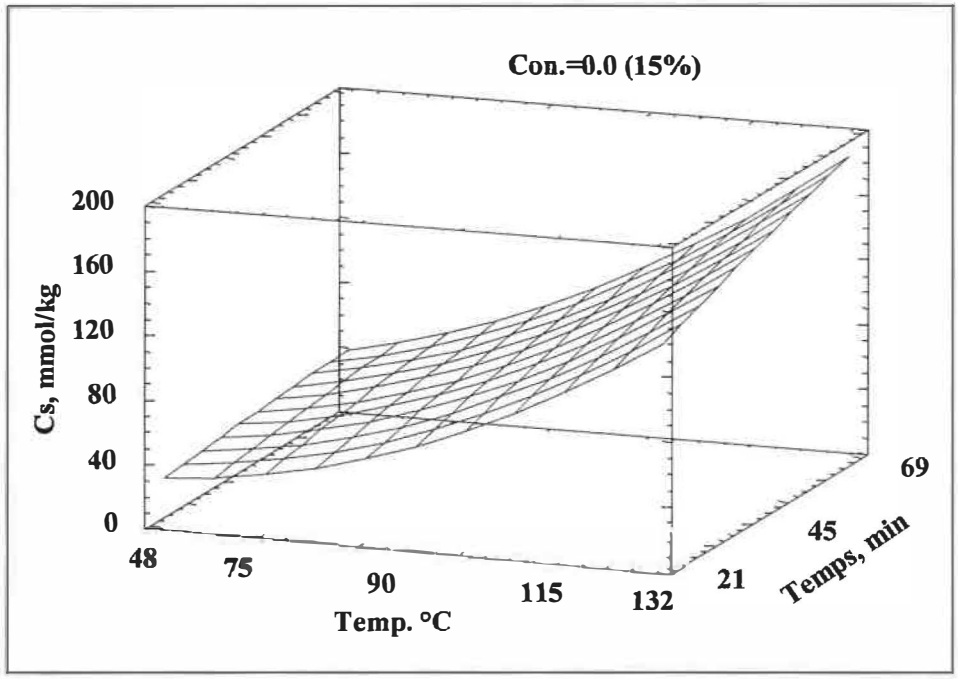

Figure 6.3 Estimated response surface for sulfonate content

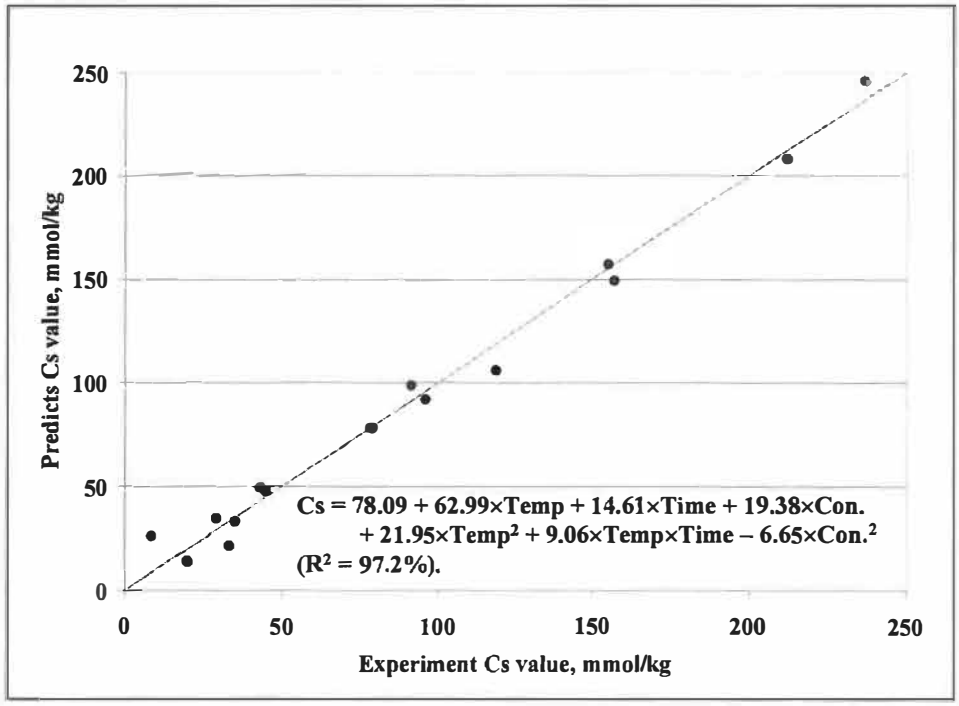

Figure 6.4 Experimental value and predicted value for sulfonate content (Cs)

6.1.2 Difference between early- and latewood in sulfonation

The work of Wu and Wilson [168] as well as those reviewed in their work indicate that the concentration of lignin is higher in EW than in LW. In contrast to these results obtained by chemical technique, Fergus [169] used ultraviolet (UV) microscopy to show that the secondary wall of both EW and LW have the same lignin distribution, while the middle lamella and cell corners of LW show significantly higher lignin concentration in comparison with the EW.

In this study we used the technique of sulfonation to see if there is any difference between the EW and LW by measuring the sulfonate and carboxylate contents of the sulphite-treated wood samples. Table 6.3 indicates that both the sulfonate and carboxylate contents are consistently lower for the EW than for the LW, regardless if they were cook together in whole-wood specimens or treated separately. This finding seems to follow the trend noted by Fergus [169], assuming that the sulfonation was uniform across the cell wall and its mechanism is similar in both EW and LW. Note that the degrees of sulfonation may not necessarily reflect the actual concentration of lignin because sulfonation reactions depend on the reaction conditions and the types of functional group in the lignin [170, 171]. However, our results may suggest that the X-, and Z-groups (Figure 1.4) of lignin are somewhat higher (10-15%) in latewood than that of earlywood.

The difference of early- and latewood in sulfonation will certainly influence the behavior of wood in compression. But the difference in sulfonate content is quite small. The differences in mechanical compression behaviors of EW and LW still mainly affected by the difference in physical properties of these wood zones.

Table 6.3 Sulfonate and carboxylate contents of earlywood and latewood

	Temperature °C	Time Min.	Na_2SO_3 Con., %	Sulfonate mmol/kg	Carboxylate mmol/kg
Earlywood	132	15	15	118.2	121.4
	132	45	15	170.9	134.2
	132	75	15	193.4	140.9
	132[a]	75	15	201.1	139.5
Latewood	132	15	15	133.0	135.6
	132	45	15	190.9	146.9
	132	75	15	230	153.1
	132[a]	75	15	228.1	154.9

* Note: a – earlywood and latewood were cooked separately.

6.2 Compression behaviors of sulfonated wood samples

6.2.1 Restrained and unrestrained radial compression of sulfonated wood

The sulfonated samples were compressed in radial direction, with or without restraint. The compression curves of unrestrained radial compression of sulfonated samples (Figure 6.5) are similar to the curves obtained at different temperatures (section 5.2.1.1). They also went through an elastic (region I), a plastic plateau (Region II), and a densification region (region III). There is also a brief second plateau at about 60% compression strain. However, this second plateau does not appear (Figure 6.6) when the sample is compressed with restraint and the compression stress increases at greater rate in the densification region.

The mechanical properties such as modulus of elasticity, first and second plateau stress, specific compression energy are recorded for both types of compression (with and without restrain). Another parameter, MOE2 was introduced to demonstrate the difference in the latter part of the stress-strain curve obtained by restrained and unrestrained compressions. The MOE2 is defined as the modulus at the densification region. The modulus at the elastic region (MOE) is defined earlier and is indicated in Figure 6.5 and Figure 6.6. The results are presented in Table 6.4. All data presented in the table are the average value of 5-7 individual compressions. The average coefficient of variance (CV, %) are, respectively, 18.64%, 22.06%, 12.64%, 21.18% and 8.63% for the MOE1, MOE2, SP1, SP2 and SCE, for the unrestrained compression. For the restrained compression, the CV remains at the same level excepted for the specific compression energy, which is a little higher than that for the unrestrained compression.

The physical properties of wood under unrestrained and restrained compression are plotted in Figure 6.6 to Figure 6.11. Obviously, the modulus of elastic (MOE) and the first plateau stress (SP1) are similar for these two types of compressions; they decrease linearly with the increase in sulfonate content. However, there is no second plateau for the restrained compression. The modulus at the densification region (MOE2) and the specific energy also behave differently. For the unrestrained compression these two

Table 6.4 Ion contents and mechanical properties of unrestrained and restrained compression of whole-wood sample blocks

Run	Ionic groups		Mechanical properties								
			Unrestrained compression					Restrained compression (RS)			
	Sul. Mmol /kg	Car. mmol /kg	MOE MPa	MOD2 MPa	SP1 MPa	SP2 MPa	SCE MJ /m3	MOE MPa	MOE2 MPa	SP1 MPa	SCE MJ /m3
(0)	0	0	140	176.2	2.56	18.55	5.33	100.2	530.1	2.73	5.83
1	157.3	117.0	41.50	118.4	0.98	11.75	2.78	27.23	543.2	1.12	4.23
(2)	78.7	110.9	75.64	159.2	1.94	17.33	4.62	57.07	548.7	1.96	4.96
3	33.3	94.8	99.58	154.9	2.42	20.09	5.05	77.25	518.4	2.59	5.56
4	118.9	134.5	60.94	152.1	1.63	14.12	3.75	52.81	510.3	1.40	4.61
5	212.3	136.5	21.77	98.24	1.02	10.05	2.83	27.61	475.1	0.92	4.28
6	20.1	95.6	86.47	168.6	2.46	21.11	5.70	111.1	504.2	2.46	6.00
(7)	78.4	110.9	64.10	153.2	1.81	17.65	5.16	74.06	492.8	1.95	4.83
8	42.9	104.4	69.66	167.3	2.54	21.54	4.94	73.97	494.4	2.54	5.78
9	91.2	122.3	63.60	143.6	2.06	16.29	3.78	70.26	498.9	1.90	5.15
10	29.1	92.9	75.02	162.3	2.49	22.51	5.03	108.9	463.3	2.63	6.21
11	8.4	80.6	97.58	184.6	2.81	20.86	5.56	90.76	492.9	2.85	5.84
(12)	78.3	111.3	71.36	163.9	1.91	17.75	4.58	69.26	498.6	2.14	5.21
13	95.8	119.9	82.82	155.4	1.78	14.4	4.05	78.173	526.9	1.88	4.88
14	155.3	123.3	55.78	112.5	1.23	12.3	3.38	39.65	479.6	1.41	4.79
(15)	77.8	110.1	77.11	164.7	1.89	17.73	5.06	76.89	506.1	2.06	5.26
16	35	105.7	105.10	166.2	2.62	19.43	5.67	122.3	498	2.53	5.78
17	44.7	117.2	70.48	179.4	2.28	17	5.04	89.71	480	2.48	6.02
(18)	78.3	111.7	64.20	153.2	1.89	18	4.56	70.89	486.2	2.20	5.55
19	236.9	145.4	16.20	114.2	0.61	8.01	2.28	22.59	442.8	0.69	4.36

* Sul. – Sulfonate; Car. – Carboxylate; Samples will be identified as S1-S19 for unrestrained compression, and RSS1-RSS19 for restrained compression in all the text.

parameters also decrease linearly with increasing of sulfonate content. However, for the restrained compression, the specific compression energy is somewhat higher than that for the unrestrained compression. It decreases linearly with the increase in sulfonate content when the sulfonate content is low (<120 mmol/kg), but remains relatively stable at higher sulfonate content. The modulus at the densification region (MOE2) for the

restrained compression remains relatively stable at all levels of sulfonate content. All these differences resulted from a high lateral expansion at a high compression strain, for both types of compression. The results suggest that the lateral movement of fibers in the samples mainly determines the compression stress at high strain. The characteristics of sample would have little effect on the stress at this stage.

Direct comparison of stress-strain curves obtained in a restrained and unrestrained compression also shows these differences (Figure 6.12). The stress-strain curves for the restrained and unrestrained compression remain similar when the strain is 50% or less. The stress increases rapidly beyond 50% strain when the sample is compressed with restraint. On the other hand, when the sample is compressed without restrain, it increases relatively slow and shows a short second plateau. This is because the unrestrained compression provides the fibers with a certain freedom of lateral movement, particularly in the tangential direction, reducing the compression stress beyond about 50% strain. It appears that the lateral displacement of fibers takes place at about 50% strain. At this point, most of the EW fibers are collapsed as discussed earlier. However, in the restrained compression, such lateral displacement of fibers is minimized, increasing substantially the stress in the densification zone, and preventing the occurrence of a secondary plateau. This difference proves again that the second plateau is the result of the fiber separation.

Microscopic observation indicates that fiber deformation is similar in restrained and unrestrained compressions at 50% strain (Figure 6.13, Figure 5.7 C). However, fiber separations are greatly limited in the restrained compression at 65% strain (Figure 6.14 and Figure 5.10). Similar observation is also reported by Thiruvengadaswamy et al. [81] who claimed that the restrained samples display much less damage (cracks) than unrestrained ones under identical loading conditions. But the relative modulus is the same for these two types of compression.

In summary, the samples behave similarly under the two types of compressions at low compression strain (<50%). However, at higher strain they behave differently due to the fiber displacement and the lateral expansion in the compression without restraint.

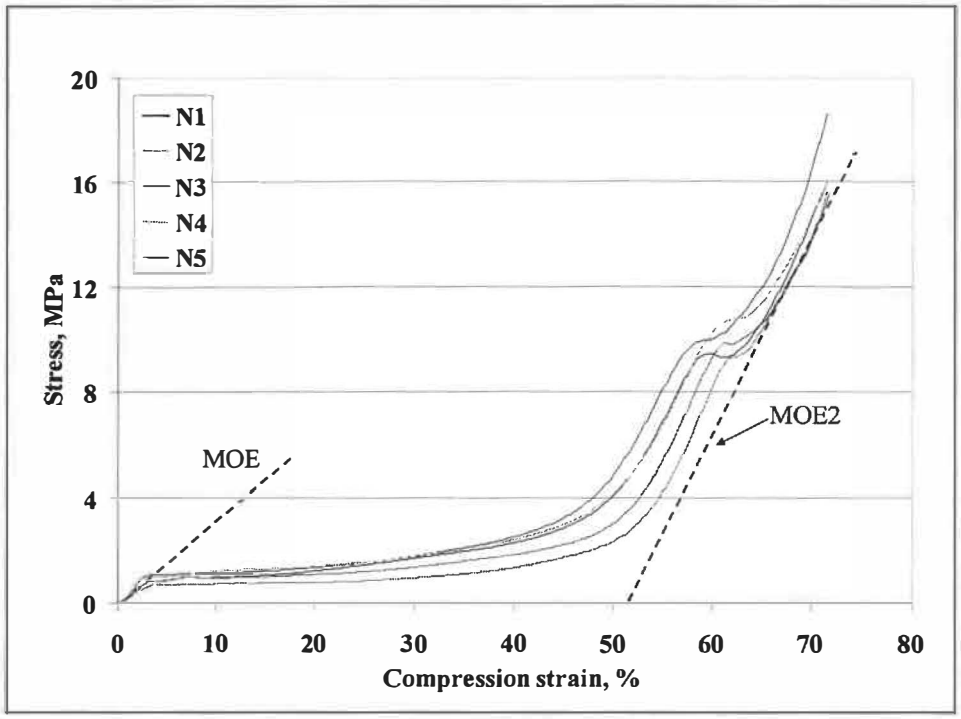

Figure 6.5 Stress-strain curves of typical unrestrained compression of sulfonated sample (S5, Cs=212 mmol/kg)

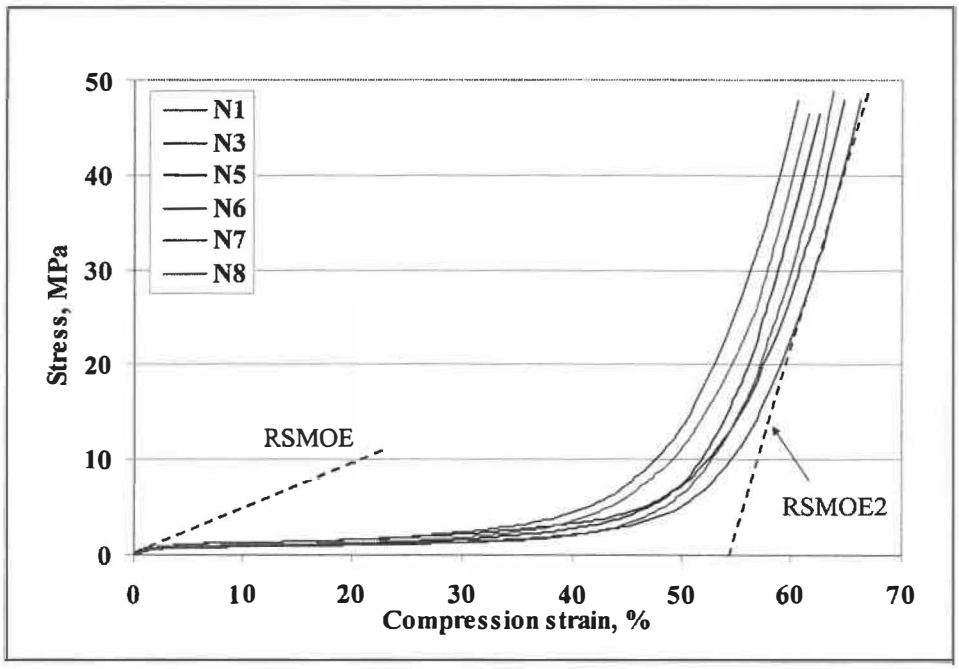

Figure 6.6 Stress-strain curves of typical restrained compression of sulfonated sample (RSS5, Cs = 212 mmol/kg)

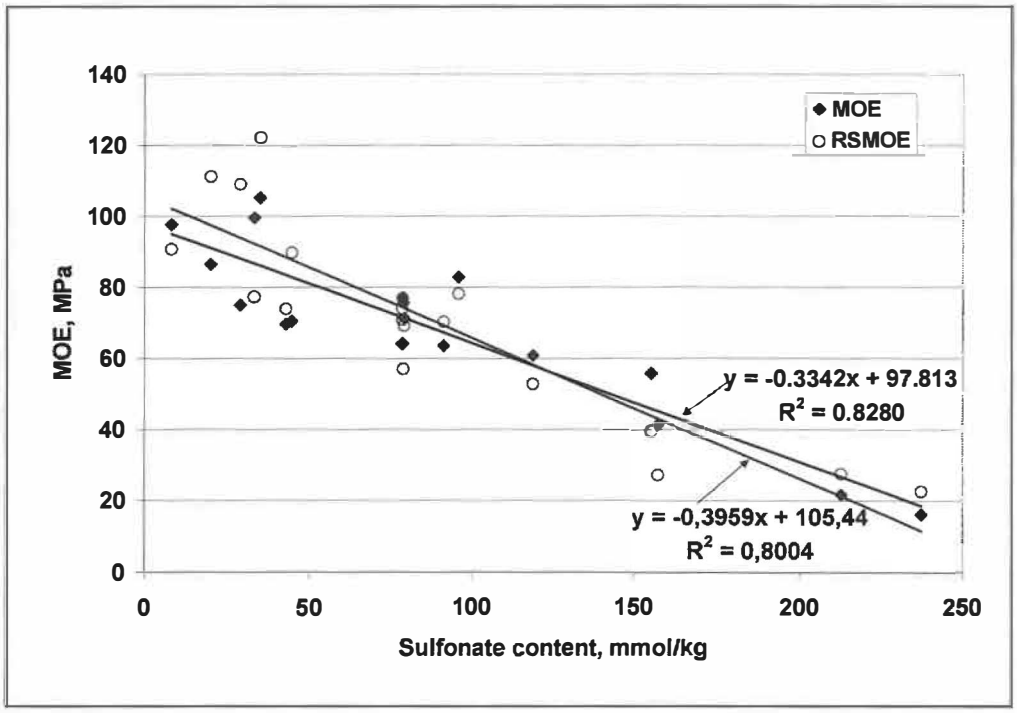

Figure 6.7 MOE VS. sulfonate content for unrestrained and restrained compressions

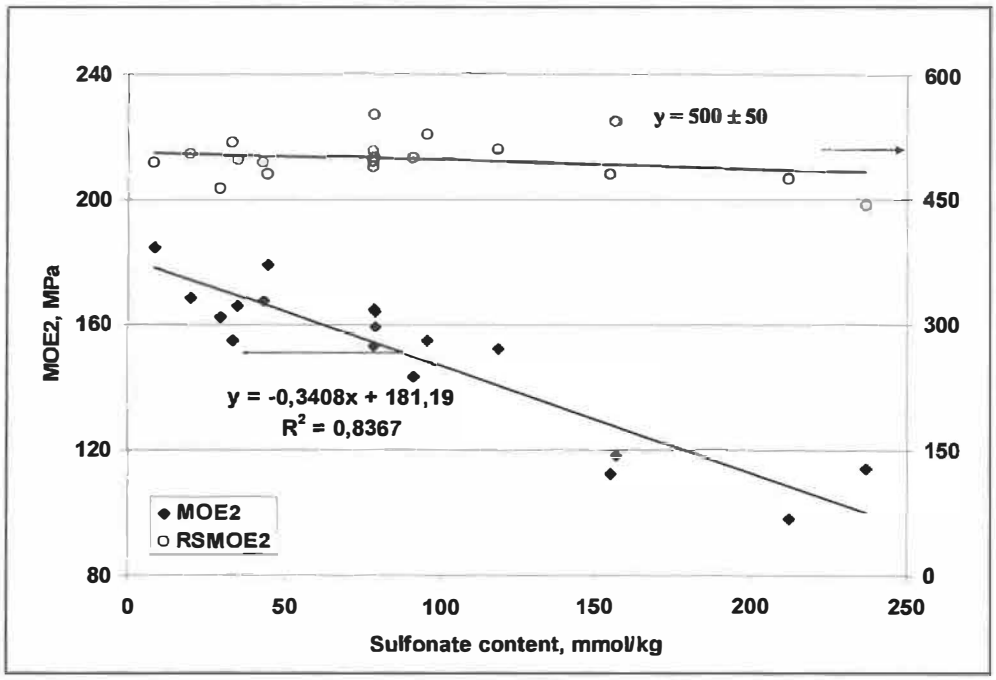

Figure 6.8 MOE2 Vs. sulfonate content for unrestrained and restrained compressions

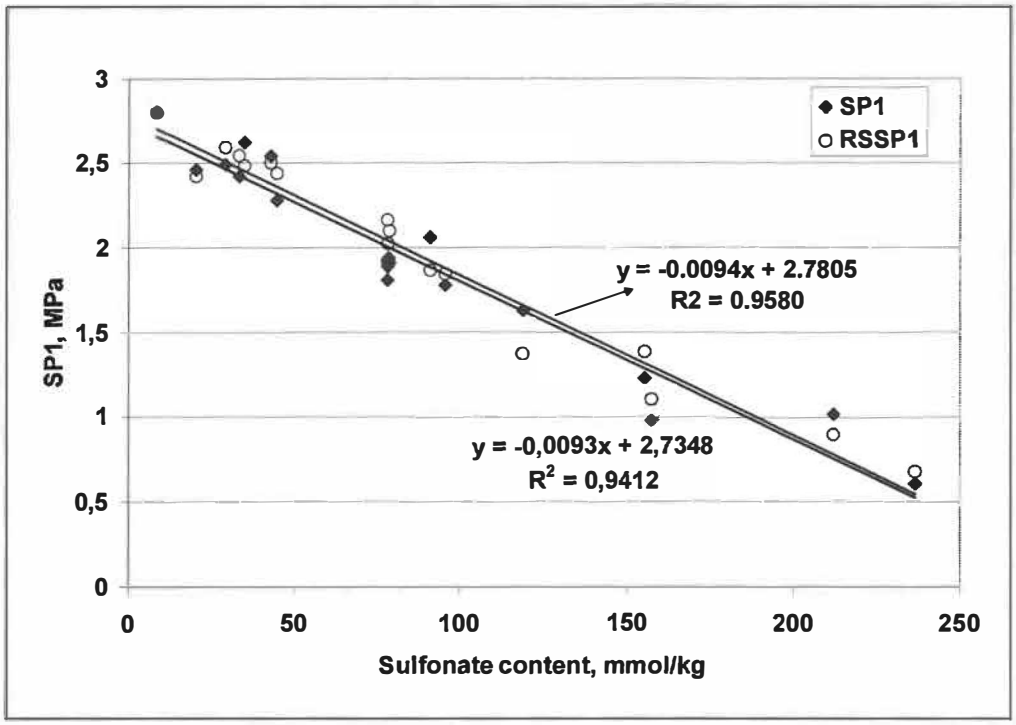

Figure 6.9 SP1 VS. sulfonate content for unrestrained and restrained compressions

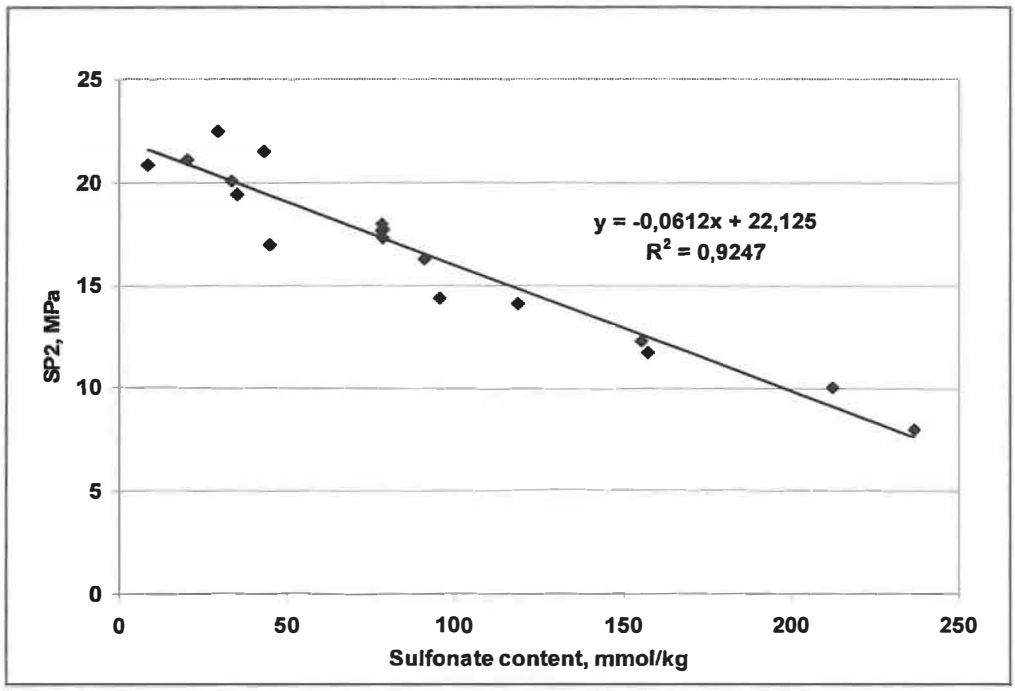

Figure 6.10 SP2 VS. sulfonate content for unrestrained compression (no second plateau for restrained compression)

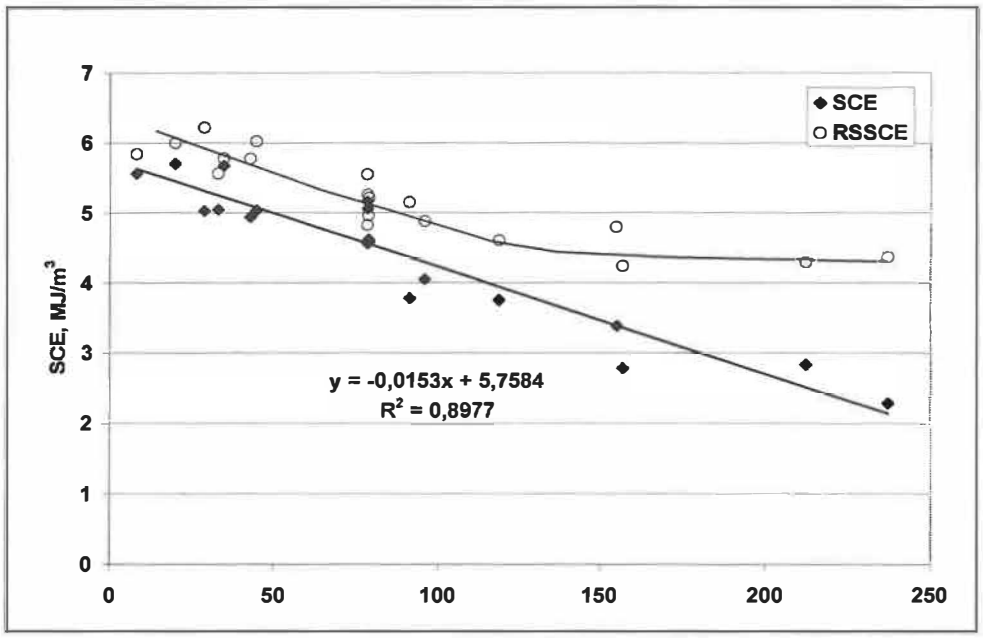

Figure 6.11 SCE VS. sulfonate content for unrestrained and restrained compressions

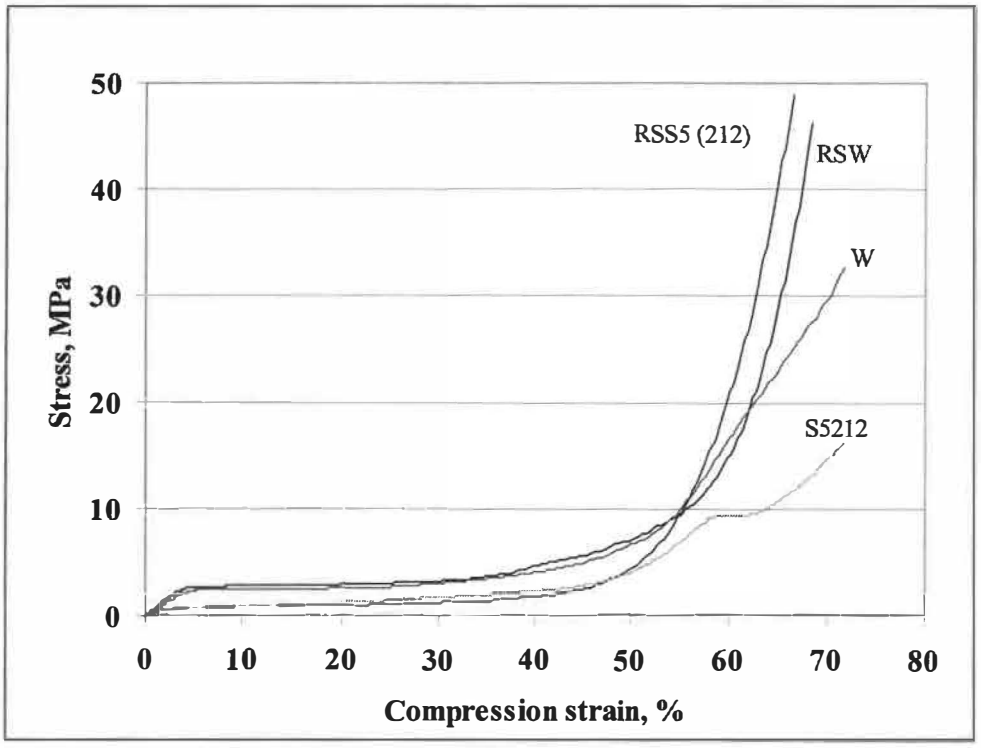

Figure 6.12 Stress-strain curves of restrained and unrestrained compression of water-saturated (RSW, W) and sulfonated samples (RSS5, S5, Cs =212 mmol/kg)

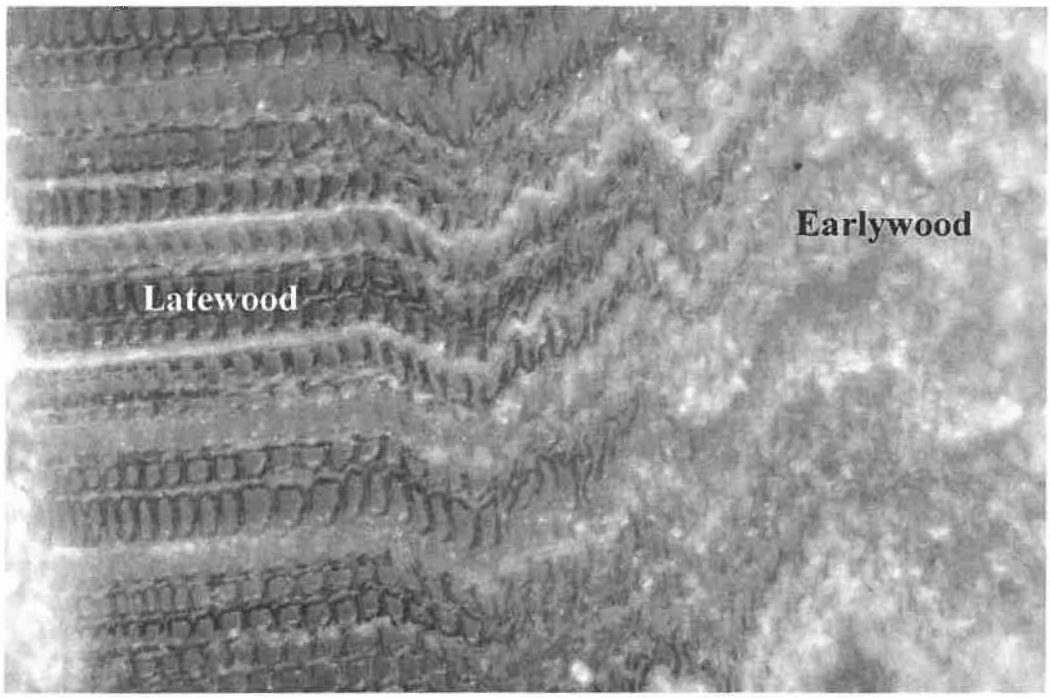

Figure 6.13 Restrained compression of water saturated sample (50% strain). Similar deformation is also observed with unrestrained compression

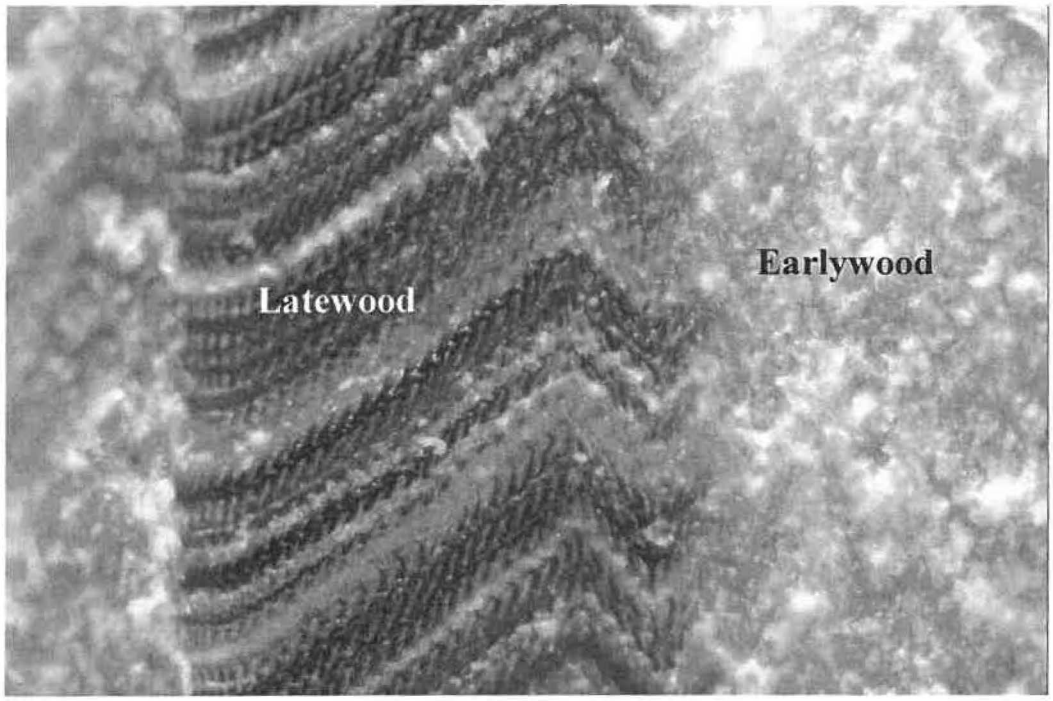

Figure 6.14 Restrained compression of water saturated sample (65% strain). Less severe fiber separation when compared with unrestrained compression

6.2.2 Relationship between mechanical properties and sulfonate content

The effects of sulfonate content on the mechanical properties of samples compressed without restrain are analyzed by using of software called *Statgraphic plus 4.1*. Table 6.5 summarizes the regression models and the analysis of variance for the mechanical properties. Since all the P-values in the ANOVA table are less than 0.01, there are statistically significant relationships between the physical properties and the sulfonate content, at 99% confidence level. The correlation coefficient ranges between -0.9702 to -0.9099, indicating a relatively strong relationship between the variables.

Table 6.5 ANOVA and regression models for mechanical properties and sulfonate content for unrestrained compressions

Properties	Relationship	R^2	Correlation Coeff.	F-Value	Standard error
MOE1	MOE1 = 181.1880 – 0.3408Cs	0.84	-0.9147	0.0000	9.8372
MOE2	MOE2 = 97.8133 – 0.3342Cs	0.83	-0.9099	0.0000	9.9534
SP1	SP1 = 2.7348 – 0.0093Cs	0.94	-0.9702	0.0000	0.1521
SP2	SP2 = 22.1247 – 0.0612Cs	0.92	-0.9616	0.0000	1.1408
SCE	SCE = 5.7585 – 0.0153Cs	0.90	-0.9474	0.0000	0.3369

Figure 6.15 to Figure 6.19 illustrate the linear relationship between the physical properties (MOE, MOE2, SP1, SP2, and SCE) and the sulfonate content. Clearly, these properties are highly associated with the sulfonated content. The R^2 indicates that the model as fitted explains 83-92% of the variability in physical properties.

The stress-strain relationships of samples having various levels of sulfonation are presented in Figure 6.20. The stresses in the elastic and the plastic zones decrease as the degree of sulfonation increases, signifying the influence of chemical softening of cell wall. As discussed earlier, the softening of wood tissue by sulfonation provokes a second stress plateau, the extent of which appears to be directly associated with the degree of sulfonation (Figure 6.18, Figure 6.20). The sulfonate content seems to have no influence in the position of second plateau. As the sample is compressed at different temperature, the second plateau appears at about 60% strain, where the LW sustains

substantial stress and yield. This yield point is mainly caused by fiber separation and/or buckling of radial files of LW fibers as demonstrated in section 6.2.1.

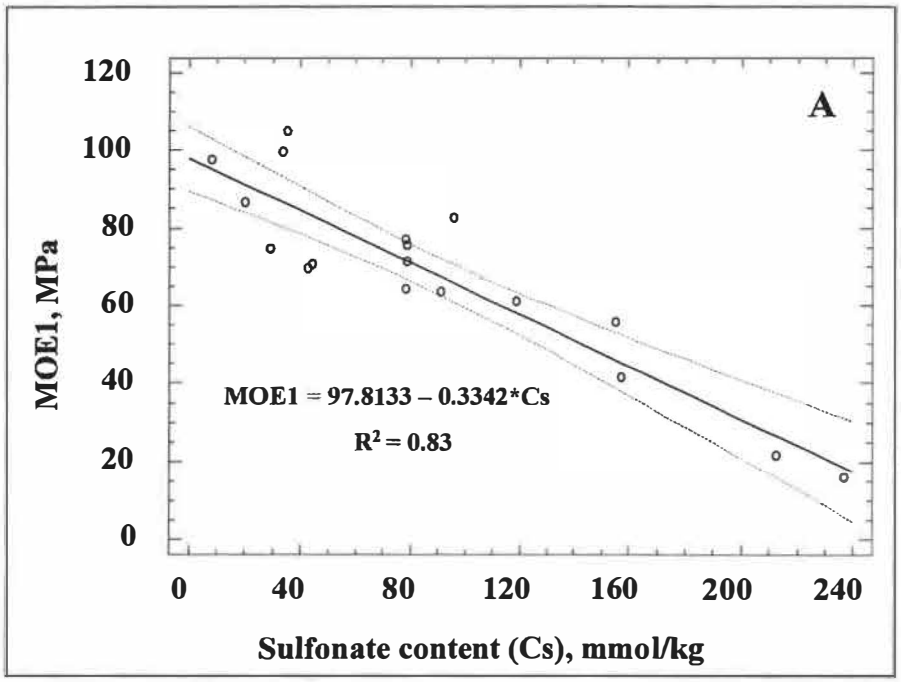

Figure 6.15 Relationship of modulus of elastic (MOE) and sulfonate content (Cs) in unrestrained compression.

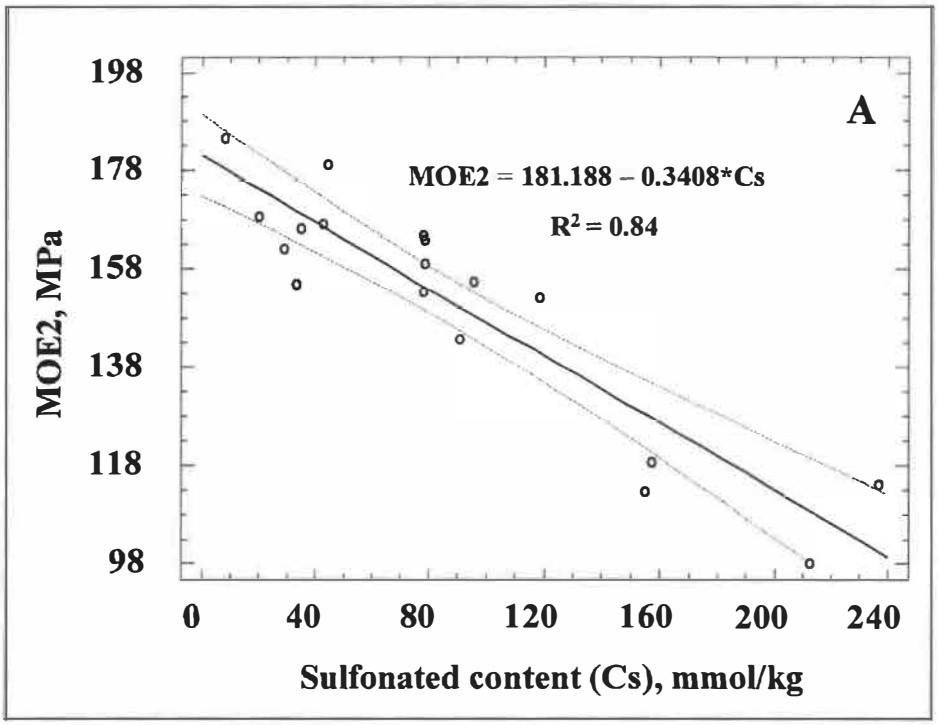

Figure 6.16 Relationship of modulus at densification region (MOE2) and sulfonate content (Cs) in unrestrained compression.

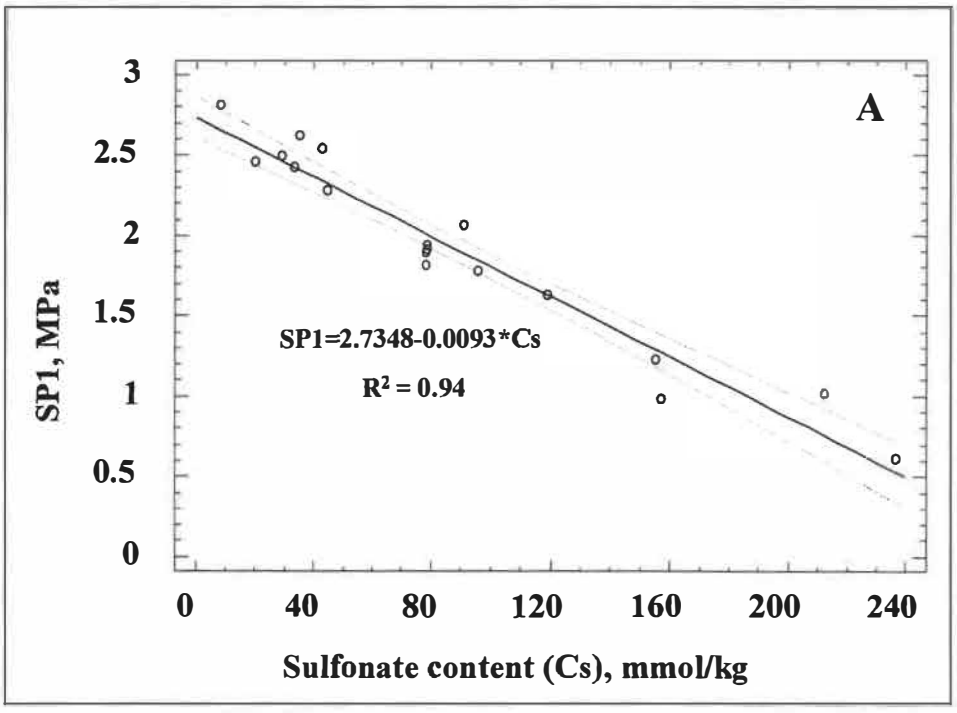

Figure 6.17 Relationship of first plateau stress (SP1) and sulfonate content (Cs) in unrestrained compression.

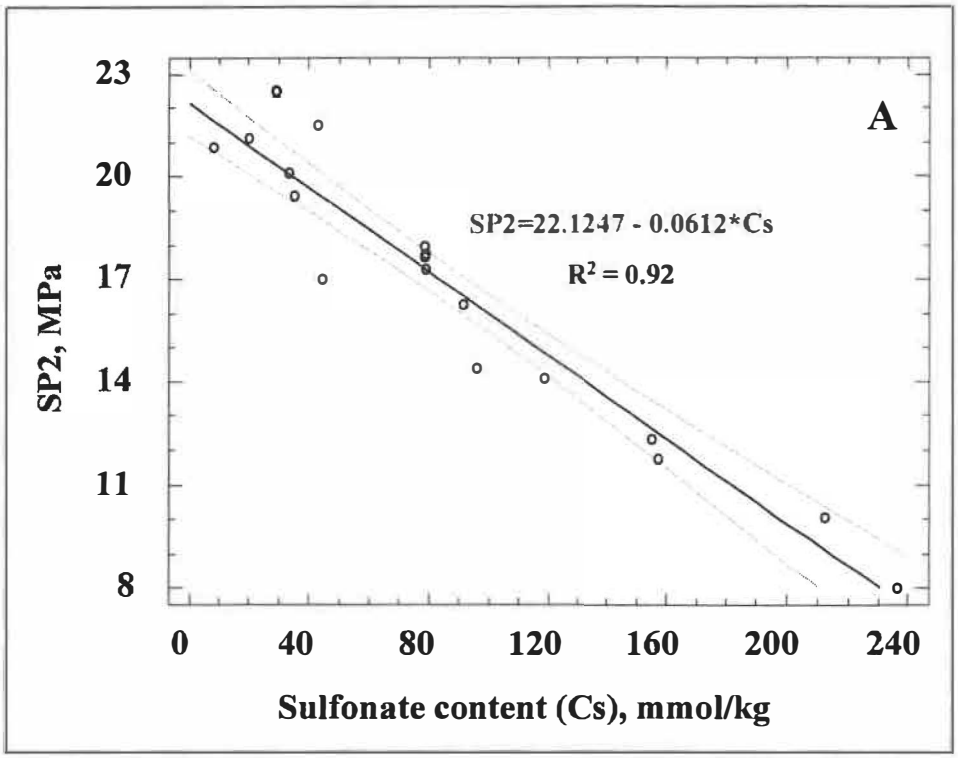

Figure 6.18 Relationship of second plateau stress (SP2) and sulfonate content (Cs) in unrestrained compression.

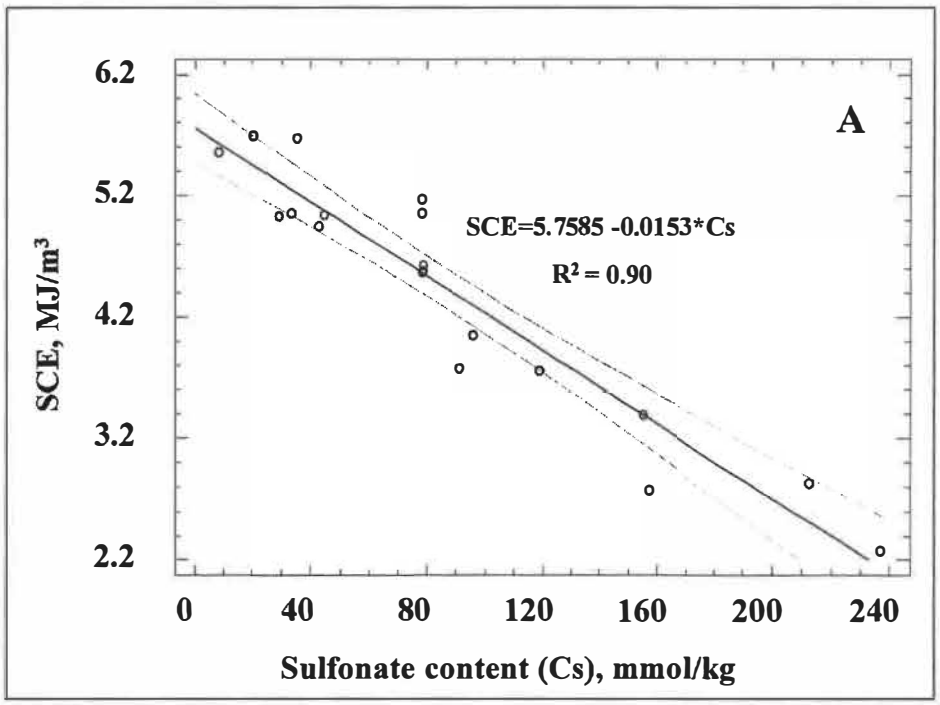

Figure 6.19 Relationship of specific compression energy (SCE) and sulfonate content (Cs) in unrestrained compression.

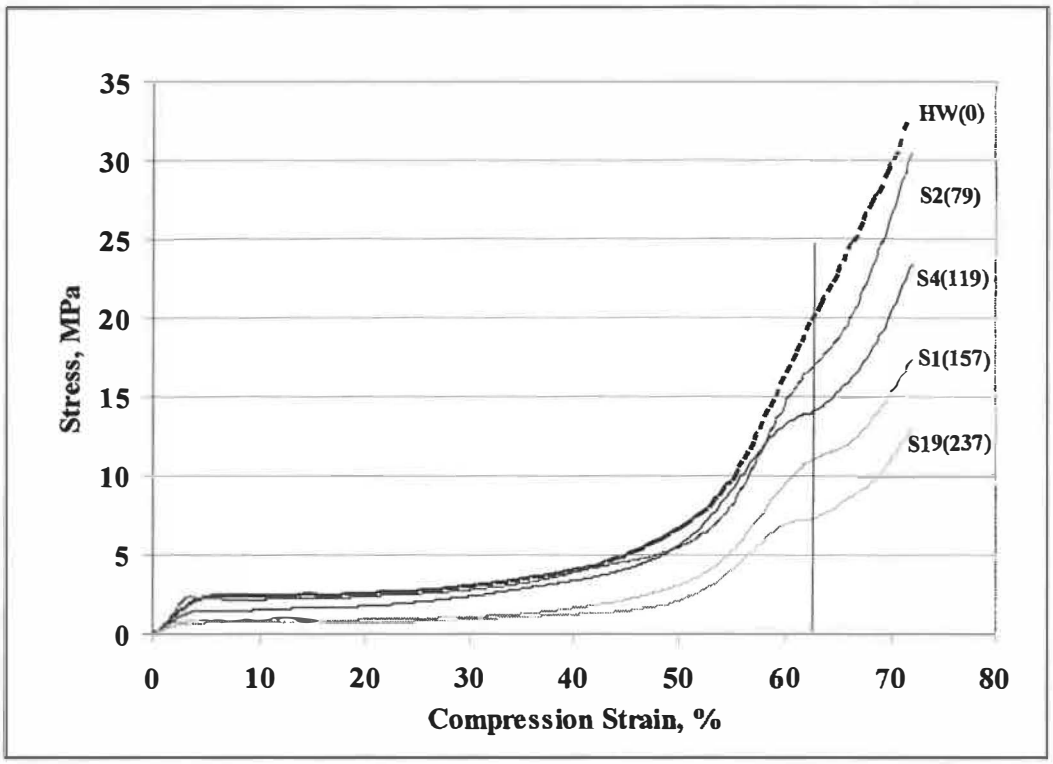

Figure 6.20 Effect of sulfonate content on stress-strain curves of unrestrained radial compressions (numbers in brackets are sulfonate contents, mmol/kg)

As in the case of thermal softening of samples (section 5.2.6), after normalization ($\sigma_n=\sigma/\sigma_y$, σ_y = SP1), the normalized curves for radial compressions at various sulfonate content fit into one curve in the elastic region (region I) and elastoplastic region (region II), as shown in Figure 6.21. In these regions, the sulfonate content does not change the form of the stress-strain curves and the wood behaves similarly at different stress levels, at various sulfonated contents. The results indicate that the deformation behavior of wood is independent of wood properties in the elastic and elasto-plastic regions, but dependent on the cellular structure of wood. Again, this finding supports the conclusion of Wolcott et al. [149] and other researchers [150, 151].

However, in the densification region (region III), the compression curve varies with sulfonate contents. This phenomenon suggests that wood behaves differently in lateral expansion and fiber separation at different sulfonate contents. However, the separation and collapse of sulfonated fibers seems to be more complicated than that of the fibers in thermally softened samples.

Following the same method used in section 5.2.6, a similar stress model for normalized stress (σ_n) in the elastoplastic region in radial compression of sulfonated samples can be obtained:

$$\sigma_n = \frac{\sigma_r}{SP1} = 1 + 0.5295 \times \left(\frac{0.5}{0.58 - \varepsilon} - 1 \right)^{0.9506}$$

Eq. 6.2

Figure 6.22 indicates that the developed model (σ_n) and the average normalized stress fit very well for the elastoplastic region. In the model, the SP1 can be obtained from the compression tests (Table 6.4) or from the model in Table 6.5. Thus a general model for the stress for this region can be expressed as follows:

$$\sigma_r = (2.7348 - 0.0093 \times C_S) \times \left[1 + 0.5295 \times \left(\frac{0.5}{0.58 - \varepsilon} - 1 \right)^{0.9506} \right]$$

Eq. 6.3

where, C_S is sulfonate content (mmol/kg) and ε is compression strain. The model also consists of two parts: the sulfonate factor and the strain factor. The general model can be used to predict a compression stress required to collapse the EW fibers at various sulfonate content at room temperature.

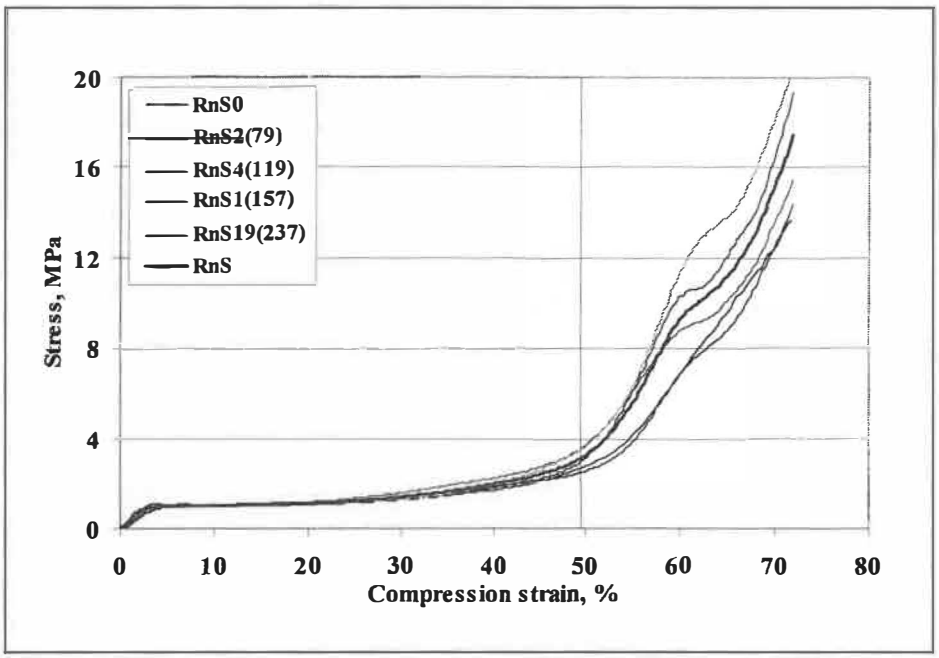

Figure 6.21 Normalized compression curves for unrestrained compressions of samples at various sulfonate contents

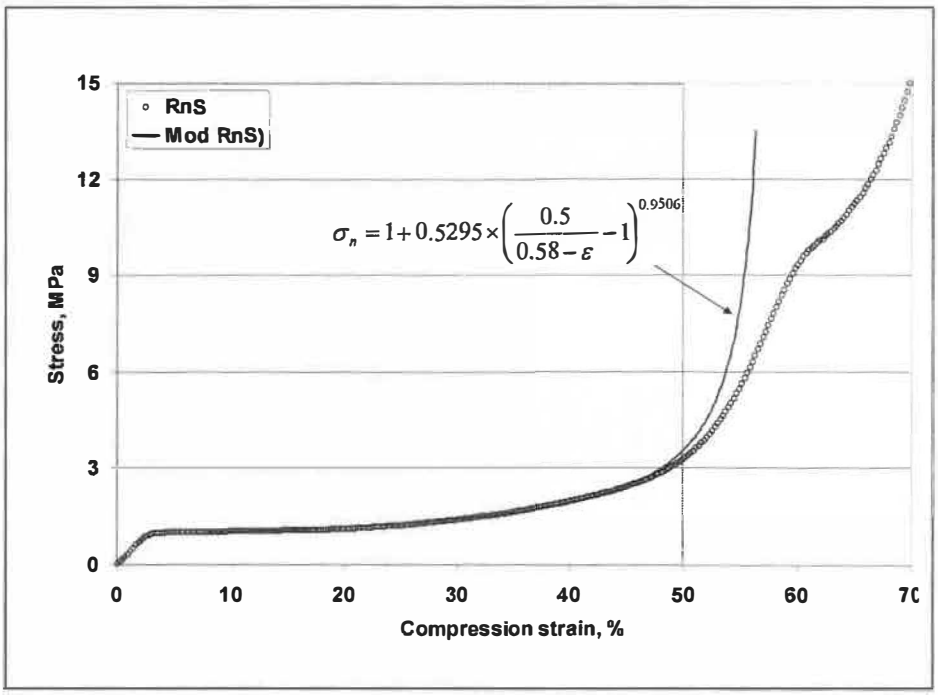

Figure 6.22 Comparison of average normalized compression curve and developed model for radial compressions of sulfonated samples

6.2.3 Comparison of thermal and chemical softening of wood

The normalized compression curves of sulfonated samples and those obtained with samples compressed at various temperatures are plotted in Figure 6.23. As expected, the curves fit into one curve for the elastic and elastoplastic regions. Figure 6.24 indicates that the average normalized curves and the separate developed models (Eq. 5.9 and Eq. 6.2) are similar for the samples treated either by sulfonation or by thermal softening. In the models, the strength coefficient c of normalized models is, respectively, 0.5112 and 0.5295 for the thermally treated and the sulfonated samples. The strain-hardening coefficients (m) are 1.0297 and 0.9507, respectively. These two coefficients are almost the same for these two types of samples. This indicates that the compression behaviors of wood in the elastic and the elastoplastic regions are independent of wood properties. The elastic properties and the collapse behaviors in the elastoplastic region are dependent only on the cellular structure of wood. Again this finding is in line with the conclusion of Wolcott et al. [149] and other researchers [150, 151].

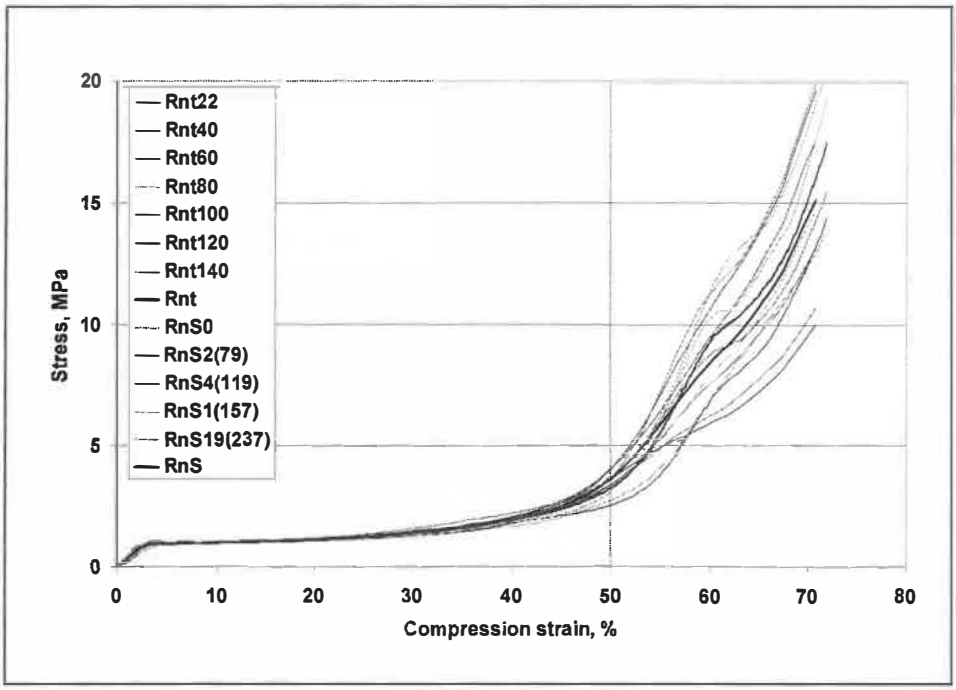

Figure 6.23 Normalized compression curves for radial compressions of sulfonated samples and that compressed at various temperatures

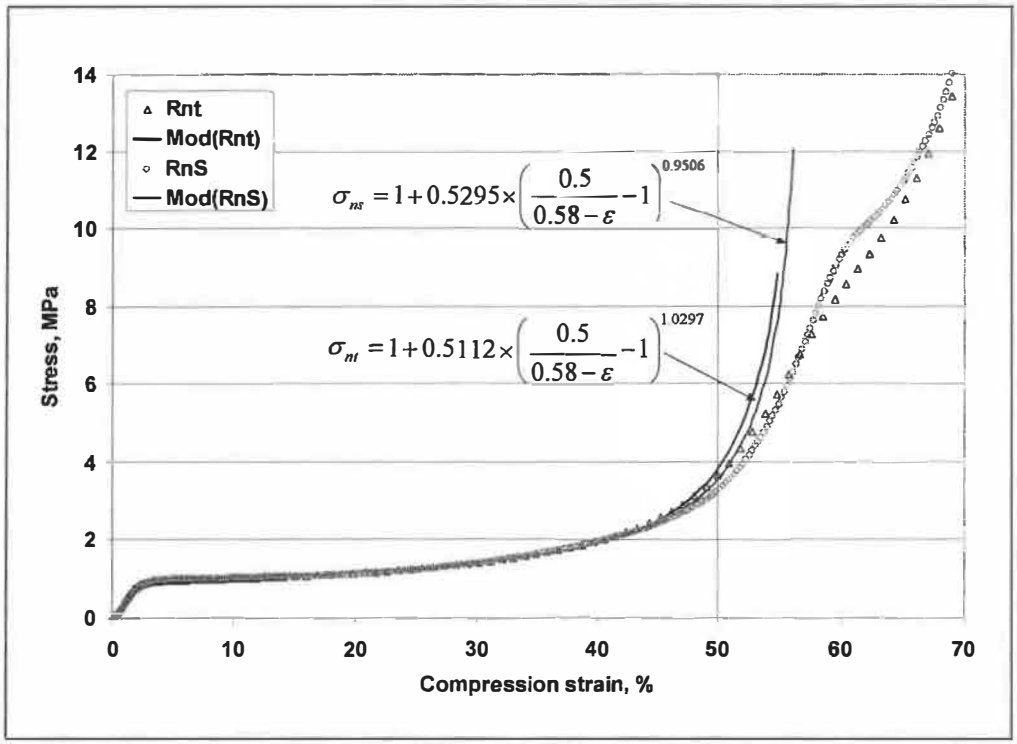

Figure 6.24 Average normalized compression curves and developed models of radial compressions for sulfonated samples and that compressed at various temperatures

However, the thermal treatment and the sulfonation of sample do modify the physical properties of wood. Figure 6.25 to Figure 6.28 compare the variation of physical properties (MOE, SP1, SP2, SCE) as a function of the heated temperature and sulfonate content of sulfonated samples. Note that the increases in sulfonate content and compression temperature decrease these physical properties steadily. These changes are the result of thermal and chemical softening of wood's main components, especially the lignin. But the mechanism of thermal softening is different from that of sulfonation. In thermal softening, the relationship between the wood properties and temperature follows Arrhenius' law. This means that the effect of thermal softening can be explained by the motion of polymer chain of the material's main components, as discussed in section 5.2.5. The thermal softening is a reversible effect, which is limited by the softening temperature of the wood's main components, particularly the lignin that has a softening temperature considerably higher than that for water saturated cellulose and hemicelluloses. For example, when the heating is conducted above the softening

temperature of lignin, about 100°C, the softening effect on wood properties diminishes, having a marginal influence above this temperature. In contrast to the thermal softening, the softening by sulfonation is an irreversible chemical softening, as discussed in section 1.2.3.1. The physical properties of wood decrease linearly with the increasing of sulfonate content. The effect continues until the lignin is fully sulfonated and completely dissolved, for example in chemical pulping. These linear-decreases in physical properties may result from the linear-decrease in the softening temperature of lignin (Figure 1.6, [40]).

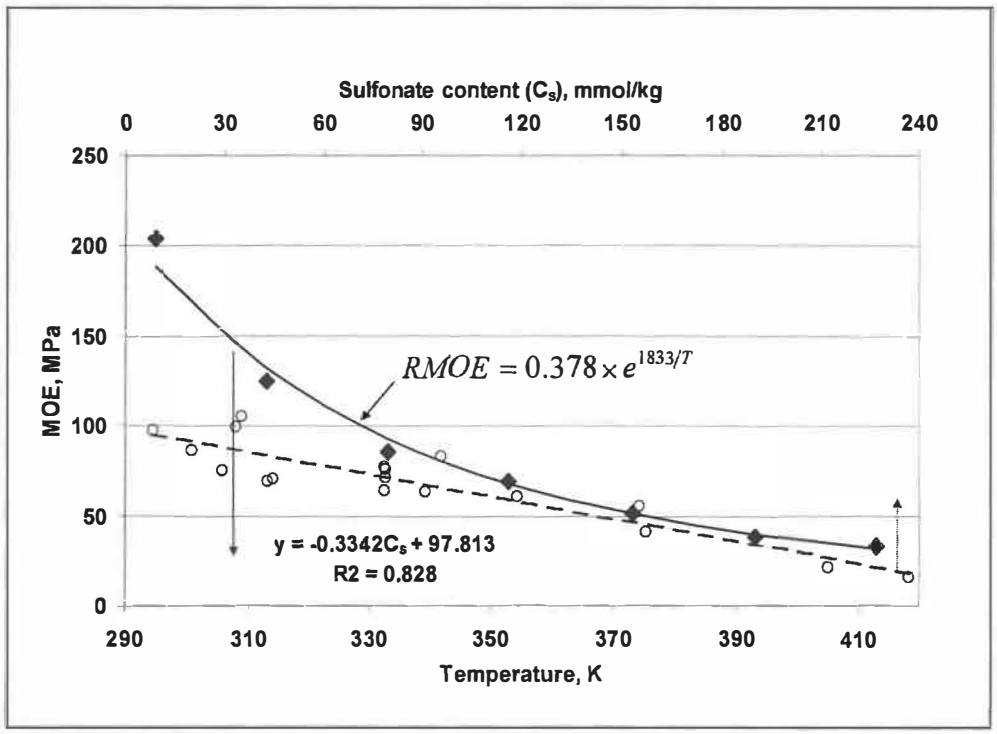

Figure 6.25 Variation of modulus of elastic (MOE) in heated and sulfonated samples

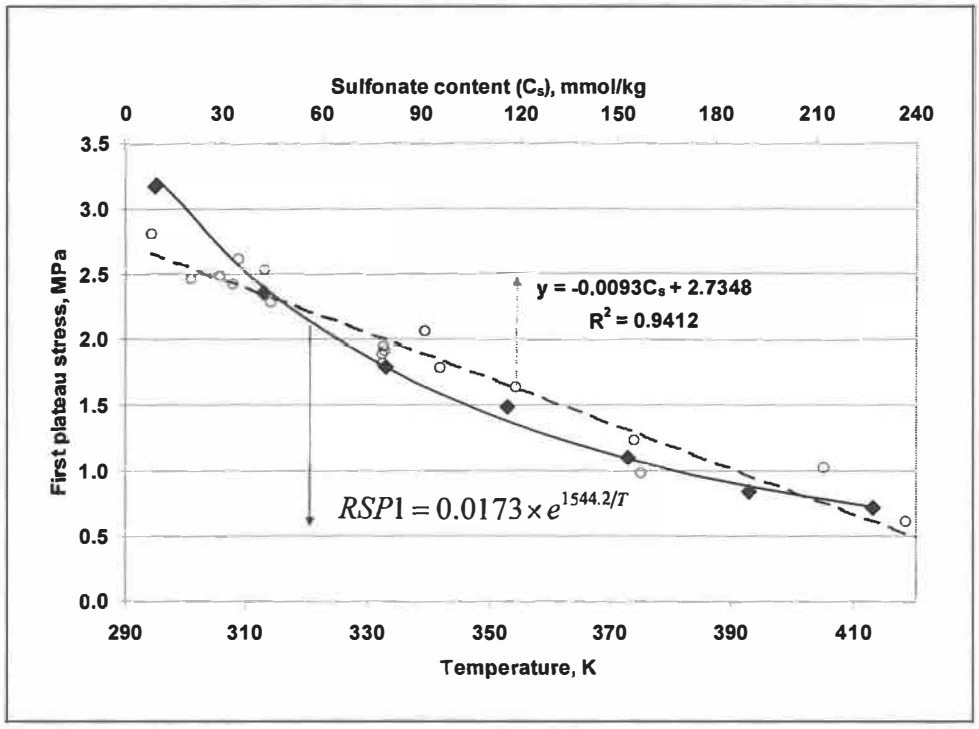

Figure 6.26 Variation of first plateau stress (SP1) in heated and sulfonated samples

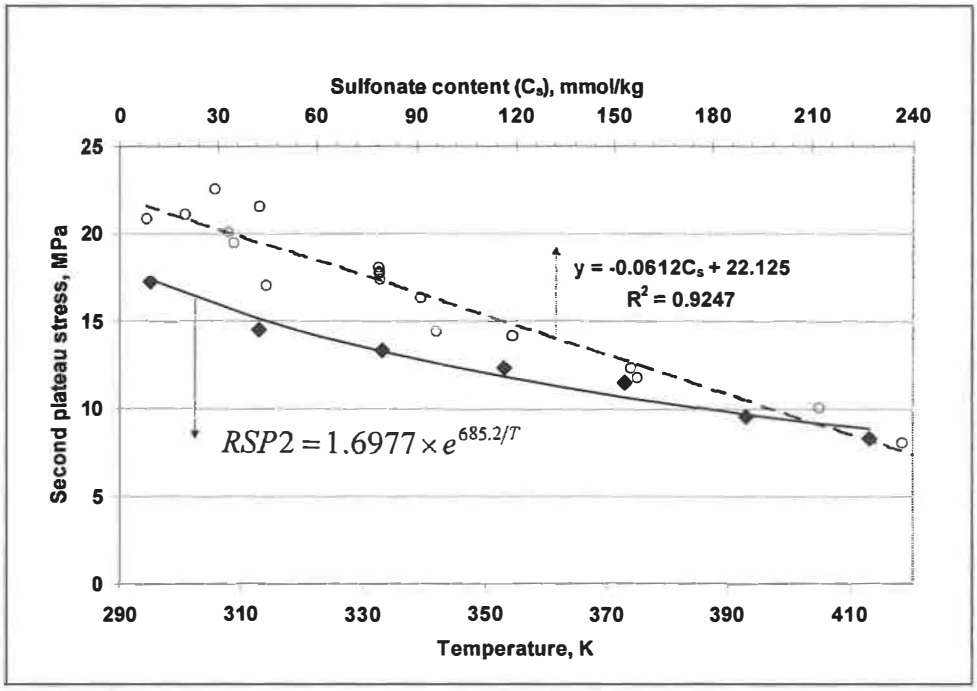

Figure 6.27 Variation of second plateau stress (SP2) in heated and sulfonated samples

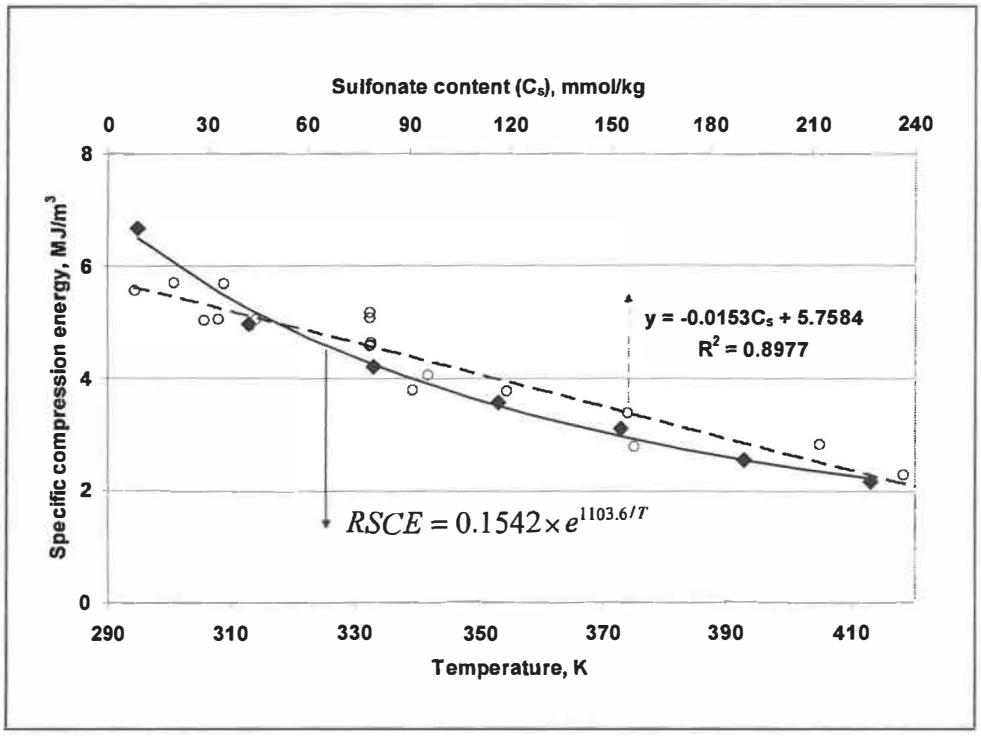

Figure 6.28 Variation of specific compression energy (SCE) in heated and sulfonated samples

6.2.4 Radial compression of early- and latewood

Wood is a biological material that exhibits great variety in properties. The variation occurs between species, between trees of the same species, and even within a single tree. One of the most striking variations amongst the conifers in temperate zone is the presence of EW and LW. The influence of these wood tissues on papermaking has long been recognized [172,173, 174, 175]. In general, the EW fibers being more flexible and conformable due to their thin cell wall produce sheet with high density and good bonding while the LW fibers having significantly thicker cell wall produce paper with high bulk and poor bonding.

In mechanical pulping the EW and LW fibers separate and develop differently [175, 176, 177, 67]. Fiber splitting or axial trans-wall failure and cross-axial breakage of EW fibers are common in refining. On the other hand, LW fibers are more resistant to such

failures. Additionally, the so-called sleeve-rolling of cell wall layers is often seen only with the thick-walled LW fibers [176, 67]. Due to their morphological differences, the EW fibers have higher energy absorption [178] but require greater refining energy [175], for a given pulp freeness, when compared with the LW fibers.

Due to their morphological differences, the EW fibers are responsible for the most deformation in radial compression of whole wood specimens. And only when the compression strain exceeded 50%, the LW fibers begin to be affected significantly. As indicate in Figure 6.29 and Figure 6.30, compression of samples consisting only EW or LW reveals the differences between these two types fiber. In radial compression, the EW exhibits a prolonged stress plateau (Figure 6.29 A and Figure 6.30 A), indicating the collapse and the significant lateral displacement of EW fibers. In contrast, the primary plastic stress plateau for the LW is not obvious (Figure 6.29 B and Figure 6.30 B) in most cases, suggesting that the collapse of LW takes place gradually. However, in some cases, a short plastic plateau does appear (Figure 6.29 B) with a stress about 8-9 MPa for water-saturated samples. This stress corresponds to a strain of 50-55% on the whole wood samples. This plateau is believed to be the result of the presence of the relatively thick-walled fibers in the transition zone between the EW and LW. However, the second plateau does not occur in samples consisting only EW or LW, even when samples are compressed to 85% strain (Figure 6.30 A). This may suggest that the provoked second stress plateau is also due to the distinct elements of EW and LW in the whole wood sample.

The results presented in Table 6.6 indicate that the first plateau stress (SP1) of EW and whole wood specimens are similar in two different treatments. This finding supports our earlier conclusion that the first plateau stress is determined only by the strength of the EW fibers. This SP1 can be used to evaluate the resistance of EW fibers in radial direction. The sulfonation treatment has a greater influence on this stress when compared with water saturation. The former reduces the SP1 by 61 %. A similar reduction in SP1 of LW is also observed.

Table 6.6 Compression of EW, LW and whole wood (WW) specimens of water-saturated and sulfonated sample

Treatment	Samples	Sul. mmol /kg	Strain %	MOE1 MPa	Mod2 MPa	SP1 MPa	SP2 MPa	SCE MJ /m^3
I Water-saturated	EW	0	70	48.01	125.0	2.61	-	3.60
	LW	0	60	51.14	145.4	(8.14)[a]	-	10.1
	WW	0	70	146	176.2	2.56	15.85	5.33
II sulfonated	SEW	201	85	16.55	233.6	1.01	-	5.82
	SLW	228	70	23.3	129.1	(2.06)	-	6.56
	SWW	212	70	21.77	98.29	1.02	10.05	2.83

* a, this is the stress at 10% compression strain, but not the first plateau stress for LW

The typical stress-strain curves for EW, LW and whole wood (WW) samples are compared in Figure 6.31 and Figure 6.32. Generally, the stress-strain curves for the EW and WW samples are similar, when the compression strain is low, for both water-saturated and sulfonated samples. On the other hand, the stress-strain curve for the LW sample is quite different. The water-saturated WW samples (Figure 6.31) gave a stress of 6.7 MPa at 50% strain. To reach this stress value, the EW has to be compressed to 59% and the LW to 11%. Since the proportion of EW in the WW sample was 78%, the EW is responsible for 95% of the total deformation of the WW sample at 50% compression strain.

This finding supports our early conclusion that the overall behavior of wood compression is mainly governed by the weaker EW while the LW contributes marginally to the total deformation. Similar compression characteristics of LW and EW at low compression strain are also noted by Dumail and Salmén [60]. The WW sample yields a compression stress of 17 MPa at 60% strain. However, the EW and the LW have to be compressed, respectively, to 71% and 37% strain to attain such a stress value. At 37% strain, the LW fibers are significantly deformed.

Similar behavior was also observed for the sulfonated samples (Figure 6.32). When the sulfonated WW sample was deformed by 70%, the deformation of the EW and the LW are 74% and 53%, respectively. This indicates that at high compression strain, the LW

can be deformed significantly. The water-saturated LW fibers that were also flattened at high compression strain as observed earlier (Figure 5.10).

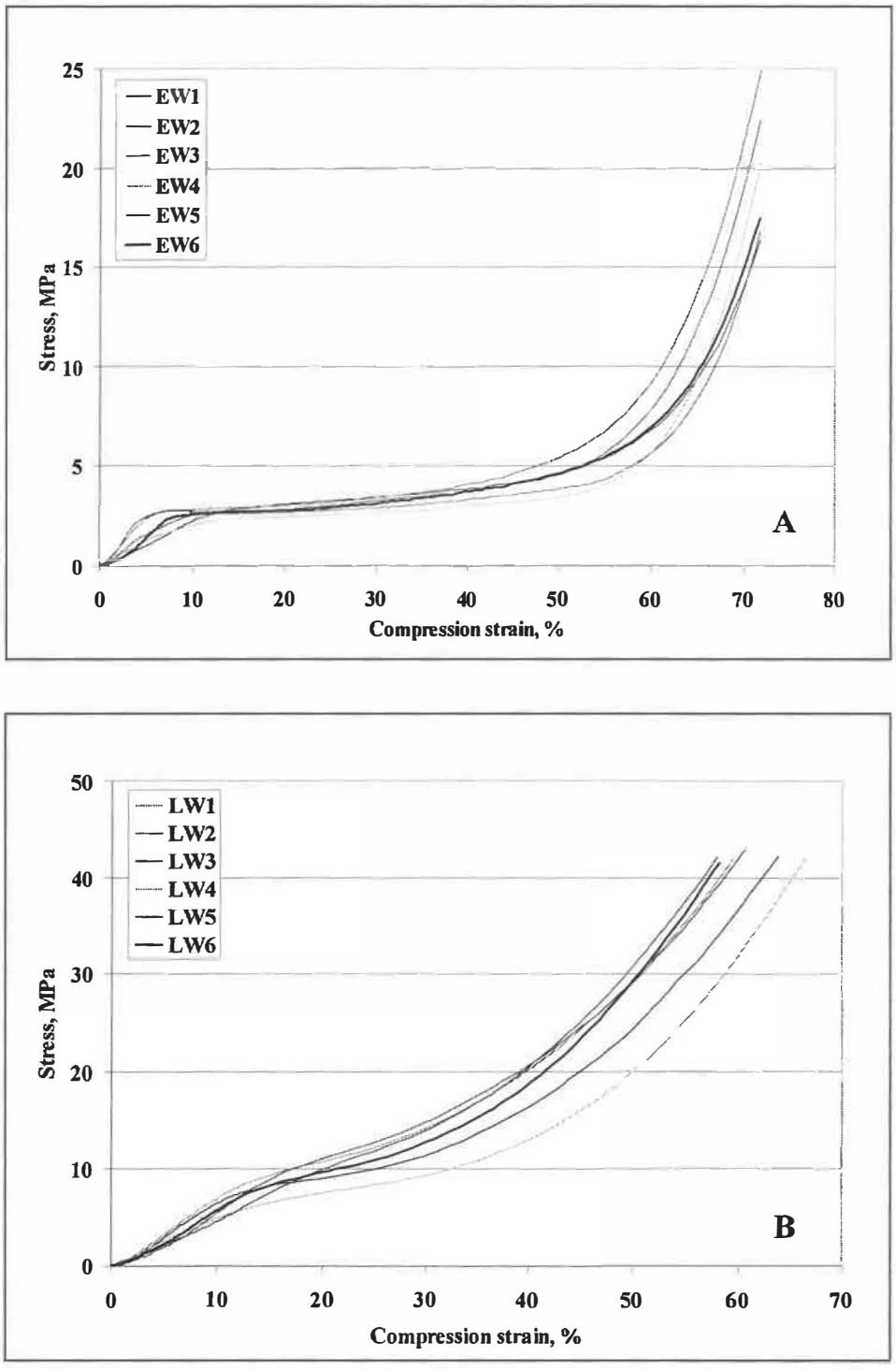

Figure 6.29 Radial compression of water-saturated samples. A: Earlywood (EW), B: Latewood (LW)

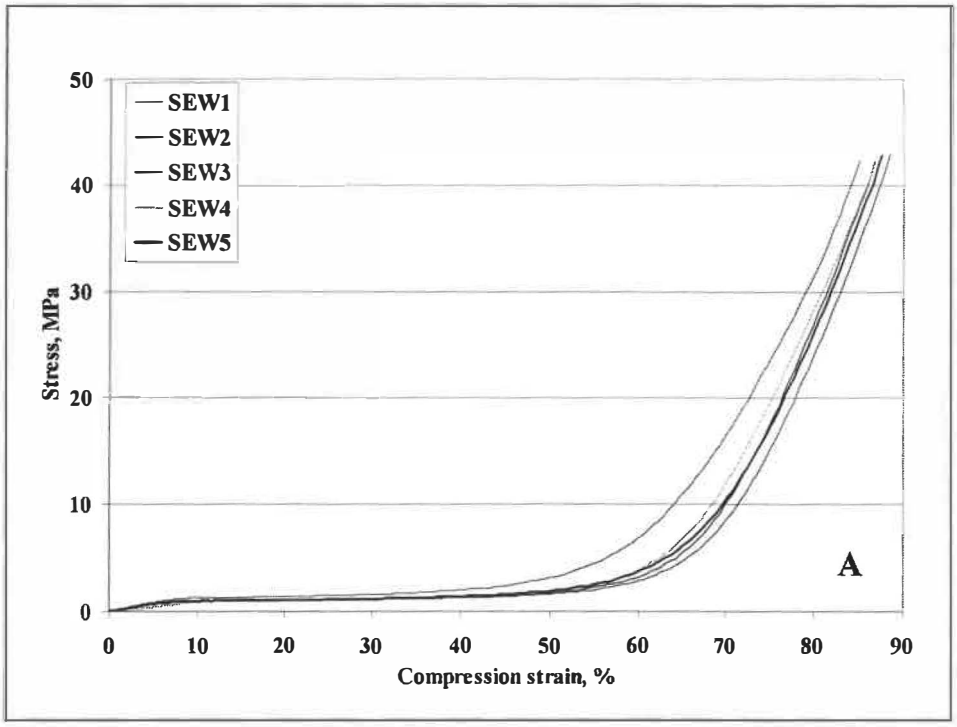

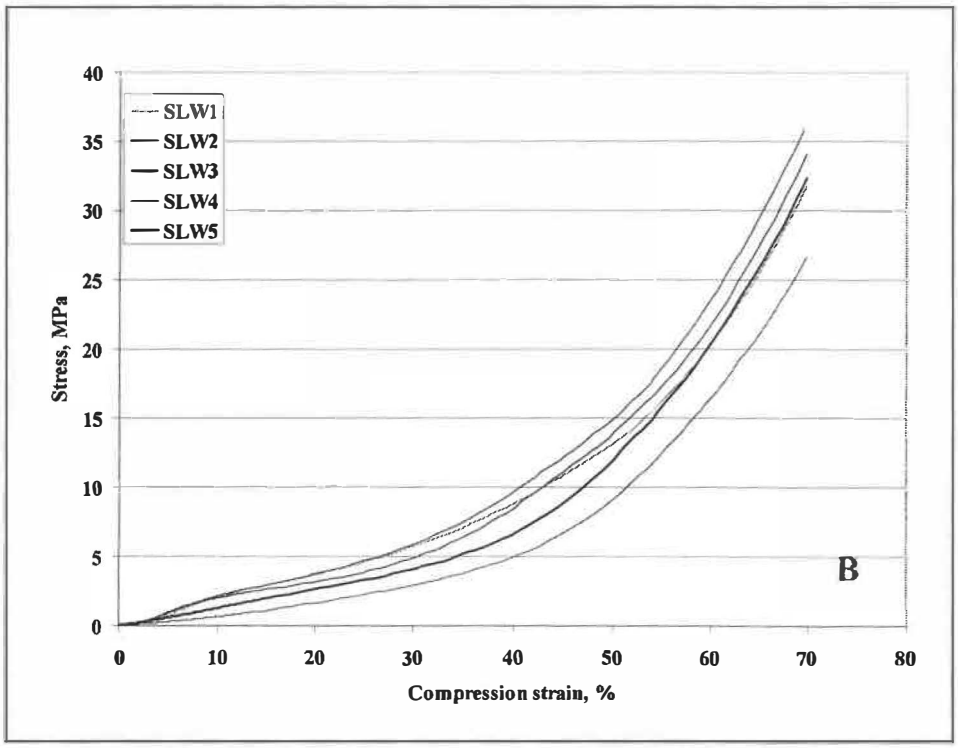

Figure 6.30 Radial compression of sulfonated samples. A: Earlywood (Cs =201 mmol/kg), B: Latewood (Cs =228 mmol/kg)

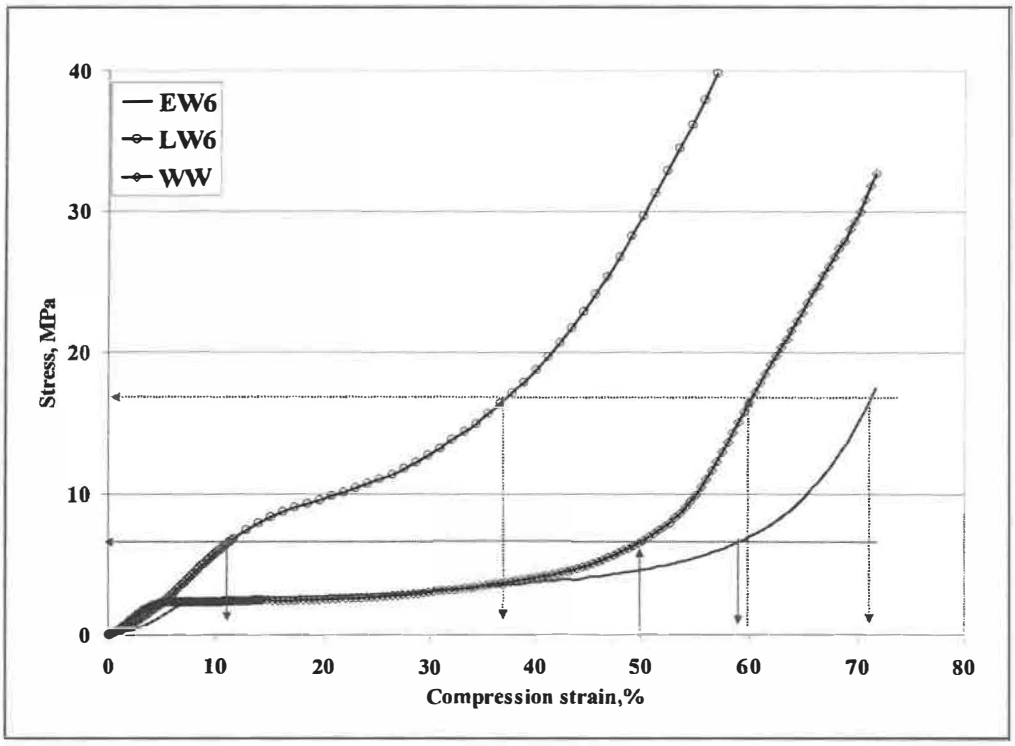

Figure 6.31 Comparison of radial compression of water-saturated EW, LW and whole wood (WW) specimens

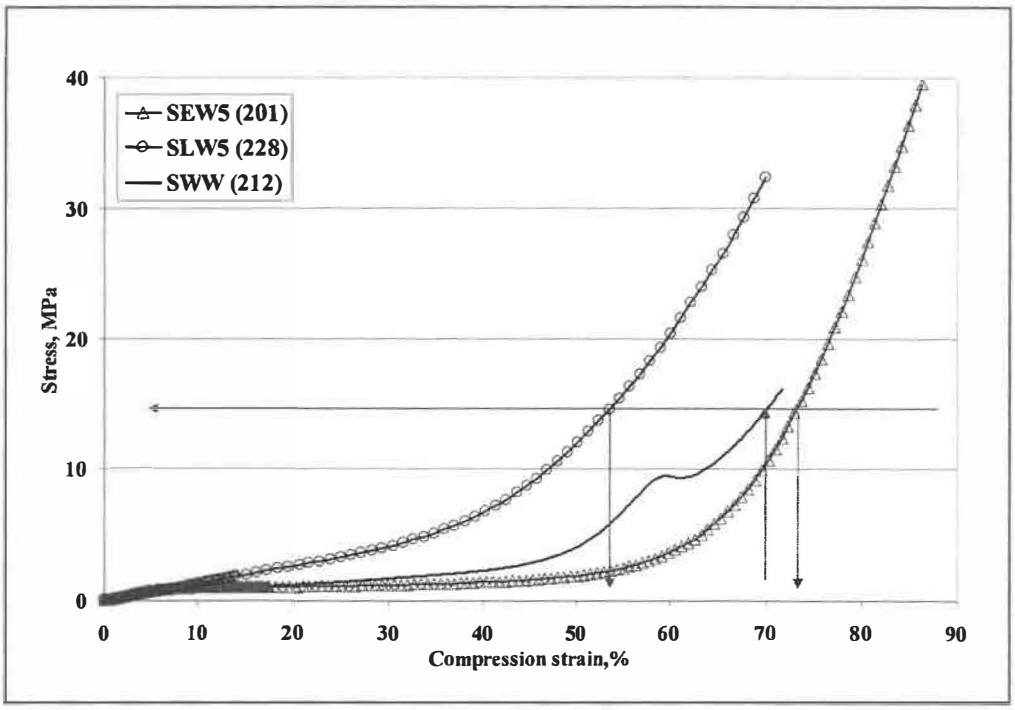

Figure 6.32 Comparison of radial compression of sulfonated EW, LW and whole wood specimens (number in bracket indicates the sulfonate content, mmol/kg)

6.3 Concluding remarks for this part

Temperature is by far the most influential factor on the level of sulfonation. Despite their differences in morphological characteristics, the EW and LW can be sulfonated to similar degree under the same conditions.

Sulfonation decreases the physical properties of wood such as modulus, specific compression energy, stress of both the primary and secondary plastic zones. However, there is no fundamental change in the form of the compression curve of the whole-wood samples at various sulfonate contents.

The normalized stress-strain curves of sulfonated samples and that of samples compressed at various temperatures can be fitted into one curve for the elastic and elastoplastic regions. This indicates that the elastic and plastic behaviors of wood under compression are independent of the wood properties. This means that the elastic property and the collapse behaviors of wood in the elastoplastic region are principally dependent on the wood's cellular structure. Increasing the compression temperature and the sulfonate content decreases all the physical properties studied. However, the mechanism of softening is different: thermal softening is the result of altering the motions of the polymer chains of all wood components. The relationship between the physical properties and the temperature follows Arrhenius' law. In contrast, sulfonation is an irreversible chemical modification of the wood components, particularly the lignin. The physical properties of wood decrease linearly with increasing sulfonate content.

A systematic comparison of the restrained and unrestrained radial compressions is made on sulfonated samples. The results indicate that, at low compression strain (<50%), the wood samples response similarly under the two types of compressions: they yield similar modulus of elasticity (MOE) and first plateau stress (SP1). However, when the compression strain exceeds 50%, where significant lateral expansion occurs, the wood samples behave differently. When the samples are compressed without restraint, a brief second stress plateau occurs at around 60% strain. At this point, fiber separation takes place due to an excessive lateral expansion. Beyond this point, the stress increases again

with increasing compression strain. The second modulus (MOE2) decreases linearly with increasing sulfonate content. However, there is no such second plateau when the sample is compressed with restraint. The stress increases rapidly in the densification region. The modulus at this stage is independent of the sulfonate content; signifying restrain manner controls the modulus at this region.

Compressions of samples consisting either of EW or LW indicate that these two types of fiber response differently. The stress-Strain curves of EW samples exhibit a prolonged plastic plateau, which is accountable to the collapse and lateral displacement of EW fibers. This primary plastic plateau exhibited by LW is not obvious, suggesting that the collapse of LW fibers was rather gradual in contrast to the EW fibers.

Radial compression of wood blocks reveals important mechanical characteristics of the components in the wood matrix. The mechanical failure follows the theory of weak-link within the wood structure. In such a case, the weak zone is situated in the EW where the fibers are large and thin-walled in comparison with those in the LW.

Following this line of thinking, we expect that the EW would breakdown earlier and faster than the LW in a refining system, and that the former would absorb most of the mechanical energy impacted by the refiner bars and thus suffer higher degree of fragmentation, when compared with the LW. Refining mixtures of low- and high-density wood would be expected to exhibit similar behavior as observed for the EW and LW.

In chemimechanical and chemithermomechanical pulping, the chips have undergone a significant change in mechanical properties, and their refining behavior would be quite different from the untreated raw material. The softening effect of sulfonation on both EW and LW would promote better fiber separation in refining (such as in CMP and CTMP), minimizing fibers breakage, particularly those in the EW. Hence, softening of the wood matrix either thermally or chemically makes both the EW and LW more amendable, providing better distribution of refining energy over the two types of tissues.

Chapter 7 - Results and discussions: Characterizing radial compression of wood by longitudinal shear

In modern refining technology, pre-treatment of chips by mechanical compression is an important process step to improve pulp quality. Therefore, compression failure of wood has received increasing attention in the past two decades or so as discussed in chapter 1. Chip refining can be regarded as a repetitive compression-decompression process that liberates fibres from the wood matrix [179]. The separation of fibres by compression, a fatigue process [80], is affected by temperature [68], stress amplitude and frequency [77]. Despite numerous research efforts on compression of wood, there is, however, no reported technique that quantitatively characterizes the mechanical properties of compressed wood.

In radial compression the early- and latewood behave differently [67, 180]. Radial compression of water-saturated wood blocks without restraint, up to 50% strain, the earlywood could account for more than 90% (depending on the proportion of earlywood in the sample) of the total deformation while the contribution of latewood is relatively small due to its thick cell wall. In the plastic deformation zone the thin-walled earlywood fibres collapse (flatten) while the latewood fibres exhibit little deformation. However, with higher strains radial rows of latewood fibres would buckle, developing microscopic fissures. Such failures could eventually lead to the breakdown of the wood matrix as the compression load increases [181].

Many methods have been used to evaluate the modification of wood matrix and fiber by refining. Some of these methods could be used to characterize the effect of compression on modification of wood matrix, such as:

1. Microscopic observation: These methods are usually used to study the locations of initial rupture and the possible rupture modes in wood under various testing conditions. The methods include: (1). Bromine stain/ KMnO4 stain [93, 182, 183] and Modified Simon stain [66, 93, 184, 185, 186, 187, 188] for light microscopic analysis. (2). Scanning electron microscopy (SEM) and image analysis [63, 72, 81, 189, 190, 191].

2. Distribution of pore volume

Quantitative information on pore size distribution of the treated and untreated specimens can be obtained by using a series of molecules of increasing size (Glucose 8 Å and different Dextran 26-1600Å) according to the techniques described in [80, 192].

3. Other methods

Other methods including mercury and liquid porosimetry [190], filler distribution [191], density distribution [193], synchrotron X-Ray microtomography [194], and confocal laser scanning microscopy (CLSM) [195, 196] can also be used to study the structural changes in fiber wall.

However, most of these methods only give limited qualitative information on a small area of surface, and many of them are too complicated to be carried out on a large scale. Most of all, these methods do not characterize the strength properties of compressed specimens.

In radial compression the physical deformation of specimen progresses gradually from earlywood towards latewood. Any physical weakening across the growth rings is expected to occur in a similar manner. The weakening effect of radial compression on strength properties of wood could be determined by a longitudinal shear in the radial plane of specimen. The objective of this chapter is to characterize the effect of radial compression on the mechanical properties of wood using a longitudinal shearing test and SEM analyses.

7.1 Pre-compression

Figure 7.1 shows stress-strain curves for samples compressed at 80°C (C2) under various compression strains. The characteristics of wood compression can be evaluated by Young's modulus (MOE), first and second plateau stress (SP1, SP2), and specific compression energy (SCE), as discussed in chapters 5 and 6. Table 7.1 presents the compression data of samples pressed under various conditions including strains of different magnitudes, 30, 50, 60 and 65%. It is obvious that for a given sample treatment the compression strain had no effect on the first plateau stress (SP1) because this stress represents the plastic response of the EW. However, the SP1 decreased with increasing temperature and sulfonation content, as discussed earlier.

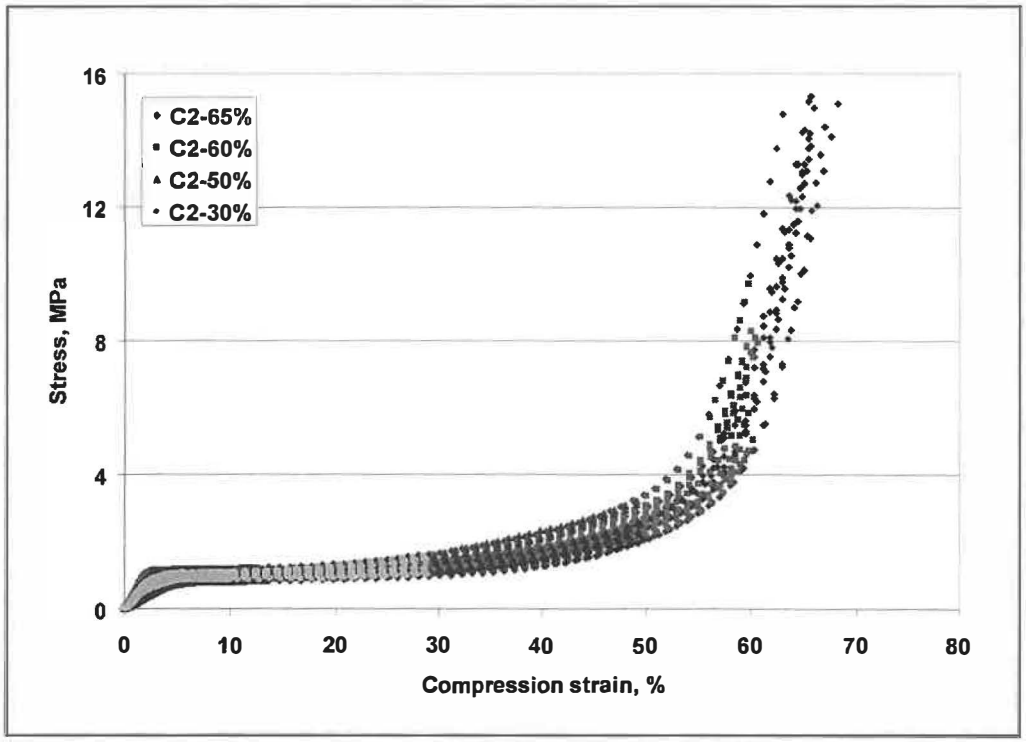

Figure 7.1 Compression curves to various strain at 80 °C (C2)

As in the case of SP1, the Young's modulus remained fairly constant for a given specimen treatment since it accounts for the elastic response of the wood matrix at low

strain. However, the treatment temperature and sulfonation significantly reduced this property.

The specific compression energy (ratio of compression energy to specimen volume) increased with increasing compression strain. Its magnitude decreased with increasing temperatures and sulfonation.

Table 7.1 Results of pre-compression

Sample	Comp. strain %		SP1, MPa	MOE, MPa	SCE, MJ/m^3	Permanent Def, %
C1: Water-saturated Comp. at 22°C	B	30	2.29 (10.4)[a]	108.3 (21.6)	0.75 (13.6)	1.0 (20.4)
	C	50	2.31 (10.8)	101.8 (38.5)	1.61 (17.4)	2.6 (18.2)
	D	60	2.37 (13.8)	91.07 (22.1)	2.48 (18.3)	3.0 (15.6)
	E	65	2.32 (15.8)	91.77 (14.1)	2.60 (9.1)	3.3 (7.8)
C2: Water-saturated Comp. at 80°C	B	30	1.03 (5.8)	44.31 (28.4)	0.30 (8.1)	1.3 (6.0)
	C	50	1.06 (7.9)	47.95 (24.5)	0.68 (13.1)	2.8 (10.2)
	D	60	1.02 (6.3)	50.05 (28.2)	1.07 (14.6)	4.3 (21.8)
	E	65	1.05 (9.1)	49.40 (30.1)	1.56 (16.8)	4.6 (16.8)
C3: W/G-saturated Comp. at 120°C	B	30	0.73 (7.1)	27.1 (21.2)	0.22 (10.0)	0.5 (26.8)
	C	50	0.74 (6.0)	29.6 (11.9)	0.54 (6.0)	2.0 (12.5)
	D	60	0.73 (9.3)	28.8 (17.3)	0.93 (18.5)	2.5 (16.5)
	E	65	0.73 (8.8)	27.0(13.5)	1.53 (20.1)	3.5 (14.6)
C4: Sulfonated Comp. at 22°C	B	30	0.91 (9.9)	49.46 (23.7)	0.28 (13.7)	0.6(31.4)
	C	50	0.83 (10.1)	44.09 (25.3)	0.62 (20.0)	1.4 (27.3)
	D	60	0.85 (10.3)	40.34 (33.0)	1.17 (11.5)	2.5 (23.0)
	E	65	0.85 (8.2)	42.23 (38.5)	1.65 (10.7)	2.8 (14.4)

* a, Figures in brackets are coefficient of variance in percentage.

There were some interesting effects of compression relative to the permanent deformation of specimens. The effects are illustrated in Figure 7.2, which shows that compression at 80°C had the greatest effect on permanent deformation, which is believed to be related to the thermosetting of lignin in the wood matrix. Interestingly, compression at 120°C yielded lower permanent deformation in comparison with that at

80°C. The reason for this phenomenon is unknown at this point. However, speculatively, it may also be related to the thermal softening of lignin. At high temperature, thoroughly softened lignin renders the wood matrix enough flexibility to spring back when the compressive force is released. Note that the sulfonated specimens showed the lowest permanent deformation, implying that sulfonation increase fiber flexibility and gave the cell wall a somewhat "spongy" character. Additional compression tests on sulfonated sample blocks confirmed this effect.

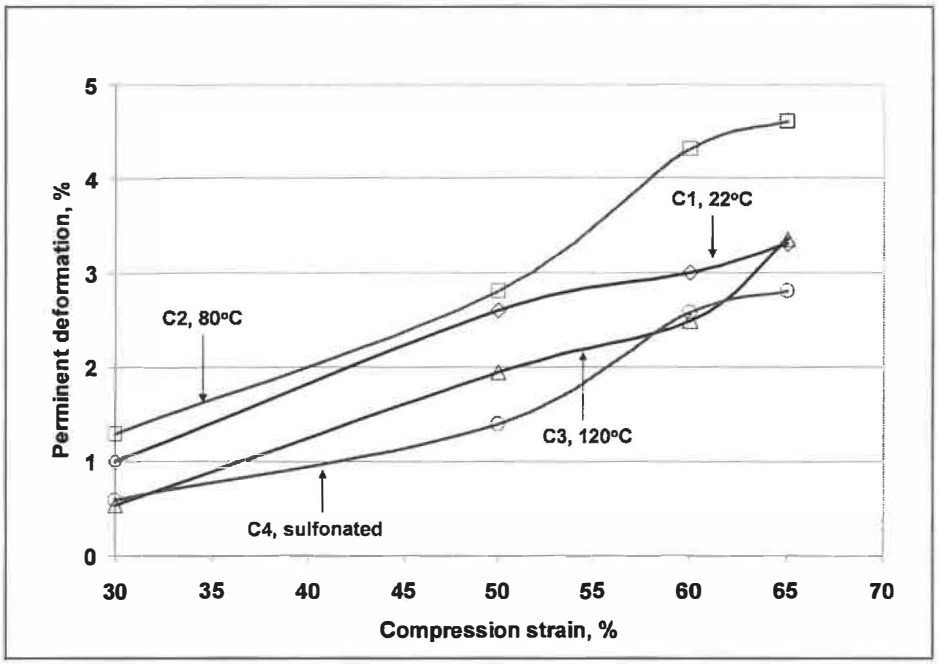

Figure 7.2 Effect of compression on permanent deformation

The coefficient of variance for the primary stress and specific compression energy are relatively small, but that of permanent deformation and modulus are relatively large in some cases. This indicates that the spring-back of wood when the compression force is removed varied a lot even under the same compression conditions. The variation of modulus resulted from the anisotropy of wood and also from the preparation of specimens, such as the roughness and non-parallelism of sample surface [82].

As discussed in the previous two chapters, when the sample was compressed without restraint, a short second plateau (SP2) occurred at about 60% compression strain. This second plateau indicates the sudden failure (fiber separation) of the wood matrix under

compression. The sudden failure is associated with the extreme lateral expansion of the sample. However, the second plateau did not appear in the samples of the third series. The only difference between the samples in the third series and that in the previous two series is the sample dimensions. Samples used in the third series had a dimensions of 11×15×28 mm (L×R×T), larger than those used in the previous series (10×10×10 mm (L×R×T). The most important difference is the tangential dimension, resulting in increased frictional force between the sample surface (LT surface) and the press platens. This larger frictional force imposes a greater restraint on the lateral expansion of sample. If the frictional force is large enough, the compression is self-restrained which is similar to the restrained compression as shown in chapter 6, and no second plateau appears.

Additional tests were conducted to demonstrate the influence of tangential dimension (LT surface area) on the behavior of wood under compression. In this part of study, ten sulfonated samples (C4F) measuring 11×15×28 mm (L×R×T) were first prepared exactly in the same way as the samples of C4E series, and then cut into two equal parts along the tangential direction. These sample pairs were placed, side by side, parallel to each other, leaving some space in between. Such arrangement allows the sample to laterally expand during the compression. The compression results are presented in Table 7.2. As indicated in Figure 7.3, these samples (C4F) exhibit a clear second plateau, but the stress-strain curves are similar when the compression strain is less than 60% strain, in comparison to C4E samples. The result shows that large dimension in tangential direction minimized lateral expansion of sample and prevented a sudden failure.

Table 7.2. Compression of two sulfonated samples with different sample dimensions

	MOE, MPa	SP1, MPa	SP2, MPa	SCE, MJ/m^3
C4E	42.23 (38.5)[a]	0.85 (8.2)	--	1.65 (10.7)
C4F	37.70 (29.53)	0.85 (10.0)	9.00 (7.15)	2.21[b] (9.61)

* a, Figures in brackets are coefficient of variance in percenage. b, Compression strain is about 70%, which is larger than that of C4E (65%).

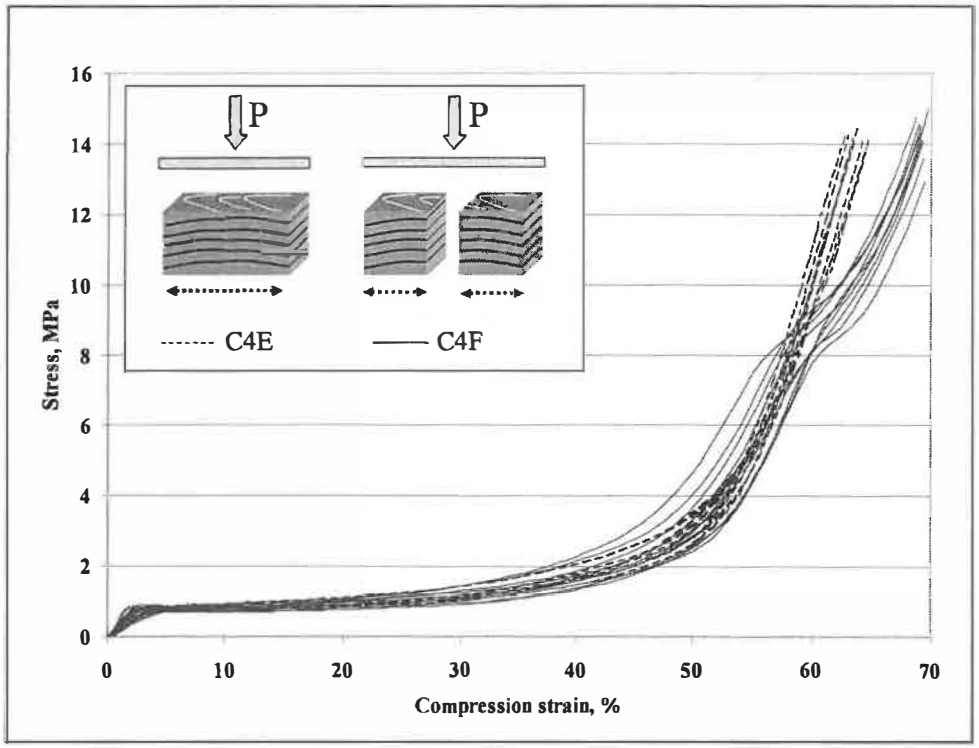

Figure 7.3 Compression curves of sulfonated samples (C4), sample with large size in tangential direction prevent sudden failure, thus no SP2 appears in this case (C4a)

7.2 Shearing test of pre-compressed samples

The shearing device used in this study was designed in such a way that two pairs of radial-longitudinal (RL) planes are created in the specimen. The reason for choosing the radial-longitudinal plane is to ensure that the shear failures take place across the entire growth ring including EW and LW.

Figure 7.4 shows the shear curves for samples pre-compressed to 65% strain at 80°C (C2S). The shear planes occurred, in most cases, successively (mode I), or less frequently, concurrently (mode II), as shown in Figure 7.5. Most of the failure planes occurred successively because of the heterogeneous nature of wood. In both failure modes, after an elastic phase (a), the shear stress reached a yield point, A, where small fissures developed mostly in the middle of the bottom side of the sample block. As the shearing load increased more fissures developed and the shear stress attained a plateau (b). In mode I, the shear stress dropped sharply when the first two failure planes appeared (point B), after which a second stress plateau occurred (c). As the shearing progressed, a second pair of shear failure planes developed at point C where the shear stress fell suddenly. The shear stress at the second plateau (c) is roughly half of that at the first plateau (b), which is $\tau_c \approx 1/2\ \tau_b$, as indicated in Figure 7.4. This relationship exists in most cases (Figure 7.4). The variation in τ_c is caused by the heterogeneity of sample and the friction force between the first shear planes and the shear device that differs in each case. When the two failure planes occurred simultaneously (mode II) the stress plateau prolonged farther than that in mode I. The shear stress disappeared as the failure planes developed.

We used shear properties such as shear modulus (G), shear yield stress (τ_y), maximum shear stress (τ_{max}), shear yield energy (E_y) and total shear energy (E_t) to characterize the shear behavior of the pre-compressed wood specimens. The shear yield stress, defined as the offset stress at 1% strain, is less than the maximum shear stress (Figure 7.4). The yield energy is the energy consumed up to the yield point A, and the total energy is the accumulative energy up to the completion of shear failure at about 27% shear strain.

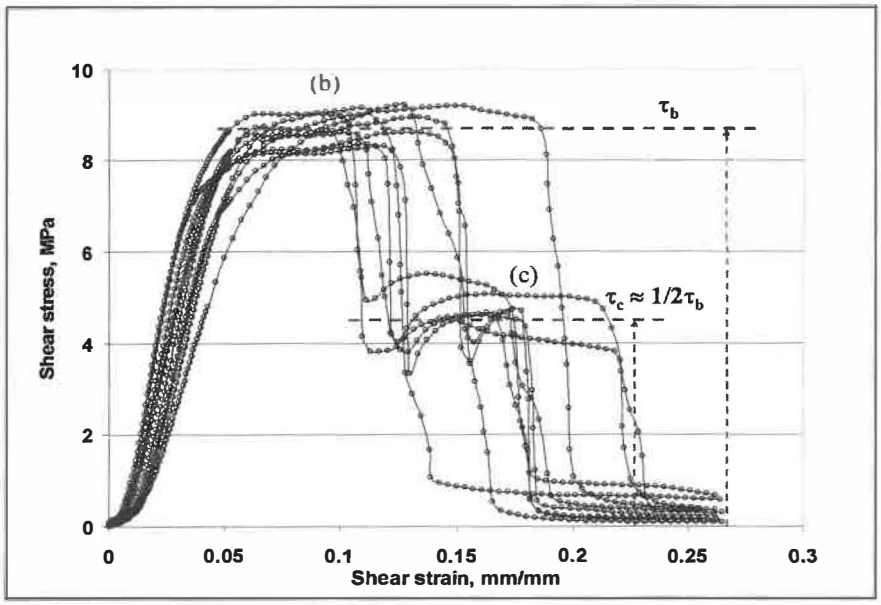

Figure 7.4 Shear curves of sample pre-compressed to 65% strain at 80 °C (C2S)

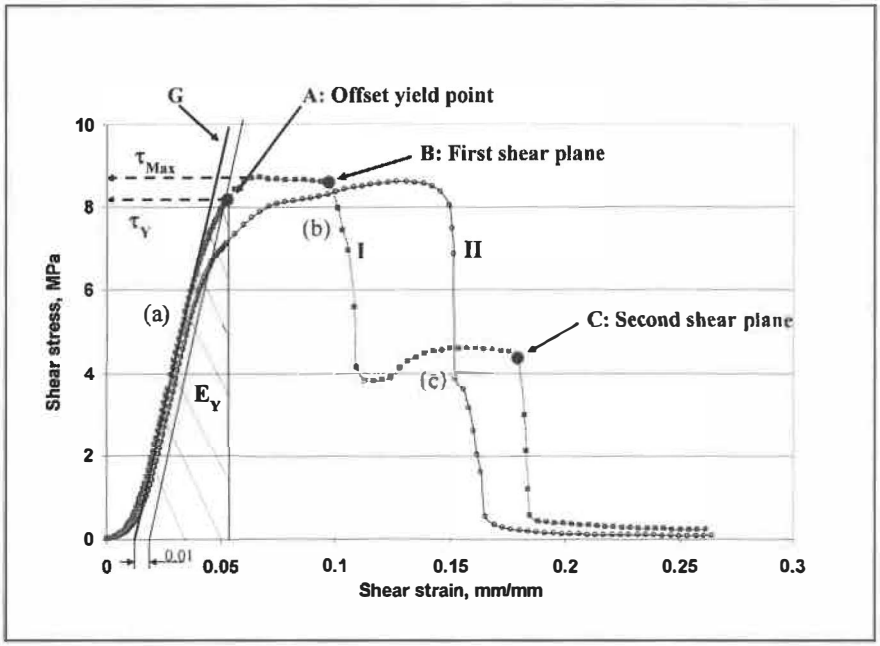

Figure 7.5 Typical shear curves, indicating two modes of shear failure: successive mode (I) and concurrent mode (II).

The results of shear tests are presented in Table 7.3. Note that two pairs of shear planes were generated in our test, thus the data presented in Table 7.3 should be divided by 2 when compared with other one-pair-surface shear methods [84, 87, 138, 139].

Table 7.3 Results of shear tests

Samples	Comp. strain (%)		Yield stress (MPa)	Max. stress (MPa)	Yield Energy (J)	Total energy (J)	Shear Modulus (MPa)
C1S: Water-saturated Comp. at 22° C	A	0	9.53 (2.9)	10.08(6.1)	0.534 (11.8)	2.10 (11.7)	261.1 (15.9)
	B	30	9.02 (6.6)	9.53 (4.1)	0.523 (16.9)	1.96 (15.5)	223.3 (16.8)
	C	50	8.37 (6.2)	8.94 (3.2)	0.499 (14.2)	1.92 (15.3)	219.1 (15.1)
	D	60	8.03 (4.4)	8.23 (2.5)	0.455 (11.3)	1.85 (16.0)	172.1 (12.0)
	E	65	7.28 (6.5)	8.01 (2.8)	0.391 (14.6)	1.66 (17.5)	156.0 (14.3)
	Dec., %		23.6(5.3)	20.5 (3.7)	26.8 (14.8)	21.0 (15.2)	40.3 (13.8)
C2S: Water-saturated Comp. at 80° C	A	0	9.16 (3.6)	9.78 (4.7)	0.473 (11.6)	1.98 (15.7)	293.5 (10.9)
	B	30	8.78 (6.7)	9.36 (2.2)	0.471 (11.2)	1.94 (16.0)	239.8 (15.1)
	C	50	8.70 (6.8)	9.27 (4.1)	0.46 (13.1)	1.89 (22.0)	243.7 (15.7)
	D	60	8.52 (4.7)	9.17 (4.2)	0.447 (10.3)	1.92 (13.5)	251.2 (8.4)
	E	65	8.09 (6.2)	8.85 (3.6)	0.408 (14.0)	1.74 (24.5)	221.6 (16.2)
	Dec., %		11.7(5.6)	9.5 (3.8)	13.7 (13.3)	12.1(18.3)	24.5 (12.0)
C3S: W/G-saturated Comp. at 120° C	A	0	8.22(10.8)	8.95 (6.5)	0.447 (12.7)	1.918 (16.7)	214.3 (21.8)
	B	30	7.86 (7.8)	8.53 (6.7)	0.429 (18.2)	1.567 (21.5)	212 (12.2)
	C	50	7.56 (8.5)	8.42 (5.4)	0.413 (20.9)	1.737 (16.0)	200.1 (20.2)
	D	60	7.34 (5.4)	8.00 (5.4)	0.401 (19.2)	1.771 (21.4)	202.6 (15.1)
	E	65	6.18 (9.9)	6.68(15.3)	0.319 (19.9)	1.226 (44.1)	188.2 (20.0)
	Dec., %		24.7 (8.5)	25.4 (7.9)	28.6 (18.2)	36.1 (23.9)	12.2 (17.9)
C4S: Sulfonated Comp. at 22° C	A	0	4.21 (5.4)	4.61 (6.3)	0.209 (16.0)	1.11 (15.8)	147.9 (25.1)
	B	30	4.03 (6.4)	4.39 (5.8)	0.192 (14.8)	1.01 (10.3)	132.6 (17.1)
	C	50	3.97 (6.9)	4.30 (8.7)	0.189 (10.3)	0.98 (18.6)	132.1 (23.4)
	D	60	3.44 (4.5)	3.78 (4.7)	0.152 (17.9)	0.88 (18.5)	127.8 (14.9)
	E	65	3.17 (5.8)	3.64 (6.9)	0.138 (19.9)	0.86 (25.7)	123.7 (14.2)
	Dec., %		24.7 (5.8)	21.0 (6.5)	34.0 (18.9)	22.5 (17.8)	16.4 (15.8)

* Dec., % is percentage of the total decrease for samples compressed to 65% strain compared to uncompressed samples.

* All tests were conducted at room temperature. Figures in brackets are coefficient of variance in percentage.

The maximum shear stress for an uncompressed water saturated sample (C1S, 0%) and that preheated at 120 °C for 15 minutes (C3S, 0%) are 5.4 MPa and 4.5 MPa, respectively. These figures are in agreement with that reported by Johansson et al. [84] who obtained a maximum stress of 5.1 MPa and 4.0 MPa for samples treated under similar conditions. The shear moduli obtained in this study are 130 MPa and 107 MPa for the samples indicated above, which are somewhat higher than those reported, 84 and 80 MPa, respectively [82].

The shear fracture energy is believed to be closely related to the fiber separation energy, this relationship has been accounted by many researchers [84, 87, 197, 198]. In our study, we obtained a shear energy of about 803.03 J/m^2. Since there is no complete failure surface created at the yield point, we believe that the actual fiber separation energy would be a little higher than this value. This result is comparable with that of Johansson et al. [84] who reported a failure energy of about 1413 J/m^2. A fracture energy of 1400 J/m^2 was presented by Koran [198]. On the other hand, much lower values, 100-140 J/m^2 are also reported [87, 197]. These discrepancies might be attributed to the differences in the shearing techniques used.

Figure 7.6 to Figure 7.10 present the variations of shear properties as a function of pre-compression strain (the void and full marks represent the experimental data and average values, respectively). In general, the radial compression had little effect on shear properties when the compression strain was less than 50%. This is because most of the compression energy is absorbed by the flexible earlywood fibres. Due to their high flexibility the earlywood fibres would suffer little physical damages. Meanwhile, the thick-walled latewood fibres would be relatively unaffected. But the shear properties fell sharply when the compression strain reached about 60% where significant structural damages occurred in both earlywood and latewood. The drastic changes in shear properties indicate the failure of latewood fibres. The possible failures include mainly buckling and separation of radial files of latewood and early wood fibres as well [180].

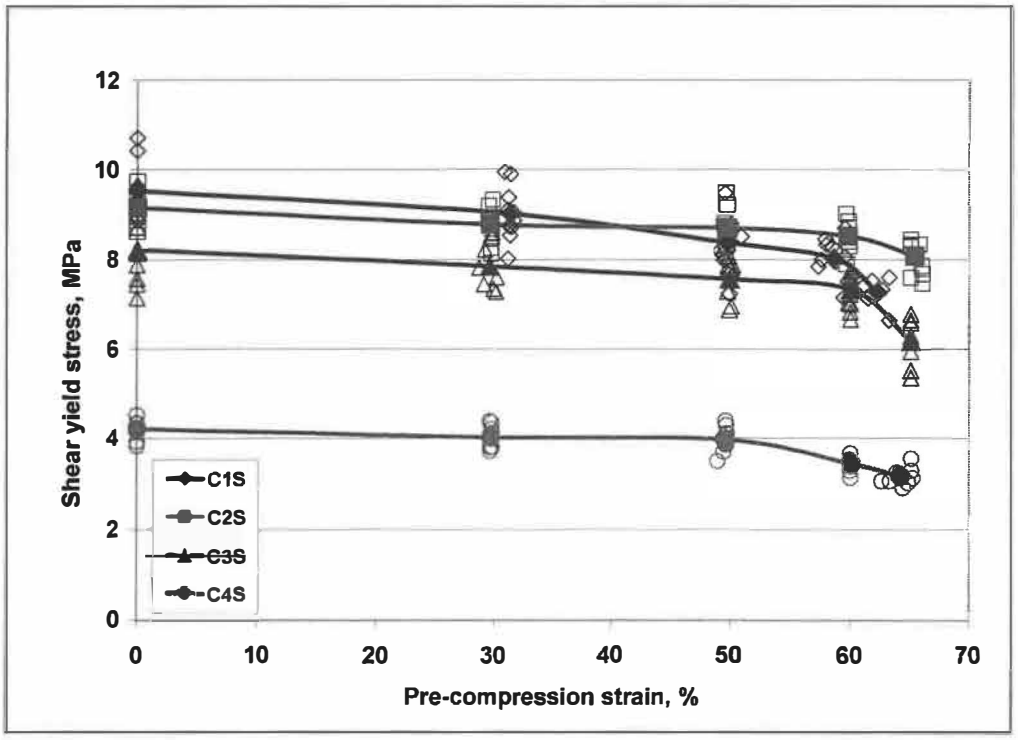

Figure 7.6 Effect of pre-compression on shear yield stress

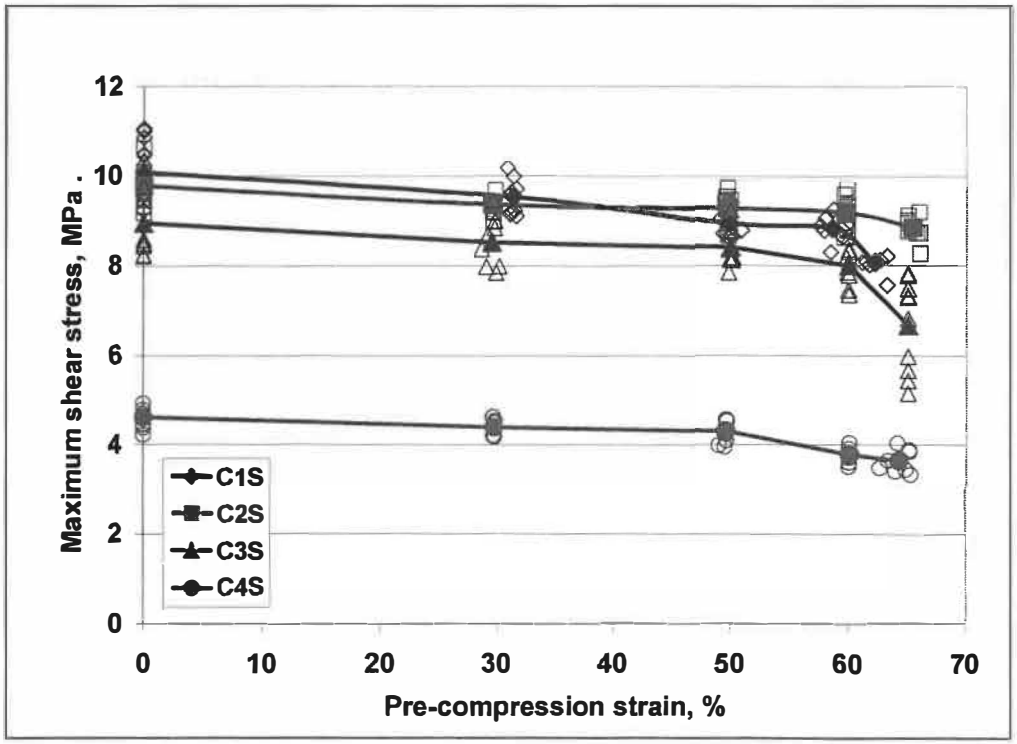

Figure 7.7 Effect of pre-compression on maximum shear stress

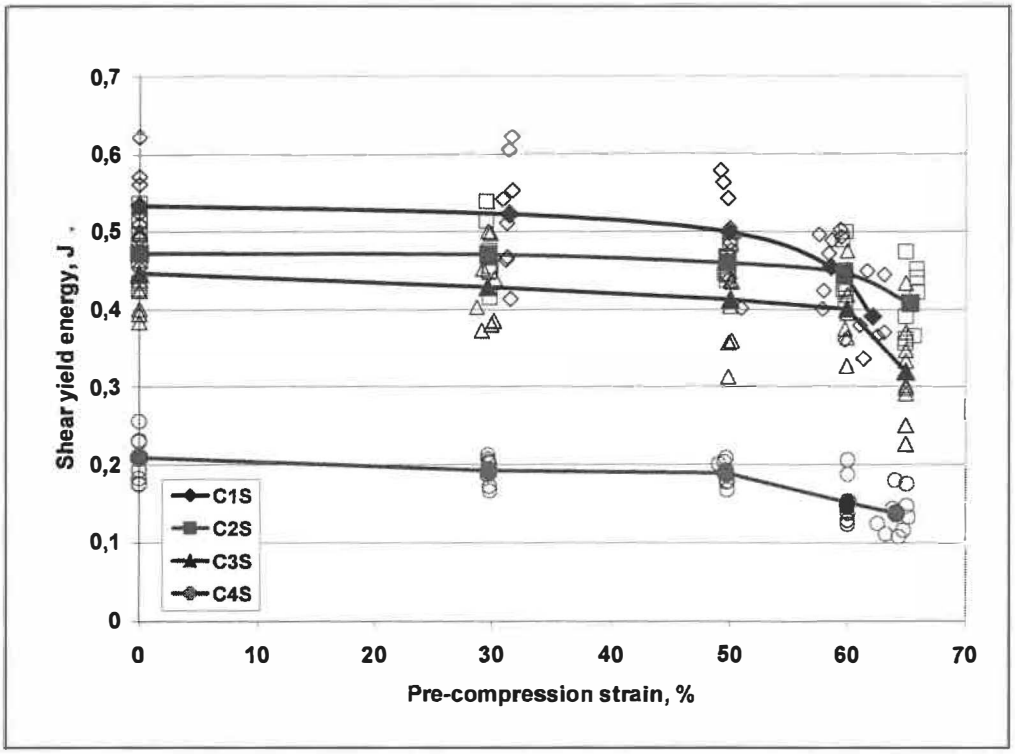

Figure 7.8 Effect of pre-compression on shear yield energy

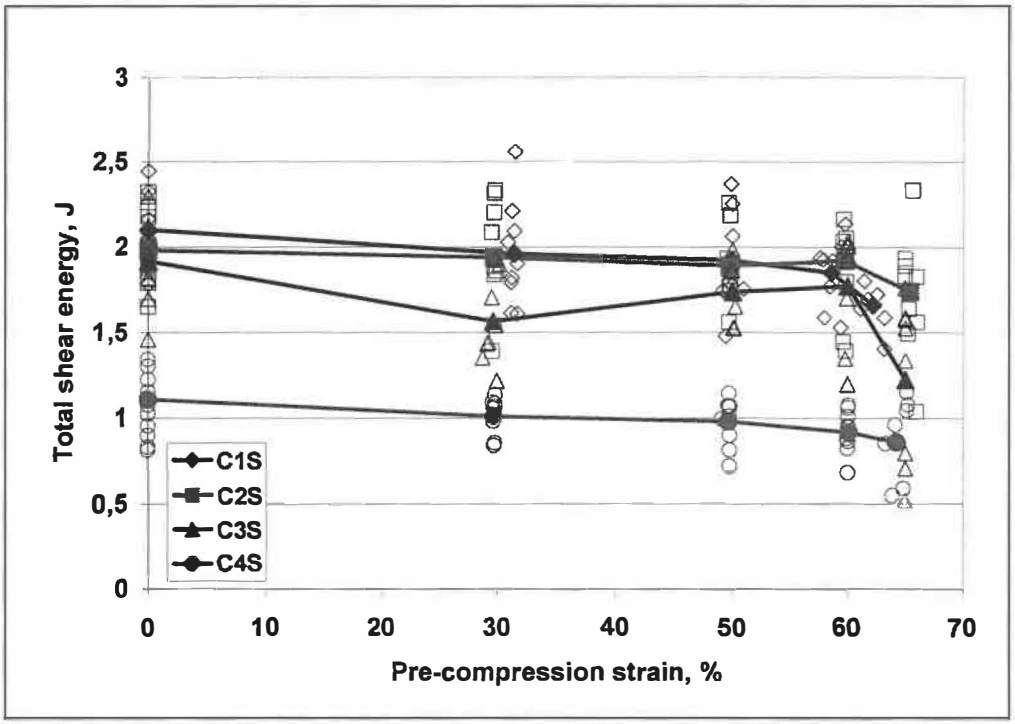

Figure 7.9 Effect of pre-compression on total shear energy

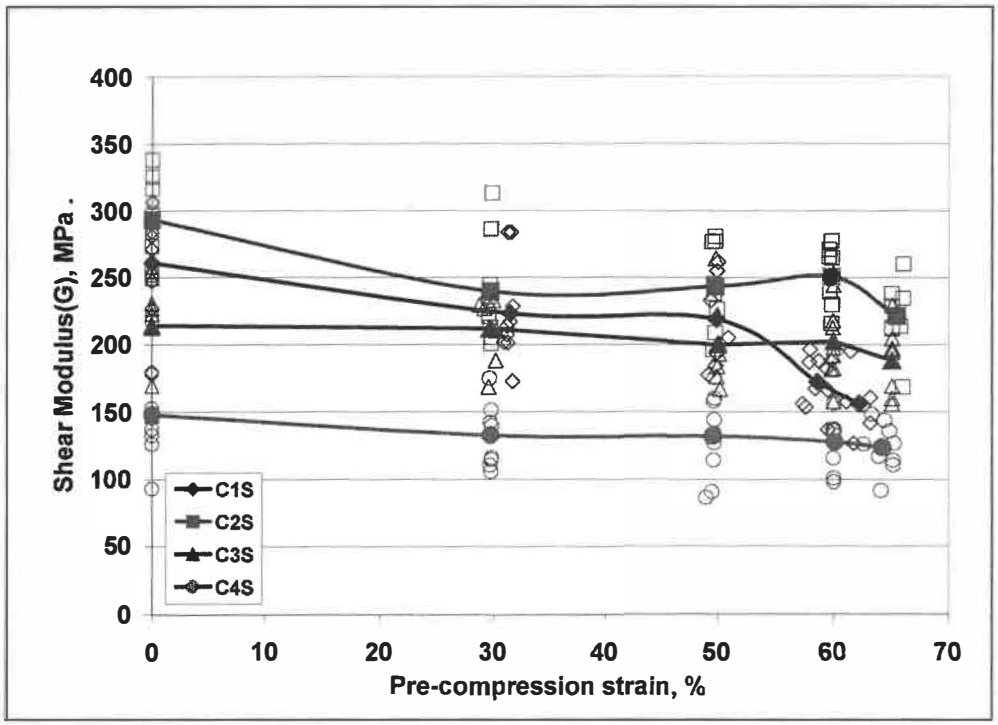

Figure 7.10 Effect of pre-compression on shear modulus

The pre-compression conditions had significant influence on the shear characteristics. Among the treatment conditions, sulfonation had the most significant impact on shear properties. In fact, sulfonation facilitates fiber separation by softening the lignin in the wood [199, 200]. Pre-compression at 120°C had much less effect when compared to the sulfonation, but the decreases in shear properties were quite evident when compared with those pre-compressed at lower temperature. At lower compression temperatures of 22°C and 80°C the changes in shear properties were comparable when the compression strain was about 50% or less. But the differences became statistically significant at high compression strain of 60% or higher where important physical damages to the wood matrix are expected to occur. However, compression at 80°C had minimum effect on reducing the shear properties as indicated in Figure 7.11 (Note that this pre-compression temperature yielded the largest permanent deformation, Figure 7.2 shows). Speculatively, the thermosetting of lignin at 80°C minimized the compression effect on the wood matrix (e.g. fiber collapse and separation), thus minimizing the adverse impact on the shear properties.

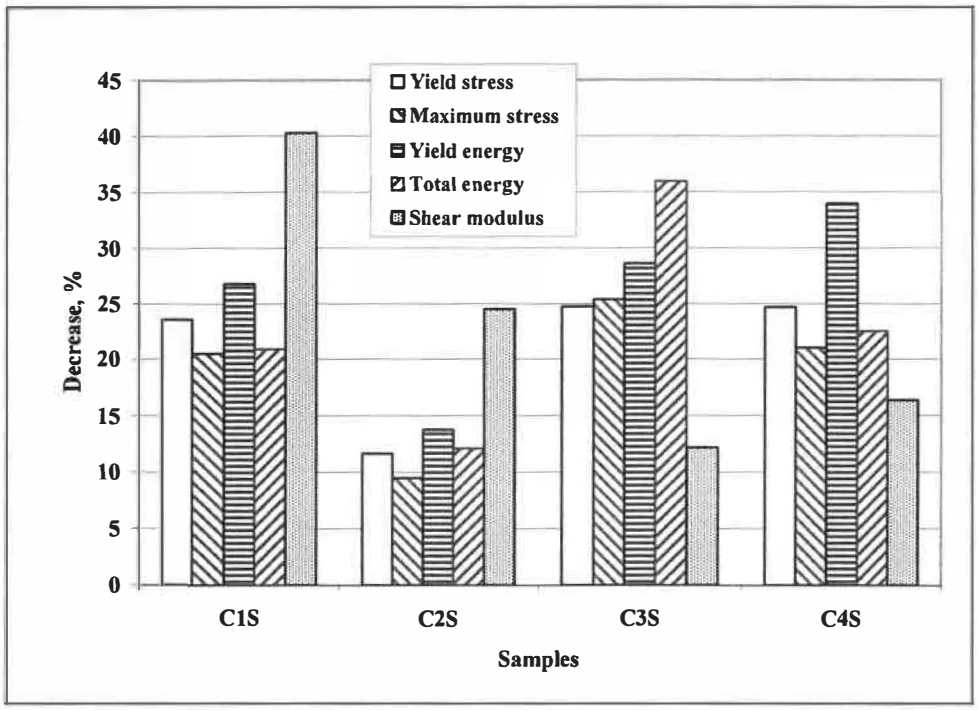

Figure 7.11 Total decrease in shear properties by pre-compression to 65% strain

The relationships between pre-compression energy and shear properties such as yield stress, maximum shear stress, shear modulus, shear yield energy and total shear energy with the SCE are presented in Figure 7.12 to Figure 7.16, respectively. In these illustrations, we use specific compression energy (SCE), defined earlier as the ratio of compression energy to the volume of the specimen (MJ/m^3), to express the correlation. Obviously, treatments at high temperature and sulfonation decrease the shear yield energy to some extents (when compression strain is 0%). Compression induced decreases in shear yield energy can be reflected from the ratio of four slopes, which is 1.08/1.01/2.66/1. This implies that compression at 120°C is more efficient in weakening the wood block in terms of energy consumption in shear, while the other three treatment conditions generally remain at the same level. This implies that compression at 120°C greatly facilitates fiber separation. However, this doesn't necessary mean that refining these pre-compressed chips could lead to any energy saving, because fiber separation energy only accounts for a small part of the total refining energy. The total refining energy is mainly determined by the energy consumed in fiber property development,

which is mainly dependent on the fiber separation mode. SEM observation (section 7.3) indicates that pre-compression at low temperature facilitates fiber separation in S_1/ S_2 interface, which is the favorite mode for developing fiber properties. Franzier et al [74] also recommended that pre-compression should be conducted at temperature well below 120°C. However, the optimum pre-compression conditions need to be further investigated by refining these pre-compression chips. However, in all circumstances, the compression should be done with high compression strain (>60%) in order to effectively compress both the EW and LW.

This finding also suggests that the changes in shear properties are highly related to the energy applied during the pre-compression of wood samples. The shearing technique developed in this study may also be used to characterize the physical damages of wood in compression such as multi-compression and wood fatigue processes.

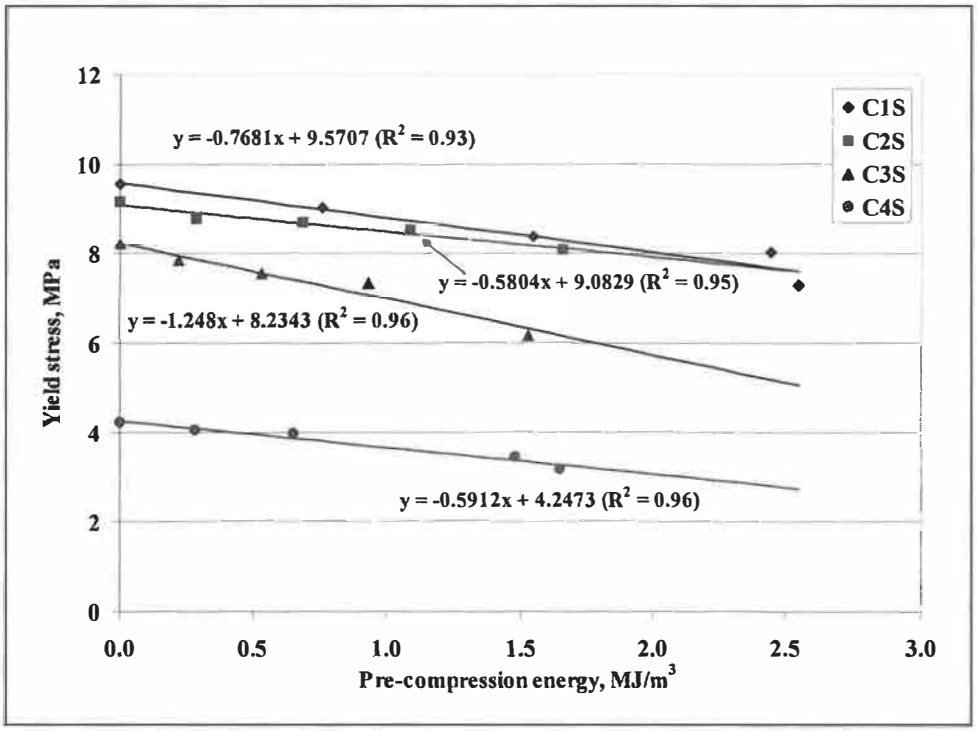

Figure 7.12 Relation of specific compression energy and shear yield stress

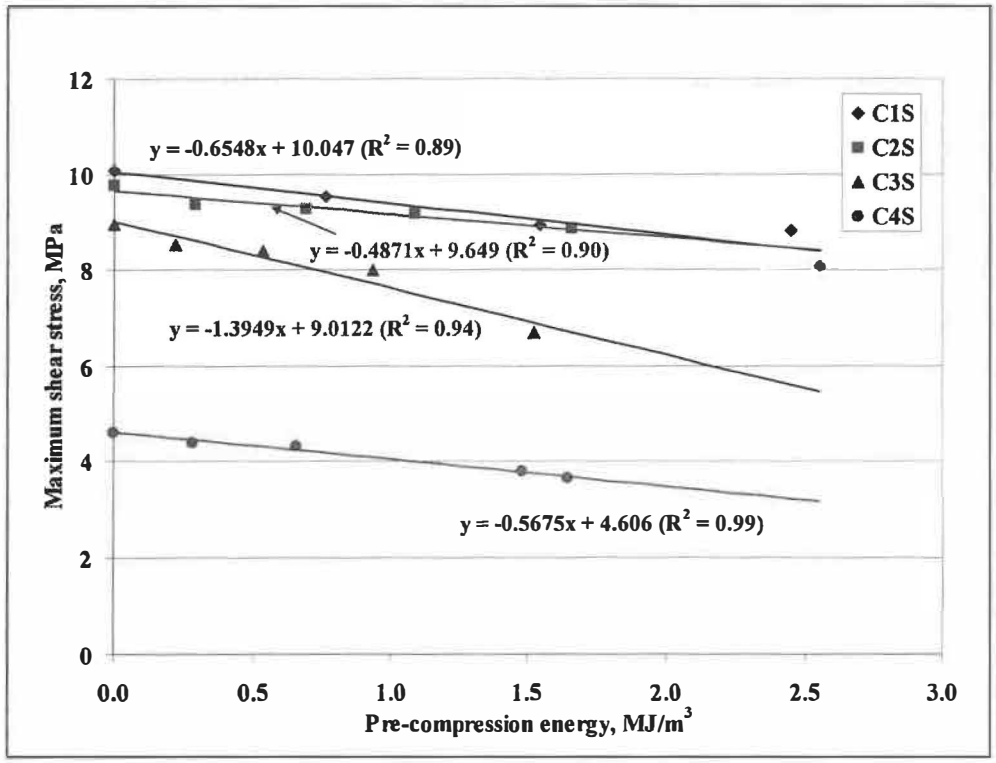

Figure 7.13 Relation of specific compression energy and maximum shear stress

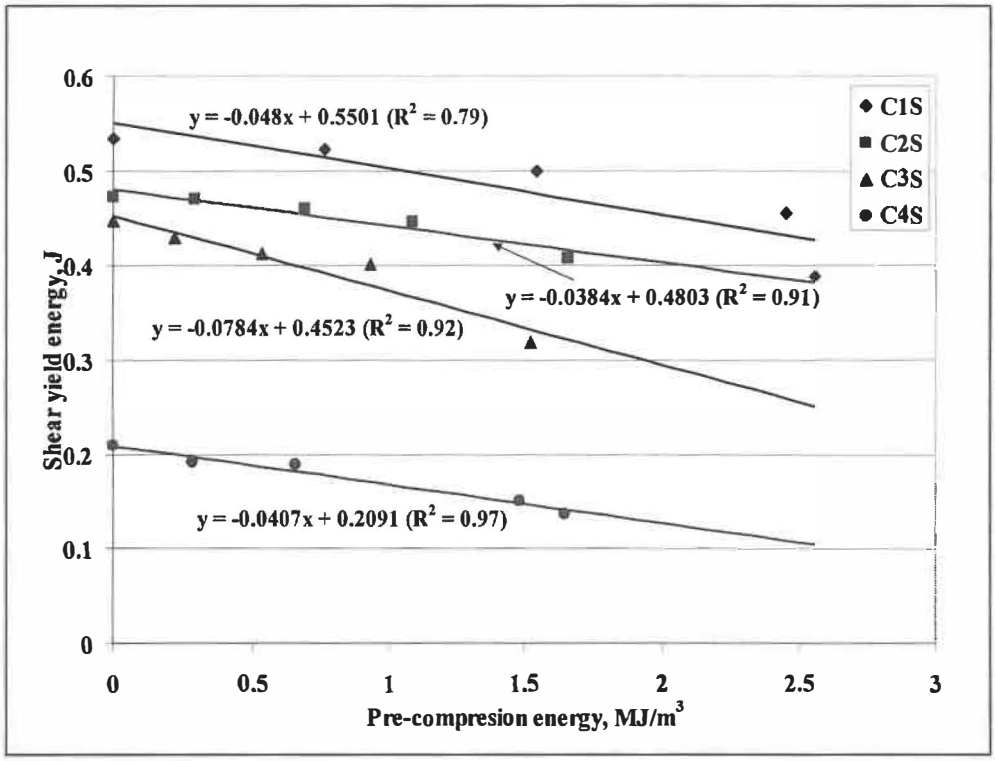

Figure 7.14 Relation of specific compression energy and shear yield energy

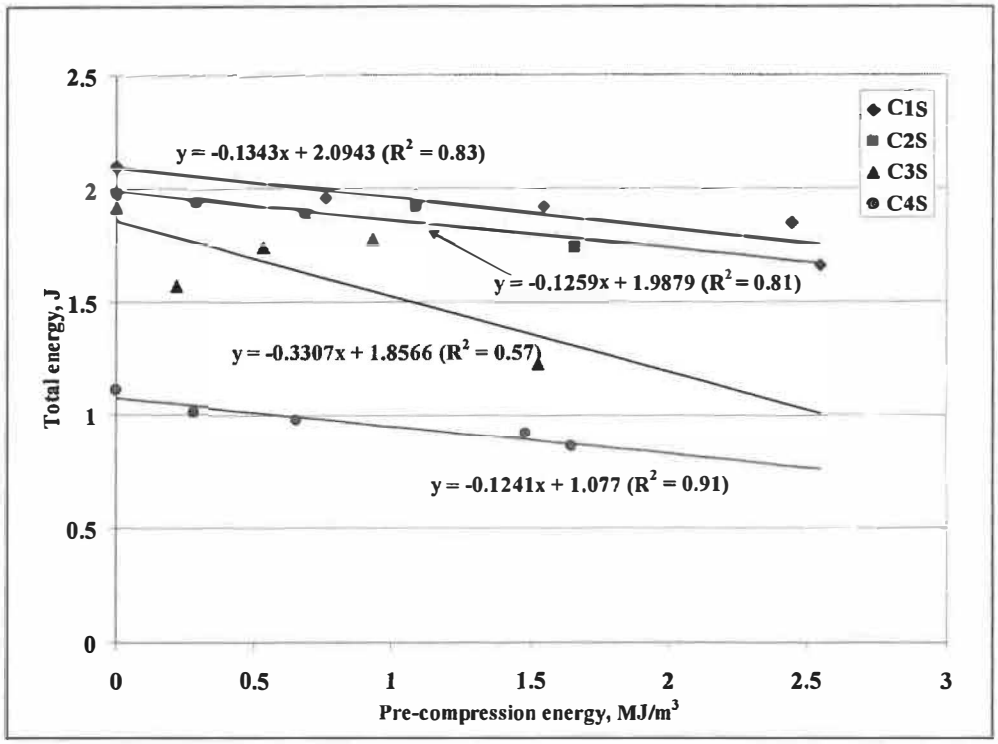

Figure 7.15 Relation of specific compression energy and total shear yield energy

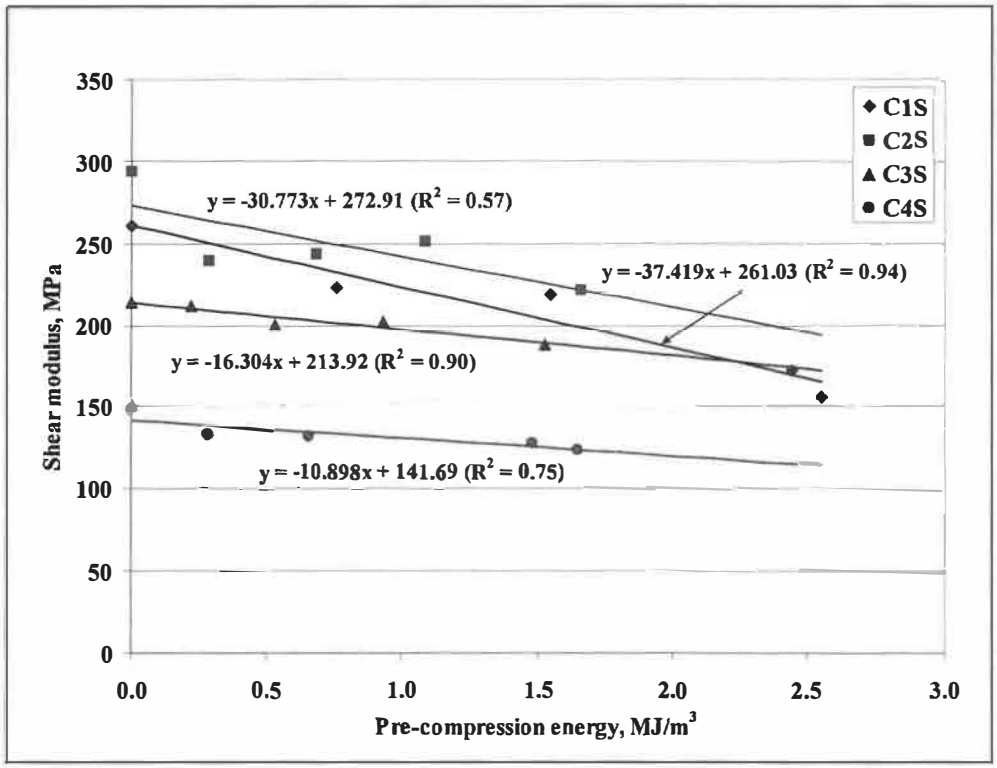

Figure 7.16 Relation of specific compression energy and shear modulus

7.3 SEM observation

The effect of pre-compression at different conditions on shear failures of wood can be revealed by SEM. The characteristics of three groups of samples used in the third series of experiment will be discussed here. Sample identification was indicated in the top-left corner of the micrographs, such as A0RL, etc. The first letter of the identification A, B, or C corresponds to the samples C1S, C2S and C4S, which were pre-compressed at 22°C (A-water saturated, and C-sulfonated), 120°C (B-saturated with water/glycerol). The second letter is a number indicating the compression strain in percentage. The third and the forth letters, RL or TL represent the radial-longitudinal plane (radial plane) and the tangential-longitudinal plane (tangential plane), respectively. The terms used for describing the fiber separation are similar as those indicated in Figure 2.2.

7.3.1 Surface characteristics of sample pre-compressed at 22 °C (C1S)

Figure 7.17 to Figure 7.20 show the SEM micrographs of radial and tangential planes of uncompressed samples. The fibers are separated in inter-cell (IC) mode in both planes. Intact pit membranes are firmly attached in most places on the radial surface. Some broken fibers are visible on tangential plane, with S_1 exposed in some places.

For samples compressed to 65% strain (Figure 7.21 to Figure 7.25), LW fibers are also separated in IC mode, similar to what is seen in the uncompressed samples. In contrast, the EW fibers are separated in trans-wall (TW) and intra-wall (IW) modes producing ribbons of cell wall and many fibers broken longitudinally (Figure 7.21). In some cases, fiber separation occurred within the S_2 layer, generating large area of S_2 surface or detached lamellae of S_2 (Figure 7.22, Figure 7.23). The characteristics of the tangential planes of samples compressed to 65% strain are similar to those of uncompressed specimens (Figure 7.24). Failures at cell corners and between cells are also evident in some locations (Figure 7.25). These characteristics indicate that, in high strain radial compression, structural weakening occurred between cells, between different cell wall

layers, and even within the S_2 layer. These failures can provoke longitudinal cleavage or cell wall delamination.

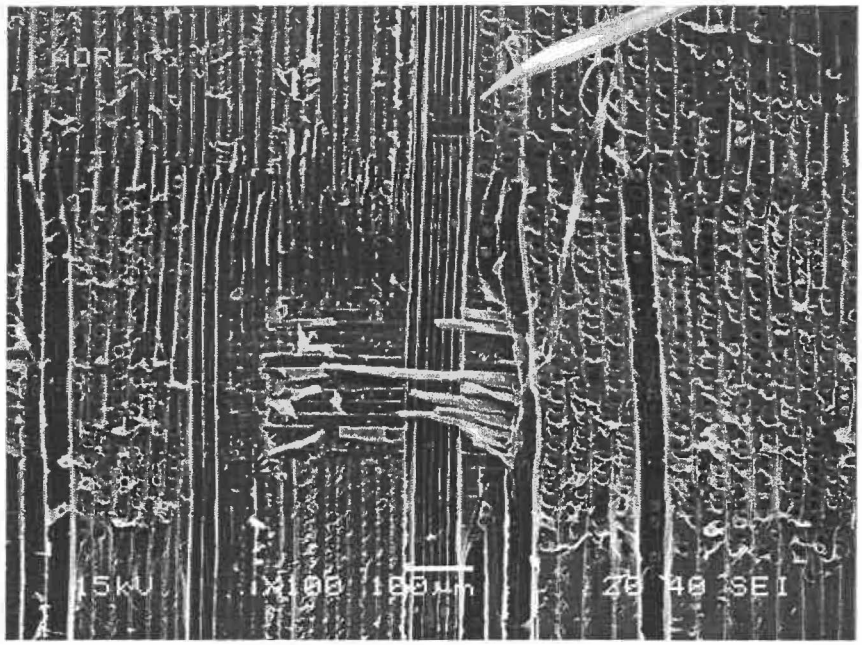

Figure 7.17 Radial fracture surface of uncompressed sample. Most fibers are separated in inter-cell mode and remained intact.

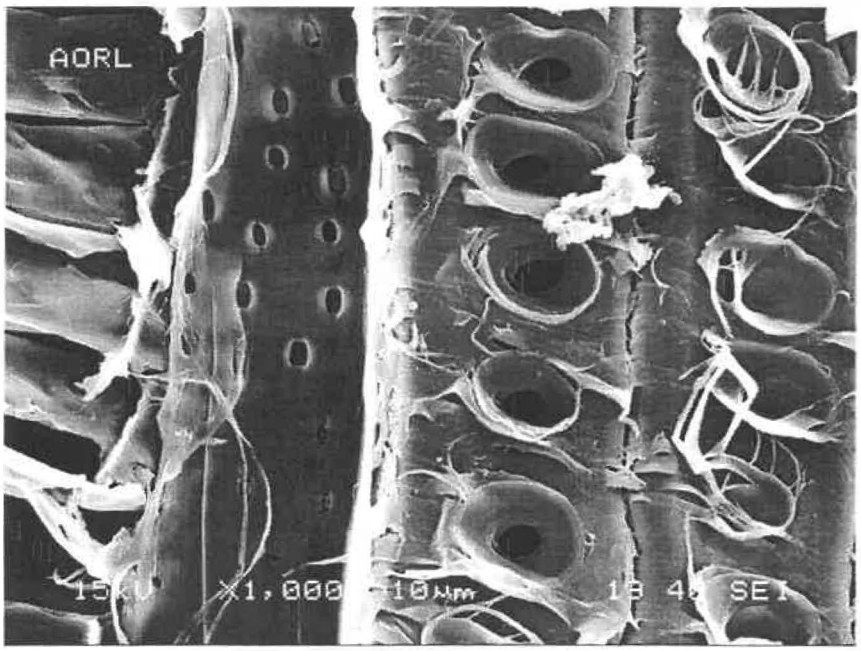

Figure 7.18 Radial fracture surface of uncompressed sample. Most fibers are separated from the CML with intact pit boarder firmly attached.

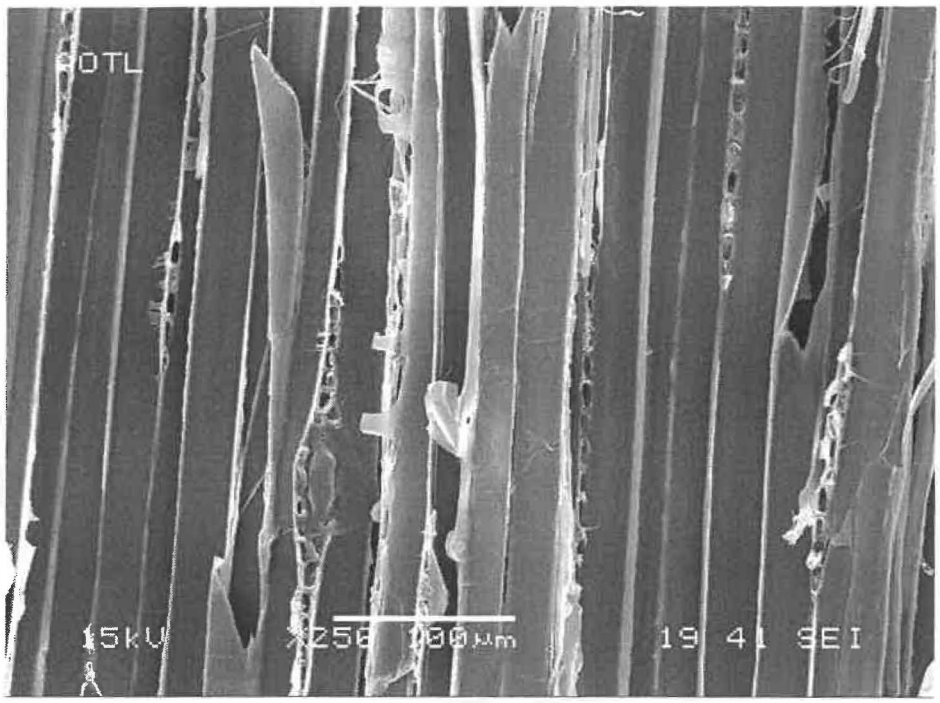

Figure 7.19 Tangential fracture surface of uncompressed sample. Some fibers are broken.

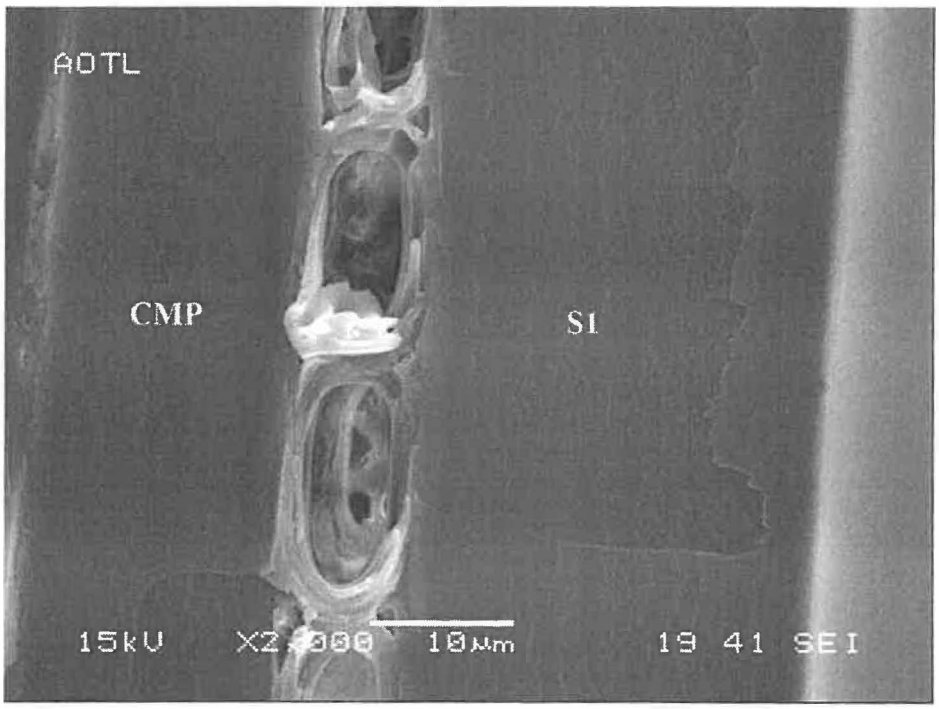

Figure 7.20 Tangential fracture surface of uncompressed sample. Fibers are separated from the CML and S_1. Ray cells are cut at the surface of fracture.

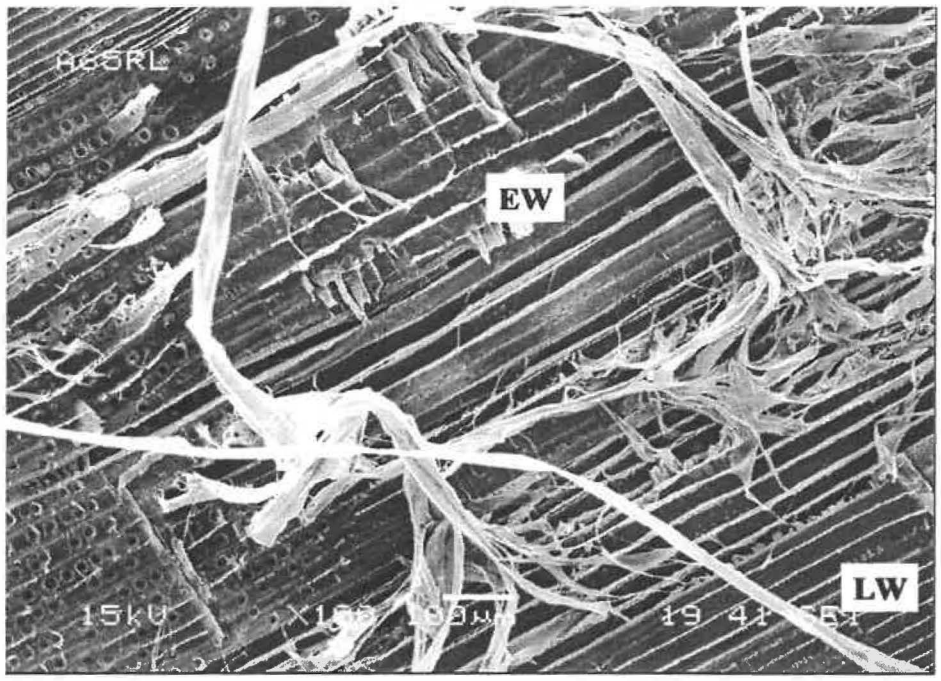

Figure 7.21 Radial fracture surface of sample pre-compressed to 65% at 22 °C. Many fibers are separated in trans-wall mode.

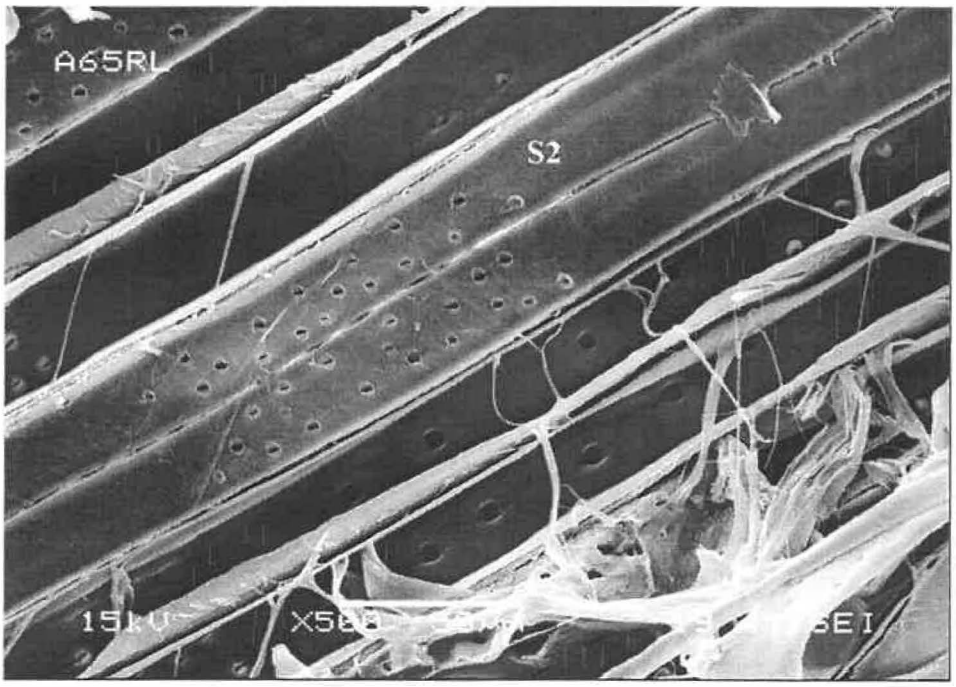

Figure 7.22 Radial fracture surface of sample pre-compressed to 65% strain at 22°C. Some fibers are separated in intra-wall mode with exposed S_2, indicating the weakening of the interface of S_1/ S_2 by high strain compression.

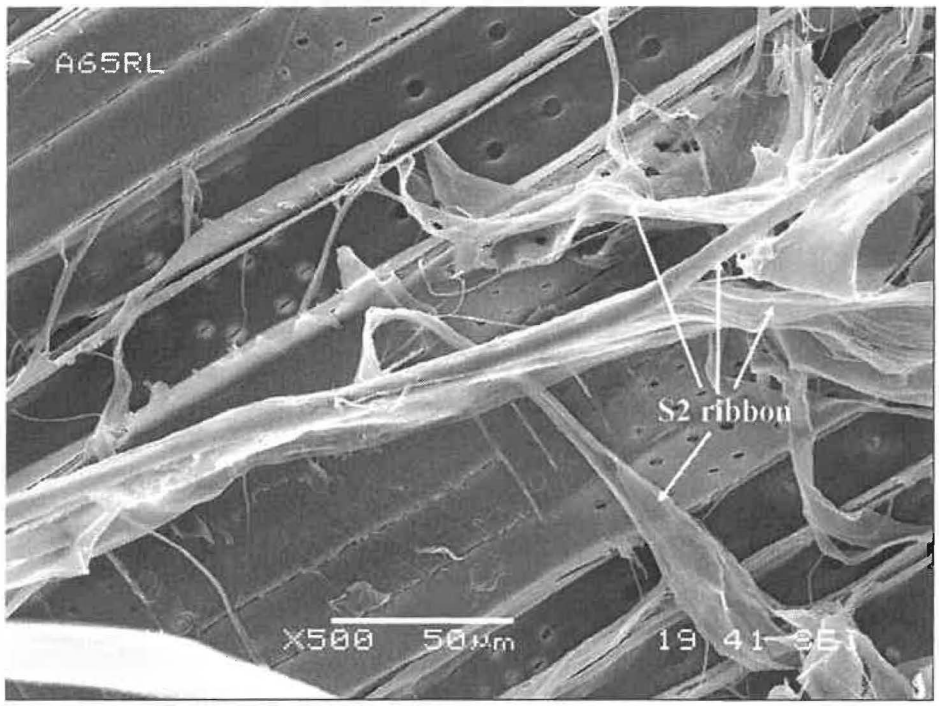

Figure 7.23 Radial fracture surface of sample pre-compressed to 65% strain at 22°C. Longitudinally broken fiber with layers of S_2 separated, indicating the weakening within S_2 layer by high strain compression.

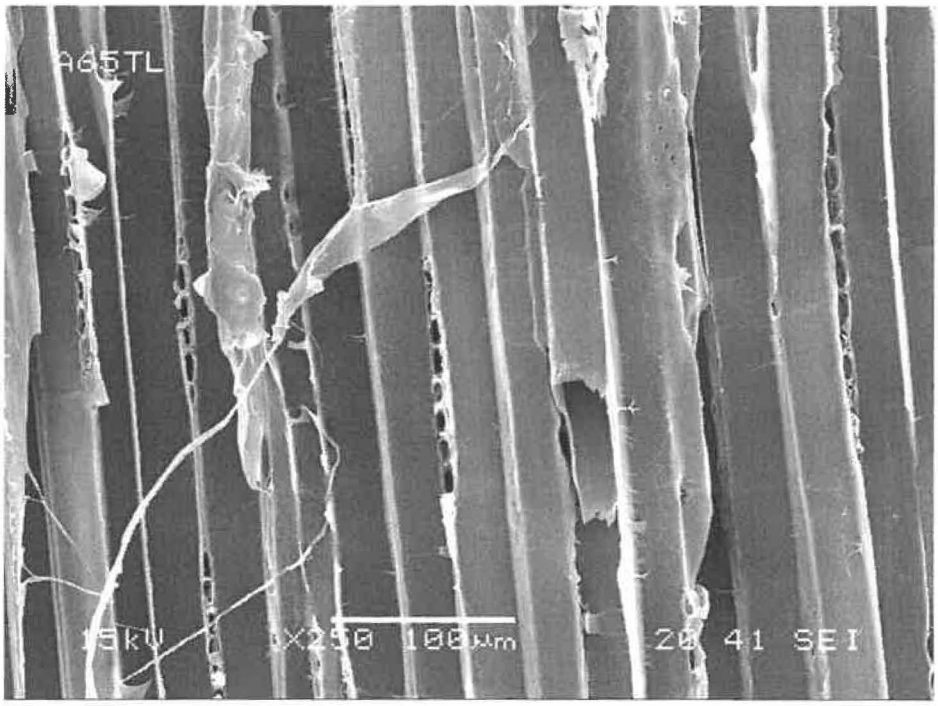

Figure 7.24 Tangential fracture surface of sample compressed to 65% at 22 °C. Some fibers are broken as uncompressed sample does.

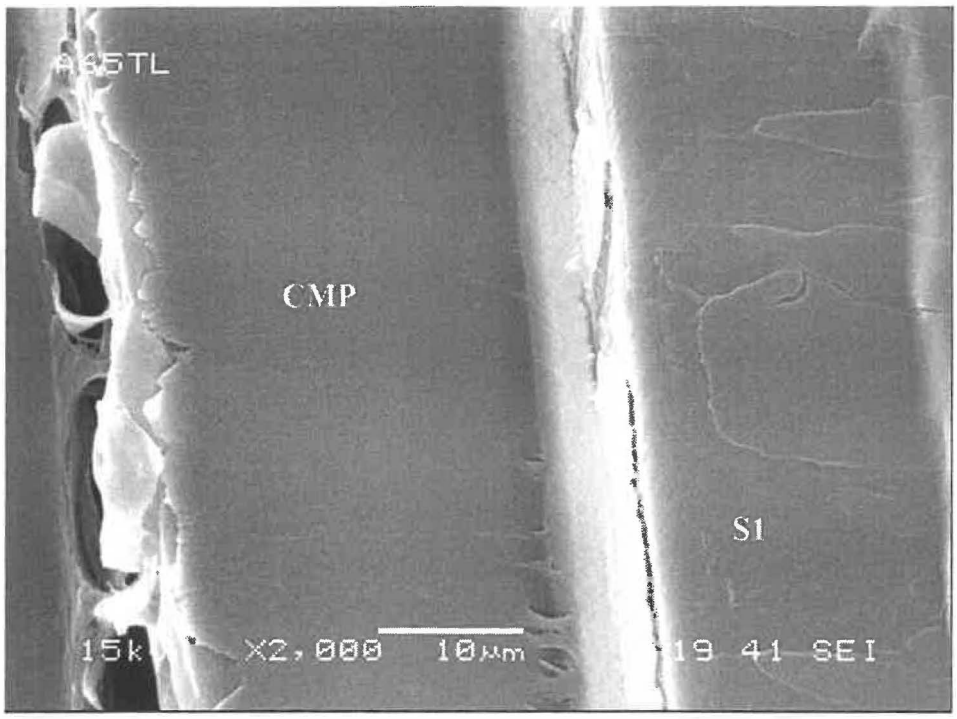

Figure 7.25 Tangential fracture surface of sample compressed to 65% at 22 °C. Some fibers are ruptured at cell corners and between cells.

7.3.2 Surface characteristics of sulfonated samples pre-compressed at 22°C (C4S)

Figure 7.26 to Figure 7.29 show the SEM micrographs of radial and tangential planes of uncompressed sulfonated samples. In radial plane, the fibers were separated in IC mode with a clean surface that is covered with intact CML. Little S_1 surface is exposed (Figure 7.26 and Figure 7.27). This is because, at high sulfonation level, the fibers tend to separate in the lignin-rich ML, exposing a more smooth fiber surface. On the tangential plane, the fibers also separated in the ML, but some broken fibers were also visible (Figure 7.28 and Figure 7.29). Similar observation was also reported by Johansson et al. [84].

For the sulfonated samples compressed to 65% strain, the fracture plane occurred across several layers of fibers (Figure 7.30). Fiber separation that occurred between middle lamellae and in the interface of P/ S_1 showed more exposed S_1 on the intact fiber surface

on radial plane(Figure 7.31, Figure 7.32). These properties indicate that radial compression introduces failures in the interface of P/S_1. The biggest difference was observed on tangential plane, where fibers were separated without significant damages (Figure 7.33). The fibers were separated with CML on the surface. The separated fibers were flattened readily without cut but with exposed S_1 and S_2 on the bending area (Figure 7.34, Figure 7.35). This indicates that pre-compression which collapsed fibers once renders fiber more flexibility although most fibers sprang back when the compression force was released.

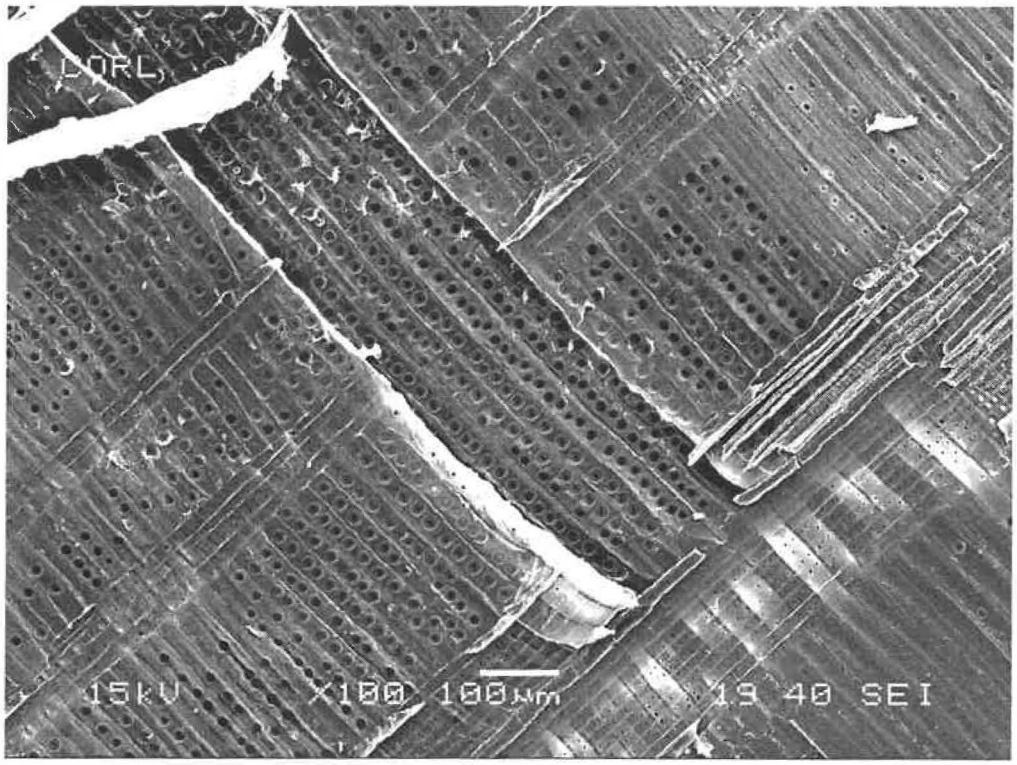

Figure 7.26 Radial fracture surface of uncompressed sulfonated sample. Fibers are separated in an inter-cell mode and remained intact.

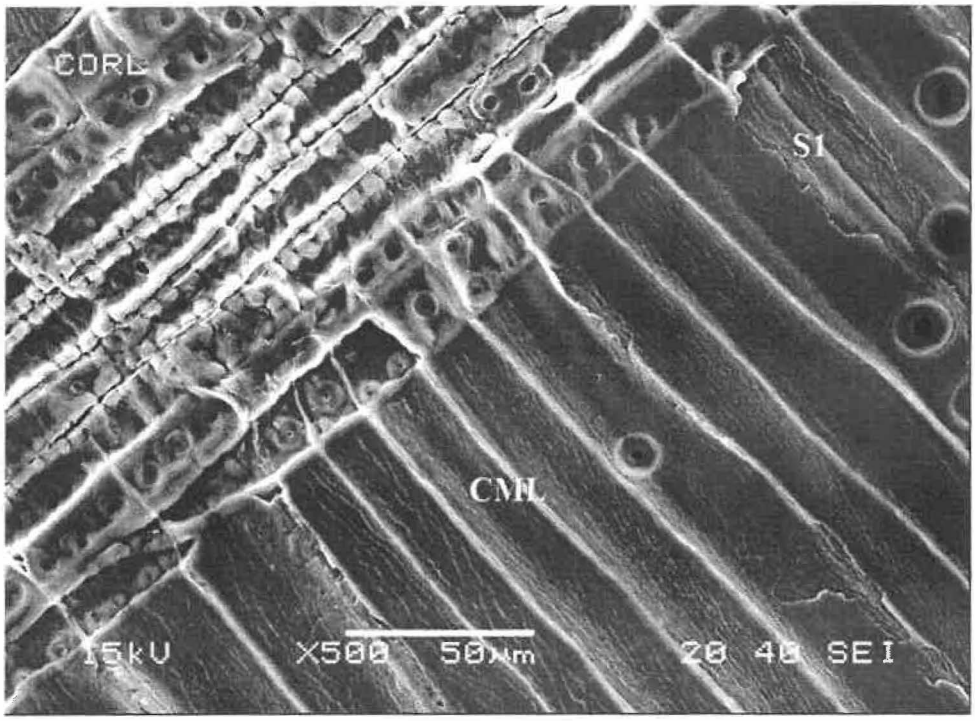

Figure 7.27 Radial fracture surface of uncompressed sulfonated sample. Fiber surfaces are covered with CML and very little exposed S_1.

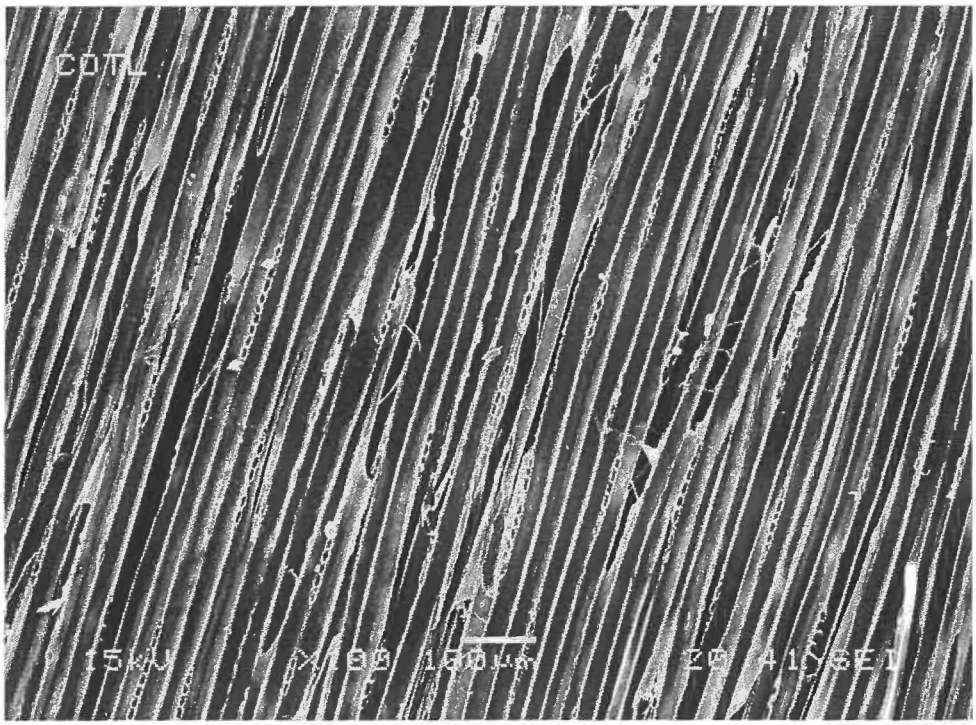

Figure 7.28 Tangential fracture surface of uncompressed sulfonated sample. Some fibers are broken.

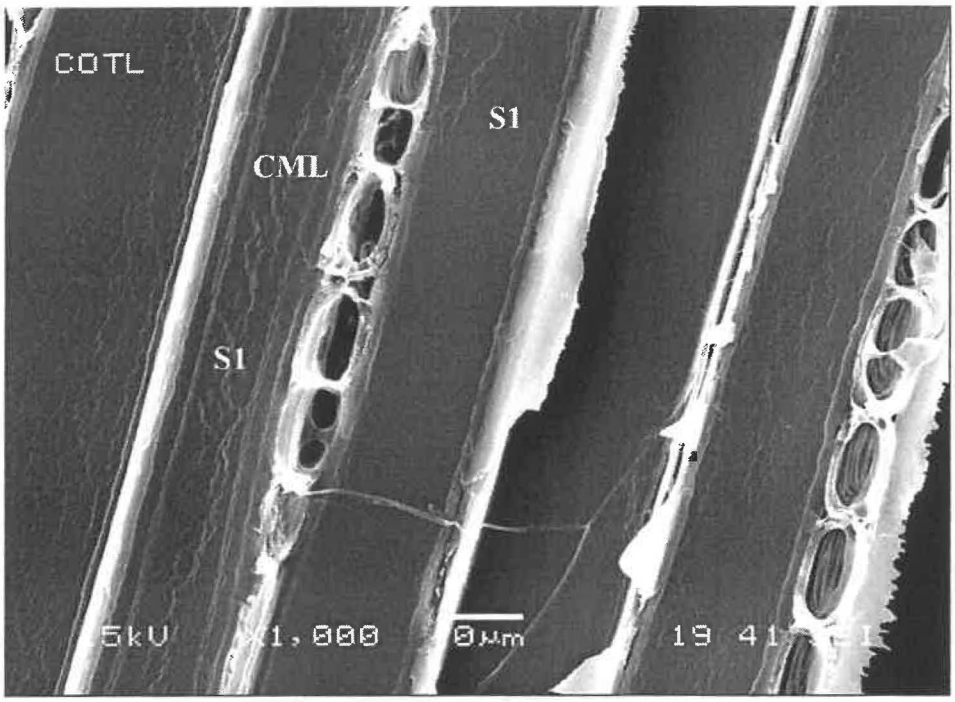

Figure 7.29 Tangential fracture surface of uncompressed sulfonated sample. Fiber surfaces are covered mostly by CML and S_1.

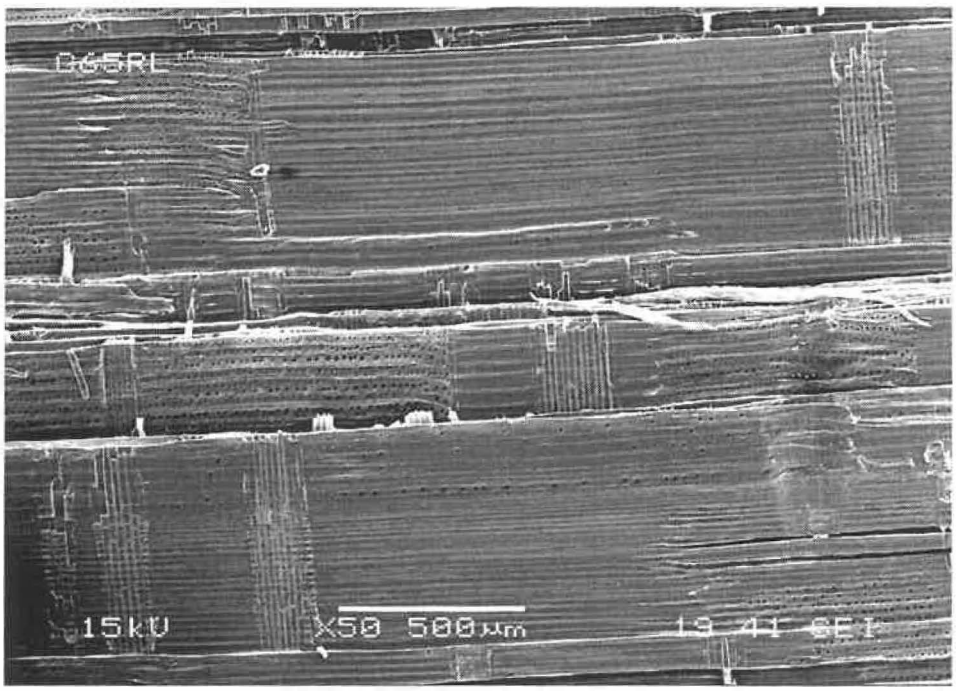

Figure 7.30 Radial fracture surface of sulfonated sample compressed to 65%. Fibers are separated in an inter-cell mode and remained intact. Fracture planes went across several layers of fibers.

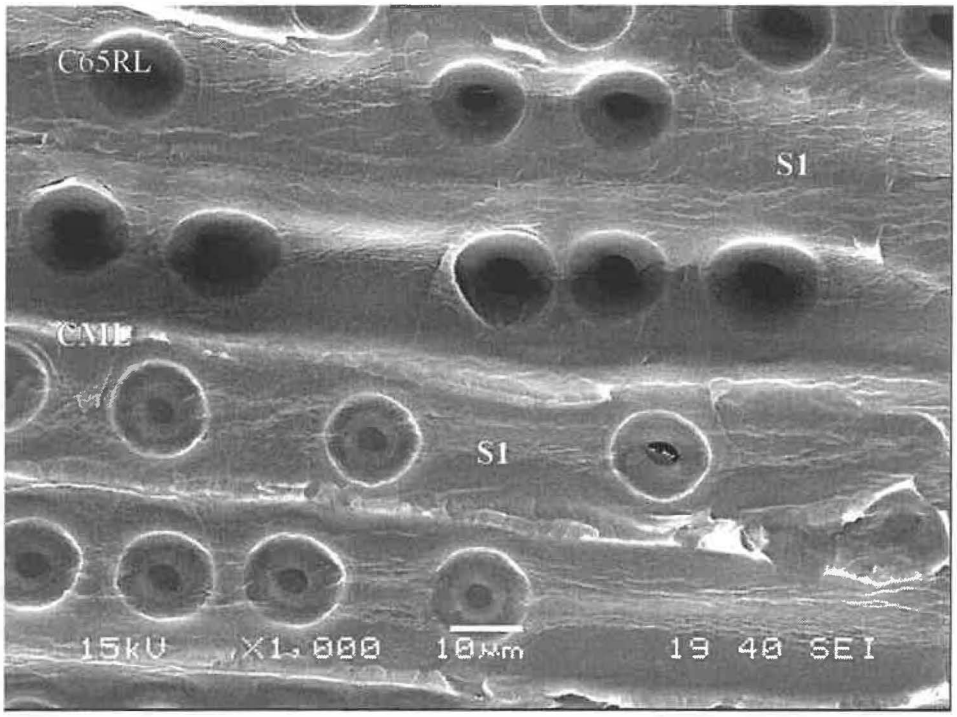

Figure 7.31 Radial fracture surface of sulfonated sample compressed to 65%. Separated fibers are covered with S_1.

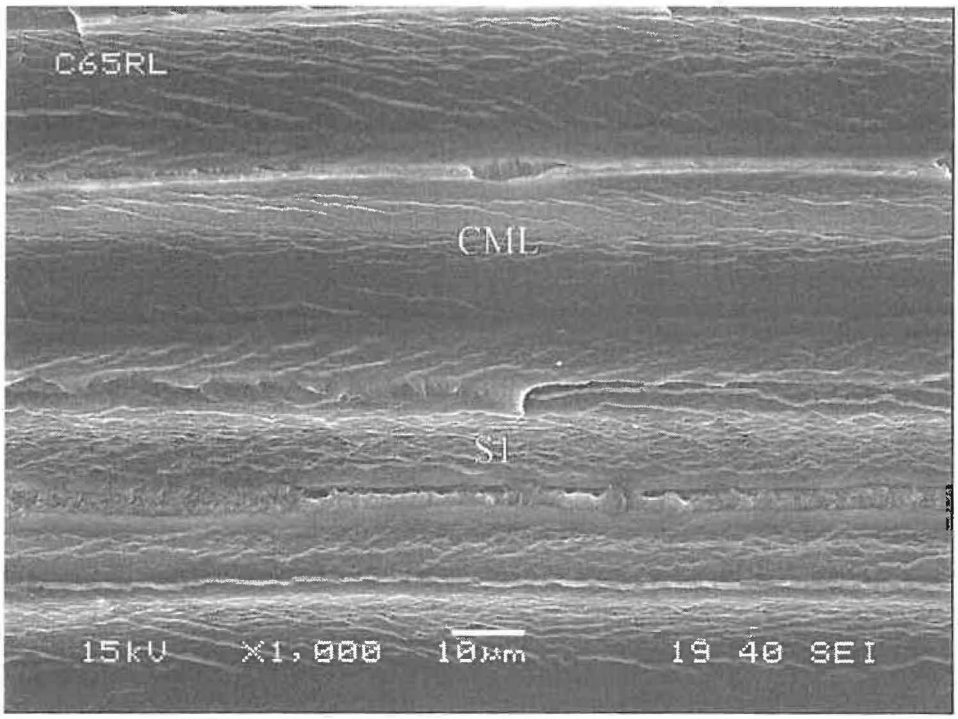

Figure 7.32 Radial fracture surface of sulfonated sample compressed to 65%. Separated fibers exposed CML and S_1.

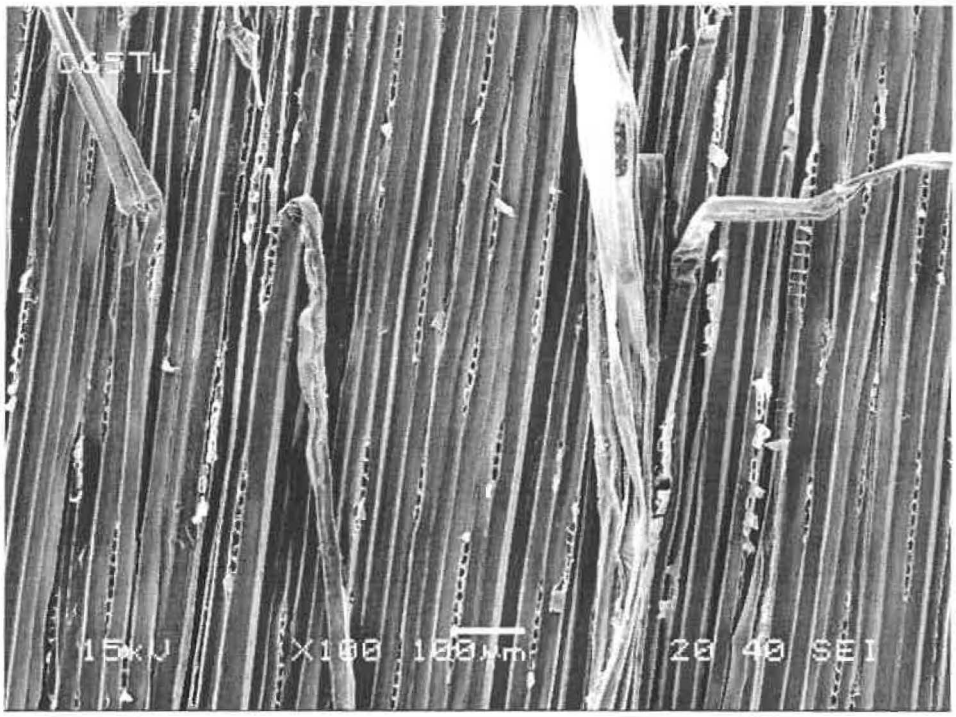

Figure 7.33 Tangential fracture surface of sulfonated sample compressed to 65%. Many fibers are separated readily with cut.

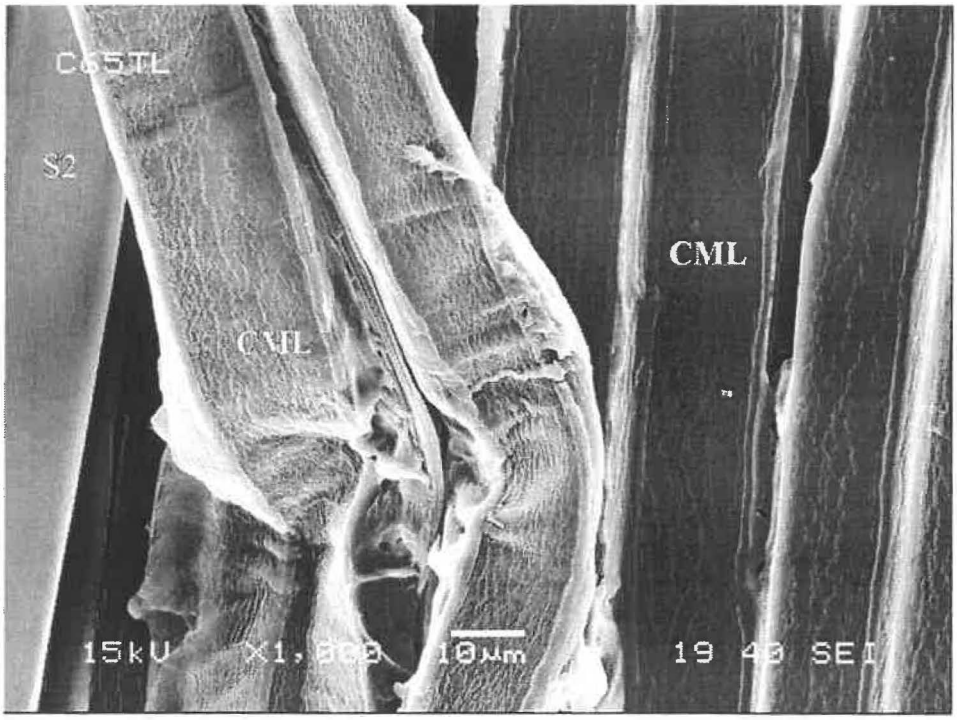

Figure 7.34 Tangential fracture surface of sulfonated sample compressed to 65%. Fibers are flattened easily under external forces without cut.

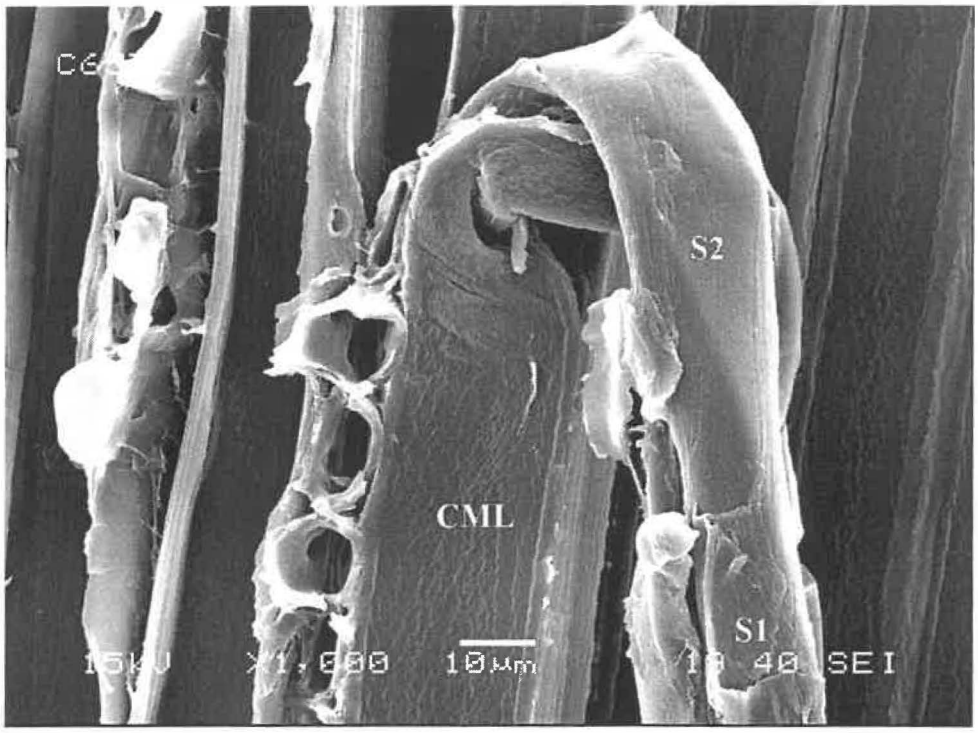

Figure 7.35 Tangential fracture surface of sulfonated sample compressed to 65%. Fibers are flattened without cut and have exposed S_2 in bend area.

7.3.3 Surface characteristics of sample pre-compressed to different strains at 120 °C (C3S)

Figure 7.36 to Figure 7.39 are the SEM micrographs showing the radial and tangential planes of uncompressed samples that were pre-heated at 120°C for 15 minutes. The EW fibers were extensively broken, but the LW fibers were mainly separated in the ML (Figure 7.36 and Figure 7.37). In some cases, the ML was slightly broken, exposing the S_1 (Figure 7.38). On tangential plane, the fibers were separated either in the ML or at the interface of P/ S_1 (Figure 7.39).

As the samples were pre-compressed at high temperature (120°C, 50% strain), more EW fibers remained intact in comparison with the uncompressed one (Figure 7.40). The separated EW fibers showed large area of S_2. These fibers are flattened readily and even folded without cut (Figure 7.41 and Figure 7.42). The LW fibers were separated both in

the ML and between the P/S_1 interfaces, exposing much more S_1 on the surface (Figure 7.43 and Figure 7.44). On tangential plane (Figure 7.45 and Figure 7.46), we noted that the pre-compression flattened fibers, and the broken CML layers were loosely attached onto the fiber surface or peeled off from the fiber surface exposing S_1. In some cases, the S_1 layer was completely stripped off exposing the S_2 layer.

For the samples pre-compressed to 65% strain at 120 °C, the degree of EW damage was smaller than that for the uncompressed ones but larger than that for those compressed to 50% strain (Figure 7.47). Some separated EW fibers with S_2 layer exposed collapsed readily without cut (Figure 7.48). A large difference was observed on the LW fibers compressed to 65% strain (120 °C) when compared to those compressed to 50% strain at the same temperature. In such case, most of CML was peeled off form fiber surface, exposing large area of S_1 layer (Figure 7.49). In many cases, the LW fibers were stripped away from the main wood matrix, leaving the CML sheath attached onto the surface of the adjacent fibers. The stripped LW fibers showed extensive area of S_2 layer (Figure 7.50 and Figure 7.51). This indicates that high strain compression has weakened in interface between CML/ S_1 and S_1/S_2 of the LW fibers. The LW fibers compressed to 65% strain behaved differently from those compressed to 50% strain, indicating that increasing compression strain form 50% to 65% has greatly modified the fiber wall of the LW fibers. On tangential plane, the extensive compression produced fibers with ridged surface (Figure 7.52); longitudinal cleavage was also observed (Figure 7.53), as shown in Figure 5.23. All these structural modifications of fiber wall could be attributed to the flattening, dislocation, lateral expansion, and rotation of fibers created by the high strain compression.

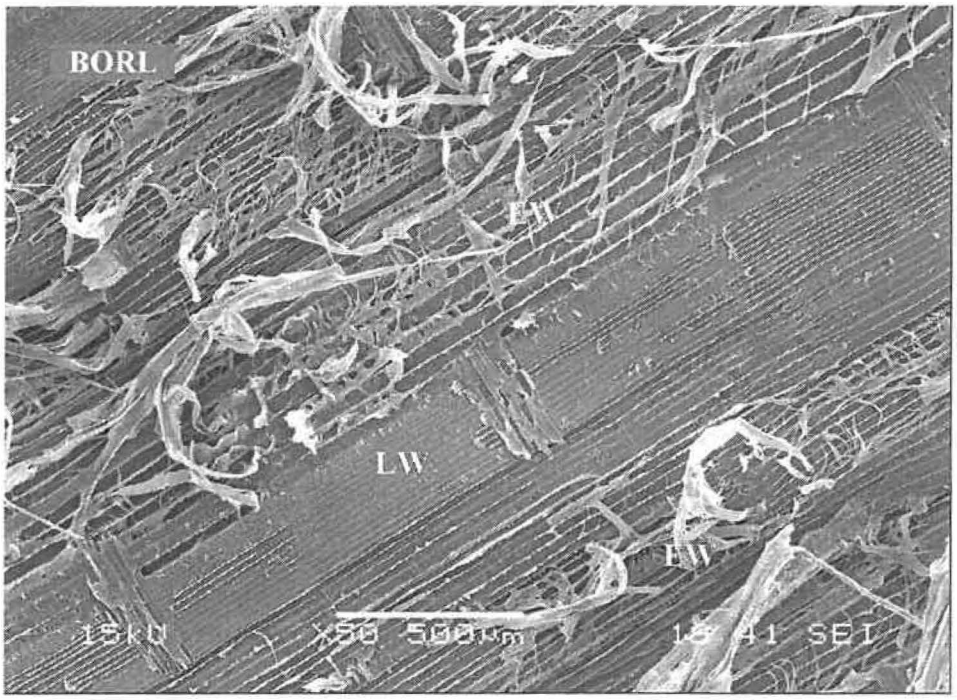

Figure 7.36 Radial fracture surface of uncompressed sample pretreated at 120°C for 15 minutes. Fibers are separated in inter-cell and trans-wall modes. The EW fibers are extensively broken.

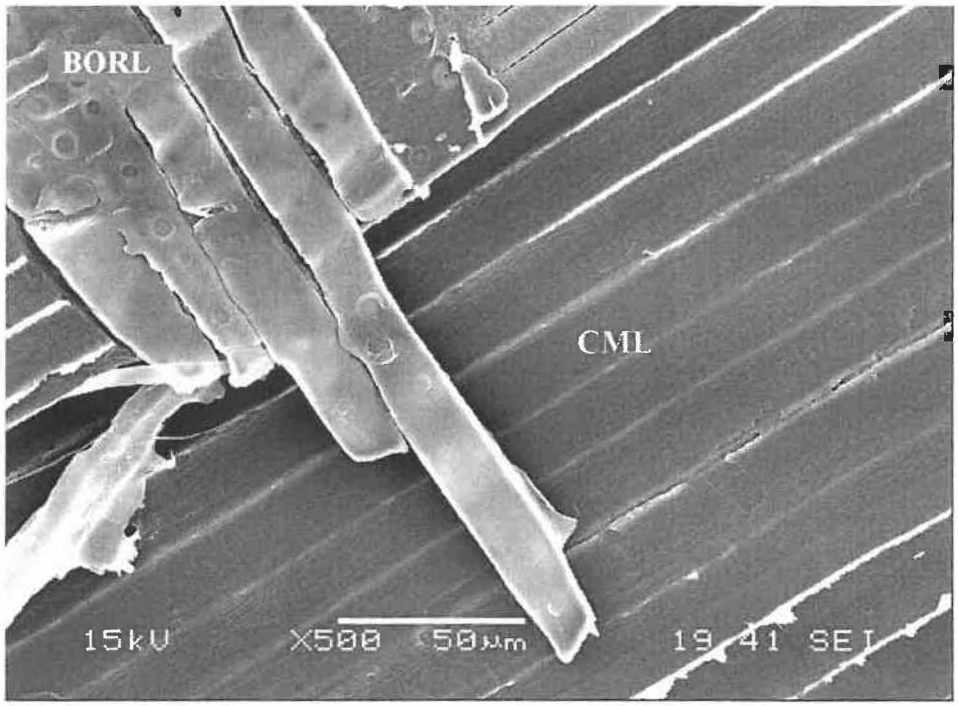

Figure 7.37 Radial fracture surface of uncompressed sample pretreated at 120°C for 15 minutes. The LW fibers remained intact with exposed CML.

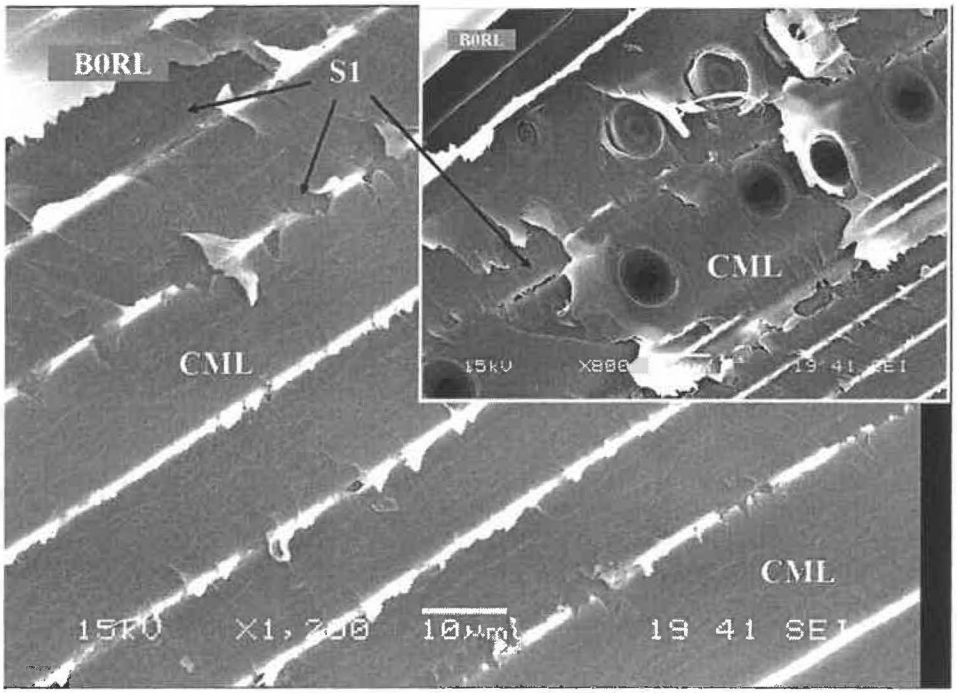

Figure 7.38 Radial fracture surface of uncompressed sample pretreated at 120°C for 15 minutes. The fibers remained intact with broken CML.

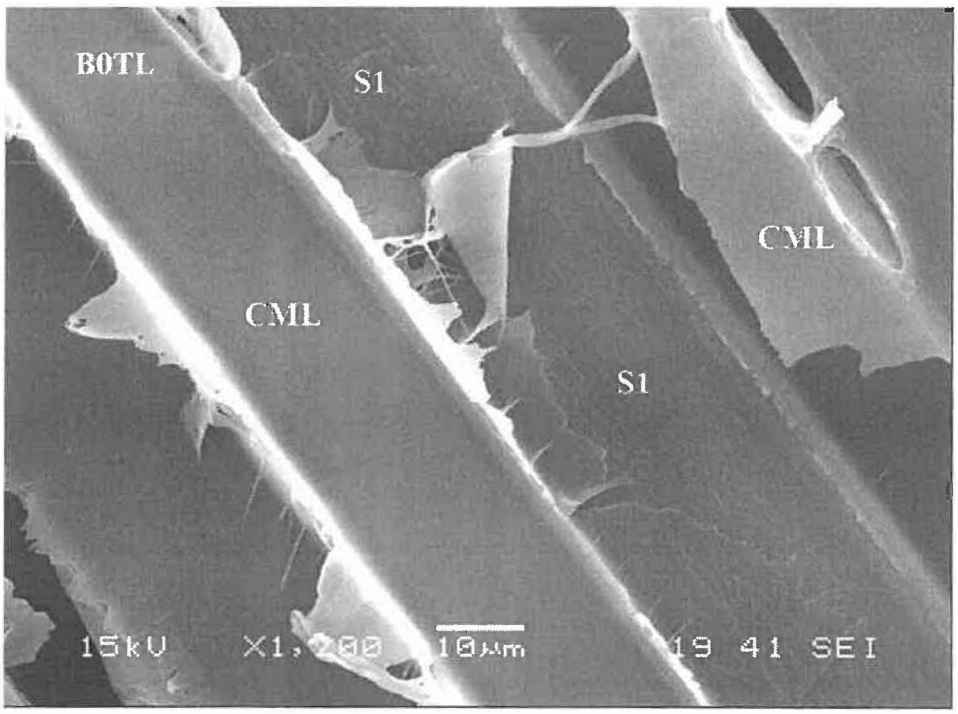

Figure 7.39 Tangential fracture surface of uncompressed sample pretreated at 120°C for 15 minutes. The fibers remained intact with exposed S_1 in some places.

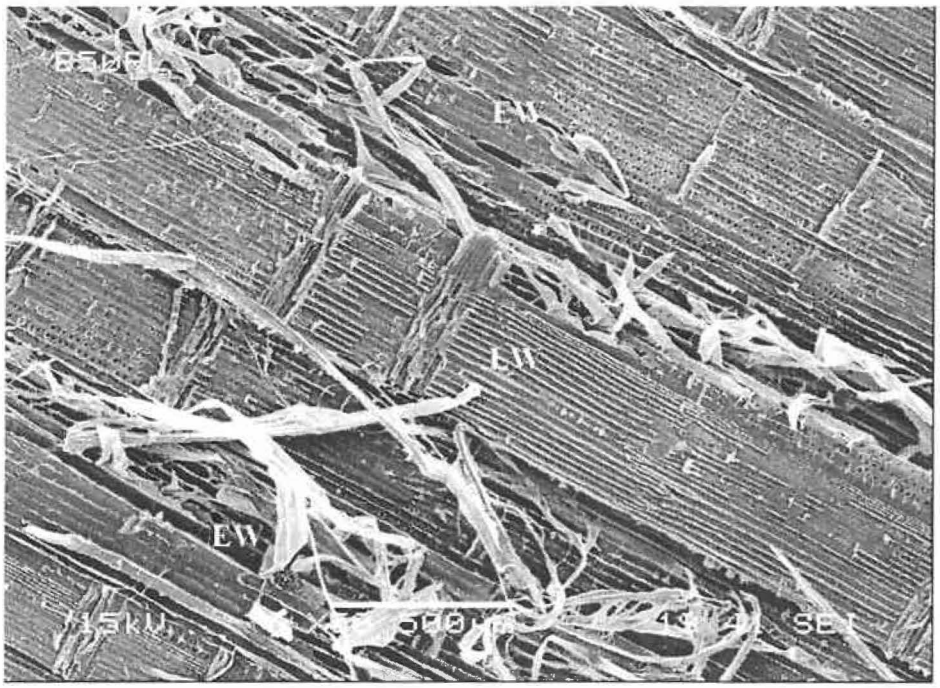

Figure 7.40 Radial fracture surface of sample compressed to 50% at 120°C. Most fibers are separated in inter-cell mode. The EW fibers are broken in some places.

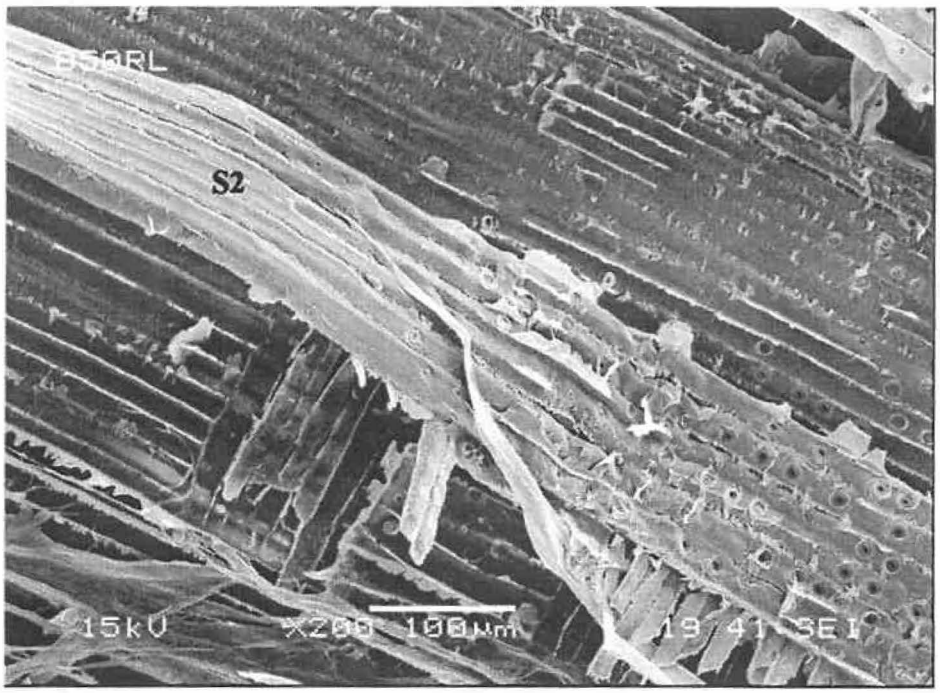

Figure 7.41 Radial fracture surface of sample compressed to 50% at 120°C. Layers of EW fibers with exposed S_2 are separated between the ray cells and tracheids.

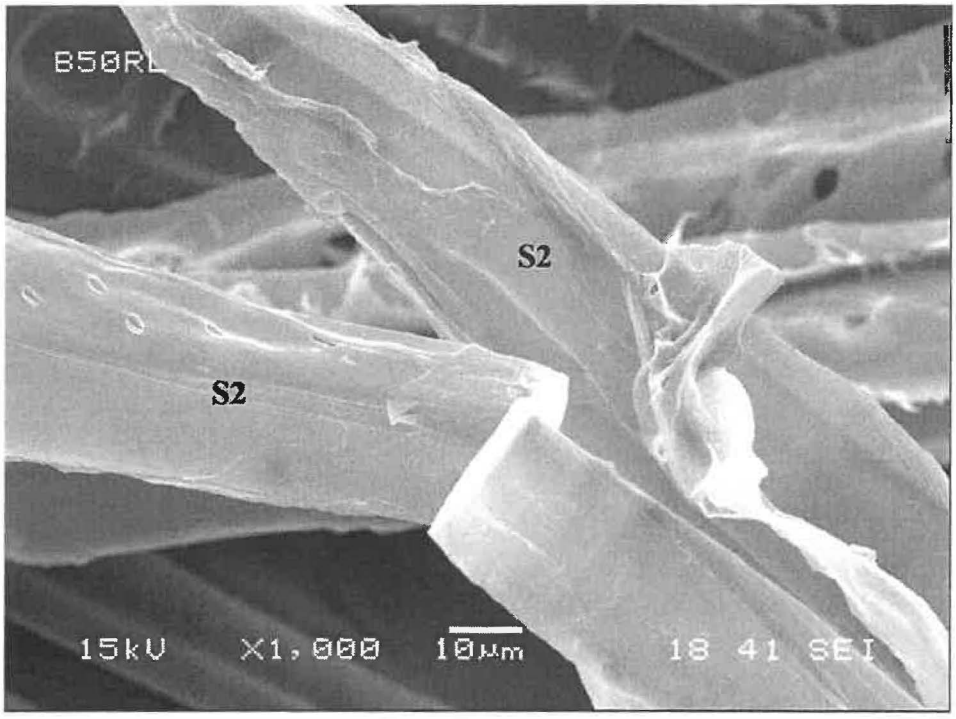

Figure 7.42 Radial fracture surface of sample compressed to 50% at 120°C. The separated EW fibers are flattened with exposing S_2.

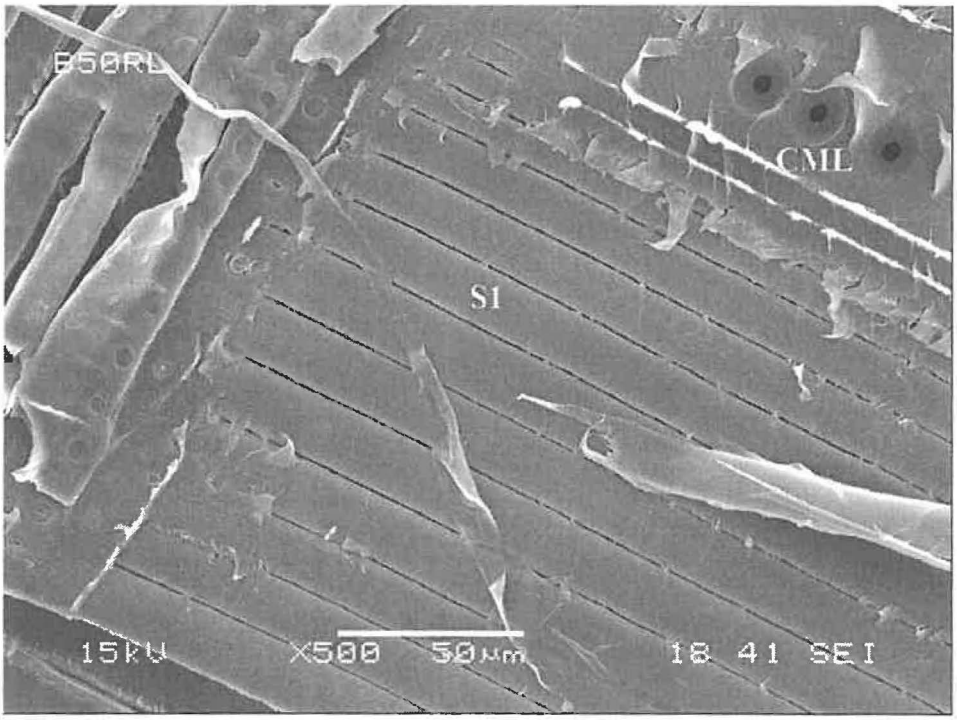

Figure 7.43 Radial fracture surface of sample compressed to 50% at 120°C. The LW fibers are covered with S_1 and CML.

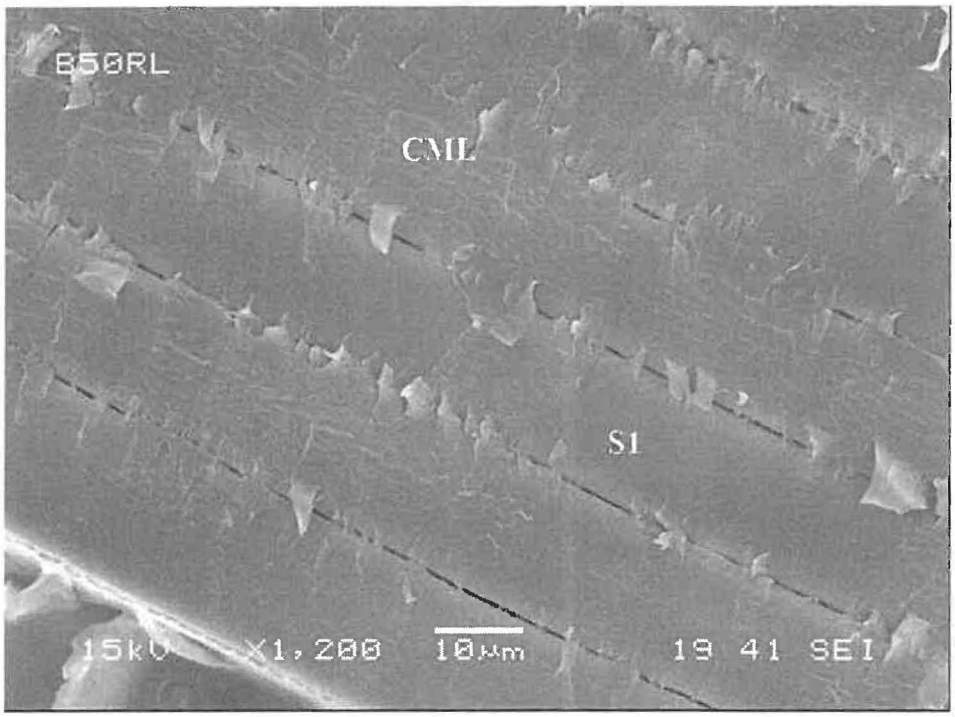

Figure 7.44 Radial fracture surface of sample compressed to 50% at 120°C. The LW fibers are covered with S_1 and broken CML.

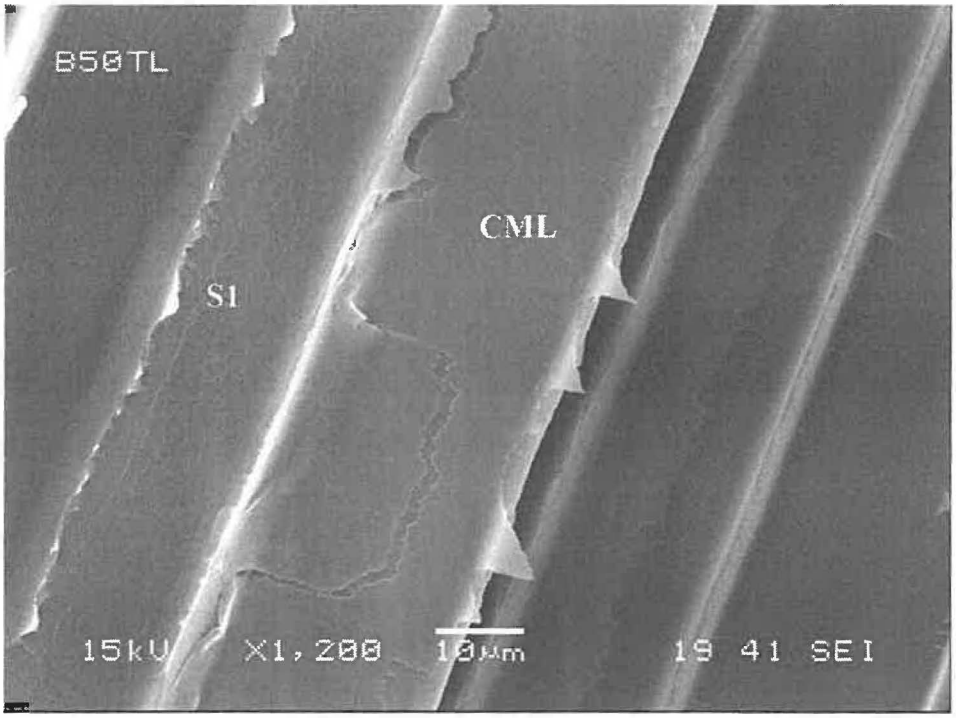

Figure 7.45 Tangential fracture surface of sample compressed to 50% at 120°C. The EW fibers are covered with S_1 and broken CML.

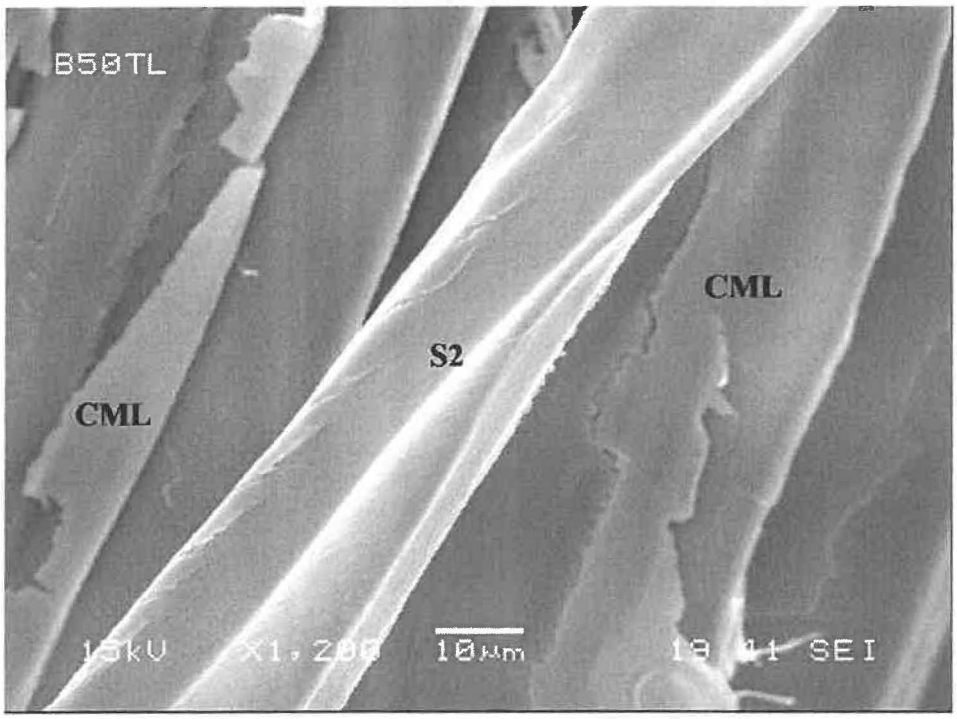

Figure 7.46 Tangential fracture surface of sample compressed to 50% at 120°C. The EW fibers are covered with broken CML or S_2.

Figure 7.47 Radial fracture surface of sample compressed to 65% at 120°C. Most fibers are separated either in inter-cell and trans-wall mode.

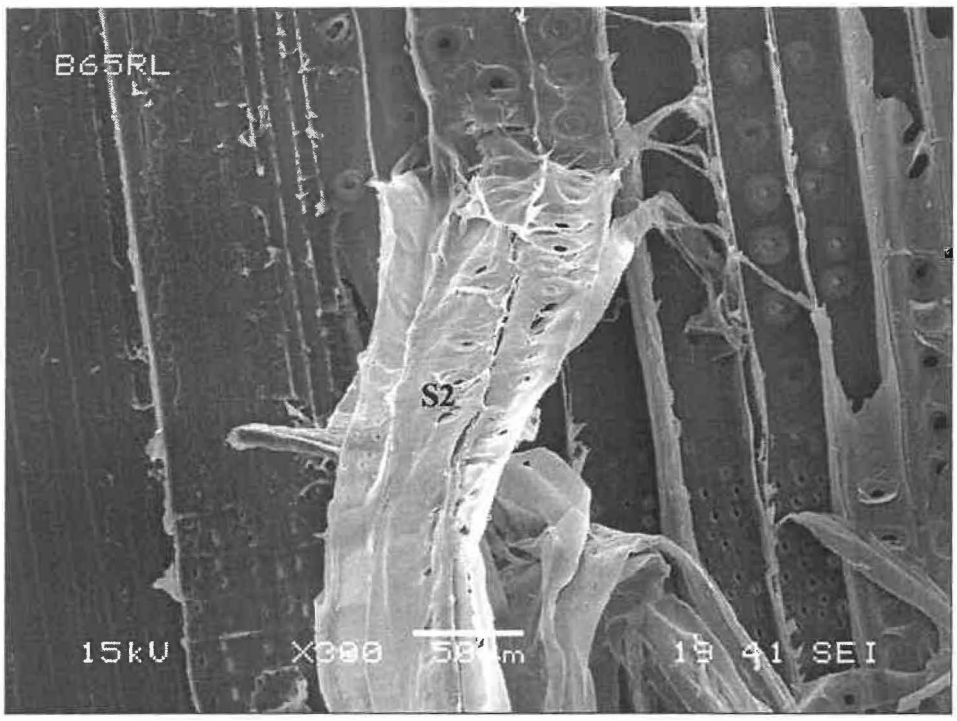

Figure 7.48 Radial fracture surface of sample compressed to 65% at 120°C. Layers of EW fibers separated with S_2 exposed are collapsed.

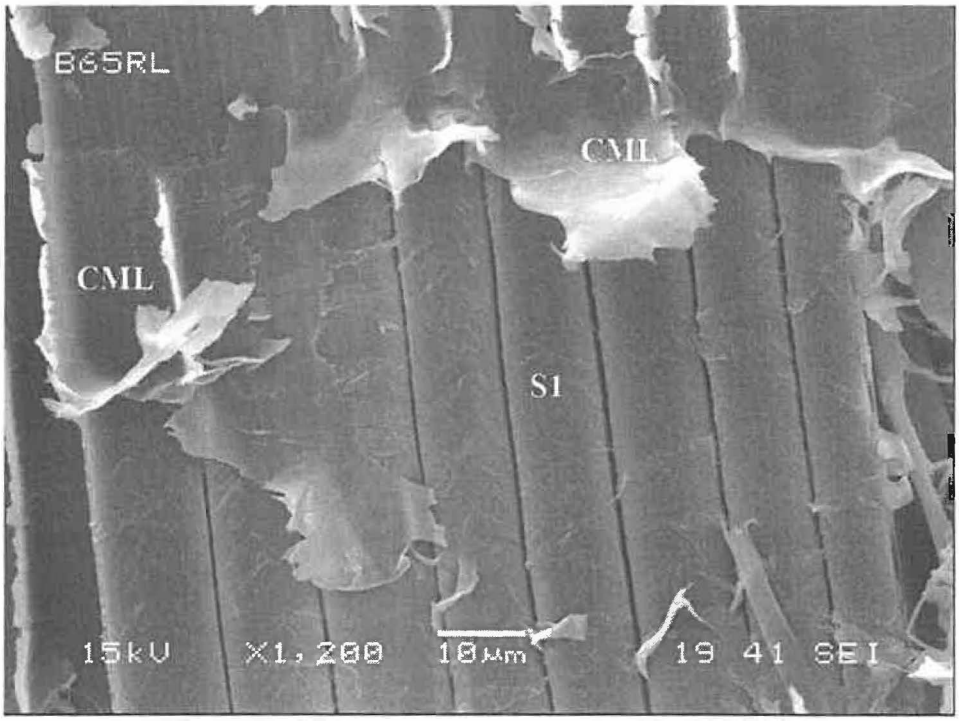

Figure 7.49 Radial fracture surface of sample compressed to 65% at 120°C. The LW fibers with S_1 exposed and CML loosely attached.

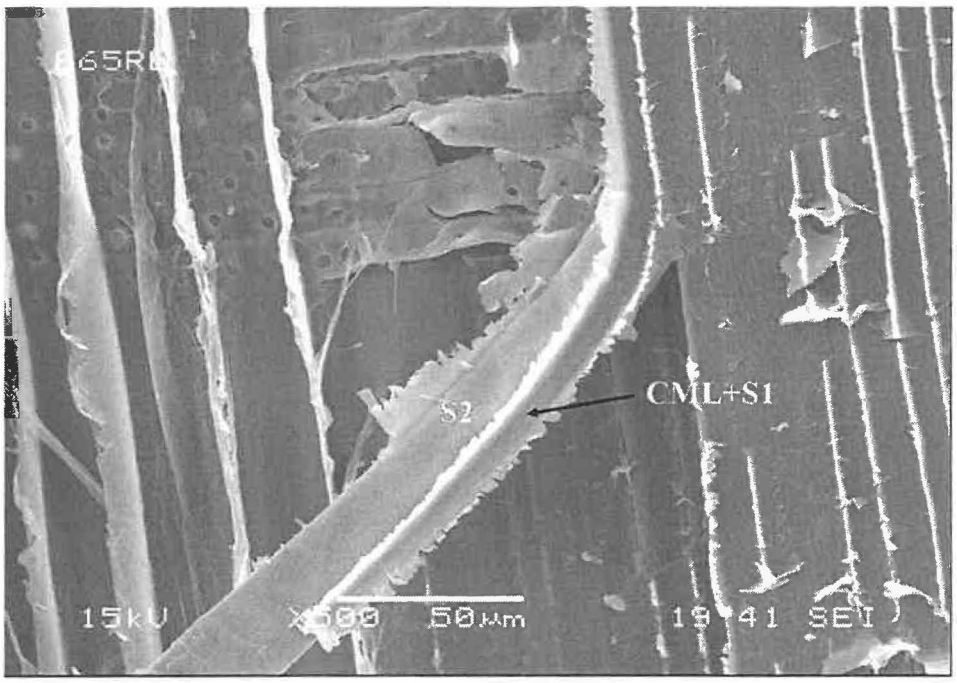

Figure 7.50 Radial fracture surface of sample compressed to 65% at 120°C. The LW fibers are separated from the wood matrix exposing S_2 and CML.

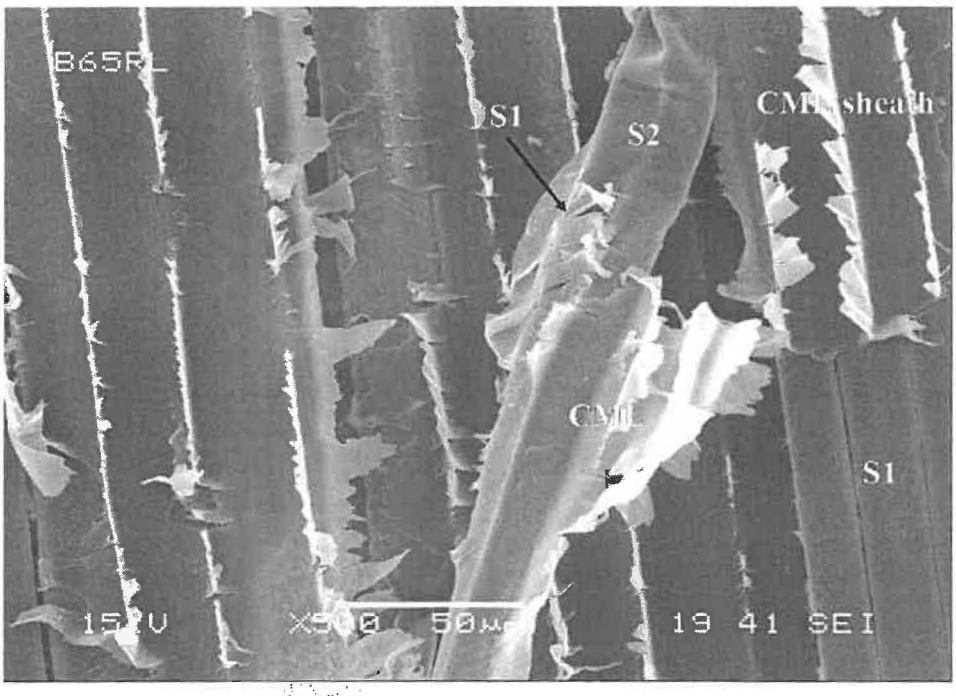

Figure 7.51 Radial fracture surface of sample compressed to 65% at 120°C. The LW fibers are flattened and separated fiber with exposing S_2, or S_1+CML loosely attached.

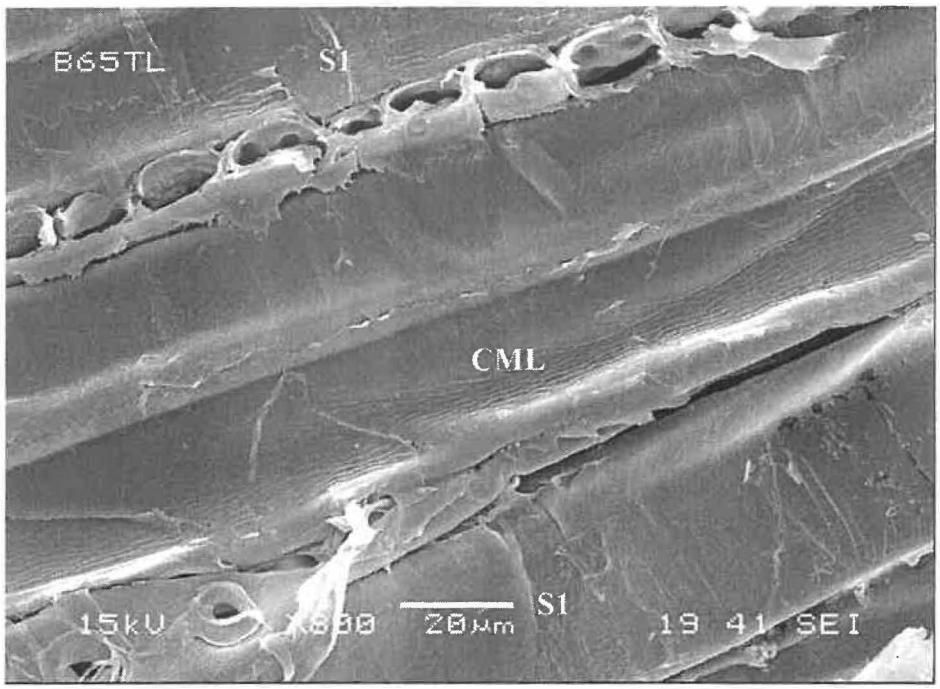

Figure 7.52 Tangential fracture surface of sample compressed to 65% at 120°C. The fibers are partly separated in inter-cell mode with buckled fiber wall.

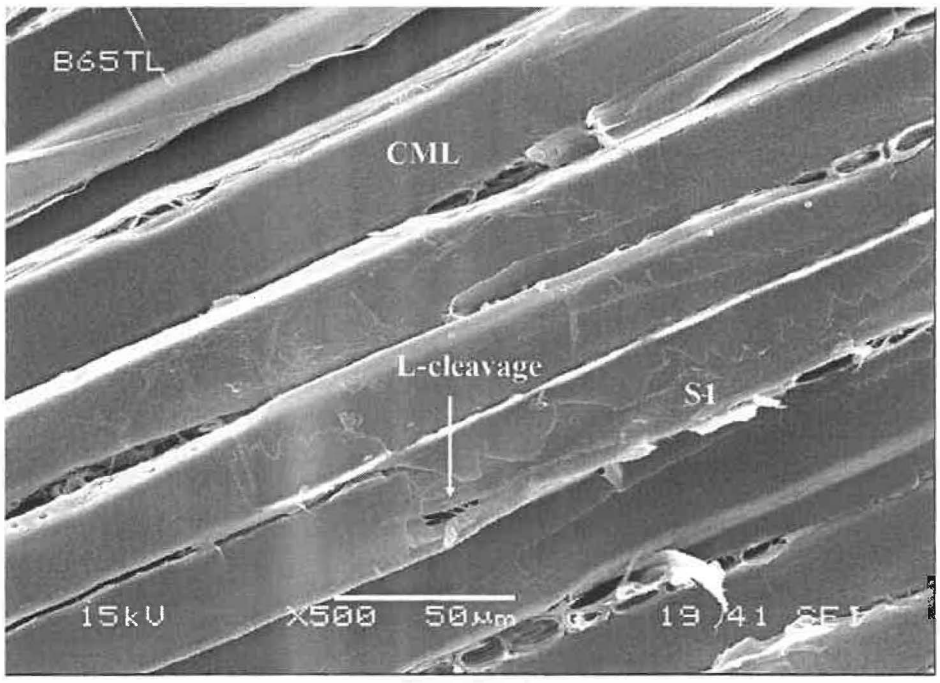

Figure 7.53 Tangential fracture surface of sample compressed to 65% at 120°C. The fibers are partly separated in inter-cell mode, exhibiting longitudinal cleavage in fiber wall.

In summary, fiber separation in the ML is common in the sulfonated and preheated samples without pre-compression. The separated fibers remain intact exposing little S_1 layer. However, extensively damaged EW fibers are evident in the samples preheated at 120 °C for 15 minutes.

For the pre-compressed samples, the effects of compression are largely determined by the pre-compression conditions. For the sulfonated samples, fiber separation still takes place in the ML, but produces much more S_1 layer on the surface. Sulfonation renders the fibers more flexible and more collapsible preventing fibers being cut under stress. Low temperature pre-compression facilitates trans-wall (TW) separation mode, and frequently creates fibers separation between S_1/S_2 and within S_2. On the other hand, high temperature pre-compression reduces damages to the EW fibers, and greatly modifies LW fibers. The LW fibers are separated typically between the P/S_1. In some instances, the LW fibers are stripped away from the main wood matrix, leaving the $CML+S_1$ sheath attached onto the adjacent fibers. High strain compression also generates longitudinal cleavages. The combined effect of high strain and high temperature weakened the S_1/S_2 interface and within S_2 in LW fibers.

The pre-compression strain also plays an important role in modifying the structure of wood fiber, especially the LW fibers. However, the LW fibers experience structural changes only when a compression strain of greater than 50% is applied. Hence, in mechanical pulping, a high compression ratio should be used to effectively modify the LW fibers. The important influence of high strain compression on the shear properties of wood has been discussed earlier in section 7.2.

7.4 Effect of pre-compression in relation to refining

An earlier study on the effect of chip compression in TMP [57] indicated that the pre-compressed chips produced TMP (100-200 ml CSF) with 18-25% less specific energy consumption when compared with the untreated chips. Long fiber content, tensile index and TEA are also considerably increased. The influence of compression on the physical properties of wood in relation to refining has been discussed in section 5.2.7. Microscopic observation reveals that these improvements may also attribute to following four possible aspects on microstructure modifications:

First, high strain compression loosens the wood matrix and facilitates fiber separation in subsequent refining. Second, due to the distinct difference in fibril orientation between P/S_1 and S_1/S_2, compression weakens particularly these interfaces, as shown in Figure 7.54. Further, owning to the extreme buckling of the radial wall (S_2) in high-strain compression, the linkages between micro-fibrils may also be disrupted because of the micro-slips created by high strain compression (Figure 7.55). These structural changes produce longitudinal cleavage or delamination of the S_2 layer. The latter mode of failure facilitates the development of fiber property (external and internal fibrillations) in refining. Finally, despite the possible spring-back of the fibers after compression, the once-collapsed fibers become much more flexible and collapsible in the refiner. This nature of fiber might greatly reduce the effect of fiber cutting in subsequent treatments, decrease refining energy and improve pulp properties.

Research [113] indicated that keeping all other parameters constant, a reduction in wall thickness or and increase in fiber splitting reduces surface roughness and increase the light-scattering coefficient. Moreover, the presence of micro-cracks in the fiber surface layers largely influence the bonding ability of fibers [112]. However, a usual TMP contains a high portion of un-collapsed fibers, and low amount of split fibers (10-15%). The latter proportion is much inferior to that in groundwood, 40-50%. The un-collapsed and un-split fibers are responsible for the increased roughness of paper made from mechanical fibers. To improve sheet smoothness and bonding ability, it is necessary to reduce the proportion of un-collapsed fibers and increase fiber splitting by means of

high strain compression prior to refining the chips. However, further research is needed to fully exploit the benefits of pre-compression.

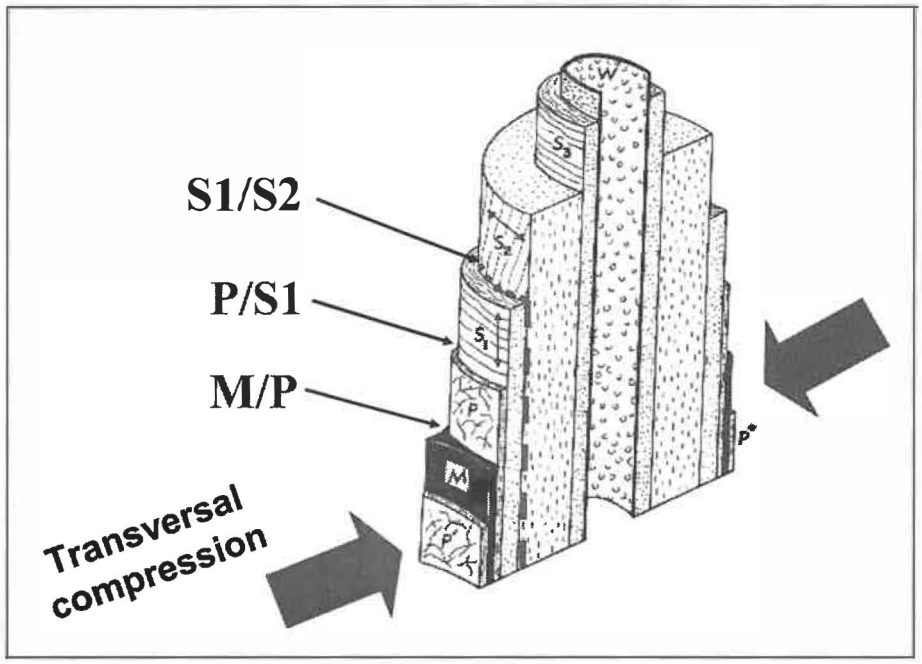

Figure 7.54 Effect of static compression on the interfaces of fiber layers

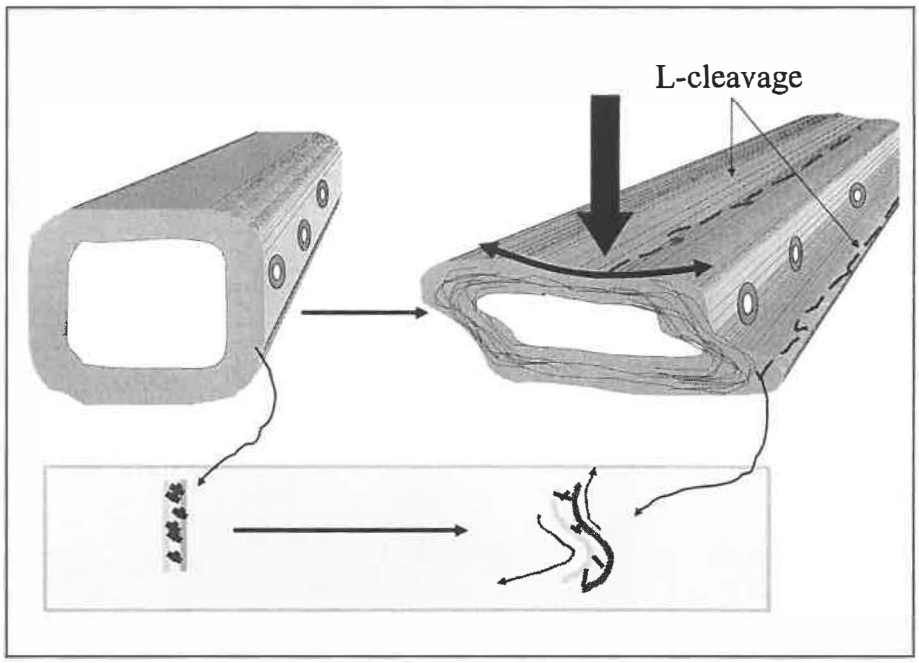

Figure 7.55 Effect of transversal compression on delamination of S_2 layer and longitudinal cleavage of fibers

7.5 Concluding remarks on this part

The degree of permanent deformation of sample blocks caused by transversal compression is affected by the compression temperature and sulfonation content. It is noted that compression at 80°C produces the greatest permanent deformation when compared to other temperatures. Sulfonated specimens have the lowest permanent deformation.

Generally, radial compression has little effect on shear properties when the compression strain is less than 50%. Beyond this compression strain the shear properties fall sharply, indicating significant structural damages in both early- and latewood. The pre-compression conditions have significant influence on the shear characteristics of wood; the sulfonation being the most significant. However, in all the cases, shear properties of wood specimens are closely associated with the specific compression energy consumed by the specimens in the pre-compression processes.

High-strain compression modifies a wood block in four possible levels: loosening the wood matrix; weakening the locations between different layers (P/ S_1, S_1/ S_2); disrupting the linkages between micro-fibrils within the S_2 layer; and flexibilizing fibers. However, the conditions of pre-compression also play an important role in determining the nature of structural failures. For example, low temperature compression promotes failures between S_1/S_2 and within the S_2 layer, while high temperature (120°C) combined with high strain (higher than 50%) favors the modification of LW fibers. All these effects of pre-compression may lead to savings in refining energy and improvement on pulp properties.

The shear technique developed in this investigation can be satisfactory used to quantify the structural weakening of a wood matrix produced by static radial compression, and could be a good method in evaluation of wood weakening under similar compressions such as cyclic compression and fatigue process.

Chapter 8 - Conclusions

Wood responses similarly in both radial and tangential compressions, regardless of compression temperature. It exhibits an elastic deformation followed by an elastoplastic and a densification (fracturing) stages. However, it behaves differently in longitudinal compression.

The compression temperature greatly affects the compression energy. A single compression of large strain (70%) requires, respectively, 3.5-4.9 kWh/t and 0.6-0.7 kWh/t at 22°C and 120°C. These energies represent only 0.2% and 0.03% of the total specific energy consumption in a typical TMP.

The compression modulus, the first and second plateau stresses, and the specific compression energy have been used to characterize the behaviors of wood under compression at different stages. Among them, the second plateau stress was defined and used for the first time to describe the fiber separation at densification stage. The relationships between these four parameters and the temperature follow the Arrhenius' Law for compressions in radial, tangential and longitudinal directions, meaning that the effect of thermal softening can be explained by the motion of polymer chain of the wood main components.

For radial and tangential compressions, the normalized compression curves obtained at various temperatures fit into one unique curve that can be used to characterize the elastic and elastoplastic regions. The resulting curve indicates the predominant influence of the tubular structure of fibers upon the behaviors of wood in these two regions. However, the temperature influences the behaviors of wood in the densification region.

The following general mathematic models are developed to express the stress in the elastoplastic region in radial and tangential compressions:

$$\sigma_r = 0.0173 \times e^{1544.2/T} \times \left[1 + 0.5112 \times \left(\frac{0.5}{0.58 - \varepsilon} - 1 \right)^{1.0297} \right]$$

$$\sigma_t = 0.0141 \times e^{1652.8/T} \times \left[1 + 0.2322 \times \left(\frac{0.5}{0.58 - \varepsilon} - 1 \right)^{1.3598} \right]$$

The model consists of two independent factors - the temperature and strain factors. A similar model for sulfonated sample was also obtained. These models were used for the first time to predict the resistance of EW fibers at various temperatures. According these models, the compressive stress required to flatten the EW fibers under refining conditions is about 0.62-1.53 MPa. This stress is much higher than the average stress between two refiner bars (0.45 MPa). This may explain the high-energy consumption in refining. However, the high strain pre-compression (70% strain), which flatten wood fibers and create fiber separation, could reduce the fiber transverse resistance by 70-85%. Therefore, in subsequent refining of the pre-compressed chips, an average compressive force of 0.45 MPa will readily flatten most of these fibers. This approach may potentially change the refining process from a fatigue process to a more efficient breakdown process.

In sulfonation, the temperature is by far the most influential factor on the level of sulfonation. Despite their differences in morphological characteristics, the EW and LW fibers are sulfonated to similar sulfonate content, under the same conditions. When the EW and LW are compressed separately they response differently. The EW samples exhibit a prolonged plastic plateau, indicating the collapse and the significant lateral displacement of the EW fibers. On the other hand, the LW does not show a distinct primary plastic plateau, suggesting that the LW fibers collapse gradually in contrast to the EW fibers

Sulfonation decreases the physical properties such as modulus, specific compression energy, stress in the primary and the secondary plastic zones. However, there is no fundamental change in the form of the compression curve when the sample blocks contain both the EW and LW, regardless of the sulfonate content.

The normalized stress-strain curves for the sulfonated samples and those for samples compressed at various temperatures can fit into one single curve in the elastic and elastoplastic regions. These relations might suggest that the compression behaviors of

wood in these regions are independent of wood properties. The elastic response and the plastic collapse of fibers are mainly dependent on the cellular structure of wood fiber. Increasing the compression temperature or sulfonate content decreases all these physical properties. However, the mechanism of softening is different: thermal softening is a reversible effect due to the movement of polymer chains of all wood components. The relationships between the physical properties and temperature follow Arrhenius' law. In contrast, sulfonation is an irreversible chemical modification of the wood components, particularly the lignin. The physical properties of wood decrease linearly with increasing sulfonate content.

A systematic analysis of the results obtained from the comparison of sulfonated samples with and without restraint indicates that wood responses similarly when the compression was conducted at strain less than 50%. Thus, the samples have similar modulus of elastic (MOE) and first plateau stress (SP1). However, when the compression strain exceeded 50%, the samples behave differently exhibiting significant lateral expansion of the wood matrix. When the compression was carried out without restraint, a second short plateau occurred at about 60% strain. At this stage, fiber separation happened due to the excessive lateral expansion. Beyond 60% strain, the stress increases again with increasing compression strain. The modulus (MOE2) at this stage decreases linearly with the increase of sulfonate content. In the case of compression with restraint, there is no second plateau. The stress increases rapidly in the densification region. The modulus for this zone is independent of the sulfonate content, and is controlled by the restraint.

Shearing tests on pre-compressed samples indicated that low strain (<50%) radial compression has little effect on the shear properties (shear modulus, shear maximum stress, shear yield stress, shear yield energy, total shear energy). Compression with strain above 50% greatly reduces the shear properties, indicating significant structural damages in both EW and LW.

The pre-compression conditions (temperature and sulfonation) have significant influence on the shear characteristics; the sulfonation content being the most important. However, in all cases, the change of shear properties such as shear modulus, shear yield

stress, maximum stress, and yield energy of wood is closely associated with the specific compression energy spent in the pre-compression processes.

Under radial and tangential compression, wood behaves similarly. The transverse compression creates longitudinal cleavage of fibers. High-strain (>50%) radial compression modifies the wood matrix in four aspects: loosening the wood matrix; weakening the interfaces of P/S_1 and S_1/S_2); disrupting the linkages between micro-fibrils within S_2 layer; and flexibilizing fibers. However, pre-compression conditions also influence the nature of structural failures; compression at low temperature benefits fiber failure between S_1/S_2 and delamination of the S_2 layer. Compression with high compression strain (>50%) (120°C) favors structural modification of LW fibers at high temperature.

The shear technique developed in this investigation can be satisfactory used to quantify the structural weakening of a wood matrix caused by static radial compression, and could be a useful method for characterizing structural damages in wood pretreated at compressions such as cyclic compression and fatigue process.

This study suggests that static compression with large strain (>50%) modifies wood block in two aspects: first, it flattens the wood fibers, greatly decreases the fiber's transverse resistance. Second, it modifies fiber's microstructure at different levels, which may pre-set a more favorite fiber separation mode and fiber development process, rendering the wood more suitable for further processing into a mechanical pulp with improved quality. All these may potentially change the refining process from a fatigue process to a more efficient breakdown process, and finally result in pulp quality improvements and energy saving in refining.

BIBLIOGRAPHY

1. Adrian J.B., "The 24th Leask Survey: Equipment Sales Tailed Off but There Has Been A Rebound in 2001", Pulp and Paper Canada, 102(4):10-17 (2001).

2. Anonymous. Annual Review, Pulp and Paper International, Vol. 32-42, (July, 1989-2002).

3. Yuan, Z., Mcgarry, P., Schmidt, J., Heitner, C., Cunkle, G., Seltzer, R., Wolf, J. -P., Fairbank, M., "Application of Yellowing Inhibitors to Mechanical Papers Using a Pilot Liquid Application System", of 87th Annual Meeting, PAPTAC, Book C: C43-C52 (2001).

4. Sundholm, J., "Can We Reduce Energy Consumption in Mechanical Pulping?", Intl. Mech. Pulp. Conf., Oslo, Norway, p. 133-142 (1993).

5. Sundholm, J., "Mechanical Pulping", Papermaking Science and Technology, Book 5, p. 20, Fapet Oy, Finland (1999).

6. Page, D.H., "The Beating of Chemical Pulps—The Action and the Effects", Transaction of the Ninth Fundamental Research Symposium, Cambridge, U.K., September 1989, Mechanical Engineering Publication Ltd. London, Vol.1 p.1-38 (1989).

7. Atack, D., Stationwala, M. I., Karnis, A., "What Happens in Refining", Intl. Mech. Pulp. Conf., Washington, USA, p. 115-130 (1983).

8. Karnis, A., Atack, D., Stationwala, M. I., "What Happens in Refining (Part II)", Intl. Mech. Pulp. Conf., Stockholm, Sweden, p. 35-45 (1985).

9. Pearson, A.J., "Towards A Unified Theory of Mechanical Pulping and refining", Intl. Mech. Pulp. Conf., Washington, USA, p. 131-138 (1983).

10. Karnis, A., "The Mechanism of Fiber Development in Mechanical Pulping", J. Pulp and Paper Science 20(10): J280-J288 (1994).

11. Petit-Conil, M., Robert, A., Pierrard, J. M., "Fundamental Principles of Mechanical Pulping from Softwoods and Hardwoods", Cellulose Chem. Technology, 31:93-104 (1997).

12. Steenberg, B., "A Model of Refining as a Special Case of Milling", Intl. Symposium on Fundamental Concepts of Refining, Appleton, USA, p. 16-18 (1980).

13. Barnet, A.J., "The 21st Annual Leask Survey: "World Refiner Capacity now at 104, 162 Tonnes A Day", Pulp and Paper Canada, 97(3): 13-16 (1996).

14. Barnet, A.J., "The 23rd Annual Leask Survey: "The Mechanical Pulping Market has Matured", Pulp and Paper Canada, 99(3): 12-14 (1998).

15. Kurdin, J.A., Tantalo, L., "Mechanical Pulping by Extrusion", Intl. Mech. Pulp. Conf., Vancouver, Canada, p. 105-110 (1987).

16. May, W.D., Atack, D., "Study of Fiber Removal in a Laboratory Method of Mechanical Pulping and Its Implications in the Production of New Types of Mechanical Pulp", Intl. Mech. Pulp. Conf., p. 1-16 (1964).

17. Harpole, G.B., Leatham, G.F., Myers, G.C., "Economic Assessment of Biomechanical Pulping", Intl. Mech. Pulp. Conf. , Helsinki, Finland, Vol. 2 : 398-408 (1989).

18. Sundholm, J., "KUITU Energy Efficient Mechanical Pulping", Interim report 1988-1990, Ministry of Trade and Industry, Energy Department, Finland, Reviews B: 97 (1991).

19. Kokta, B.V., Vit, R., "New Ultra-high-yield V-Pulping Process", 73rd Annual Meeting, Technical Section CPPA, Book A: A143-A149 (1987).

20. Kokta, B.V., "Process for Preparing Pulp for Paper Making", Can. Pat., 1,230,208 (Dec. 15, 1987).

21. Sundholm, J., Mannström, B., Heikkurinen, A., Särkilahti, A., Finnish Pat. No. FI-89610 (Oct. 25, 1993).

22. Höglund, H., Bäck, R., Falk, B., Jackson, M., "Thermopulp™- A New Energy Efficient Mechanical Pulping Process," Intl. Mech. Pulp. Conf., Ottawa, Canada, p. 213-225 (1995).

23. Cannell, E., "Mechanical Pulping Technologies Focus on Reducing Refining Energy", Pulp and Paper, 73(5): 63-70 (1999).

24. Argger, H., "RTS bring A New Intensity to TMP (Production at Perlen Papier, Switzerland), Pulp Paper Europe 2(5): 16-19 (1997).

25. Vuorio, P., Bergquist, P., "New Refiner Segments Technology to Optimize Fiber Quality and Energy Consumption of Refiner Mechanical Pulp", Intl. Mech. Pulp. Conf., Helsinki, Finland, p. 565-577 (2001).

26. Scott, G.M., Alhtar, M., Myers, G.C., Sykes, M. Swaney, S., R.E., "An Update on Biopulping Commercialization", 3rd Economy & Ecology in Papermaking Technology, Helsinki, Finland, p. 37-43 (2001).

27. Fengel, D., Wegener, G., "Wood- chemistry, Ultrastructure, Reactions", Walter de Gruyter, Berlin. New York, p. 430-437 (1984).

28. Katz, S., Liebergott, N., Scallan, A.M., "A Mechanism for the Alkali Strengthening of Mechanical Pulps" Tappi J., 64(7): 97-100 (1981).

29. Katz, S., Scallan, A.M., "Ozone and Caustic Soda Treatments of Mechanical Pulp", Tappi J. 66(1): 85-87 (1983).

30. Bohn, W.L., Sferrazza, M.J., "Alkaline Peroxide Mechanical Pulping - A Revolution in Mechanical Pulping", Intl. Mech. Pulp. Conf., Helsinki, Finland, p. 184-200 (1989).

31. Heimburger, S., Quick, T., Sabourin, M., Tremblay, S., Shaw, G., "One-and Two-stage APTMP (Alkaline Peroxide Thermomechanical Pulp); Route to High-Brightness Pulp", Tappi J. 79(8): 139-144 (1996).

32. Lanouette, R., Valade, J., Thibault, J., "Optimization of an Alkaline Peroxide Interstage Treatment of Jack Pine (Pinus banksiana Lamb.) Using a D-Optimal Design", The Canadian. J. of Chemical Engineering, 75 (1): 70-78 (1997).

33. Lanouette, R., Thibault, J., Valade, J.L., "High-yield pulping of jack pine", TAPPI 81(10): 143-149 (1998)

34. Tyrväinen, J., Law, K. N., Valade, J. L., "Alkaline-Peroxide Inter-Stage Treated Mechanical Pulp from Jack Pine (*Pinus Banksiana*), Part I. Introduction and Pulp Physical Properties", Pulp and Paper Canada 98 (6): T191-T196 (1997).

35. Tyrväinen, J., Law, K. N., Valade, J. L., "Alkaline-peroxide Inter-Stage Treated Mechanical Pulp from Jack Pine (*Pinus Banksiana*), Part II. Pulp Optical properties, Color Reversion, Extractives Content and Process Implications", Pulp and Paper Canada, 98 (7): T223-T227 (1997).

36. Barbe, M.C., Janknecht, S., Sauriol, J.F., "The Importance of Chip Impregnation on Refiner Pulp Quality", Intl. Mech. Pulp. Conf., Oslo, Norway, Poster presentation No. 2, Pulping and Process Technology Session: 17-38 (1993).

37. Adler, E., "The Chemical Structure of Lignin", Svensk Kem. Tidskr. 80(9): 279-90 (1968).

38. Beatson, R.P., Heitner, C., Atack, D., "Factors Affecting the Sulfonation of Spruce", J. of Pulp and Paper Science, 10(1): J12-J17 (1984).

39. Ingruber, O.V., Kocurek, M.J., Wong, A., "Pulp and Paper Manufacture, Vol. 4, Sulfite Science &Technology", 3rd, TAPPI & CPPA, The Joint Textbook Committee of The Paper Industry, p. 160 (1985).

40. Atack, D., Heitner, C., "Dynamic Mechanical Properties of Sulfonated Eastern Black Spruce", CPPA Trans. of Technical Section 5(4): TR99-TR108 (1979).

41. Ebringerova, A., Kosikova, B., Kacurakova, M., "Structural Changes in Hardwood Lignin-polysaccharide Complex upon Steaming", Drev. Vysk. 38(3): 23-30 (1993).

42. Puls, J., Dietrichs, H.H., "Separation of Lignocellulose into Highly Accessible Fiber Materials and Hemicellulose Fraction by the Steaming-extraction Process", Energy from Biomass Conf., Brighton, p. 348-353 (1980).

43. Nicholas, D.D., Thomas, R.J., "Influence of Steaming on Ultrastructure of Bordered Pit Membrane in Loblolly Pine", Forest Prod. J. 18(1): 57-59 (1968).

44. Jackson, M., Akerlund, G., "Preheating and Refiner Housing Pressure affecting Quality of TMP and CTMP", Tappi J. 67(1): 54-58 (1984).

45. Lunan, W.E., Miles, K.B., May, W.D., Harris, G., Franzen, R., "High Pressure Refining and Brightening in Thermomechanical Pulping", Tappi Pulp. Conf., Houston, USA, Book1, p. 239-253(1983).

46. Sachs, I. B., Leatham, G. F., Myers, G. C., "Biomechanical Pulping of Aspen Chips by Phanerochaete chrysosporium: Fungal Growth Pattern and Effects on Wood Cell Walls", Wood and Fiber Science, 21(4): 331-342 (1989).

47. Chen, Y.-R., Schmidt, E.L., Olsen, K.K., "Effect of Compression of Green Wood Chips on Conidial Germination and Colonization of Biopulping Fungus, Phanerochaete chrysosporium", Wood and Fiber Science, 30(1): 18-26 (1998).

48. Bajpai, P., Bajpai, P.K., Akhtar, M., Jauhari, M. B., "Biokraft Pulping of Eucalyptus with Selected Lignin-degrading Fungi", J. of Pulp and Paper Science, 27(7): 235-239 (2001).

49. Murton, K., "The Effect of Chip Compression of TMP Properties", Appita J. 49(5): 313-318(1996).

50. Parkinson, A., Tessier, P., Lee, C.L., "Effect of Compression Ratios of Screw Feeders during Multistage Impregnation on Black Spruce Chips and Fibers", Tappi J. 79(7): 149-156 (1996).

51. Heitner, C., Beatson R.P., Atack, D., "Ultra-high Yield Pulping. Part V. High Compression Impregnation of Softwood Chips with Sodium Sulphite – A Method of Producing CMP with High Wet and Dry Strength ", Intl. Mech. Pulp. Conf., Stockholm, Sweden, p. 101-108 (1985).

52. Sabourin, M.J., "Evaluation of A Compressive Pretreatment Process in TMP Properties and Energy Requirements", Pulp and Paper Canada, 101(2): 50-56 (2000).

53. Kure, K.-A., Dahlqvist, G., Sabourin, M.J., Helle, T., "Development of Spruce Fiber Properties by a Combination of a Pressurized Compressive Pretreatment and High Intensity Refining", Intl. Mech. Pulp. Conf., Houston, TX, USA, p. 427-433 (1999).

54. Sabourin, M.J., Vaughn, J., Wiseman, N., Cort, J.B., Galatti, P., "Mill Scale Results on TMP Pulping of Southern Pine with Pressurized Chip Pretreatment", Proc. 87th Annual Meeting of PAPTAC, Book C: C9-C17 (2001).

55. Sabourin, M., Aichinger, J., Wiseman, N., "Effect on Increasing Wood Chip Defiberation on Thermomechanical and Chemi-Thermomechanical refining Efficiency". Intl. Mech. Pulp. Conf., Quebec, Canada, p.163-170 (2003).

56. Law, K.N., Lanouette, R., Yang, K.C., "A New Approach to Mechanical Pulping – Pretreatment of Chips by Normal-to-Grain Compression Prior to Refining", Intl. Mech. Pulp. Conf., Houston, USA, p. 229-256 (1999).

57. Law, K.N., Lanouette, R., Yang, K.C., "Effect of Compression on Refining Energy and Pulp Properties of Birch TMP", Appita J. 53(4): 296-299 (2000).

58. Law, K.N., Lanouette, R, Yang, K.C., "A New Approach to Mechanical Pulping – Pretreatment of Chips by Normal-to–Grain Compression Prior to Refining", Tappi J. 83(9): 63 (2000). (http://www.tappi.org/public/tappi_journal.asp).

59. Uhmeier, A., Salmén, L., "Repeated Large Radial Compression of Heated Spruce", Nordic Pulp and Paper Research J. 3:171-176 (1996).

60. Dumail, J.F., Salmén, L., "Compression Behavior of Spruce Wood Under Large Plastic Deformations", Nordic Pulp and Paper Research J., 4:239-242 (1996).

61. Dumail, J.F., Salmén, L., "Compression Behavior of Saturated Wood Perpendicular to Grain Under Large Deformations - Comparison Between Water-Saturated and Ethylene Glycol-Saturated Wood", Holzforschung, 51(4): 296-302 (1997).

62. Uhmeier, A., Morooka, T., and Norimoto, M., "Influence of Thermal Softening and Degradation on the Radial Compression Behavior of Wet Spruce", Holzforschung, 52(1): 77-81 (1998).

63. Thiruvengadaswamy, R., Ouellet, D., "On the Generation of Structural Damage in Wood by Cyclic Compressive Loading", J. of Pulp and Paper Science, 24(8): 247-253 (1998).

64. Deisnto, W., Morooka. T., Norimoto, M., Kitajima, T., "Stress Relaxation of Sugi (*Cryptomeria Japonica* D. Don) Wood in Radial Compression Under High Temperature Steam", Holzforschung, 53(5): 541-546 (1999).

65. Tabarsa, T., Chui, Y.H., "Stress-Strain Response of Wood under Radial Compression. Part I. Test Method and Influences of Cellular Properties", Wood and Fiber Science, 32(2): 144-152 (2000).

66. Bergande, A., and Salmén, L., "Lamellar Cracks, Do They Appear During Radial Compression of Wood", Nordic Pulp and Paper Research J., 12(4): 216-219 (1997).

67. Law, K.N., "Mechanical Behavior of Early- and Latewood Under Compression Load", Intl. Mech. Pulp. Conf., Helsinki, Finland, Vol. 1, p. 159-166 (2001).

68. Renaud, M., Rueff, M., Rocaboy, A. C., "Mechanical Behavior of Saturated Wood under Compression, Part 2: Behavior of Wood at Low Rates of Strain, Some Effects of Compression in Wood Structure", Wood Science and Technology, 30:237-243 (1996).

69. Tabarsa, T., Chui, Y.H., "Characterizing Microscopic Behavior of wood under Transverse Compression. Part II. Effect of Species and Loading Direction", Wood and Fiber Science, 33(2): 223-232 (2001).

70. Watanabe, U., Fujita, M., Norimoto, M., "Transverse Young's Moduli and Cell Shapes in Coniferous Early Wood", Holzforschung, 56 (1):1-6 (2002).

71. Ethington, R.L., Eskelsen, V., Gupta, R., "Relationship between Compression Strength Perpendicular to Grain and Ring Orientation", Forest Products J., 46 (1):84-86 (1996).

72. Kucera, L.J., Bariska, M., "On the Fracture Morphology in Wood. Part 1 A SEM-study of Deformations in Wood of Spruce and Aspen upon Ultimate Axial Compression Load", Wood Science and Technology 16:241-259 (1982).

73. Gong, M., Smith, I., "Failure of Softwood under Static Compression Parallel to Grain", Journal of the Institute of Wood science, 15 (4):204-210 (2000).

74. Franzier, W.C., Williams, G.J., "Reduction of Specific Energy in Mechanical Pulping by Axial Precompression of Wood," Pulp and Paper Canada 83(6): 87-92 (1982).

75. Berg, J.-E., Gradin, P.A., "Effect of Temperature on Fracture of Spruce in Compression, Investigated by use if Acoustic Emission Monitoring", J. of Pulp and Paper Science 26(8): 294-299 (Aug. 2000).

76. Renaud, M., Rueff, M., Rocaboy, A.C., "Mechanical Behavior of Saturated Wood Under Compression, Part I: Behavior of Wood at High Rates of Strain", Wood Science and Technology, 30:153-164 (1996).

77. Salmén, L., "The Effect of the Frequency of a Mechanical Deformation on the Fatigue of Wood", Intl. Mech. Pulp. Conf., Stockholm, Sweden, p. 146-152 (1985).

78. Salmén, L., Fellers, C., "The Fundamentals of Energy Consumption During Viscoelastic and Plastic Deformation to Wood", Transactions of Technical Section, CPPA, p. TR93-TR99 (Dec. 1982).

79. Ouis, D., "On The Frequency Dependence of the Modulus of Elasticity of wood", Wood Science Techn. 36:335-346 (2002)

80. Salmén, L., Tigerström, A., Fellers, C., "Fatigue of Wood - Characterization of Mechanical Defibration", J. of Pulp and Paper Science, 11(3): 68-73 (1985).

81. Thiruvengadaswamy, R., Ouellet, D, "An Image Analysis Method to Quantify Fibre Separation in Wood Subjected to Fatigue Load", Intl. Mech. Pulp. Conf., Houston, USA, p. 221-228 (1999).

82. Wolcott, W.P., Kasal, B., Kamke, F.A., Dillard, D.A., "Testing Small Wood Specimens in Transverse Compression", Wood and Fiber science 21(3):320-329 (1989).

83. Lai, Y.Z., and Iwamida, T., "Effects of Chemical Treatments on Ultra-High-Yield Pulping 1. Fiber Separation", Wood Science and Technol. 27:195-203 (1993).

84. Johansson, L., Peng, F., Simonson, R., "Effects of Temperature and Sulfonation on Shear Deformation of Spruce Wood ", Wood Science and Technology, 31:105-117 (1997).

85. Law, K.N., Koran, Z., "Torsional-Shear Stress of Wood at Various Temperatures", Wood Science and Technology, 15:227-235 (1981).

86. Bendtsen, B.A., "Rolling Shear Characteristics of Nine Structural Softwoods", Forest Products J., 26(11): 51-56 (1976).

87. Ottestam, C., Salmén, L., "Fracture Energy of Wood; Relation to Mechanical Pulping", Nordic Pulp and Paper research J., 16 (2):140-142 (2001).

88. Leask, R.A., Kocurek, M.J., "Mechanical pulping", Pulp and Paper Manufacture Vol.2, 3rd ed., Joint Textbook Committee of the Paper Industry, p. 93-97 (1987).

89. Peel. J.D., "Paper Science and Paper Manufacture", Angus Wild Publications Inc., Vancouver & Bellingham, Canada, p.99-116 (1999).

90. Corson, S.R., "Aspects of Mechanical Pulp Fiber Separation and Development in a Disc Refiner", Paperi ja Puu – Paper and Timber, 7: 802-814 (1989).

91. Zink, A.G., Pellicane P. J., Shuler, C. E., "Ultrastructural Analysis of Softwood Fracture Surfaces", Wood Science and Technology 28:329-338 (1994).

92. Franzen, R.G., "General and Selective Upgrading of Mechanical Pulps", Intl. Mech. Pulp. Conf., Stockholm, Sweden, p. 19-33 (1985).

93. Johnsen, P.O., Skinnarland, I., Helle, T., Houen, P.J., "Distribution of Lignin and other Materials of Particle Surfaces in Mechanical Pulps", Intl. Mech. Pulp. Conf., Ottawa, Canada, p. 93-99 (1995).

94. Genco, J.M., "Principles of Processes in Stock Preparation and Refining", TAPPI, Pulp. Conf., Orlando, Florida, USA, 1:74-95 (1999)

95. Stevens, W.V., "Principles of Stock Preparation and Refining and Refiner Systems" TAPPI, Pulp. Conf., Orlando, Florida, USA, 1:97-111 (1999).

96. Annergren, A., "Fundamentals of Pulp Fiber Quality and Paper Properties", TAPPI, Pulp. Conf., Orlando, Florida, USA, 1:29-39 (1999).

97. Atack, D., Stationwala, M.I., Karnis, A., "What Happens in Refining- Part I", Pulp and Paper Canada, 85(12): 119-124 (1984).

98. Miles, K.B., May, W.D., "Flow of Pulp in Chip Refiner" J. of Pulp and Paper Science 16(2): J63-J72 (1990).

99. Brecht, W., "Method for Comparative Evaluation of Bar-Equipped Beating Devices", TAPPI J. 50(8): 40-44 (1967).

100. Leider, P.J., Nissan, A.H., "Understanding the Disk Refiner – Mechanical Treatment of Fibers", TAPPI J. 60(10): 85-89 (1977).

101. Turt, V., "Effect of Refining on Fiber Properties", M. S. Thesis, University of Maine, Orono, Maine, USA, (1994).

102. Kerekes, R.J, "Characterization of Pulp Refiners by A C-Factor", Nordic Pulp Paper Res. J., 5(1): 3-8 (1990).

103, Dahlqvist, G., "Advances in Fundamental Refiner Control", Intl. Mech. Pulp. Conf., OSLO, Norway, p. 208-214 (1993).

104. Strand, B., "Quality Control of High Consistency Refiners", Intl. Mech. Pulp. Conf., Stockholm, Sweden, p. 127-136 (1997).

105. Alami, R., Boileau, I., Harris, G., Lachaume, J., Karnis, A., Miles, K.B., and Roche, A., "Evaluation of The Impact of Refining Intensity on Energy Reduction in Commercial Size Refiners: The Effect of Primary Stage Consistency", Intl. Mech. Pulp. Conf., Ottawa, Canada, p. 203-212 (1995).

106. Strand, B.C., Mokvist, A., Falk, B., Jackson, M., "The Effect of Production Rate on Specific Energy Consumption in High Consistency Chip Refining", Intl. Mech. Pulp. Conf., OSLO, Norway, p. 143-151 (1993).

107. Härkönen, E., Tienvieri, T., "The Influence of Production Rate on Refining in a Specific Refiner", Intl. Mech. Pulp. Conf., Ottawa, Canada, p. 177-182 (1995).

108. Strand, B.C., Hartler, N., "Modeling and Optimization of Full Scale Chip Refining", Intl. Mech. Conf., Stockholm, Sweden, p. 46-54 (1985).

109. Münster, H., Dahlqvist, G., "Operational Experience with the First Commercial High Speed Refiner at Perlen Papier AG Switzerland", Intl. Mech. Pulp. Conf., Ottawa, Canada, p. 197-203 (1995).

110. Chagaev, O., Stationwala, M.I., Allem, R., "The Role of Fiber Collapse in Mechanical Pulping", Intl. Mech. Pulp. Conf., Houston, TX, USA, p. 155-169 (1999).

111. Reme, P.A., Kure, K.-A., Gregersen, Ø.W., Helle, T., "Optimal Mechanical Pulp Fibers for Improved Publication Paper: Targets and Treatments", Intl. Mech. Pulp. Conf., Houston, TX, USA, p. 171-182 (1999).

112. Mohlin, U.-B., "Fiber Development during Mechanical Pulp Refining", Intl. Mech. Pulp. Conf., Ottawa, Canada, p. 71-77 (1995).

113. Reme, P.A., Helle, T., "Quantitative Assessment of Mechanical Fiber Dimensions during Defibration and Fiber Development", J. of Pulp and Paper Science, 27(1): 1-7 (2001).

114. Geirtz, H.W., "Basic Wood Raw Material Properties and Their Significance in Mechanical Pulping", Intl. Mech. Pulp. Conf., Helsinki, Finland, p.1-15 (1977).

115. Brill, J.W., "Effects of Wood and Chip Quality on TMP Properties", Intl. Mech. Pulp. Conf., Stockholm, Sweden, p. 153-161 (1985).

116. Harter, N., "Wood Quality Requirements, Process Adaptation and Necessary Sacrifice", Intl. Mech. Pulp. Conf., Stockholm, p. 109-119 (1985).

117. Corson, S.R., "Influence of Wood Quality Characteristics on TMP and RMP from New Zealand-Grown Radiata Pine", Appita J. 37(5): 400-408 (1984).

118. Corson, S.R., "Wood Characteristics Influence Pine TMP Quality", Intl. Mech. Pulp. Conf., Minneapolis, USA, p. 243-251 (1991).

119. Rudie, A.W., Morra, J., St.-Laurent, J. M., Hickey, K. L., "The Influence of Wood and Fiber Properties on Mechanical Pulping", Tappi J. 77(6): 86-90 (1994).

120. Tyrväinen, J., "Wood and Fiber Properties of Norway Spruce and Its Suitability for Thermomechanical Pulping", Finnish Society of Forest Science, p. 20-27 (1995).

121. Göran, A., "Fundamentals of Pulp Fiber Quality and Paper Properties", TAPPI Pulp. Conf., Orando, Florida, USA, p. 29-39 (1999).

122. Kollmann, F.F.P., Côté, W.A., Jr., "Principles of Wood Science and Technology. I: Solid wood" , N. Y., Springer-Verlag N. Y. Inc, p. 9-12 (1968).

123. Kocurel, M.J., Stevens, C.F.B., Pulp and Paper Manufacture Volume 1, "Properties of Fibrous Raw Materials and their Preparation for Pulping", TAPPI & CPPA, The Joint Textbook Committee of the Paper Industry, 3rd. p. 22-43, (1983).

124. Kollmann, F.F.P., Côté, W.A. Jr., "Principles of Wood Science and Technology. I: Solid wood", N. Y., Springer-Verlag N. Y. Inc., p. 18-42 (1968).

125. French, J., Conn, A.B., Batchelor, W. J, Parker, I.H., "Effect of Fibre Fibril Angle on Some Hand sheet Mechanical Properties", Appita J. 53(3): 210-215, 226 (2000).

126. Arsmstrong, J.P., Kyanka, G.H., Thorpe, J.L., "S2 fibril angle – Elastic Modulus Relationship of TMP Scotch Pine Fibers ", Wood Science 10(2): 72-80 (1977).

127. Sjöström, E., "Wood Chemistry, Fundamentals and Applications", Academic Press, New York, p. 1-20 (1981).

128. Berg, J.-E., Gradin, P.A., "A Micromechanical Model of the Deterioration of a Wood Fiber", J. of Pulp and Paper Science 25(2): 66-71 (1999).

129. Mark, R.E., "Cell Wall Mechanics of Tracheids", New Haven and London, Yale University Press, USA. p. 1-26 (1967).

130. Kerr, A.J., Goring, D.A.I., "The Ultrastructural Arrangement of the Wood Cell Wall", Cellulose Chemistry and Technology 9: 563 (1975).

131. Baker, C.F., Punton, V.W., "Fundamentals of Papermaking", Transactions of the Ninth Fundamental Research Symposium, Cambridge, Vol. 1, p. 1-38, Published by Mechanical Engineering Publication Limited, London (1989).

132. Salmen, L., Kolseth, P., Ruvo, A., "Modeling the softening Behavior of wood fibers", J. of Pulp and Paper Science, 11(4):J102-J107 (1985).

133. Browning, B.L., "The Chemistry of Wood" Interscience Publishers, a division of John Wiley & Sons, New York · London, p. 7-56 (1963).

134. Goldstein, I.S., Gould, R.F., "Wood Technology: Chemical Aspects", ACS Symposium Series 43, American Chemical Society, Washington, D.C., USA, p. 1-23 (1977).

135. Fengel, D., Wegener, G., "Wood- Chemistry, Ultrastructure, Reactions", Walter de Gruyter, Berlin New York, USA, p. 167-174 (1984).

136. Haun, J.L., Britt K.W., "Hand Book of Pulp and Paper Technology," Van Nostrand Reinhold, New York, USA, p. 25-31 (1970).

137. Katz, S., Beatson R., Scallan, T., "The Determination of Strong and Weak Acidic Groups in Sulphite Pulps", Svensk Papperstidn, 87(6): R48-R53 (1984).

138. Dumail J.F., Olofsson, K., Salmen L., "An Analysis of Rolling shear of Spruce Wood by the Iosipescu Method", Holzforschung, 54(4):420-426 (2000).

139. Gindl, W., Teischinger, A., "Comparison of the TL-Shear Strength of Normal and Compression Wood of European Larch", Holzforschung, 57(4):420-426 (2000).

140. Sadoh T., "Mechanism of Dimensional Stabilization of Wood by Polyethylene Glycol Treatment", Mokuzai Gakkaishi 14, 353-357 (1968).

141. Koran, Z., "Electron Microscopy of Radial Tracheid Surfaces of Black Spruce Separated by Tensile Failure at Various Temperatures", Tappi J., 50(2):60-67 (1967).

142. Sadoh, T., Ohgoshi, M., "Viscoelastic Properties of Wood in Swelling System II: Viscoelastic Properties of Wood Swollen with Ethylene Glycol and Ployethylene Glycols" Mokuzai Gakkaishi 20(4):177-181 (1974).

143. Sperling, L.H. "Introduction to Physical Polymer Science", John & Willey & Sons, USA, p. 254-272 (1986).

144. Lawrence H. Van Vlack, "Elements of Materials Science and Engineering", 5th ed. Addison-Wesley Publishing Company, USA, p.122-139 (1985).

145. Bjorkman, A., Salmén, L., "Studies on Solid Wood. II. The Influence of Chemical Modifications on Viscoelastic Properties", Cellulose Chemistry and Technology 34:7-20 (2000).

146. Wolcott, M.P., Kamke, F.A., Dillard, D.A., "Fundamentals of Flake Board Manufacture: Viscoelastic Behavior of The Wood Component", Wood and Fiber Science 22 (4): 345-361 (1990).

147. Hearn, E.J., "Mechanics of Materials", An Introduction to the Mechanics of Elastic and Plastic Deformation of Solids and Structural Components, 2nd ed. Pergamon Press, USA, p. 743-749 (1985).

148. Ludwik, P. "Elemene der echologischen Mechanik", Springer, Berlin, 1909. From: Alexander Mendelson, "Plasticity: Theory and Application" 2nd ed., Robert E. Krieger Publishing Company, Inc., USA, p. 7-20 (1983).

149. Wolcott, M.P., "Modeling Viscoelastic Cellular Materials for The Pressing of Wood Composite", Ph.D dissertation, Virginia Polytechnic Institute and state University, Blacksburg, VA. USA. (1990).

150. Rusch, K.C., "Load-Compression Behavior of Flexible Foams", J. Appl. Polymer Science 13:2297-2311 (1969).

151. Dai, C., Steiner, P.L., "Compression Behavior of Randomly Formed Wood Flake Mats", Wood and Fiber Science 25(4):349-358 (1993).

152. Liu. Y., Morooka T., Norimoto M., "The Large Compressive Deformation of Wood in The Transverse Direction: Relationships between Stress-strain Diagrams and Specific Gravities of Wood", Mouzai Gakkaishi. 39, p.1140-1145 (1993).

153. Uhmeier A., Morooka T., Norimoto M., "Influence of Thermal Softening and Degradation on The Radial Compression Behavior of Wet Spruce", Holzforschung 52 (1): 77-81 (1998).

154. Baumeister, T., Avallone, A., Baumeister III, T., "Marks' Standard Handbook for Mechanical Engineers", 8th Ed., McGraw-Hill Book Company, USA, p.5-56 (1978).

155. Bardage, S.L., Daniel, G., Singh, A., "Three dimensional Analysis of The Collapse Behavior of Kraft-Cooked Norway Spruce Fibers", Wood and Fiber Science 34(3):382-390 (2002).

156. Jang H.F., "A Theory for The Transverse Collapse of Wood Pulp Fibers", 12th Fundamental Research Symposium, Oxford, UK., p.193-210 (September, 2001).

157. Dunford, J.A., Wild, P.M., "Cyclic Transverse Compression of Single Wood-Pulp Fibers", J. of Pulp and Paper Science 28(4):136-141 (2002).

158. Nyren, J., "The Transverse compressibility of Pulp Fibers", Tech. Sect., CPPA, 72 (10):T321-T323 (1971).

159. Hartler, N., Nyren, J., "Influence of Pulp Type and Post-treatments on the Compressive Force Required for Collapse", TAPPI, Special Technical Association Publication 8:265-277 (1970).

160. Page, D.H., "The beating of chemical pulps- the action and the effects", Fundamentals of Papermaking: Transaction of Fundamental Research Symposium, Cambridge, UK., p.1-38 (1989)

161. Goncharov, V.N., Smirnova, E.A., Shemyakin, E.V., "Method for The determination of Stress between Refiner Blades", *Bum. Promst.* (27):134-138, English Trans., (1970).

162. Senger, J., Siadat, A., Ouellet, D., Wild, P., "Measurement of Normal and Shear Force during Refining Using a Piezoelectric force sensor", Intl. Mech. Pulp. Conf., p.403-407 (2003).

163. Miles, K.B., "Simplified Method for Calculating the Residence Time and Refining iin a Chip Refiner" , Paperi Ja Puu 73 (9):852-857 (1991).

164. Law, K.N., "A New Insight into Chip Refining", Appita J. 53(5): 393-397 (2000).

165. Kerekes, R.J., "Is There Untapped Potential in Pulp Refining", Pulp and Paper Canada, 104(12):21-23 (2003).

166. Schmidt, S.R., Launsby, R.G., "Understanding Industrial Designed Experiments", 4th. Ed., Chapter 3 (1-62), Chapter 4 (1-74), Chapter 7 (1-9). Air Academy Press, Colorado, USA, (1994).

167. Beatson, R.P., Heitner, C., and Atack, D. "Factors Affecting the Sulphonation of Spruce". J. of Pulp and Paper Science 10(1):J12-J17 (1984).

168. Wu, Y.-T., and Wilson, J.W. "Lignification within Coniferous Growth Zones". Pulp Paper Mag. Can. 68(4):T159-T164 (1967).

169. Fergus, B.J., Procter, A.R., Scott, J.A.N., and Goring, D.A.I. "Distribution of Lignin in Sprucewod as Determined by Ultraviolet Microscopy". Wood Science Technol. 3(2):117-138 (1969).

170. Gellerstedt, G., and Zhang L. "Reactive Structures in High Yield Pulping. Part 2. Monomeric End Groups and Detached Side Chain Structures". Nordic Pulp Paper Res. J. 7(2):75-80 (1992).

171. Lindholm, C.-A., and Kurdin, J.A. "Chemimechanical Pulping". In: Mechanical Pulping (ed. Sundholm, J.), Finnish Paper Engineers' Association and TAPPI, Finland, p. 222-249 (1999).

172. Prasad, V., and Luner, P. "Physical Properties of Paper Made from Springwood and Summerwood Fibers". SUNY College of Environmental Science and Forestry, ESPRI Research Report 38-II-12 (1964).

173. Smith, W.E., and Byrd, V.L., "Fiber Bonding and Tensile Stress-strain Properties of Earlywood and Latewood Hand Sheets". U.S. Forest. Serv. Paper FPL 193: 11 p. (1972).

174. Hasuika, M., "Physical Properties and Macrostructure of Earlywood and Latewood Pulp Sheets". J. Japan Wood Res. Soc. 19(11):547-553 (1973).

175. Murton, K.D., Richardson, J.D., Corson, S.R., and Duffy, G.G., "TMP Refining of Radiata Pine Earlywood and Latewood Fibers". Intl. Mech. Pulp. Conf. Helsinki, Finland, p.361-371 (2001).

176. Mohlin, U.-B. "Fibre Development During Mechanical Pulp Refining". J. of Pulp and Paper Science 23(1):J28-J33 (1997).

177. Reme, P.A., Johnsen, P.O., and Helle, T. "Changes Induced in Early- and Latewood by Mechanical Pulp Refining", Nordic Pulp Paper Res. J. 14(3):256-262 (1999).

178. Hickey, K.L., and Rudie, A.W., "Preferential Energy Absorption by Earlywood in Cyclic Compression of Loblolly Pine". Intl. Mech. Pulp. Conf., OSLO, Norway, Poster Session:81-86 (1993).

179. Pearson, A.J., Pulp and Paper Technology Series, No. 6,"A Unified Theory of Refining", Joint Textbook committee of the Paper Industry, TAPPI, P. 6 (1990).

180. Mao, C.B., Law, K.N., Kokta, B.V., "Effect of Sulfonation on the Compression Behavior of Early-and Latewood", Pulp and Paper Canada 105 (12): T273-277 (2004).

181. Mao, C., Law, K.N., Kokta, B.V., "Characterizing Radial Compression of Wood by Longitudinal Shear", 90th Pulp and Paper Annual Meeting, PAPTAC, Montreal, Canada, p. B5-B10 (2004).

182. Gregersen, Ø.W., Skinnarland, I., Johnsen, P.O., Helle, T., "Qualitative Methods for The Study of Lignin Distribution in Wood and Surface Layers of Unbleached Pulp Fibers and Paper". J. of Pulp Paper Science, 21(8): J285-J287 (1995).

183. Saka, S., "Evaluation of the Quantitative Assay of Lignin Distribution by SEM-EDXA- Technique", Wood Science and Technology 16: 1-18 (1982).

184. Simons, F.L., "A Stain for Use in the Microscopy of Beaten Fibers". TAPPI J., 33(7): 312-314 (1950).

185. Wurz, O., "Studying the Degree of Beating of Chemical Pulps with the Simons Stain", The Papermaker, 158(6): 59 (1969).

186. Blanchette, A.R., Akhtar, M., Attridge, M.C., "Using Simons Stain to Evaluate Fiber Characteristics of Biomechanical Pulps", TAPPI J., 75(11): 121-124 (1992).

187. Karnis, A., "The Mechanism of Fiber Development in Mechanical Treatment", J. of Pulp and Paper Science, 20(10): J280-288 (1994).

188. Kibblewhite, R.P., Bailey, D.G., "Measurement of Fiber Cross-Section Dimensions Using Image Processing", Appita J., 41 (4): 297 (1988).

189. Kure, K.-A., "The Alteration of the Wood Fibers in Refining", Intl. Mech. Pulp. Conf, Stockholm, Sweden, p. 137-150 (1997).

190. Kettle, J., Matthews, P., Ridgway, C., Wagberg, L., "Investigation of the Pore Structure of Paper by Novel Porosimetric Techniques: Application to Super and Soft-Nip Finishing", Fund. Papermaking Materials, 11th Fund. Res. Symp., Cambridge, UK, 2:1355-1392 (1997).

191. Gibbon, D. L., Simon, G.C., Cornelius, R.C., "New Electron and Light-Optical Techniques for Examining Papermaking, with and Emphasis on Cross-Sectional Studies", Tappi Papermaking Conf. Washington DC, USA, p. 227-254 (1998).

192. Stone, J.E., Scallan, A.M., "A Structural Model for the Cell Wall of Water-Swollen Wood Pulp Fibers Based on Their Accessibility to Macromolecules", Cellulose Chemistry and Technology 2:343-358 (1968).

193. Szikla, Z., Paulapuro, H., "Changes in Z-Direction Density Distribution of Paper in Wet Pressing", J. of Pulp and Paper Science 15(1): 11-17 (1989).

194. Samuelsen, E.J., Gregersen, O.W., Houen, P.J., Helle, T., Raven, C. Snigirev, A., "Three-Dimension Imaging of Paper by Use of Synchrotron X-ray Microtomography", J. of Pulp and Paper Science, 27(2): 50-53 (2001).

195. Mangin, P.J., Béland, M.-C., Cormier, L.M., "Paper Surface Compressibility and Printing", Intl. Printing Graphic Art Conf., Technical section, CPPA, p. 19-31 (1994).

196. Robertson, A. G., Jiang, H. F., Seth, R. S., "Transverse Dimensions of Wood-Pulp Fiber by Confocal Laser Scanning Microscopy and Imaging Analysis", J. Mater. Science 27: (6391-6400).

197. Attack, D., May, D., Morris, E.L., Sproule, R.N., "The Energy of Tensile and Cleavage Fracture of Black Spruce", Tappi, J.44 (8): 555-567 (1961).

198. Koran, Z., "Tensile Properties of spruce under different conditions", Wood and Fiber 11 (1):38-49 (1979).

199. Mutton, D.B., Tombler, G., Gardner, P.E., and Ford. M.J., "The sulphonated chemimechanical pulping process", Pulp and Paper Canada, 83(6): 120-128 (1982).

200. Heitner C., Hattula, T., "Ultra-high-yield pulping part VI: The effect of sulphonation on the development of fibre properties", J. of Pulp and Paper Science 14(1): J6-J11, (1988).

RECENT PUBLICATIONS AND PRESENTATIONS

1. MAO, C.B., K.N. LAW, B.V. KOKTA, "Characterizing Radial Compression of Wood by Longitudinal Shear", Preprints Vol. B, pp. B1291-B1296, 90th Pulp and Paper Annual Meeting, PAPTAC, Montreal (Jan., 2004). The paper has been accepted for publication in APPITA Journal.

2. MAO, C.B., K.N. LAW, B.V. KOKTA, "Effect of Sulfonation on the Compression Behavior of Early –and Latewood", Pulp and Paper Canada 105 (12): T273-277 (2004). This paper presented at 89th Pulp and Paper Annual Meeting in Montreal, QC, Canada (Jan. 28-30, 2003).

3. MAO, C.B., K.N. LAW, B.V. KOKTA. "Mechanism of Wood Compression". Presentation at Canadian Pulp and Paper Graduate Students Seminars, PAPTC 90th Pulp and Paper Annual Meeting, Montreal (Jan., 2004).

4. MAO, C.B., K.N. LAW, B.V. KOKTA, "Compressibility of Early – and – Latewood and Its Influence on Mechanical Pulping". Presentation at The CTIA/WFGA/PCC Wood Technology workshop, Joint Canadian Tree Improvement Association, Western Forest Genetics Association and Poplar Council of Canada 2002 Conference, Edmonton, Alberta (July 2002).

5. B.V. KOKTA, K.N. LAW, MAO, C.B., "Fiber Morphology and Soda-sulfite Pulping of Switchgrass". 11th International Symposium on Wood and Pulping Chemistry, Nice, France, Vol.2, pp. 283-287 (2001).

6. K.N. LAW, B.V. KOKTA, MAO, C.B., "Fiber Morphology and Soda-sulfite Pulping of Switchgrass". Bioresource Technology 77:1-7 (2001).

7. K.N. LAW, B.V. KOKTA, MAO, C.B., "Differentiation of Jack Pine from Other Conifers by Analysis of Color Appearance from Chemical Test". Journal of Wood Chemistry and Technology 20(1): 61-70 (2000).

Appendix 1

- **"Characterizing Radial Compression of Wood by Longitudinal Shear"**

  The paper was presented at 90th Pulp and Paper Annual Meeting, PAPTAC, Montreal (Jan., 2004), and has been accepted for publication in APPITA Journal.

Telephone: (03) 9532 4534
Intern'l +61 3 9532 4534
Facsimile: (03) 9532 4534
Intern'l +61 3 9532 4534
Email:
ateched@ozonline.com.au

Appita

51 Carlingford Street
Elsternwick
Victoria 3185
Australia

Technical Editor

23 January, 2004

Dr Kwei-Nam Law
Pulp & Paper Research Centre
P. O. Box 500
Trois-Rivières
Quebec, Canada G9A 5H7

Dear Ken,

Your paper titled **'Characterizing Radial Compression of Wood by Longitudinal Shear'** has been accepted for publication in *Appita Journal*. The referee has made the attached comments, which we would like you to consider and modify your paper as necessary. Also the number of figures must be reduced to no more than 12.

Would you please send me an electronic copy of the final version of your paper. Microsoft Word format is preferred. This version should comply strictly with the *Appita Journal* - Guidelines for Authors.

I look forward to seeing your paper published in *Appita Journal*.

Yours sincerely,

K Maddern

Dr Ken Maddern

CHARACTERIZING RADIAL COMPRESSION OF WOOD BY LONGITUDINAL SHEAR

Changbin Mao, Kwei-Nam (Ken) Law, and Bohuslav V. Kokta

Centre intégré en Pâtes et Papiers
Université du Québec à Trois-Rivières
3351 boul. des Forges, Trois-Rivières, QC G9A 5H7

RÉSUMÉ

Dans cette étude nous avons développé une technique de cisaillement pour obtenir des données qui peuvent être utilisées pour quantifier l'effet de la compression sur les caractéristiques mécaniques des spécimens de bois. Nous trouvons que les propriétés de cisaillement du bois sont influencées par les conditions de compression telles que la température et la sulfonation, et qu'elles sont étroitement reliées à l'énergie spécifique de compression.

ABSTRACT

In this work we have developed a shearing technique which produces data that can be used to quantify the effect of compression on mechanical characteristics of specimens. We find that shear properties are affected by the compression conditions such as temperature and sulfonation, and highly correlated with the specific compression energy.

INTRODUCTION

In modern refining technology, pre-treatment of chips by mechanical compression is an important process step to improve pulp quality. Therefore, compression failure of wood has received increasing attention in the past two decades or so [1-12]. Chip refining can be regarded as a repetitive compression-decompression process that liberates fibres from the wood matrix [1]. The separation of fibres by compression, a fatigue process [4], is affected by temperature [8], stress amplitude and frequency [5]. Despite numerous research efforts on compression of wood, there is, however, no reported technique that quantitatively characterizes the mechanical properties of compressed wood.

In radial compression early- and latewood behave differently [13, 14]. Radial compression of water-saturated wood blocks without restraint, up to 50% strain, the earlywood could account for more than 80% (depending on the proportion of earlywood in the sample) of the total deformation while the contribution of latewood is relatively small due to its thick cell wall. In the plastic deformation zone the thin-walled earlywood fibres collapse (flatten) while the latewood fibres exhibit little deformation. However, with higher strains radial rows of latewood fibres would buckle, developing microscopic fissures. Such failures could eventually lead to the breakdown of the wood matrix as the compression load increases.

Microscopic observation [15-18] is usually used for characterizing mechanical failures and physical changes in the wood matrix. The optical technique gives limited qualitative information over a small area. Imagine analysis has also been used [18] to characterize failures in wood. Like other optical methods, it provides only an approximate quantitative physical estimation. Unfortunately, the optical methods do not characterize the strength properties of compressed specimens.

In radial compression the physical deformation specimen progresses gradually from earlywood towards latewood. Any physical weakening across the growth rings is expected to occur in a similar manner. The weakening effect of radial compression on strength properties of wood could be determined by a longitudinal shear in the radial plane of specimen. The objective of this study is to characterize the effect of radial compression on the mechanical properties of wood using a longitudinal shearing test.

EXPERIMENTAL

Sample Preparation

Sample blocks were prepared as described in [14]. The principal experimental procedures are shown in Fig. 1. At least 10 replicates were made for each experimental condition; a total of 200 specimens were tested. Before the compression test, specimens C1 and C2 were presoaked in water under vacuum ovemight at room temperature while specimens C3 in water-glycerol mixture (1:8 by vol). Samples C4 were impregnated with a 10%-Na_2SO_3 solution, under vacuum, at room temperature for 8 hours, and then cook in a M/K laboratory digester at 132°C for 75 minutes. A liquor-to-wood ratio of 22 was used. The sulfonated specimens were thoroughly washed and kept in water until further testing.

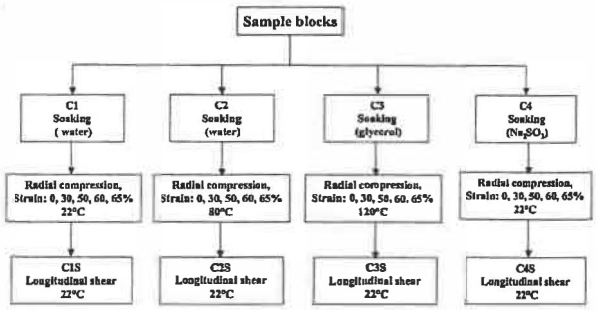

Fig. 1. Experimental design

Compression Test

Static compression, in radial direction of growth rings, was conducted by means of an Instron machine (model 4200), using a loading speed of 3 mm/min. Data were collected at a rate of 5 per second. As shown in Fig. 1, samples C2 and C3 were preheated in water and water-glycerol at 80°C and 120 °C for 15 min, respectively. It took about 7 min to reach these temperatures inside the sample blocks. The heated specimens were pressed either in water or water-glycerol mixture at these temperatures. The specimens C1 and C4 were compressed at 50% relative humidity and 22 °C. After compression the samples were kept in water under vacuum for 2 hours and then kept over night to restore their water-saturated state, after which their dimensions were re-measured before being subjected to shear test.

Shear Test

Shearing tests were performed using the same Instron machine with a special sample holding device as shown in Fig. 2. To conduct the shearing test the specimen block was placed onto a platform keeping it in a restrained position with the grain direction parallel to the shearing piston, that is in parallelism with the

direction of the applied force. The samples were sheared to a maximum strain of 27% at a speed of 10 mm/min. Data were collected at a rate of 20 per second. Two pairs of failure surface were created on radial plane of each block.

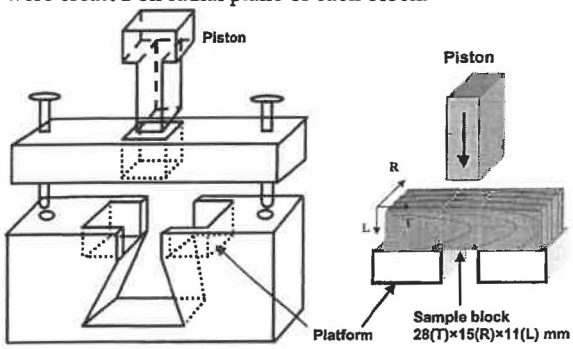

Fig. 2. Shearing Device

RESULTS AND DISCUSSION

Compression:

The characteristics of wood compression was discussed previously [14]. TABLE I presents the compression data of samples pressed in various conditions, and at 30, 50, 60 and 65% strain. Since the primary stress plateau (SP1) represents the intrinsic property of earlywood and is, therefore, independent of the magnitude compression strain. As such, its variation was relatively small within a sample group, Table 1 indiactes. However, the SP1 decreased with increasing compression temperature or with sulfonation.

As in the case of SP1, the Young's modulus was not supposed to be affected by the compression strain for a given specimen treatment since it accounts for the elastic response of the wood matrix. However, the treatment temperatures and sulfonation significantly reduced this property.

TABLE I. RESULTS OF COMPRESSION

Sample	Compression strain %	Primary stress plateau (SP1) MPa	Young's modulus MPa	Specific compression energy, MJ/m^3	Permanent Deformation %
C1: Water- saturated Comp. at 22°C	30	2.29 (10.4)*	108.3 (21.6)	0.75 (13.6)	1.0 (20.4)
	50	2.31 (10.8)	101.8 (38.5)	1.61 (17.4)	2.6 (18.2)
	60	2.37 (13.8)	91.07 (22.1)	2.48 (18.3)	3.0 (15.6)
	65	2.32 (15.8)	91.77 (14.1)	2.60 (9.1)	3.3 (7.8)
C2: Water- saturated Comp. at 80°C	30	1.03 (5.8)	44.31 (28.4)	0.30 (8.1)	1.3 (6.0)
	50	1.06 (7.9)	47.95 (24.5)	0.68 (13.1)	2.8 (10.2)
	60	1.02 (6.3)	50.05 (28.2)	1.07 (14.6)	4.3 (21.8)
	65	1.05 (9.1)	49.40 (30.1)	1.56 (16.8)	4.6 (16.8)
C3: Glycerol- saturated Comp. at 120°C	30	0.73 (7.1)	27.1 (21.2)	0.22 (10.0)	0.5 (26.8)
	50	0.74 (6.0)	29.6 (11.9)	0.54 (6.0)	2.0 (12.47)
	60	0.73 (9.3)	28.8 (17.3)	0.93 (18.5)	2.5 (16.5)
	65	0.73 (8.8)	27.0(13.5)	1.53 (20.1)	3.5 (14.6)
C4: Sulfonated Comp. at 22°C	30	0.91 (9.9)	49.46 (23.7)	0.28 (13.7)	0.6(31.4)
	50	0.83 (10.1)	44.09 (25.3)	0.62 (20.0)	1.4 (27.3)
	60	0.85 (10.3)	40.34 (33.0)	1.17 (11.5)	2.5 (23.0)
	65	0.85 (8.2)	42.23 (38.5)	1.65 (10.7)	2.8 (14.4)

* Figures in brackets are coefficient of variance in percentage

The specific compression energy (ratio of compression energy to specimen volume) increased with increasing compression strain. Its magnitude decreased with increasing temperatures and sulfonation.

There were some interesting effects of compression relative to the permanent deformation of specimens (TABLE I). The effects are illustrated in Fig. 3 which shows that compression at 80°C had the greatest effect on permanent deformation, which is believed to be related to the thermosetting of lignin in the wood matrix. Interestingly, compression at 120°C yielded lower permanent deformations in comparison with that at 80°C. The reason for this phenomenon is unknown at this point. However, speculatively, it may be related to the ease of springback of the wood matrix at this high temperature when the compressive forces is released. Noteworthily, the sulfonated specimens showed the lowest permanent deformation, implying that sul-

fonation gave the cell wall a somewhat "spongy" character. Additional compression tests on sulfonated sample blocks confirmed this effect.

Shear:

The shearing device used in this study was designed in such a way that two pairs of radial-longitudinal (RL) planes are created in the specimen. The reason for choosing the radial-longitudinal plane is to ensure that the shear failures take place across the entire growth ring including early- and latewood. These shear planes occurred, in most cases, successively (mode I), or less frequently, concurrently (mode II), as shown in Fig. 4. Most of the failure planes occurred successively because of the heterogeneous nature of wood. In both failure modes, after an elastic phase (a), the shear stress reached a yield point, A, where small fissures developed mostly in the middle of the bottom side of the sample block. As the shearing load increased more fissures developed and the shear stress attained a plateau (b). In mode I, the shear stress dropped sharply when the first two failure planes appeared (point B), after which a second stress plateau occurred (c). As the shearing progressed, a second pair of shear failure planes developed at point C where the shear stress fell suddenly. When the two pairs of failure plane occurred simultaneously (mode II) the stress plateau prolonged farther than that in mode I. The shear stress disappeared as the failure planes developed.

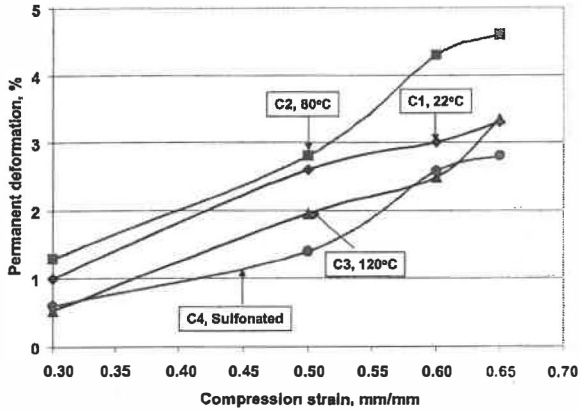

Fig. 3. Effect of compression on permanent deformation

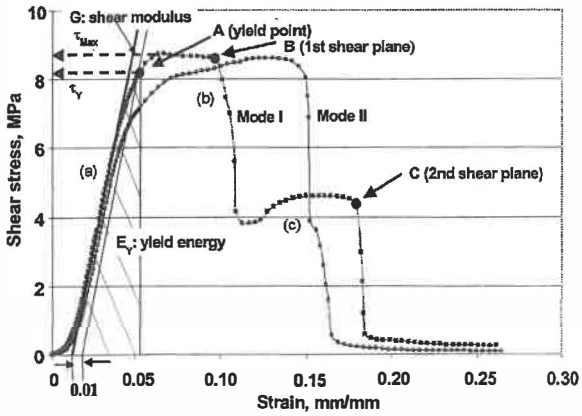

Fig. 4. Typical shear curves

We used shear modulus (G), yield stress (τ_y), maximum stress (τ_{max}), yield energy (E_y) and total energy (E_t) to characterize the shear behavior of the pre-compressed wood specimens. The shear yield stress, defined as the offset stress at 1% strain, is less than the maximum shear stress (Fig. 4). The yield energy is the energy consumed up to the yield point, A, and the total energy is the accumulative energy up to the completion of shear failure at about 27% shear strain. The mean coefficient of variance of the above 5 parameters were 6.3, 5.5, 16.3, 18.8 and 14.9%, respectively.

Figs. 5-9 present the variations of shear properties as a function of pre-compression strain. In general, the radial compression had little effect on shear properties when the compression strain was less than 50%. This is because most of the compression energy is absorbed by the flexible earlywood fibres. Due to their high flexibility the earlywood fibres would suffer little physical damages. Meanwhile, the thick-walled latewood fibres would be relatively unaffected. But the shear properties fell sharply when the compression strain reached about 60% where significant structural damages occurred in both earlywood and latewood. The drastic changes in shear properties indicate the failure of latewood fibres. The possible failures include mainly buckling and separation of radial files of latewood and early wood fibres as well [14].

The pre-compression conditions had significant influence on the shear characteristics. Among the treatment conditions, sulfonation had the most significant impact on shear properties. In fact, sulfonation facilitates fibre separation by softening the lignin in wood [19, 20]. Pre-compression at 120°C had much less effect when compared to the sulfonation. At lower compression temperatures of 22°C and 80°C the changes in shear properties were comparable when the compression strain was about 50% or less. But the differences became statistically significant at high compression strain of 60% or higher where important physical damages to the wood matrix are expected to occur. However, compression at 80°C had minimum effect in reducing the shear properties (Note that this pre-compression temperature yielded the largest permanent deformation, Fig. 4 shows. Speculatively, the thermosetting of lignin at 80°C minimized the compression effect on the wood matrix (e.g. fiber collapse and separation), thus minimizing the adverse impact on the shear properties.

The relations between pre-compression energy and shear properties such as shear yield stress, maximum shear stress, shear modulus, shear yield energy and total shear energy, are presented in Figs. 10-14, respectively. In these illustrations we use the specific compression energy, defined earlier as the ratio of compression energy to volume of specimen (MJ/m3), to express the correlation.

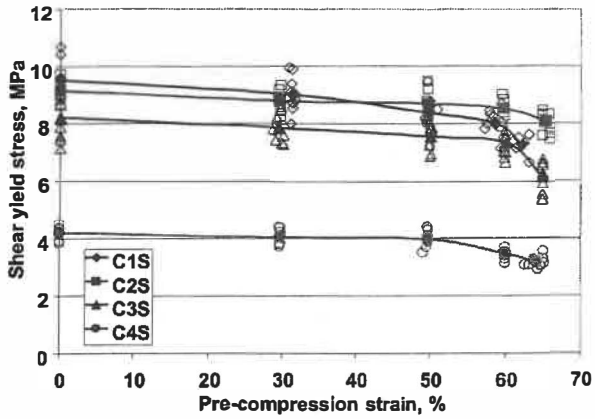

Fig. 5. Effect of pre-compression strain on shear yield stress

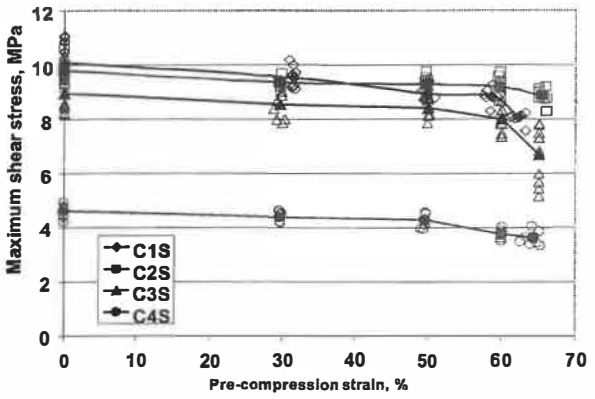

Fig. 6. Effect of pre-compression strain on maximum shear stress

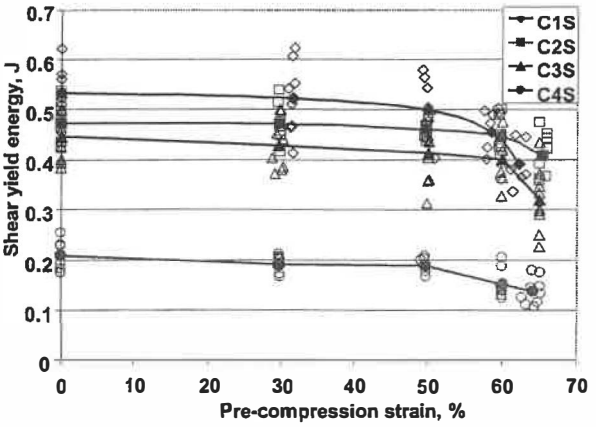

Fig. 7. Effect of pre-compression strain on shear yield energy

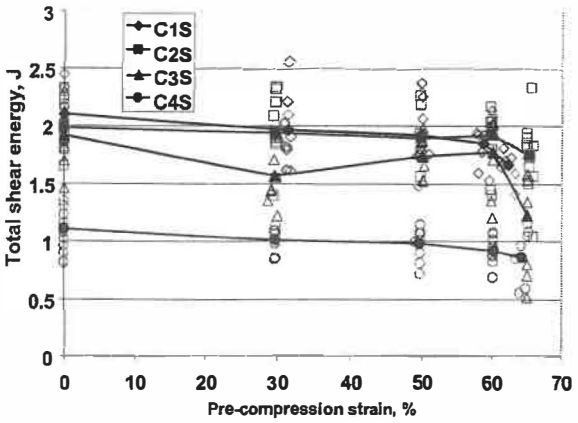

Fig. 8. Effect of pre-compression strain on total shear energy

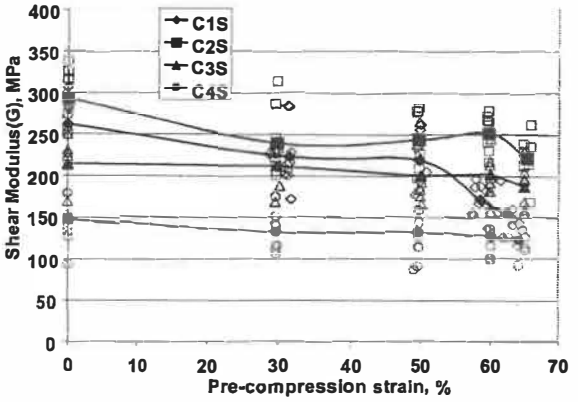

Fig. 9. Effect of pre-compression strain on shear modulus

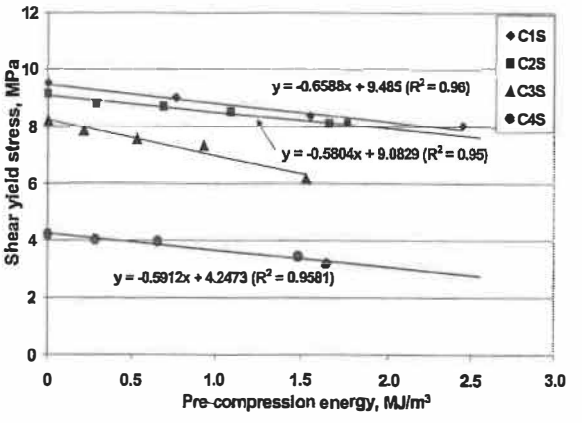

Fig. 10. Relation of specific compression energy and shear yield stress

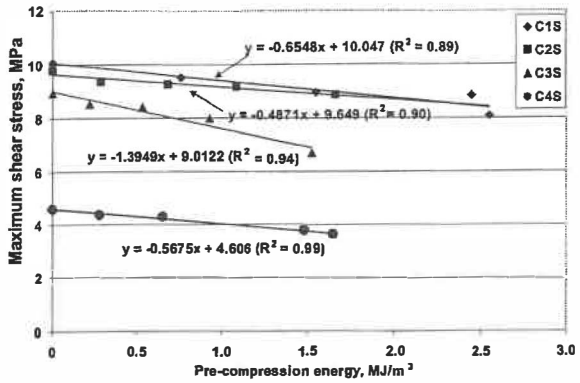

Fig. 11. Relation of specific compression energy and maximum shear stress

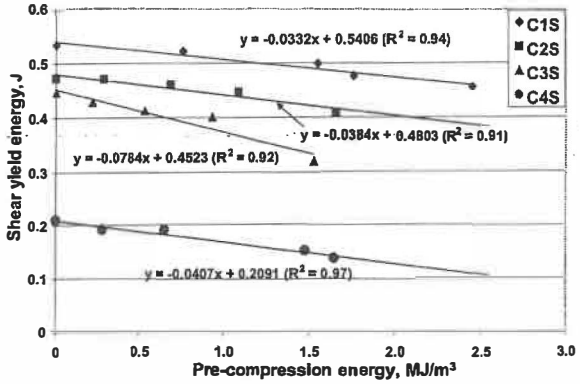

Fig. 12. Relation of specific compression energy and shear yield energy

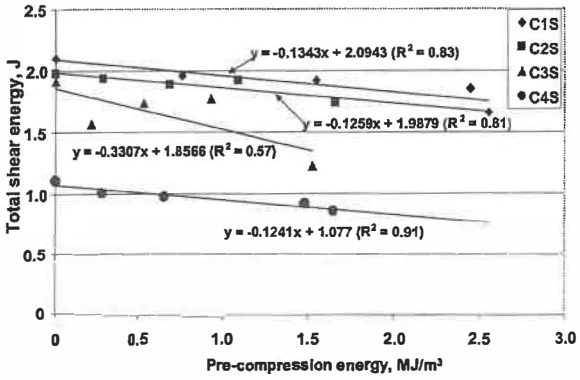

Fig. 13. Relation of specific compression energy and total shear energy

As seen in Figs. 10-14, the shear properties of wood specimens are closely associated with the specific compression energy consumed by the specimens in the pre-compression processes. This finding suggests that the changes in shear properties are highly related to the energy applied during the pre-compression of wood samples, and that shearing test could be used to characterize the physical damages in wood.

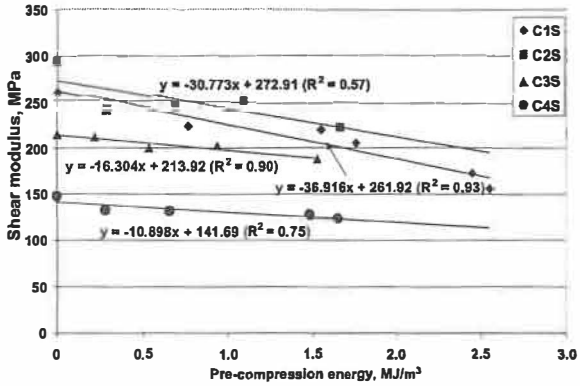

Fig. 14. Relation of specific compression energy and shear modulus

CONCLUSION

For a given compression condition (temperature or sulfonation) compression strain of low magnitude, about 50% or less, there is little changes in strength characteristics. However, the properties decrease with increasing compression temperatures or with sulfonation.

As results of compression, permanent deformation is affected by the temperature and sulfonation. Compression at 80°C produces the greatest permanent deformation when compared to other temperatures. Sulfonated specimens have the lowest permanent deformation.

With the shearing technique used in this study, the shear planes occur, in most cases, successively, or less frequently, concurrently.

Generally, radial compression has little effect on shear properties when the compression strain is less than 50%. Beyond this compression strain the shear properties fall sharply, indicating significant structural damages in both early- and latewood.

The pre-compression conditions have significant influence on the shear characteristics; the influence of pretreatment by sulfonation being the most significant.

Shear properties of wood specimens are closely associated with the specific compression energy consumed by the specimens in the pre-compression processes.

ACKNOWLEDGEMENTS

We want to thank the Natural Science and Engineering Research Council of Canada for its financial support in this work.

REFERENCES

1. PEARSON, A.J., "A Unified Theory of Refining", *Pulp and Paper Techn. Series, No. 6*, Joint Textbook committee of the Paper Industry, TAPPI, p. 6 (1990).
2. SALMÉN, L. and FELLERS, C., "The Fundamentals of Energy Consumption during Viscoelastic and Plastic Deformation of Wood", *Trans. Techn. Sect.*, CPPA (PAPTAC): TR93-99 (1982).
3. SABOURIN, M. J., "Evaluation of a Compressive Pretreatment Process in TMP Properties and Energy Requirements", *Pulp Paper Can.* 101(2): 50-56 (2000).
4. SALMÉN, L., TIGERSTRÖM, A. and FELLERS, C., "Fatigue of Wood - Characterization of Mechanical Defibration", *J. Pulp Paper Sci.* 11(3): 68-73 (1985).
5. SALMÉN, L., "The Effect of the Frequency of a Mechanical Deformation on the Fatigue of Wood", *Proc. Intl. Mech. Pulp. Conf.*: 146-152 (1985).

6. RENAUD, M., RUEFF, M. and ROCABOY, A.C., "Mechanical Behavior of Saturated Wood under Compression, Part I: Behavior of Wood at High Rates of Strain", *Wood Sci. Techn.* 30:153-164 (1996).
7. RENAUD, M., RUEFF, M. and ROCABOY, A. C., "Mechanical Behavior of Saturated Wood under Compression. Part II: Behavior of Wood at Low Rates of Strain, some Effects of Compression in Wood Structure", *Wood Sci. Techn.* 30:237-243 (1996).
8. UHMEIER, A. and SALMÉN, L., "Repeated Large Radial Compression of Heated Spruce", *Nordic Pulp Paper Res. J.* 3:171-176 (1996).
9. DUMAIL, J.F. and SALMÉN, L., "Compression Behavior of Spruce Wood under Large Plastic Deformations", *Nordic Pulp Paper Res. J.* 4:239-242 (1996).
10. SABOURIN, M. J., "Evaluation of a Compressive Pretreatment Process in TMP Properties and Energy Requirements", *Pulp Pap. Can.* 101(2): 50-56 (2000).
11. LAW, K. N., LANOUETTE, R., YANG, K. C., "Effect of Compression on Refining Energy and Pulp Properties of Birch TMP", *Appita J.* 53(4): 296-299 (2000).
12. LAW, K. N., LANOUETTE, R, YANG, K. C., "A New Approach to Mechanical Pulping – Pretreatment of Chips by Normal-to–Grain Compression Prior to Refining", *Tappi J.* 83(9): 63 (2000). (http://www.tappi.org/public/tappi_journal.asp).
13. LAW, K.N., "Mechanical Behavior of Early- and Latewood under Compression Load", *Proc. Intl. Mech. Pulp. Conf.*, 1:159-166 (2001).
14. MAO C., LAW, K.N., KOKTA, B.V., "Effect of Sulfonation on the Compression Behavior of Early- and Latewood", *Proc.(CD) 89th PAPTAC Annual Meeting, Montreal*, Canada, (2003).
15. KUCERA, L.J., BARISKA, M., "On the Fracture Morphology in Wood. Part 1 A SEM-study of Deformations in Wood of Spruce and Aspen upon Ultimate Axial Compression Load", *Wood Sci. Techn.* 16:241-259 (1982).
16. BERGANDE, A., and SALMÉN, L., "Lamellar Cracks, do They Appear During Radial Compression of Wood", *Nordic Pulp Paper Res. J.* 12(4): 216-219 (1997).
17. THIRUVENGADASWAMY, R., OUELLET, D., "On the Generation of Structural Damage in Wood by Cyclic Compressive Loading", *J. of Pulp Paper Sci.* 24(8): 247-253 (1998).
18. THIRUVENGADASWAMY, R., OUELLET, D., "An Image Analysis Method to Quantify Fibre Separation in Wood Subjected to Fatigue Load", *Proc. Intl. Mech. Pulp. Conf.*:221-228 (1999).
19. MUTTON, D.B., TOMBLER, G., GARDNER, P.E. and FORD, M.J., "The Sulphonated Chemimechanical Pulping Process", *Pulp Paper Can.* 83(6): 120-128 (1982).
20. HEITNER, C. and HATTULA, T., "Ultra-High-Yield Pulping. Part VI: The Effect of Sulphonation on the Development of Fibre Properties", *J. Pulp Paper Sci.* 14(1): J6-J11 (1988).

Appendix 2

- **"Effect of Sulfonation on the Compression Behavior of Early –and Latewood"**

The paper has been published in Pulp and Paper Canada 105 (12): T273-277 (2004), and was presented at 89th Pulp and Paper Annual Meeting in Montreal, QC, Canada (Jan. 28-30, 2003).

Effect of sulfonation on the compression behaviour of early — and latewood

By C. Mao, K.N. Law and B.V. Kokta

Abstract: Sulfonation is an important technique for producing mechanical pulp with improved papermaking properties. This study examines the response of early- and latewood to the treatment of sulfonation, and their mechanical behaviour under compression force. Upon sulfonation, the compressive stress of the plastic region is reduced by 63.58 and 67.49% for the earlywood and latewood, respectively. Hence, this chemical treatment would make the wood more amendable in refining and produce better pulp quality.

Wood is a biological material that exhibits great variety in properties. The variation occurs between species, between trees of the same species, and even within a single tree. One of the most striking variations amongst conifers in the temperate zone is the presence of earlywood (EW) and latewood (LW). The influence of these wood tissues on papermaking has long been recognized [1-6]. In general, the EW fibres being more flexible and conformable due to their thin cell wall produce a sheet with high density and good bonding, while the LW fibres having significantly thicker cell wall produce paper with high bulk and poor bonding.

In mechanical pulping the EW and LW fibres separate and develop differently [6-9]. Fibre splitting or axial trans-wall failure and cross-axial breakage of EW fibres are common in refining. On the other hand, LW fibres are more resistant to such failures. Additionally, the so-called sleeve-rolling of cell wall layers is often seen only with the thick-walled LW fibres [7, 9]. Due to their morphological differences the EW fibres have higher energy absorption [10], but require greater refining energy [6] for a given pulp freeness as compared with the LW fibres.

The mechanical properties of wood can be modified to make it more amendable in mechanical pulping, improving its papermaking characteristics. The most common techniques used to change the mechanical behaviour of wood include thermal [11-13] and chemical [14-17] treatments. In chemimechanical or chemithermomechanical pulping, a question arises whether the EW and LW differ in chemical reaction when treated under the same conditions. It is also of interest to know how a chemical treatment such as sulfonation affects their mechanical behaviour, particularly under compressive load, which is one of the two major refining forces. The present work tends to shed some light on these two aspects.

MATEIRALS AND METHODS

Materials: Samples were taken from a 1-metre log (above ground) of a freshly felled 65-year old white spruce [Picea glauca (Moench) Voss], excluding the heartwood and all natural defects. Whole-wood specimens consisting of both EW and LW, having a nominal dimension of 10x10x10 mm (in air-dry condition), and containing five to seven growth rings, were prepared in such a way that the growth rings were, more or less, parallel to the tangential plane. The exact dimension of the water-saturated specimens was measured using a digital sliding calliper to the nearest 0.01mm, at 22°C. The over-all average volumetric proportion of EW was about 78%; LW represented 22%. Specimens containing only EW or LW measured 10 (longitudinal) × 10 (tangential) × 3mm (radial) and 10 × 10 × 1.9mm, respectively, were also prepared for certain tests.

Methods:

—*Sulfonation:* Sulfonation of water-saturated samples was carried out in a laboratory digester (M/K System) using a central composite design, Table I. In the process, 15 specimen blocks (approximately 8 g, o.d.) were placed in a stainless-steel basket and cooked with 1.1 L of chemical solution. The initial pH of the treatment liquor was about 9.7, which dropped only slightly after cooking. The treated samples were thoroughly washed with running tap water and kept in distilled water at 4°C for further testing.

The degree of sulfonation was evaluated by determining the acidic groups in the treated samples, which were first disintegrated in a blender before being refined in a PFI mill (5,000-20,000 revolutions). The resulting pulps were then treated with 0.1N HCl twice, each for 45 minutes, and thoroughly washed. The acidic groups were determined by conductivity titration as described in [18] by means of an automatic titration system composing of a Metrohm titration unit (765 Dosimat), and a conductivity meter (Thermo Orien model 150).

—*Compression test:* We conducted radial compression tests (relative to the growth rings) using an Instron machine (model 4201) in a controlled environment (50% RH, 22°C). In most cases, the water-saturated specimens were compressed without restraint at a loading speed of 3 mm/min. The maximum strain was set at 70%. Data were collected at 5-10 data per second. For each sample type, the average test value was calculated using the results of at least five specimens. For compar-

C. MAO,
Centre intégré
en Pâtes et Papiers, UQTR,
Trois-Rivières, QC
maoc@uqtr.ca

K.N. LAW,
Centre intégré
en Pâtes et Papiers, UQTR,
Trois-Rivières, QC

B.V. KOKTA,
Centre intégré
en Pâtes et Papiers, UQTR,
Trois-Rivières, QC

TABLE I. Central composite design of the experiment (19 runs).

Code value (CV)		-1.68	-1	0	1	1.68	
Actual value	Temp. °C	20	48.4	90	131.6	160	AV= 90+41.62CV
	Time Min.	5	21.2	45	68.8	85	AV= 45+23.78CV
	Con. %	0	6.1	15	23.9	30	AV= 15+8.92CV

TABLE III. Sulfonate and carboxylate contents of earlywood and latewood.

	Temp. °C	Time min	Na_2SO_3 Con.kl%	Sulfonate mmol/kg	Carbo xylate mmol/kg
Early-wood	132	15	15	118.2	121.4
	132	45	15	170.9	134.2
	132	75	15	193.4	140.9
	132[a]	75	15	201.1	139.5
Late-wood	132	15	15	133.0	135.6
	132	45	15	190.9	146.9
	132	45	15	230	153.1
	132[a]	75	15	228.1	154.9

Note: a — earlywood and latewood were cook separately.

TABLE II. Experiment conditions and results of sulfonation and compression of whole-wood sample blocks.

Run	Temp. C°	Time min Con. %	Na_2SO_3 /kg	Sul. mmol /kg	Car. mmol	SPI MPa	SP_2 MPa	Toug. MPa
1	131.6	68.8	6.1	157.3	117.0	0.98	11.75	2.78
2	90	45	15	78.7	110.9	1.94	17.33	4.62
3	48.4	68.8	6.1	33.3	94.8	2.42	20.09	5.05
4	131.6	21.2	6.1	118.9	134.5	1.63	14.12	3.75
5	131.6	68.8	23.9	212.3	136.5	1.02	10.05	2.83
6	48.4	21.2	6.1	20.1	95.6	2.46	21.11	5.70
7	90	45	15	98.4	110.9	1.81	17.65	5.16
8	90	5	15	42.9	104.4	2.54	21.54	4.94
9	90	85	15	91.2	122.3	2.06	16.29	3.78
10	20	45	15	29.1	92.9	2.49	22.51	5.03
11	90	45	0	8.4	80.6	2.81	20.86	5.56
12	90	45	15	98.3	111.3	1.91	17.74	4.58
13	90	45	30	95.8	119.9	1.78	14.4	4.05
14	131.6	21.2	23.9	155.3	123.3	1.23	12.3	3.38
15	90	45	15	97.8	110.1	1.89	17.73	5.06
16	48.4	21.2	23.9	35	105.7	2.62	19.43	5.67
17	48.4	68.8	23.9	44.7	117.2	2.28	17	5.04
18	90	45	15	98.3	111.7	1.89	18	4.56
19	160	45	15	236.9	145.4	0.61	8.01	2.28

Note: Sul. — sulfonate; Car. — carboxylate; SPI — stress plateau 1; SP2 — stress plateau 2; Toug — toughness. The standard deviations are 0.343, 5.740 and 0.443 for the SP1, SP2 and toughness, respectively.

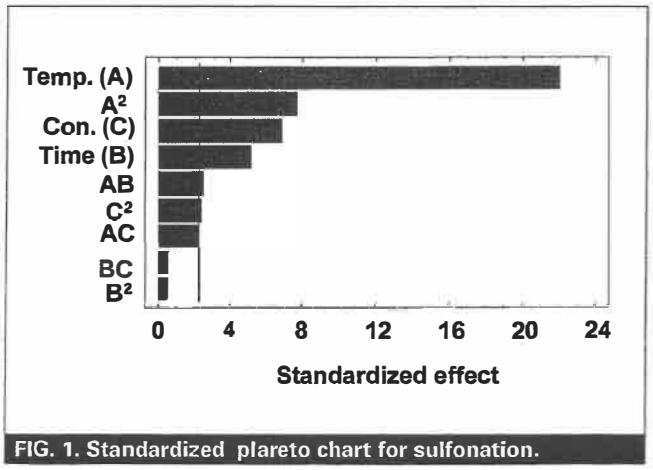

FIG. 1. Standardized plareto chart for sulfonation.

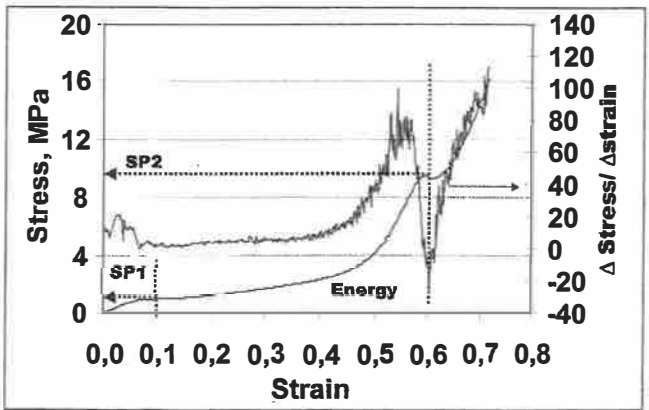

FIG. 2. Definition of stress of the primary plastic plateau (SP1) and that of second plastic plateau (SP2).

ative purpose, some specimens were compressed with restraint in specially made device that limits the lateral expansion of specimen under compression.

RESULTS, DISCUSSION

Factors Affecting Sulfonation: Beatson et al. [19] reported that the total SO_2, pH and reaction time have significant effect on the sulphur content of lignin in the treated spruce wood. In this study we found that among the variables studied the reaction temperature is the most influential on the level of sulfonation, Fig. 1). The effect of sodium sulphite concentration and treatment time are also significant, but to a lesser extent when compared with the temperature, as the following equation (coded values) indicates: Sul. = 78.09 + 62.99*Temp. + 14.61*Time + 19.38*Con. + 21.95*temp.2 + 9.06*Temp.*Time - 6.65*Con.^{2} (R^2 = 97.2%). The results on sulfonation are shown in Table II.

Earlywood vs. Latewood: The work of Wu and Wilson [20] as well as those reviewed in their work indicate that the concentration of lignin is higher in EW than in LW. In contrast to these results obtained by chemical techniques, Fergus [21] used ultraviolet (UV) microscopy to show that the secondary wall of both EW and LW have the same lignin distribution, while the middle lamella and cell corners of LW show significantly higher lignin concentration in comparison with the EW.

In this study, we used the technique of sulfonation to see if there is any difference between the EW and LW by measuring the sulphonate and carboxylate contents of the sulphite-treated wood samples. Table III indicates that both the sulphonate and carboxlate contents are consistently lower for the EW than for the LW, regardless if they were cooked together in whole-wood specimens or treated separately. This finding seems to follow the trend noted by Fergus [21], assuming that the sulfonation was uniform across the cell wall and its mechanism is similar in both EW and LW. Note that the degrees

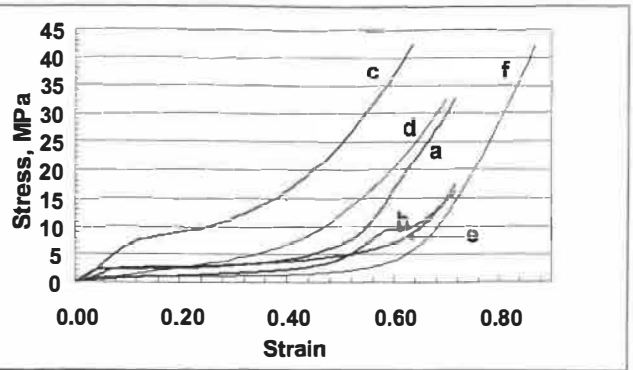

FIG. 3. Effect of sulfonation on stress-strain relationship of specimens compressed without restraint: a) untreated ww; b) sulfonated WW (212 mmol/kg); c) untreated LW; d) sulfonated LW (228 mmol/kg); e) untreated EW; f) sulfonated EW (201 mmol/kg).

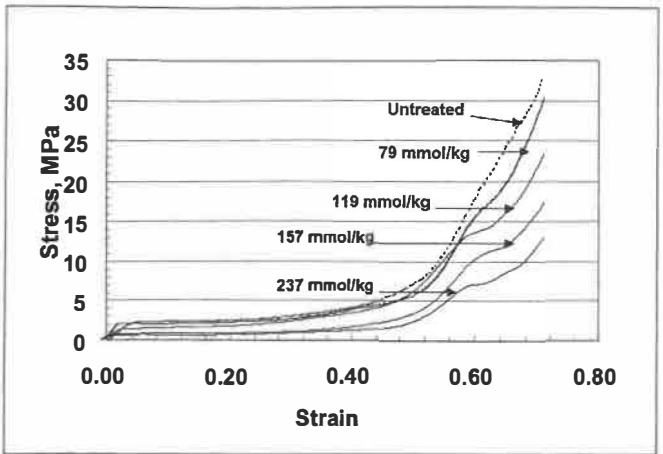

FIG. 4. Effect of sulfonate content on stress-strain curves of whole-wood specimen compressed without restraint.

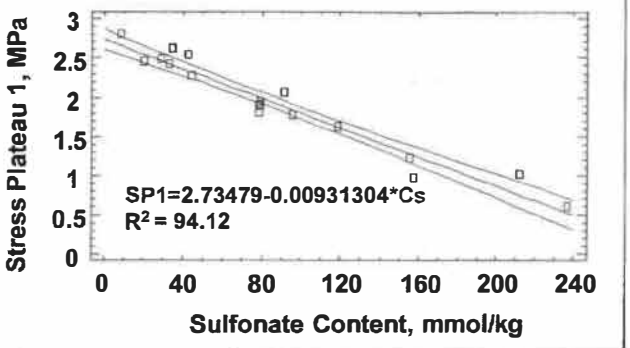

FIG. 5. Relationship of the first plateau stress (SP1) and sulfonate content of the whole-wood specimens compressed without restraint.

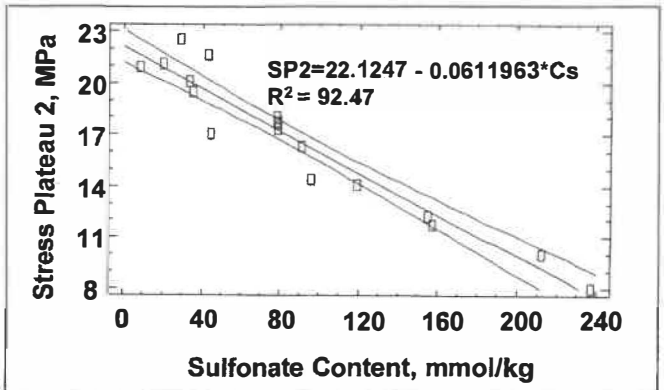

FIG. 6. Relationship of the second plateau stress (SP2) and the sulfonate content of the whole-wood specimens compressed without restraint.

of sulfonation may not necessarily reflect the actual concentration of lignin, because sulfonation reactions depend on the reaction conditions and the types of functional group in the lignin [22, 23].

Typical Compression Curve and Definitions: A typical compression curve (lower curve of Fig. 2) can be characterized by its slope (upper curve of Fig. 2). The characteristic of the elastic region is not considered here because of its relatively large variation, which is probably due to the small specimens used in the study. The stress of the primary plastic plateau (SP1) is taken at 10% deformation, while the stress used to represent the stress of the secondary plateau (SP2) is defined as the stress at a point that is determined by the slope curve; it is located at the point corresponding to the bottom of the slope curve's valley, which is in the neighbourhood of 60% strain. Note that the secondary plastic plateau occurs only when the strain exceeds 50%, particularly in whole-wood specimens that have been sulfonated.

Stress-Strain Relationship: A series of compression curves for the sulfonated and untreated specimens are illustrated in Fig. 3. Each curve represents the average of five to seven measurements. The untreated whole-wood (WW) samples (curve a) exhibit a typical stress-strain curve as described by others [24-26]: An elastic region follows an extended plastic deformation and a sharp rise in stress (densification zone). The plastic plateau is usually described as the collapse of EW. However, our experience indicates that a lateral displacement of EW fibres and separation of LW fibres in the transition zone also contribute to the plastic deformation, when the compression is conducted without restraint. The rapid increase in stress at the beginning of the densification zone may signify the end of the lateral displacement of the EW and the beginning of densification of the EW.

Sulfonation decreased the elastic and plastic stresses (Fig. 3, curve b). What is noteworthy is that after a initial densification, a second stress plateau appeared at about 60% strain. This may indicate the weakening effect of sulfonation on the LW. This initial failure of LW may be characterized by fibre separation in radial direction and/or bucking of radial file of fibres. The second plastic stress plateau was usually relatively brief in comparison with the first plastic stress plateau. Softening of wood by heating can also provoke a second stress plateau at about 60% strain, as reported by Uhmeier and Salmén [27]. When the strain increases further the stress rises sharply again.

In the compression of LW, the primary plastic stress plateau was not obvious (Fig. 3, curves c and d), indicating that the collapse of LW was rather gradual in contrast to that of EW (curves e and f). Note that the stress was substantially reduced by sulfonation (curve d). When compared with the untreated LW, the sulfonated LW exhibited a 67.49% reduction in compressive stress of the plastic region. However, the form of the compression curve for the sulfonated LW was similar to that for the untreated specimen. It is interesting to note that there was no second stress plateau even when the LW was sulfonated, suggesting that there was no sudden failure. In contrast to the LW, the EW exhibit a prolonged plastic plateau (Fig. 2, curves e and f), indicating the collapse and the significant lateral displacement of EW fibres. The drop in compression stress in this region was 63.58%. The densification of EW progressed without showing a second stress plateau. Similar compression characteristics of LW and EW are also noted by Dumail and Salmén (28).

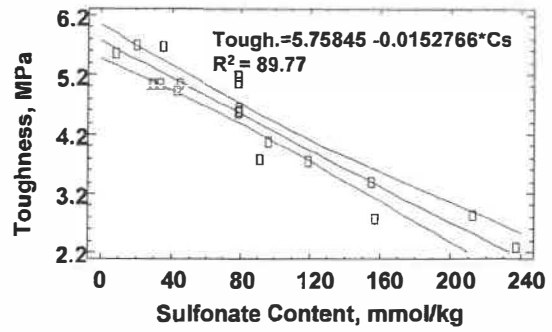

FIG. 7. Relationship of the toughness and the sulfonate content of whole-wood specimens compressed without restraint.

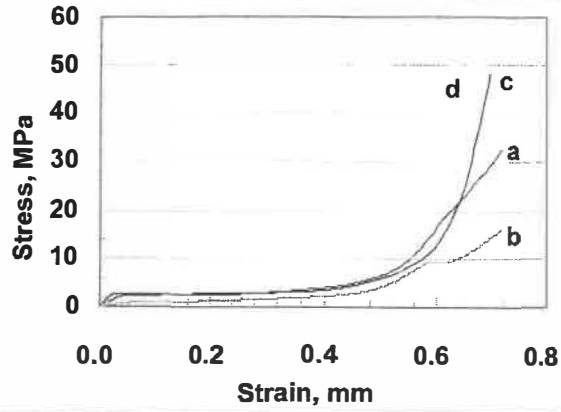

FIG. 8. Comparison between compression with restraint and without restrain of whole-wood specimens: a) untreated without restraint; b) sulfonated without restraint; c) untreated with restraint; d) sulfonated with restraint.

The stress-strain relationships of WW specimens having various levels of sulfonation are shown in Fig. 4. The stresses in the elastic and the plastic zones decrease as the degree of sulfonation increases, signifying the influence of chemical softening of the cell wall. As discussed earlier, the softening of wood tissue by sulfonation provokes a second stress plateau. The extent of this stress plateau appears to be directly associated with the degree of sulfonation, Figs. 4, 6. This second stress plateau appears only at large deformation, at about 60% strain, at which point the LW undergo substantial stress, forcing it to yield probably in the transition zone. This yield point could probably be caused by fibre separation and/or buckling of radial files of LW fibres.

Relationships of Stress and Toughness with Sulfonate Content: The influences of sulfonate content on the stress of the primary plastic plateau (SP1) and that of the secondary plastic plateau (SP2) are shown in Table II, and illustrated, respectively, in Figs. 5 and 6. Obviously, both stresses are closely correlated with the sulfonate content. The toughness of the compressed specimen, defined as the compression energy (area under the compression curve, Fig. 4) divided by the volume of the specimen, is shown in Fig. 7. This property is also highly associated with the sulfonate content.

In chemimechanical and chemithermomechanical pulping the chips have undergone a significant change in mechanical properties, and their refining behaviour would be quite different from the untreated raw material. As a result, we would expect different refining energy, fibre separation mode and pulp quality. A detailed analysis of the effect of sulfonation in chemimechanical pulping has been discussed [29].

Compression with Restraint vs. Without Restraint: Radial compression without restraint (curves a and b in Fig. 8) provides the fibres with a certain freedom of lateral movement, particularly in the tangential direction, reducing the compression stress beyond about 50% strain. It appears that the lateral displacement of fibres takes place at about 50% strain. In compression with restraint (curves c and d in Fig. 8), such lateral displacement of fibres is minimized, increasing substantially the stress in the densification zone, and prevents the occurrence of a secondary stress plateau. With sulfonation (curve d), the densification process occurs faster when compared to the untreated specimen (curve c), indicating an increase in fibre collapsibility by sulfonation.

CONCLUDING REMARKS

Radial compression of a wood block can reveal important mechanical characteristics of the component elements in the wood matrix. Mechanical failure follows the theory of weak-link within the wood structure. In such a case, the weak zone is situated in the EW where the fibres are large and thin-walled in comparison with those in the LW. In this study, the stress of the primary plastic plateau may be used to characterize the mechanical strength of EW while that of the secondary plastic plateau characterize the LW.

Following this line of thinking, we expect that the EW would break down earlier and faster than the LW in a refining system, and that the former would absorb most of the mechanical energy impacted by the refiner bars, and thus suffer higher degree of fragmentation compared to the LW. This has in fact been previously observed in atmospheric refining [9]. Refining mixtures of low- and high-density wood would be expected to exhibit similar behaviour as observed for the EW and LW.

Sulfonation decreases the compression stress of both the primary plastic region and the secondary plastic zone, and the toughness of wood compressed at large deformation. There is no fundamental change in the form of the compression curve of the whole-wood blocks containing both EW and LW. However, the softening effect of sulfonation on both EW and LW would promote better fibre separation in refining (such as in CMP and CTMP), minimizing fibres breakage, particularly those in the EW. Hence, softening of the wood matrix either thermally or chemically makes both the EW and LW more amendable, providing better distribution of refining energy over the two types of tissues.

ACKNOWLEDGEMENTS

The authors thank the Natural Science and Engineering Research Council of Canada for its financial support.

LITERATURE

1. PRASAD, V., LUNER, P. Physical properties of paper made from springwood and summerwood fibers. ESPRI Research Report 38-II-12. Syrocus, SUNY College of Environmental Science and Forestry (Oct. 2, 1964).
2. SMITH, W.E., BYRD, V.L. Fiber bonding and tensile stress-strain properties of earlywood and latewood handsheets. Paper FPL 193. Madixon, U.S. Forest. Serv., 11 p. (1972).
3. IFJU, G., LABOSKY, P. JR. Study of Loblolly pine growth increments. (1). Wood and tracheid characteristics. (2) Pulp yield and related properties. *Tappi J.* 55(4):524-534 (1972).
4. HASUIKA, M. Physical properties and macrostructure of earlywood and latewood pulp sheets. *J. Japan Wood Res. Soc.* 19(11):547-553 (1973).
5. LAW, K.N., VALADE, J.L., DANEAULT, C. Chemimechanical pulping of Tamarack. (2). Effects of pH and sodium sulfite. *Cellul. Chem. Technol.* 23(6):733-741 (1989).
6. MURTON, K.D., RICHARDSON, J.D., CORSON, S.R., DUFFY, G.G. TMP refining of radiata pine earlywood and latewood fibres. Proc., Intl. Mech. Pulp. Conf., Helsinki, 361-371 (2001).
7. MOHLIN, U.-B. Fibre development during mechanical pulp refining. *JPPS* 23(1):J28-J33 (1997).
8. REME, P.A., JOHNSEN, P.O., HELLE, T. Changes induced in early- and latewood by mechanical pulp refining. *Nordic Pulp Paper Res. J.* 14(3):256-262 (1999).
9. LAW, K.N. Mechanical behavior of early- and latewood under compression load. Proc., Intl. Mech. Pulp. Conf., Helsinki, 159-166 (2001).
10. HICKEY, K.L., RUDIE, A.W. Preferential energy absorption by earlywood in cyclic compression of Loblolly pine. Proc., Intl. Mech. Pulp. Conf., Poster

Session, Oslo, 81-86 (1993).
11. STATIONWALA, M.I., ATACK, D. Thermal softening of untreated and chemically treated eastern black spruce. Preprints, TS, CPPA Annual Meeting, Montreal, B63-B65 (1974).
12. UHMEIER, A., SALMÉN, L. Repeated large radial compression of heated spruce. *Nordic Pulp and Paper Res. J.* 3:171-176 (1996).
13. JOHANSSON, L., PENG, P., SIMONSON, R. Effects of temperature and sulfonation shear deformation of spruce wood. *Wood Science and Technology* 31(2):105-117 (1997).
14. ATACK, D., HEITNER, C. Dynamic mechanical properties of sulfonated eastern black spruce. Proc., Intl. Mech. Pulp. Conf., Toronto, 1-12 (1979).
15. HEITNER, C, ATACK, D. Dynamic mechanical properties of sulfite-treated aspen. *Paperi ja Puu* 66(2): 84-89 (1984).
16. OSTBERG, G., SALMÉN, L. Effects of sulfonation on properties of different cell wall layers. *Nordic Pulp Paper Res. J.* 3(1):8-12 (1988).
17. HEITNER, C., SALMÉN, L. Effect of sulfonation on the fatigue properties of wood. Nord. *Pulp Paper Res. J.* 9(3):182-186 (1994).
18. KATZ, S., BEATSON, R.P., SCALLAN, A.M. The determination of strong and weak acidic groups in sulphite pulps. *Svensk Paperstidin.* 6:R48-R53 (1984).
19. BEATSON, R.P., HEITNER, C., ATACK, D. Factors affecting the sulphonation of spruce. *JPPS* 10(1):J12-J17 (1984).
20. WU, Y.-T., WILSON, J.W. Lignification within coniferous growth zones: *Pulp Paper Can.* 68(4):T159-T164 (1967).
21. FERGUS, B.J., PROCTER, A.R., SCOTT, J.A.N., GORING, D.A.I. Distribution of lignin in sprucewood as determined by ultraviolet microscopy. *Wood Sci. Technol.* 3(2):117-138 (1969).
22. GELLERSTEDT, G., ZHANG L. Reactive structures in high yield pulping. Part 2. Monomeric end groups and detached side chain structures. *Nordic Pulp Paper Res. J.* 7(2):75-80 (1992).
23. LINDHOLM, C.-A., KURDIN, J.A. Chemimechanical pulping. *Mechanical Pulping. Ed. J.* Sundholm. Atlanta: Finnish Paper Engineers' Association and TAPPI, 222-249 (1999).
24. DUMAIL, J.F., SALMÉN, L. Compression behaviour of saturated wood perpendicular to grain under large deformation. *Holzforschung* 51(4):296-302 (1997).
25. UHMEIER, A., MOROOKA, T., NORIMOTO, M. Influence of thermal softening and degradation on the radial compression behavior of wet spruce. *Holzforschung* 52(1):77-81 (1998).
26. Tabarsa, T., Chui, Y.H. Stress-strain response of wood under radial compression. Part I. Test method and influences of cellular properties. *Wood Fiber Sci.* 32(2):144-152 (2000).
27. UHMEIER, A., SALMÉN, L. Repeated large radial compression of heated spruce. *Nordic Pulp Paper Res. J.* 3:171-176 (1996).
28. DUMAIL, J.F., SALMÉN, L. Compression behaviour of spruce wood under large plastic deformations. *Nordic Pulp Paper Res. J.* 4239-242 (1996).
29. SINKEY, J.D. Analyzing the effects of sulfonation in softwood chemi-mechanical pulping. *Paper Trade J.* 167(14):23-30 (1983).

Résumé: La sulfonation est une technique importante de production de pâte mécanique dotée de meilleures propriétés de fabrication. La présente étude examine la réponse du bois initial et du bois final au traitement par sulfonation et leur comportement mécanique sous une force de compression. La sulfonation réduit la contrainte de compression de la région plastique de 63,58 % et 67,49 pour le bois initial et le bois final, respectivement. Ce traitement chimique rendrait donc le bois plus facile à raffiner et permettrait de produire une pâte de meilleure qualité.

Reference: MAO, C., LAW, K.N., KOKTA, B.V. Effect of sulfonation on the Compression behaviour of early- and late-wood. *Pulp & Paper Canada* 105(12): T273-277 (December, 2004). Paper presented at the 89th Annual Meeting in Montreal, QC, ON January 28 to 30, 2003. Not to be reproduced without permission of PAPTAC. Manuscript received on March 31, 2004. Revised manuscript approved for publication by the Review Panel on May 21, 2004.

Keywords: SULFONATION, SPRING WOOD, SUMMER WOOD, MECHANICAL PULPING, COMPRESSION STRENGTH, REFINING, PULP PROPERTIES, MECHANICAL PULPS.